

THE DETERMINATION OF CRACK PROPAGATION RATES OF
REFLECTION CRACKING THROUGH ASPHALT SURFACINGS

by

TIMOTHY NICHOLAS BROOKER, B.Sc

This thesis is submitted to the Council for National Academic Awards in partial fulfilment of the requirements for the Degree of Doctor of Philosophy.

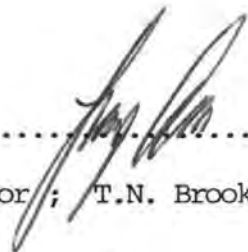
This work was undertaken within the Department of Civil Engineering at Plymouth Polytechnic, Plymouth, in collaboration with the University of Birmingham, the Transport and Road Research Laboratory (TRRL), U.K. and Devon and Cornwall County Council Highways Departments.


October 1986

DECLARATION

While registered as a candidate for the degree for which this submission is made , the author has not been a registered candidate for any other award of the C.N.A.A or of a University during the research programme .

All work described in this thesis is wholly original and was carried out by the author except where specifically noted by reference . Assistance recieved in the research work and preparation of this thesis is acknowledged .

.....

Author ; T.N. Brooker .

.....

Supervisor ; Prof' C.K. Kennedy .

LIBRARY STORE

| PLYMOUTH POLYTECHNIC LIBRARY | |
|------------------------------|--------------|
| Accr. No | 70 5500417-X |
| Class No | T-625.85 BRO |
| Contl. No | X700603017 |

STATEMENT OF ADVANCED STUDIES

The author has undertaken the following advanced studies in connection with the program of research .

DIRECTED READING

The published proceedings of the five conferences known as the " Ann Arbor " conferences held in 1962/7/72/7/82 .

COURSES / SEMINARS / CONFERENCES

The author has attended the following meetings -

- (i) The 1983 "Deflectograph" Short Course held at Plymouth Polytechnic .
- (ii) The 1983 meeting of the European Flexible Pavement Study Group held at Plymouth Polytechnic .
- (iii) The 2nd International Conference on the Bearing Capacity of Road and Airfield Pavements , held at Plymouth Polytechnic in 1986 .
- (iv) Appropriate research seminars , lectures and other meetings of 'Professional' Bodies throughout the period of the research .

ACKNOWLEDGEMENTS

The author is indebted to the many staff at Plymouth Polytechnic who gave freely of their time in support of this project .

The author wishes to express his gratitude in particular to Prof' C.K. Kennedy , formerly Head of Department of Civil Engineering , Plymouth Polytechnic , and to Dr G.D. Lees , Head of Department of Transport and Highway Engineering , University of Birmingham , who supervised this thesis and gave generously of their time for discussion and support .

Thanks are also due to Mr M.D. Foulkes for his assistance and to Miss M. Hall for all her understanding .

THE DETERMINATION OF CRACK PROPAGATION RATES OF
REFLECTION CRACKING THROUGH ASPHALT SURFACINGS

T.N. BROOKER

ABSTRACT

A large proportion of the U.K. highway network constructed in the 1960's and 1970's contains lean concrete roadbase with bituminous surfacing. Pavements containing relatively high strength lean concrete have rarely required structural maintenance (thick overlay or reconstruction) but have required maintenance because of reflection cracking where the surfacing cracks above cracks in the lean concrete. The time of appearance of this cracking is very variable (2-20 years).

Field observations indicate that roadbase transverse crack spacings are often greater than 5m. Reflection cracking at these long spacings can be caused by thermal stresses. This project identifies conditions under which thermal reflection cracking will occur and develops a predictive model that allows estimation of the combined effect of thermal and traffic stresses. Finite element analyses indicate that initial crack development is likely to be caused by thermal stresses and final cracking will be assisted by traffic stresses.

A temperature model has been developed to determine roadbase daily temperature range and surfacing temperature on a mean monthly basis. Thermal reflection cracking is considered to result from daily cycle fatigue rather than an extreme low temperature mechanism. A test rig has been developed to apply cyclic crack opening movements and simulative tests have been accelerated to 0.1Hz by using a "bitumen stiffness" fatigue criterion.

Finite element results, displacements recorded during tests and tensile creep tests to determine mix stiffness, enable dc/dN and K_1 values and material constants (A,n) to be determined. This fracture mechanics interpretation of test results serves as the basis of the predictive model for thermal reflection cracking that is consistent with observations from an untrafficked road.

The combined estimate of thermal and traffic stresses cannot however explain reflection cracking at <5m spacings. This cracking apparently initiates at the surface and is probably influenced by other mechanisms.

CONTENTS

| | Page No. |
|---|----------|
| 1.0 INTRODUCTION - STATE OF THE ART | |
| <u>The Problem of Reflection Cracking</u> | |
| 1.1 Road construction in the U.K. | 1 |
| 1.2 The influence of reflection cracks on the failure modes of composite pavements | 3 |
| 1.3 The mechanisms of reflection cracking | 4 |
| <u>Variables That Influence the Growth Rate of Reflection Cracking and the Performance of Composite Pavements</u> | |
| 1.4 Roadbase strength and crack spacing | 6 |
| 1.5 The crack resistance of asphalt surfacings | 8 |
| <u>Research to Date (1984)</u> | |
| 1.6 Summary of reflection cracking in the U.K. | 12 |
| 1.7 Assumptions for simplification of the analysis of thermal stresses | 15 |
| 1.8 Research into thermal reflection cracking | 18 |
| 1.9 The scope of this project | 24 |
| 2.0 PROCESSING OF TEMPERATURE DATA | |
| 2.1 Daily temperature cycles and crack opening movements | 26 |
| 2.2 A temperature model for composite pavements | 28 |
| 2.3 The 6th power effect | 33 |
| 2.4 Warping restraint effects | 35 |
| 2.5 Sub-base friction restraint effects | 43 |
| 2.6 The magnitude of crack-opening movements | 45 |
| 3.0 TEST AND ANALYTICAL METHODOLOGY | |
| 3.1 Introduction to simulative testing | 48 |
| 3.2 Reasons for accelerated testing | 52 |

| | Page No | |
|-----|---|-----|
| 3.3 | Fracture mechanics | 52 |
| 3.4 | Finite element analysis | 58 |
| 3.5 | Consistency of crack-opening movements | 64 |
| 4.0 | BITUMEN STIFFNESS AS A REDUCED PARAMETER IN ACCELERATED TESTING | |
| 4.1 | Introduction to accelerated testing | 68 |
| 4.2 | Observations of the influence of bitumen stiffness in the fracture process | 69 |
| 4.3 | Temperature compensation for the non-sinusoidal daily cycle | 77 |
| 4.4 | Temperature corrections for the variation of mean daily temperature within each month | 85 |
| 4.5 | Cyclic conditions of bitumen stiffness and suitable test temperatures | 87 |
| 5.0 | TEST PROCEDURES | |
| 5.1 | Asphalt mix proportions and the preparation of test samples | 92 |
| 5.2 | Details of the test rig | 98 |
| 5.3 | Measurement of crack growth during testing | 103 |
| 5.4 | Tensile creep tests to determine the effective modulus of materials during testing | 103 |
| 6.0 | TEST RESULTS | |
| 6.1 | Observations | 113 |
| 6.2 | Bitumen stiffness interpretation of test results | 122 |
| 6.3 | Fracture mechanics interpretation of test results | 124 |
| 7.0 | A PREDICTIVE MODEL FOR THERMAL REFLECTION CRACKING DEVELOPED FROM SIMULATIVE TESTING | |
| 7.1 | Introduction | 132 |
| 7.2 | External parameters, roadbase and climate | 133 |
| 7.3 | Design parameters | 139 |
| 7.4 | Material properties and Stress Intensity Factors | 142 |

| | Page No |
|--|---------|
| 7.5 Prediction of thermal reflection cracking | 146 |
| 8.0 SUMMARY AND RECOMMENDATIONS FOR FURTHER WORK | |
| 8.1 Mix Design | 152 |
| 8.2 Combined thermal and traffic stresses | 155 |
| 8.3 Surface crack initiation | 157 |
| 9.0 CONCLUSIONS | |
| 9.1 The incidence of reflection cracking | 160 |
| 9.2 The assessment of temperature and thermal stresses | 161 |
| 9.3 Simulative testing and fracture mechanics | 162 |
| 9.4 The influence of thermal stresses in reflection cracking | 164 |
| REFERENCES | 168 |
| APPENDIX | |
| A Temperature Model for Composite Pavements | A1 |

LIST OF TABLES

Page No.

| | | |
|-------|---|-----|
| 1 . 1 | Predicted and observed crack spacings . | 8 |
| 1 . 2 | Thermal expansion of concrete . | 18 |
| 2 . 1 | Mean monthly temperatures for the air & bituminous, concrete and composite pavements at depths 0 → 300 mm. | 29 |
| 2 . 2 | Mean monthly daily temperature ranges for the air & bituminous , concrete and composite pavements at depths 0 → 300 mm . | 30 |
| 2 . 3 | Comparison of mean and 6th power mean daily temperature ranges . | 34 |
| 2 . 4 | Comparison of upper and lower bound estimates for the daily temperature range that causes crack-opening | 35 |
| 2 . 5 | Temperature differences across the roadbase at the maximum and minimum points of the daily cycle at depth 100 mm in a composite pavement . | 42 |
| 2 . 6 | Estimation of slab end curl and warping restraint factors . | 43 |
| 2 . 7 | Correction factors for crack opening for subbase friction effects . | 45 |
| 2 . 8 | Daily cyclic crack opening movements in the roadbase corrected for 6th power mean , warping restraint & subbase friction restraint effects . | 46 |
| 3 . 1 | Force per metre width to produce 1 mm crack opening in 95 mm surfacing . | 64 |
| 4 . 1 | Evaluation of fatigue crack growth per cycle for actual daily cycles . | 78 |
| 4 . 2 | Evaluation of fatigue crack growth per cycle for equivalent sinusoidal daily cycles at constant temperature. | 79 |
| 4 . 3 | Temperature corrections for the daily variation of mean pavement temperature within each month . | 86 |
| 4 . 4 | Determination of equivalent monthly temperatures for a sinusoidal daily cycle at constant temperature . | 88 |
| 4 . 5 | Conditions of cyclic bitumen stiffness for two types of 50 PEN bitumen & equivalent stiffness test temperatures for testing with either 50 or 200 PEN bitumen . | 91 |
| 5 . 1 | Mix proportions as % wt mix . | 93 |
| 5 . 2 | Nominal stone sizes in the test mixes . | 97 |
| 5 . 3 | Determination of theoretical n values for the test mixes from Schapery's theory . | 112 |
| 6 . 1 | Test results for samples with 50 PEN bitumen at approx' 17°C and 27°C at 0.12Hz . | 114 |
| 6 . 2 | Test results for samples with 50 PEN bitumen at approx' 40°C and 0.12Hz . | 115 |

| | Page No. |
|---|----------|
| 6 . 3 Test results for samples with 200 PEN bitumen at approx' 17°C and 27°C at 0.12Hz . | 116 |
| 6 . 4 Test results for samples with 200 PEN bitumen at approx' 40°C and 0.12Hz . | 117 |
| 7 . 1 Daily cyclic crack opening movements in the roadbase for (5th , 25th , 50th , 75th & 95th) percentile values of the estimated normal distribution of roadbase transverse crack spacings . | 134 |
| 7 . 2 Mean and equivalent mean monthly values for the daily temperature range at the top of the roadbase & the mean temperature in the surfacing . | 135 |
| 7 . 3 The evaluation of equivalent annual fatigue life for 100 mm surfacing , oxidised bitumen & 13.5 m roadbase transverse crack spacing . | 148 |
| 8 . 1 Relative fatigue lives for surfacings with DBM base-courses and various HRA type wearing courses . | 153 |

LIST OF FIGURES

Page No.

| | | |
|-------|---|---------|
| 1 . 1 | Typical designs from the 1970 U.K. thickness design procedure . | 2 |
| 1 . 2 | Limiting critical lives for composite pavements that are relevant when reflection cracks have been present at the surface and trafficked for at least 5 MSA . | 5 |
| 1 . 3 | Frequency distributions of the spacing of roadbase transverse cracks from observations of reflection cracking at the surface at 3 sites in Devon . | 9 |
| 1 . 4 | Recent U.K. design thicknesses for composite pavements with a lean concrete roadbase . | 11 |
| 1 . 5 | Surface cracking and surface rutting based design thicknesses for bituminous surfacing over a lean concrete roadbase . | 13 |
| 1 . 6 | Longitudinal sections of a composite pavement to illustrate the thermal contraction of a lean concrete roadbase and the induced stresses in the above-crack region of the surfacing . | 16 |
| 1 . 7 | Fatigue lines derived from simulative thermal reflection cracking tests at 25°C and 0.1Hz on mixes containing AC-10 Asphalt (100 PEN) . | 22 |
| 1 . 8 | Fatigue lines derived from the results of simulative traffic induced reflection cracking tests at 25°C . | 23 |
| 1 . 9 | Flowchart of predictive model for thermal reflection cracking of asphalt surfacings , based on the results of simulative testing . | 25 |
| 2 . 1 | Pavement hourly temperature / depth profiles . | 27 |
| 2 . 2 | Bi-hourly temperature / depth profiles for bituminous, concrete and composite pavements , January , April , July and October . | 31 & 32 |
| 2 . 3 | A simplified analysis of self-weight restraint of thermal warping . | 36 |
| 2 . 4 | The limiting temperature difference for self-weight restraint of upward warping in the idealised situation where a 200 mm thick slab is supported by a rigid foundation . | 39 |
| 2 . 5 | The effect of embedment at the slab centre and distribution of the support reaction forces , in reducing the potential self-weight induced deflection at the slab ends | 40 |
| 2 . 6 | The variation of thermal and potential self-weight induced deflections along the slab , as a % of the slab end deflection . | 41 |
| 3 . 1 | A longitudinal section of a composite pavement and the basic design for the simulative test rig for asphalt surfacing samples . | 50 |
| 3 . 2 | Fatigue lines for controlled strain fatigue testing of a sandsheet mix at 25Hz and various temperatures . | 53 |

| | Page No. | |
|-------|--|-----|
| 3 . 3 | The ratio between experimentally determined n values and theoretical values predicted by schapery's theory, expressed as a function of the air void content of the mix . | 57 |
| 3 . 4 | Three examples of the PAFEC finite element mesh for half a 450 mm x 95 mm surfacing sample bonded to 12 mm thick steel plates . | 59 |
| 3 . 5 | The variation of peak positive K_1 with crack ratio . | 61 |
| 3 . 6 | Two samples of different thicknesses with identical stress distributions at the same crack ratio (c/h). | 63 |
| 3 . 7 | Master curve of equivalent mean K_1 (\bar{K}_1) for the determination of fatigue life . | 65 |
| 3 . 8 | Restraint of cyclic crack opening by the surfacing , as a function of the extent of cracking in the surfacing and the effective modulus of the basecourse . | 67 |
| 4 . 1 | The relationship between the tensile strength of both pure bitumen and bitumen / aggregate mixes and bitumen stiffness . | 70 |
| 4 . 2 | The SHELL Nomograph relating mix stiffness and bitumen stiffness at high stiffness conditions . | 72 |
| 4 . 3 | Creep tests to relate mix stiffness to bitumen stiffness for individual mixes at low stiffness conditions . | 73 |
| 4 . 4 | The three modes of tensile fracture of thin films of bitumen tested at a range of temperatures and loading rates . | 74 |
| 4 . 5 | The relationship between the mode of tensile fracture of thin films of bitumen and the test conditions of bitumen stiffness . | 75 |
| 4 . 6 | The daily cycles of surfacing and roadbase temperature for a 100 mm surfacing composite pavement . | 80 |
| 4 . 7 | Relaxation modulus and constant-rate-of-strain modulus for a rolled asphalt basecourse material . | 82 |
| 4 . 8 | The variation with temperature of the fatigue crack constant A_1 for 1 hour loading at constant K_1 . | 84 |
| 4 . 9 | The Van der Poel Nomograph for the determination of bitumen stiffness . | 89 |
| 5 . 1 | Aggregate grading curves for the test mixes in relation to the specification . | 94 |
| 5 . 2 | Exploded view of wooden mould for compaction of test samples . | 96 |
| 5 . 3 | Side elevation of the test rig with 1800 mm long test sample and section of the "closed circuit air flow " thermal cabinet for testing shorter epoxy resin bonded samples at elevated temperatures . | 99 |
| 5 . 4 | Detail of the test-rig mechanism that produces cyclic crack opening . | 100 |

| | Page No. | |
|--------|--|-----|
| 5 . 5 | Re-usable portal frame displacement gauges to monitor cyclic crack opening and cyclic displacements over a 100 mm gauge length . | 104 |
| 5 . 6 | Curves to determine the crack ratio (c/h) of partially cracked samples from the ratio of the cyclic displacements at the top and base of the samples , 95 mm surfacing . | 105 |
| 5 . 7 | Apparatus attached to the test rig for simultaneous tensile creep testing of up to four , 100x100x40 mm samples . | 107 |
| 5 . 8 | Creep curves derived from testing 100x100x40 mm samples cut from the test mixes after testing . | 108 |
| 5 . 9 | Comparison of the tensile creep curves for the test mixes with the SHELL Stiffness relationship at high bitumen stiffness . | 109 |
| 5 . 10 | LOG-LOG plots of creep compliance vs time for the wearing course mix with coated chippings containing 50 PEN bitumen . | 111 |
| 6 . 1 | Fatigue lines for 95 mm two course surfacing , derived from the test results . | 118 |
| 6 . 2 | Median lines for the crack growth vs % fatigue life expired relationship for those tests where 100% cracking occurred . | 120 |
| 6 . 3 | Correction curves for the crack ratio (c/h) determined by the gauge displacements , to account for the influence of a plastic zone at the crack tip . | 121 |
| 6 . 4 | Thermal reflection cracking fatigue life expressed as a function of bitumen stiffness . | 123 |
| 6 . 5 | Fracture mechanics interpretation of the test results, basecourse mix . | 126 |
| 6 . 6 | Fracture mechanics interpretation of the test results, wearing course mix . | 127 |
| 6 . 7 | Schapery's theory interpretation of the test results , basecourse mix . | 128 |
| 6 . 8 | Schapery's theory interpretation of the test results , wearing course mix . | 129 |
| 6 . 9 | The results of simulative tests to determine fatigue constants A,n for the test mixes . | 130 |
| 7 . 1 | Frequency distributions of observed reflection crack spacings and probable roadbase crack spacings at 6 sites in Devon . | 137 |
| 7 . 2 | Cyclic bitumen stiffness for 50 PEN bitumen at 3 levels of oxidation . | 143 |
| 7 . 3 | The results of tensile creep tests to determine mix stiffness as a function of bitumen stiffness . | 144 |

| | Page No. |
|--|----------|
| 7 . 4 Master curve of equivalent mean K_1 (\bar{K}_1) for the determination of fatigue life . | 147 |
| 7 . 5 The variation of thermal reflection cracking fatigue life with oxidation of the bitumen and surfacing thickness , for 5 roadbase crack spacings . | 149 |

LIST OF PLATES

| | |
|--|-----|
| 1 . 1 Thermal reflection cracks on untrafficked section of road at Camborne in Cornwall . | 14 |
| 5 . 1 Approx' side view of test rig with detachable temperature control cabinet in foreground . | 101 |
| 5 . 2 Approx' end view of test rig to illustrate portal frame gauges and lever arm mechanism . | 102 |

1.0 INTRODUCTION

THE PROBLEM OF REFLECTION CRACKING

1.1 Road Construction in the U.K.

There is a single national design procedure for highway pavement construction in the U.K. It has been periodically reviewed (1960/65/70/78/84)^{1,2,3}, on the basis of the performance of full-scale experimental roads at sites throughout the U.K.

A range of possible materials for pavements are specified⁴ with additional quality control for bituminous materials covered by British Standards (BS 594/4987)^{5,6}.

There are 5 basic types of roadbase material, FIG 1.1, For each roadbase material the design thickness of the various pavement layers is determined by the subgrade CBR and the predicted future traffic to be carried by the road. The normal design period is 20 years (40 years for concrete roads).

The future traffic is expressed in millions of Standard Axles (MSA), where an approximate 4th power law is used to assess the damaging effect of real traffic axle loadings as an equivalent number of Standard Axles (8175 kg). Recent¹ design thicknesses for 5 MSA and 50 MSA are illustrated, FIG 1.1.

When new roads are constructed, the choice of roadbase type depends upon local economic considerations and is thus effectively left to the contractor. Concrete roads are rarely used nowadays, probably because the 40 year design life¹ is difficult to justify and also because it can be a problem producing an acceptable running surface.

The exception to this is in urban areas, where the lower thickness and thus reduced excavation requirement is useful, as the most important consideration is often to avoid disturbing mains services.

FIG 1 . 1

TYPICAL DESIGNS FROM THE 1970 U.K. THICKNESS DESIGN PROCEDURE¹.

THERE ARE 5 PERMITTED TYPES OF ROADBASE MATERIAL FOR USE IN THE U.K.

FLEXIBLE PAVEMENTS

CONCRETE PAVEMENTS

"FULLY FLEXIBLE"
CONSTRUCTION

"COMPOSITE"
PAVEMENTS

HOT ROLLED
ASPHALT
OR DENSE
BITUMINOUS
ROADBASE

WET-MIX OR
DRY-BOUND
COMPACTED
GRANULAR
ROADBASE

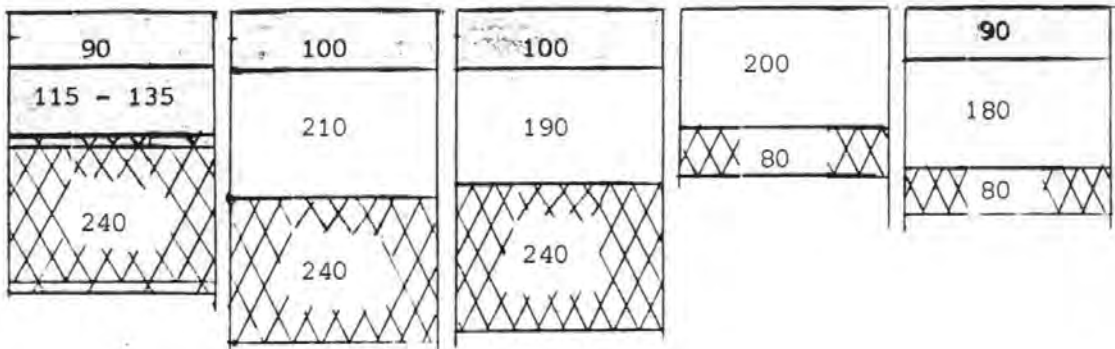
LEAN
CONCRETE OR
CEMENT-BOUND
GRANULAR
ROADBASE

PLAIN OR
REINFORCED
CONCRETE
SLAB
PAVEMENT

CONTINUOUSLY
REINFORCED
CONCRETE WITH
A BITUMINOUS
SURFACING

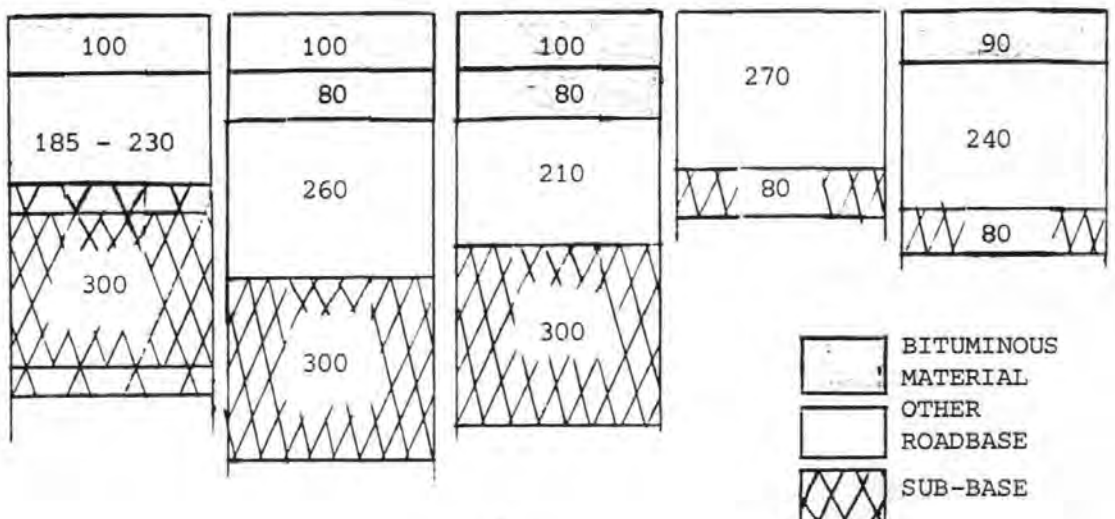
THICKNESSES FOR CUMULATIVE TRAFFIC 5 MSA (CBR 5%)

mm



THICKNESSES FOR CUMULATIVE TRAFFIC 50 MSA (CBR 5%)

mm



BITUMINOUS MATERIAL
OTHER ROADBASE
SUB-BASE

The expected terminal condition¹ for these designs (after they had carried the appropriate traffic) was to be in need of partial reconstruction or a major overlay.

The 1978 review² was concerned with a reassessment of the commercial traffic to standard axles conversion factors and with the use of cheaper "capping layer" material for the lower part of sub-bases that exceed 150mm.

The 1984 review⁷ increases layer thicknesses for most designs by 10-20% but the terminal condition is now defined as an 85% chance of survival. Also proposed layer thicknesses for HRA and DBM roadbases are now equal and the use of granular roadbases is now limited to > 20 MSA Designs.

1.2 The Influence of Reflection Cracks on the Failure Modes of Composite Pavements.

This research is primarily concerned with lean-concrete-roadbase flexible pavements, which are the only widely used type of composite pavement in the U.K. The deterioration of composite pavements is unlike that of the other types of flexible pavement, as it can be influenced by transverse cracks in the roadbase.

Transverse cracking of the roadbase is unavoidable and results from thermal and shrinkage effects whilst the material is curing and the tensile strength is not yet fully developed. The transverse cracks are in effect "natural" contraction joints and can be considered to be present throughout the service life of the pavement. Wheelpath rutting of composite pavements is usually only serious if longitudinal roadbase cracking has occurred. This is most likely to occur at slab centres where restrained thermal warping stress is greatest, or at the transverse cracks where there is lack of load transfer/shock loading effects.

Sympathetic "REFLECTION" cracking of the bituminous surfacing above transverse roadbase cracks, can occur by several mechanisms. The reflection cracking process cannot, at present, be quantified but

it is known that the appearance of reflection cracks at the surface tends to limit future life of the pavement to a further 5 MSA, FIG 1.2⁸.

In principle, if the reflection cracks can be effectively sealed, then they will not have any adverse effects on the pavement. Unfortunately, the technique used in the U.K. for sealing cracks (Overbanding) cannot absorb large movements and the seal is often broken within one or two years. Water seepage and possibly frost damage at unsealed reflection cracks will reduce both load transfer in the roadbase and sub-base support. This will aggravate the development of longitudinal cracking and wheelpath rutting. Also, spalling of the surfacing from the crack faces may result in localised early failures of the pavement.

The original concept of these lean concrete roads was that the roadbase strength should be sufficiently high to resist longitudinal cracking and yet low enough to avoid forming long slabs (5m⁺) where movements may be too large for the surfacing to resist reflection cracking. The current standards⁴ attempt this by specifying an aggregate-cement ratio between (15:1+20:1) by weight, and limiting the 20 Day crushing strength of cubes compacted to refusal, to the range of 10+20 MN/m².

1.3 The Mechanisms of Reflection Cracking

The various possible mechanisms by which reflection cracking can propagate, have been comprehensively summarised, both in the U.K. in 1962⁹ and more recently in the U.S.A. in 1980¹⁰, and so will be only briefly summarised here.

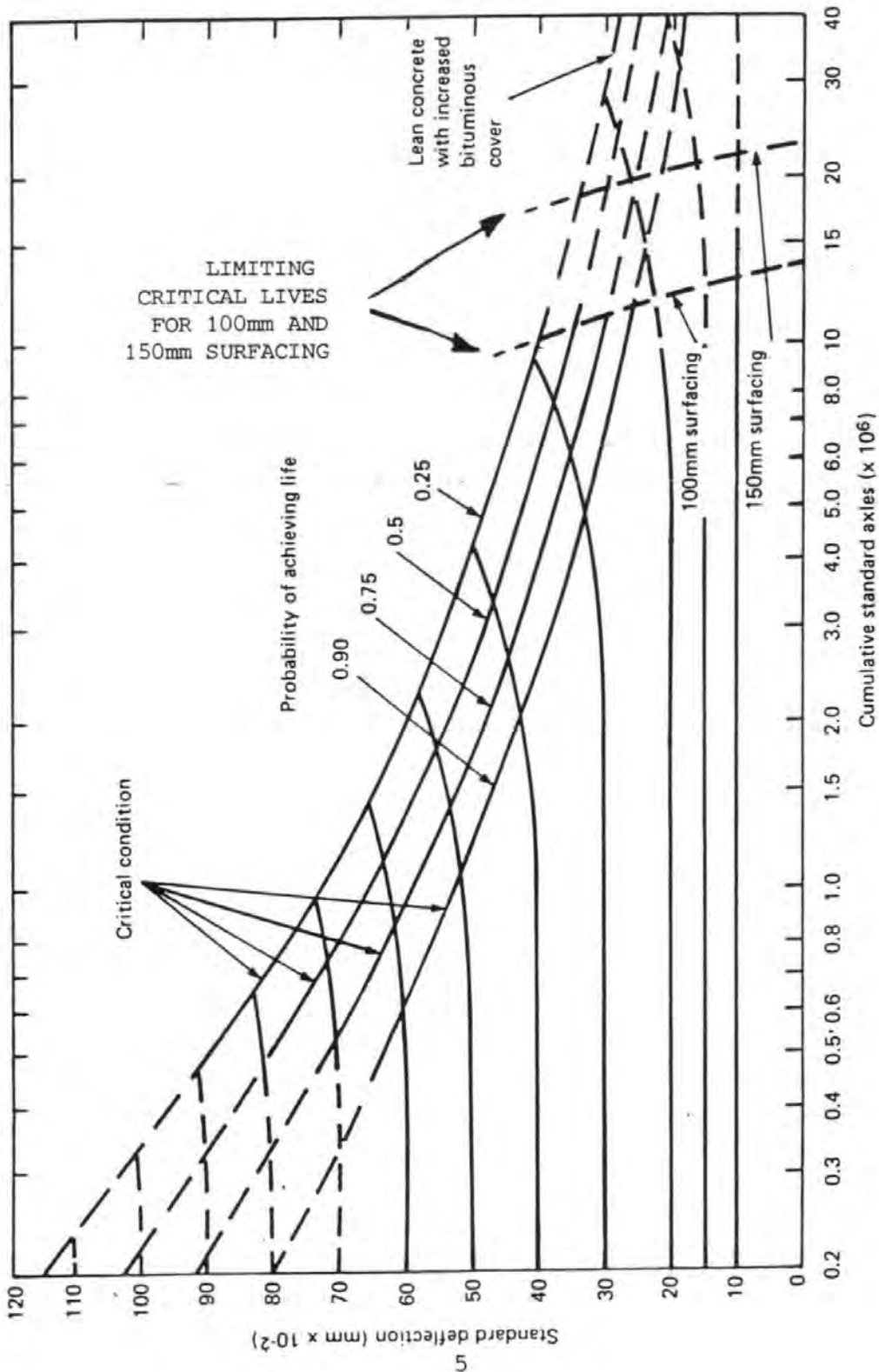
It was considered⁹ that reflection cracking could be caused by any of 5 mechanisms -

- Thermal contraction - horizontal crack opening
- Traffic loading - vertical shear crack opening
- Thermal warping
- Settlement of roadbase slabs
- Curing Shrinkage in the roadbase

FIG 1 . 2

LIMITING "CRITICAL" LIVES FOR COMPOSITE PAVEMENTS , THAT ARE RELEVANT WHEN REFLECTION CRACKS HAVE BEEN PRESENT AT THE SURFACE AND TRAFFICKED FOR AT LEAST 5 MSA .

(THE LR833⁸ RELATION BETWEEN STANDARD DEFLECTION AND LIFE FOR PAVEMENTS WITH CEMENT BOUND ROADBASES)



- but that thermal and traffic effects were responsible for most reflection cracking.

It was noted that the magnitude of horizontal movements was consistent with unrestrained thermal expansion and that cracking can occur on roads with little or no traffic, indicating that thermal stresses alone can cause reflection cracking in some situations. Also the severity of cracking on the A4 at Slough was related to traffic induced movements between concrete slabs, where these were greater than 0.015 in (0.38mm) the surfacing deteriorated rapidly at the joints.

In lean-concrete roads there are also interactions between thermal and traffic effects, i.e. thermal contraction will reduce granular interlock between roadbase slabs and this will increase traffic induced movements. It is also uncertain whether thermal warping of slabs is restrained by self-weight in all cases. Under upward warping, slabs will "rock" more easily, and aggravate traffic induced reflection cracking. Upward warping, if unrestrained, will increase the thermal contraction at the upper surface of the roadbase and thus the crack opening movements applied to the surfacing.

Settlement was considered to be uncommon on main roads in the U.K., but its effects can be observed on the A30 west of Exeter where differential settlement of adjacent slabs of lean concrete has produced longitudinal reflection cracks on embankments and oblique reflection cracks near cut-fill transitions.

Curing Shrinkage will have negligible effect providing that the surfacing is not laid before the concrete is one week old.

VARIABLES THAT INFLUENCE THE GROWTH RATE OF REFLECTION CRACKING AND THE PERFORMANCE OF COMPOSITE PAVEMENTS

1.4 Roadbase Strength - Crack Spacing

Considerable research effort has been expended in the U.K.¹¹ on full-scale experimental roads with cement-bound roadbases. The materials

used had a wide range of strengths and performance was continuously monitored until failure. The Wheatley by-pass (A40) experiment, constructed in 1963, contained 25 sections with cement-bound road bases of 3 different strength (3.8, 7.6 & 15.2 MN/m²), 4 aggregate types and 4 aggregate gradings.

By 1976, after carrying traffic estimated at 8 MSA, 4 of the 25 sections had permanent deformation of 10-16mm, but none had failed and no significant reflection cracking was observed through the 100mm asphalt surfacing used on this and almost all the other full-scale experiments.

It was concluded that although the low strength materials had performed well, there were difficulties in mixing properly with such low cement contents (less than 20:1), and this could, in practice, result in weak patches and early failures.

The probable explanation for the lack of significant reflection cracking at the Wheatley by-pass after 13 years, is that with these low roadbase strengths, the transverse crack spacings are probably less than 5m and inter-slab movements have been too small to propagate the reflection cracks within this time.

The transverse crack spacing in the roadbase is thought to be a significant factor in reflection cracking because long slabs will have greater thermal crack-opening movements, and also crack opening reduces load transfer between slabs, increasing the traffic induced vertical movements. Alternatively, short slabs will be more prone to rocking under traffic and this will also increase traffic induced movements, except where the sub-base support is very sound.

Thus there may be an optimum slab length for resistance to traffic induced reflection cracking, but thermal reflection cracking will get progressively worse with longer slabs.

Research by TAYLOR and WILLIAMS¹² has shown that the roadbase cracking is most likely to occur at the 1st or 2nd dawn, approximately 16+24

or 40+48 hours, after laying. The crack spacing will depend on the early life tensile strength of the lean concrete and the temperature fall during the night. Laboratory tests performed on a typical high strength lean concrete (18-20 MN/m² @ 28 DAYS) predicted crack spacings that are consistent with recent (1984/5) crack surveys of major roads in Devon and Cornwall, TABLE 1.1 .

TABLE 1.1. PREDICTED AND OBSERVED CRACK SPACINGS

| COMBINATIONS OF TEMPERATURE FALL AND CRACK SPACING FOR CRACKS FORMED AT 20 HOURS (1st NIGHT AFTER LAYING) | 2°C | 12 - 24 m |
|--|-----|-----------|
| | 3°C | 11 - 20 m |
| | 4°C | 9 - 17 m |
| | 5°C | 8 - 15 m |

| ROAD AND LOCATION | MOST FREQUENT OBSERVED CRACK SPACING (m) | AGE OF ROAD YEARS | SURFACING THICKNESS (mm) |
|----------------------|---|-------------------------|--------------------------------|
| A30 FINGLE GLEN | 17 | 8 | 100 |
| A30 LAUNCESTON | 10 | 8 | 100 |
| A30 IDE | 17 | 10 | 100 |
| M5 WILLAND | 7 and 10 | 10 | 145 |
| A38 PLYMPTON | 18 | 15 | 175 |
| A30 HONITON | 16 and 19 | 20 | 100 |

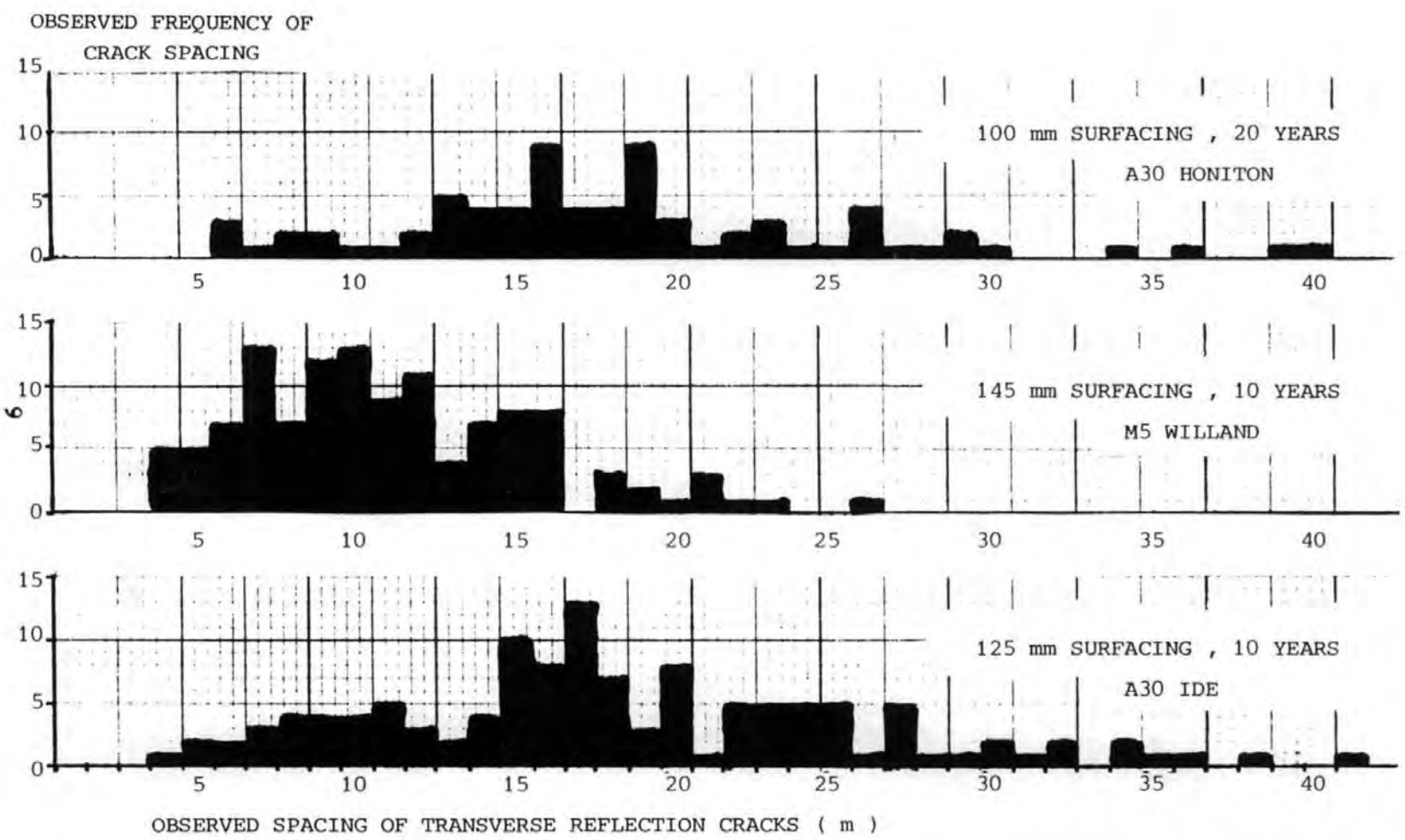
The actual frequency distributions of observed crack spacing for the most heavily cracked sites are illustrated, FIG 1.3. These crack spacings are much greater than the oft-quoted values of 3.5+5m^{3,11,13}, but apparent 16+19m spacings may contain roadbase cracks that have not reflected. It is also significant that all these roads were built before 1976, when the upper strength limit of 20 MN/m² at 28 Days was introduced, and so may contain lean concrete of higher strengths, which could indeed form actual crack spacings of 16+19m.

1.5 The Crack Resistance of Asphalt Surfacing

The mix design and thickness of asphalt surfacings have not been included as major variables in the U.K. full-scale experimental roads, where 100mm of two-course rolled asphalt has been used almost exclusively over cement-bound roadbases.

FREQUENCY DISTRIBUTIONS OF THE SPACING OF ROADBASE TRANSVERSE CRACKS
 FROM OBSERVATIONS OF REFLECTION CRACKING AT THE SURFACE AT 3 SITES
 IN DEVON .

FIG 1 . 3



A range of thicknesses of surfacing have been used for major road construction since 1970 and these mixes have recently been reviewed³, FIG. 1.4. However, the range of mix design permitted for the asphalt surfacing for major roads (>2.5 MSA) is restricted to rolled asphalt⁵ for the wearing course and a choice of DBM⁶ or rolled asphalt for the base course.

Thus the influence of the asphalt surfacing in controlling reflection cracking and other deterioration of composite pavements is still not well understood, although it has been observed¹¹ that whereas reflection cracks came through a 100mm surfacing with a 55% stone content wearing course in 5 years, a 30-40% stone content wearing course was intact for more than 10 years.

The increased life of the 30-40% stone wearing course is probably due to the higher bitumen content (7+8% wt mix) compared to (6% wt mix) for the 55% stone wearing course.

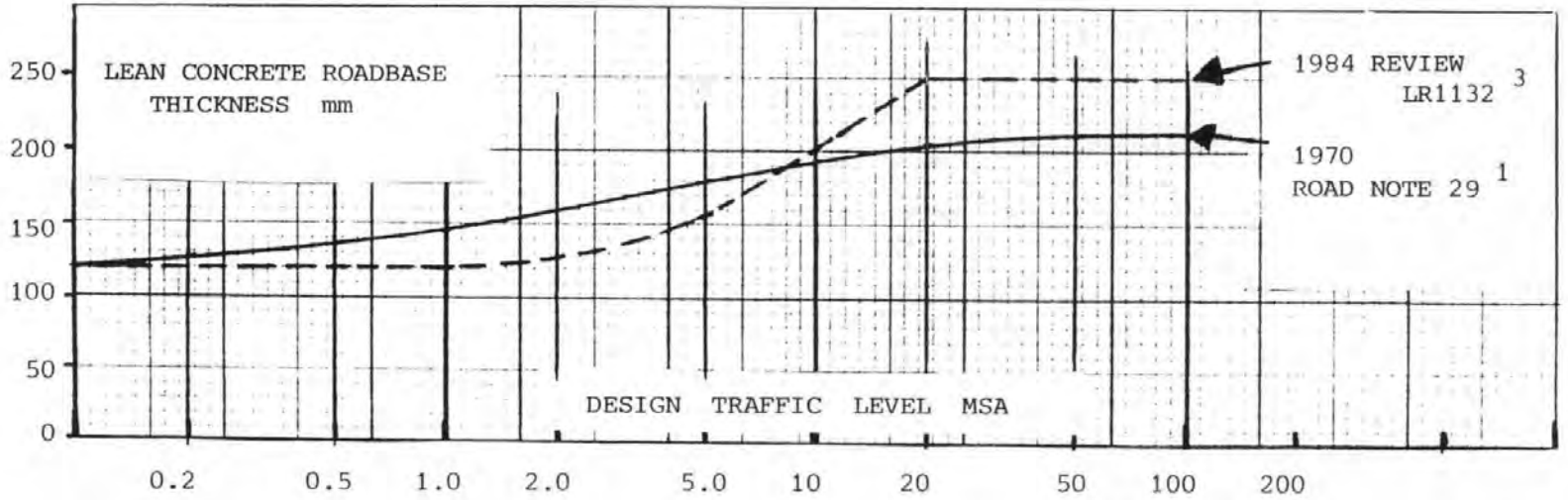
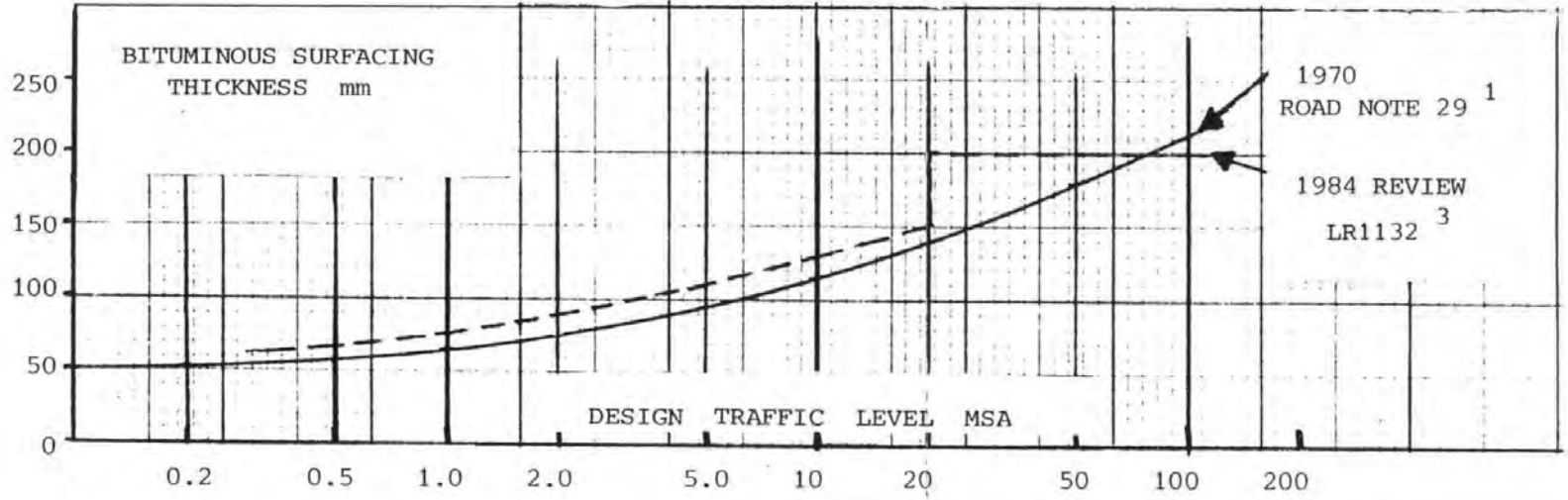
In practice the asphalt surfacing may be embrittled by hardening of the bitumen, poor compaction, or water induced "stripping" of the asphalt-aggregate bond. Localised defects such as these may well be responsible for the variable intensity of reflection cracking at different locations on the same section or road. Several experiments were reported in the period prior to 1962⁹, concerning special treatments to reduce reflection cracking of asphalt surfacings, e.g. -

- i. Rubberised bitumen in the surfacing
- ii. Bond-breaking strips (felt, paper or sand)
- iii. Small or large mesh steel reinforcement in the surfacing
- iv. Granular layers or crushed rock or gravel between the roadbase and surfacing.

These experiments were unsuccessful in that any possible savings by reduction of surfacing thickness from the 100mm commonly used at that time, were more than offset by the additional construction costs. Consequently, the use of these special treatments in the U.K. since 1962, has not been widespread.

RECENT U.K. DESIGN THICKNESSES FOR COMPOSITE PAVEMENTS WITH A LEAN CONCRETE ROADBASE .

FIG 1 . 4



RESEARCH TO DATE (1984)

1.6 Summary of Reflection Cracking (U.K.)

The co-existence of so many variables in the reflection cracking process has made it difficult to ascertain the significance of the various factors at any particular site. Past research into composite pavements in the U.K. has concentrated on the mix design of the cement-bound roadbase.

It is now realised that lean concrete of high flexural strength ($1.2-2.4 \text{ MN/m}^2$ at 28 Days) is necessary to prevent longitudinal cracking of the roadbase and ensure long life. This is the basis of the 1984, FIG 1.4, design recommendations of 250mm Roadbase and 200mm Asphalt Surfacing for any traffic level greater than 20 MSA. 20 MSA is the present upper limit of the design method developed from the results of the full-scale experiments.

The mix design of the B.S. standard asphalt surfacings has been evolving for over 50 years, but the same mixes have been used over bituminous, granular and cement bound roadbases where the stiffness and fracture toughness requirements are obviously different. Thus there must be some scope for developing improved fracture toughness mixes. The optimum mix design is achieved when the thickness criteria for failure by cracking and failure by rutting coincide, FIG 1.5. At present there is considerable difference between the two, indicating that current mixes are too brittle for use over lean concrete.

Traffic and Thermal effects are probably both significant in reflection cracking. The current design procedure,^{1,3} is based on traffic levels alone and so there is a need to investigate where thermal stresses are significant, especially with the higher strength lean concrete roadbases, which form long slabs and may have large daily thermal movements.

Thermal effects are probably most significant in areas like Devon and Cornwall where commercial traffic is light. Reflection cracks were observed after 5 years on an untrafficked extension for the Camborne by-pass, PLATE 1.1.

FIGURE 1.5
 SURFACE CRACKING AND SURFACE RUTTING BASED DESIGN THICKNESSES FOR
 BITUMINOUS SURFACING OVER A LEAN CONCRETE ROADBASE, LR1132 3

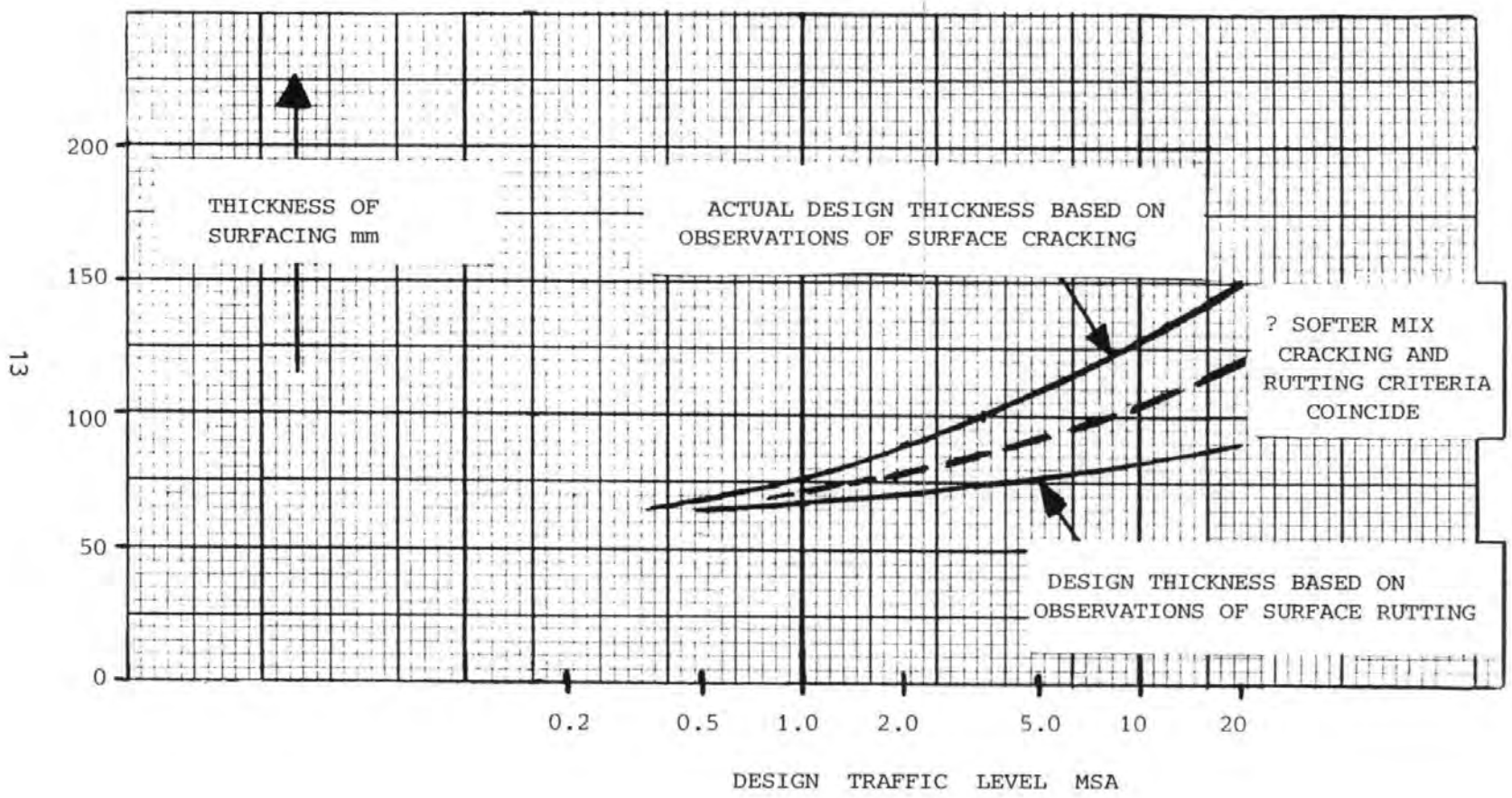


PLATE 1 . 1

" THERMAL " REFLECTION CRACKS ON UNTRAFFICKED SECTION OF ROAD AT
CAMBORNE IN CORNWALL



1.7 Assumptions for Simplification of the Analysis of Thermal Stresses

The thermal stresses can be best illustrated by first considering the thermal contraction of lean concrete slabs, and then considering the effect of adding a bituminous surfacing. FIG 1.6.

Seven assumptions can be made to simplify the analysis. The first four are summarised here and form the limits to the applicability of the analysis.

Assumptions (v) and (vi) can be clarified once the magnitude of thermal movements and the temperature gradients at roadbase depth, have been established, [SECTION 2.4 and 2.5]. Assumption (vii) can be clarified after analysis of the crack opening induced stresses [SECTION 3.5].

(i) Crack opening in the roadbase is the result of thermal contraction of two adjacent slabs and the analysis is greatly simplified when the assumption that adjacent slabs are equal in length is made. Although a wide variation of crack spacings (roadbase strength) was observed over the 500-2500m sections surveyed, FIG 1.3, the variability of crack spacing (roadbase strength) between adjacent slabs was much less than implied by FIG 1.3.

(ii) Each roadbase slab will expand and contract about its centre. This involves the least relative movement of surfaces and thus the least restraint to movement.

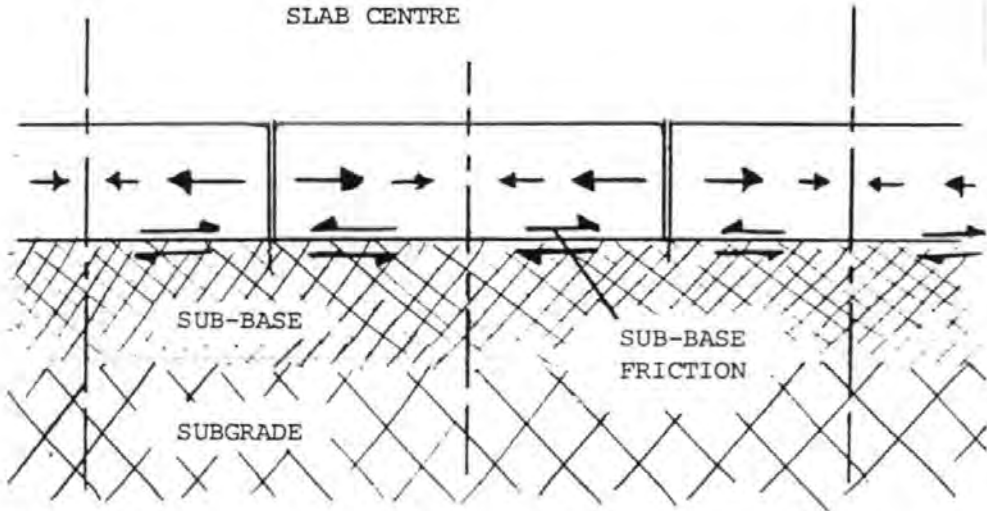
(iii) The roadbase cracks never close completely. This would reduce the size of the cycle of expansion and contraction and produce compressive stresses in the roadbase. This assumption is valid for roadbases laid in the summer or for roadbases that undergo some shrinkage, either during curing or long-term.

(iv) The bond between the surfacing and the roadbase remains intact right up to the cracks. If the bituminous emulsion usually used, is applied to the specified thickness, then it will tend to

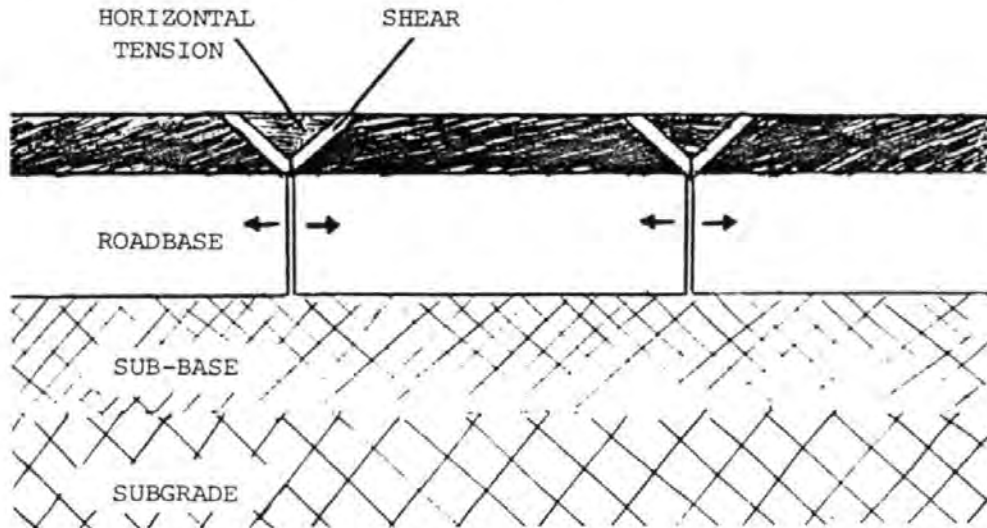
FIG 1 . 6

LONGTITUDINAL SECTIONS OF A COMPOSITE PAVEMENT TO ILLUSTRATE THE THERMAL CONTRACTION OF LEAN CONCRETE ROADBASE AND THE " INDUCED " STRESSES IN THE ABOVE-CRACK REGION OF THE SURFACING .

THERMAL CONTRACTION OF
EACH ROADBASE SLAB
IS TOWARDS THE
SLAB CENTRE



INDUCED STRESSES IN THE SURFACING



yield rather than debond.

(v) Self-weight restraint of thermal warping is not absolute. There will still be warping of a small percentage of slab length at the slab ends. The assumption that self-weight restrains warping is commonly made when calculating maximum possible stresses in the design of concrete slab pavements, because it is a conservative assumption. This is not the case with thermal reflection cracking because restraint to warping decreases crack opening movements and stresses and is thus not a conservative assumption.

(vi) The high modulus of the lean concrete (typically $3 \times 10^{10} \text{ N/m}^2$) means that the effect of sub-base friction in restraining thermal contraction of the roadbase slabs, will be almost negligible (approx 1-5%).

(vii) The stiffness of the surfacing under 24 hr cyclic loading is sufficiently low that it is incapable of restraining the thermal contraction of the lean concrete and so roadbase crack-opening will be independent of the extent of cracking in the surfacing. The surfacing will also have small internally generated tensile stresses during cooling which will tend to assist crack opening.

These assumptions mean that thermal stresses can be adequately characterised by the daily cycles of horizontal opening and closing of the transverse cracks between the roadbase slabs.

This cyclic crack opening is unrestrained by the surfacing and produces cycles of stress and strain in the above crack region of the surfacing, FIG. 1.6, the exact magnitude and distribution of which requires finite element analysis.

The thermal crack-opening between two adjacent roadbase slabs can be defined as:-

$$\text{Crack Opening, CO} = \Delta T \cdot w \cdot L \cdot \alpha \quad (\text{EQN 1})$$

where ΔT = The daily temperature range at the upper surface of the roadbase (adjusted by a factor, w , to compensate for self-weight restraint of warping).

- L = The slab length in the roadbase
 α = The coefficient of thermal expansion of the lean concrete.

A range of quoted values for the coefficient of thermal expansion of concrete made with a range of aggregates is summarised, TABLE 1.2.

TABLE 1.2 THERMAL EXPANSION OF CONCRETE

| TYPE OF AGGREGATE | COEFFICIENT OF THERMAL EXPANSION (PER °C) $\times 10^6$ | |
|---|---|-------------|
| | AIR STORAGE | WET STORAGE |
| DATA FROM BONNELL AND HARPER ¹⁴ | | |
| GRAVEL | 13.1 | 12.2 |
| QUARTZITE | 12.8 | 12.2 |
| FOAMED SLAG | 12.1 | 9.2 |
| SANDSTONE | 11.7 | 10.1 |
| BLAST-FURNACE SLAG | 10.6 | 9.2 |
| GRANITE | 9.5 | 8.6 |
| DOLERITE | 9.5 | 8.5 |
| LIMESTONE | 7.4 | 6.1 |
| PORTLAND STONE | 7.4 | 6.1 |
| DATA FROM TAYLOR AND WILLIAMS ¹² | | |
| GRITSTONE | 15.7 | |
| THAMES VALLEY GRAVEL | 12-13 | |
| LIMESTONE | 6.3 | |

1.8 Research into Thermal Reflection Cracking

Thermal reflection cracking of bituminous overlays over concrete slab pavements has been the subject of recent research in the U.S.A. (the use of composite construction from new is not widespread).

Several researchers have used finite-element programs to analyse the stresses in the above crack regions of an overlay^{15,16,17} and simulative crack opening tests have been carried out on laboratory samples of surfacing mixes^{18,19}.

Some of this research^{17,19} was concerned with the use of asphalt-rubber membranes as a tack coat/interlayer between the concrete and the surfacing.

It was found that an asphalt-rubber membrane reduced stresses in the surfacing under rapid loading (traffic stresses), but gave increased stresses when under slow loading (thermal effects) because the rubber inhibits long term viscous yield in asphalt tack coats.

The most comprehensive research to date has been at TEXAS UNIV. where Chang, Lytton and Carpenter¹⁵ developed a finite element program with a crack-tip element and determined stress intensity factors during crack growth. This enabled subsequent test results¹⁸ to be analysed by the application of fracture mechanics theory.

Thermal reflection cracking is a fatigue type process because failure occurs after many cycles of applied stress-strain. The study of fatigue crack growth is part of the theory of fracture mechanics which has been developed by:-

- GRIFFITH 1928²⁰
- WESTERGAARD 1939²¹
- IRWIN 1957²²
- PARIS et al 1963/5^{23,24}

The fatigue crack growth rate per cycle (dc/dN) and the crack-tip stress intensity factor (K_1), can be related by an equation of the form:-

$$dc/dN = A K_1^n \quad (\text{EQN 2})$$

where A,n are material constants that express the "fracture toughness" of the material. The exponent, n, was observed to be approximately 4 for crack propagation in elastic materials such as metals²³. Early fatigue tests on asphaltic concrete at OHIO STATE UNIV, reported by Majidzadeh and Ramsamooj²⁵, indicated that

a value $n = 4$ was still applicable to visco-elastic materials. This conclusion was later modified to $n = 4-8$ for low load-long life fatigue and $n = 2$ for high load-short life fatigue, with the transition point at about 10^4 Cycles²⁶.

The theory of visco-elastic fracture mechanics developed by Schapery²⁷, indicates that n is related to the slope (m) of a LOG-LOG plot of creep compliance (STRAIN/STRESS) vs time, and predicts that n will be approximately equal to 6 for most visco-elastic materials such as asphaltic concrete.

German and Lytton¹⁸ performed tests on 65 samples representing 10 different surfacing mixes and 3 types of fabric interlayers. Mostly 3" (76mm) samples were tested at 25°C and 0.1hz, and subjected to cyclic crack opening (0.75-1.9mm) by steel test platens.

Crack growth was estimated visually and by ultrasonics in the samples, and values of (dc/dN) and K_1 were obtained from the test data and used to estimate the material constants A , n . A reasonable correlation was found between the experimental results and Schapery's theory, despite the creep compliance of pure bitumen being used to calculate n , instead of asphalt concrete mix as in Schapery's original theory²⁷.

The value of the exponent, n , in the crack growth equation (EQN 2) is also indicated by the slope of a LOG-LOG plot of cyclic stress or strain vs fatigue life for a test series of identical samples. If the bulk of the material is linear-visco-elastic then both stress and strain in the samples are directly proportional to K_1 . The fatigue life is inversely proportional to the crack growth rate (dc/dN) , and so the slope of a LOG-LOG plot either stress or strain vs fatigue life will be $(-1/n)$.

The bulk of published fatigue data for asphaltic surfacing mixes produced LOG-LOG slopes of $(-1/4$ to $-1/6)$ indicating that n is in the range 4-6 for testing at frequencies of about 50hz and temperatures of about 10°C^{28,29,30}.

German and Lytton's data¹⁸ is illustrated, FIG 1.7, and this can be interpreted with the aid of a relationship between the thickness of surfacing and the fatigue life determined by Marchand and Goacolon³¹. In fact, the increase in life for greater thicknesses of surfacing will be more than indicated by FIG 1.7, because of the greater insulation provided by thicker surfacings which reduces daily thermal crack opening movements.

German and Lytton's data shows that for typical American mixes, daily crack - opening movements of (1+1.3mm) are necessary to produce thermal reflection cracking after 6+18 years (2,200 - 6,600 Cycles) in 100mm surfacings. The richer surfacing mixes used in the U.K. mean that daily crack opening movements may not be sufficient to produce reflection cracking by thermal stresses alone.

Recent finite element analyses of cracked composite pavements subjected to traffic loading, Molenaar³² indicate that the crack-tip stress intensity factors (K_1 , K_2) are greater when the load is offset rather than directly above the crack, which diminishes the value of the simulative traffic induced reflection cracking tests in the U.S.A.^{17,33} that used repeated loading directly above the crack.

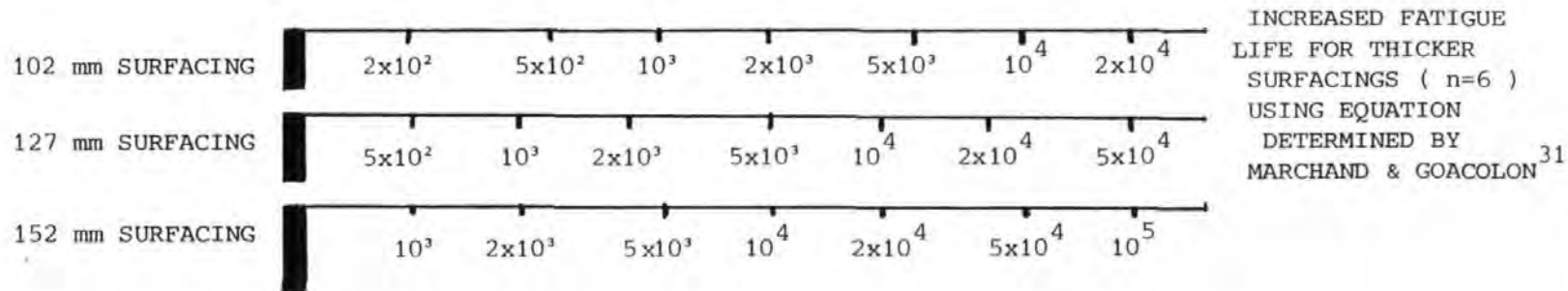
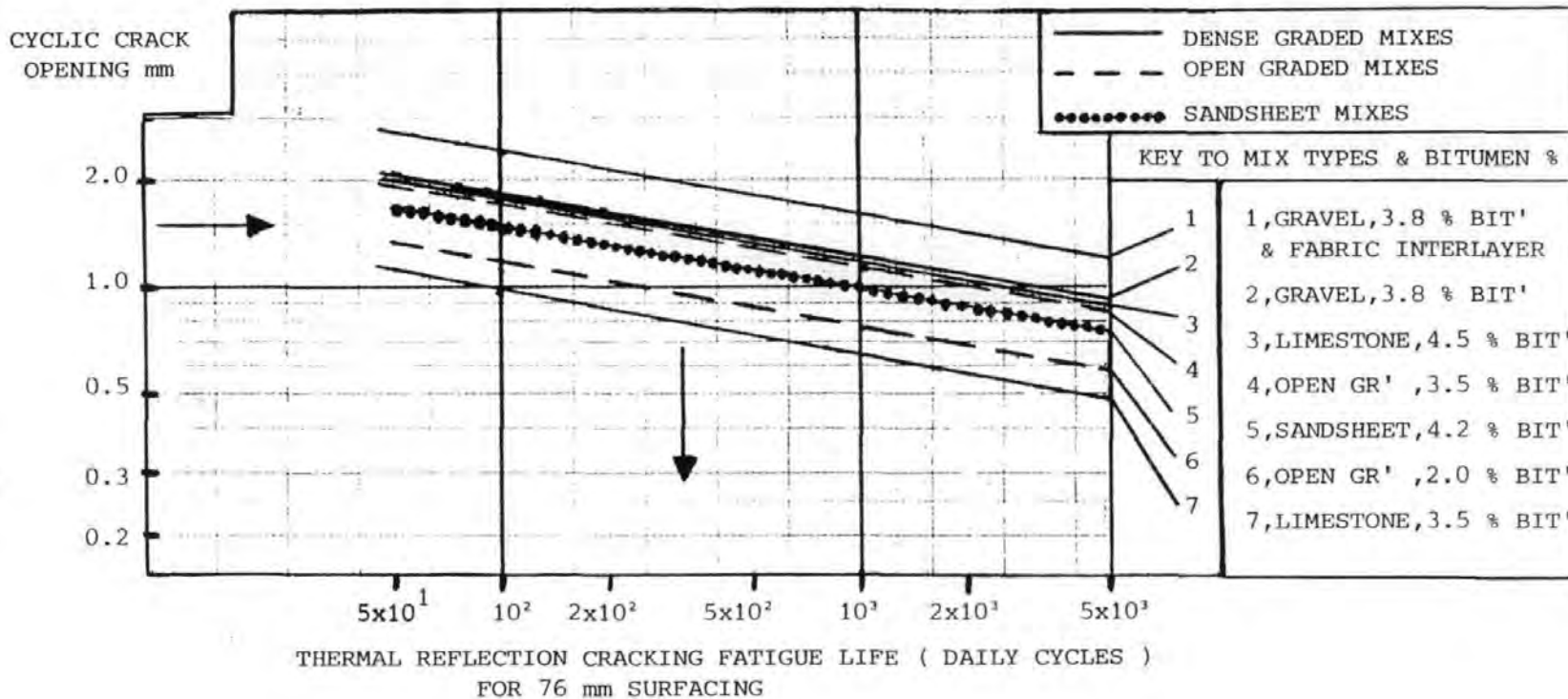
Traffic induced reflection cracking tests that used applied vertical displacements to one side of the samples, have been performed by Jimenez et al¹⁹ at ARIZONA UNIV.

An unspecified asphaltic concrete mix was used and pure asphalt and asphalt-rubber tack coats were compared but no significant difference could be observed at 25°C.

The test data are illustrated, FIG 1.8, and indicate that the differential vertical movements at cracks must be less than 0.2mm for a 100mm surfacing to last for millions of load applications.

Molenaar's analyses³² also show that the stress intensity factors (K_1 , K_2) increase with crack length for traffic loading. This is the opposite to what happens with thermal loading, where analyses¹⁵ show that K_1 decreases with crack length.

Thus thermal effects are probably more important in the early stages of crack growth and traffic effects should be more important in the final stages of crack growth, especially because of the 4+6th power relationship between the crack growth rate and K_1 .

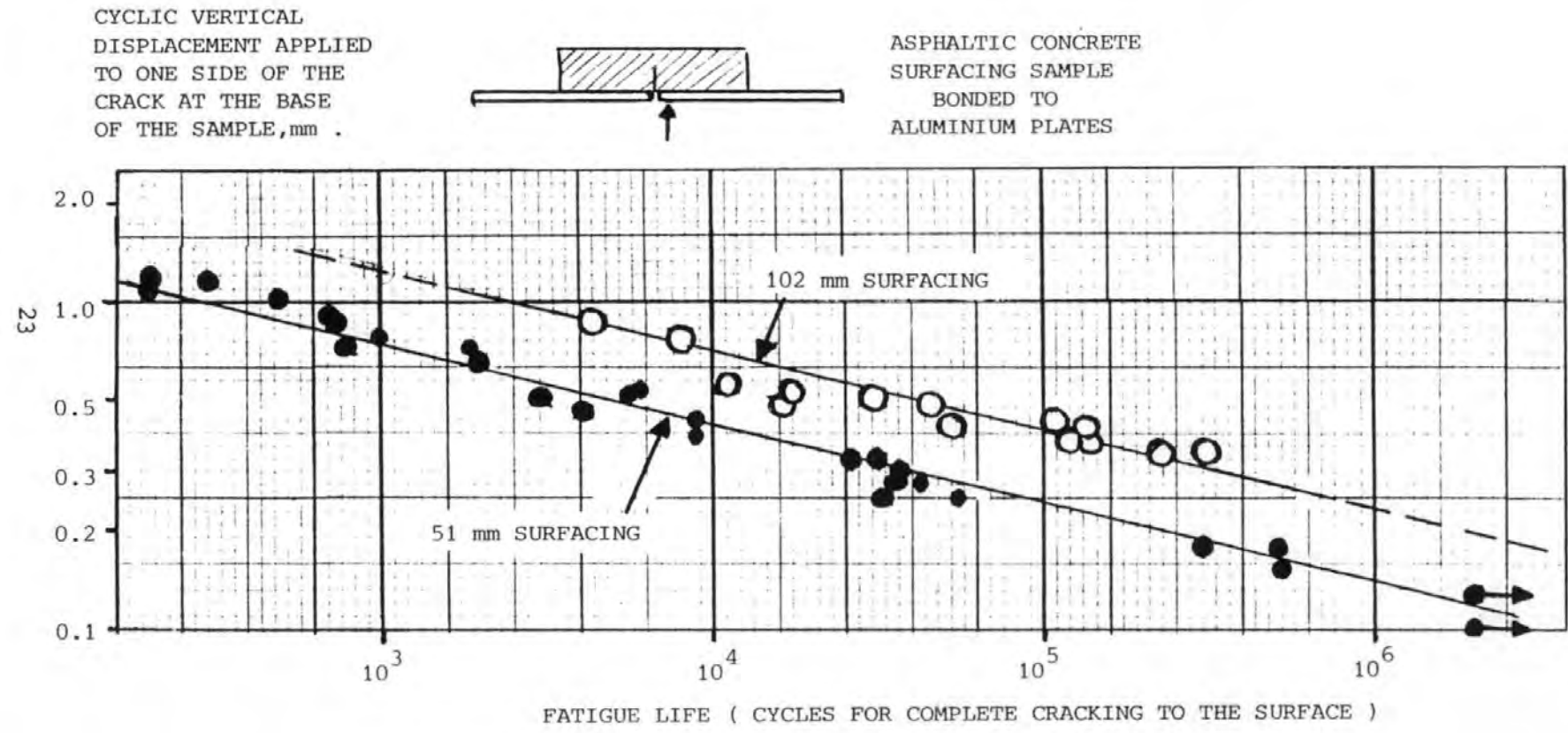


" FATIGUE LINES " DERIVED FROM SIMULATIVE THERMAL REFLECTION CRACKING TESTS AT 25°C AND 0.1 HZ ON MIXES CONTAINING AC-10 ASPHALT (100 PEN), GERMAN & LYTTON¹⁸, 1979 .

FIG 1 . 7

" FATIGUE LINES " DERIVED FROM THE RESULTS OF SIMULATIVE TRAFFIC INDUCED REFLECTION CRACKING TESTS AT 25 °C , JIMENEZ et al 19 , 1979.

FIG 1 . 8



23

1.9 The Scope of this Project.

The overall aim of reflection cracking research is to be able to design composite pavements that can adequately resist reflection cracking for 20 years or longer.

Alternately, if it is decided that reflection cracking can be tolerated, then research will help the planning of surveys to identify and seal the cracks.

The scope of this project is firstly to adapt existing T.R.R.L. temperature data to evaluate the magnitude of thermal crack-opening movements that asphalt surfacings are subjected to by the U.K. climate. To determine the resistance to cracking of U.K. surfacing mixes, it is necessary to develop a test rig that performs simulative crack opening tests. Test results will indicate the conditions where the U.K. climate can cause or influence reflection cracking. Simulative testing can be accelerated from a 24 hr cycle to 0.1hz by the use of either a raised temperature or a softer grade of bitumen.

There is evidence to suggest that the influences of test temperature and frequency on fatigue life can be combined by the use of a viscosity based parameter such as bitumen stiffness, as defined by the Van der Poel Nomograph³⁴.

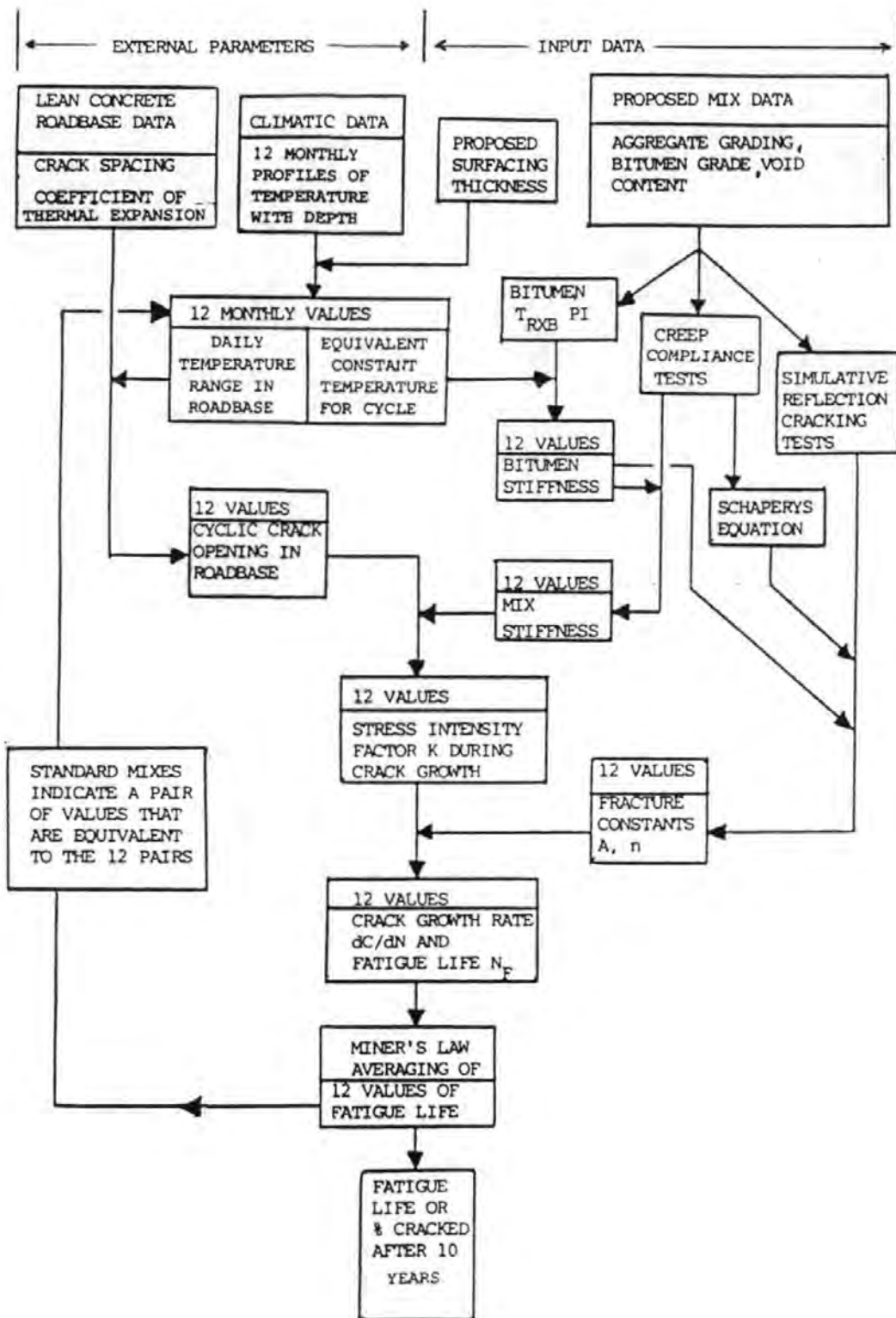
Creep compliance tests and finite element analyses of cracked two-course surfacings, are also necessary for interpretation of the test results and for the development of a predictive model for thermal reflection cracking that can be summarised by the flowchart, FIG 1.9

It is apparent that softer grades of bitumen will increase the reflection cracking fatigue life because it is a controlled-strain type process. Creep compliance tests have the potential for estimation of the decreased rutting resistance of these softer mixes in order to confirm their practicality. Thus creep tests should be included in a test program of this sort.

Reflection cracking is an extreme case of the importance of the fracture toughness properties of asphalt surfacings. A study of these properties is, however, important for considering fatigue of the fully flexible types of pavement, especially where stiffer mixes are required to avoid failure by deformation.

FIG 1 . 9

FLOWCHART OF PREDICTIVE MODEL FOR THERMAL REFLECTION CRACKING OF ASPHALT SURFACINGS , BASED ON THE RESULTS OF SIMULATIVE TESTING .



2.0 PROCESSING OF TEMPERATURE DATA

2.1 Daily Temperature Cycles/Crack Opening Movements

This chapter presents a summary, SECTION 2.2, of a detailed analysis given in the appendix. A summary only is included here to maintain the balance of the presentation.

The daily temperature cycles are more likely than the annual cycles to be the cause of thermal reflection cracking, because they are 365 times more frequent and the stresses have less time to relax.

The annual cycle can be interpreted as a month-by-month variation in the mean temperature of the daily cycle.

It is the daily temperature cycle in the roadbase that produces crack-opening movements, and it is the crack-opening movements at the upper surface of the roadbase that are applied to the surfacing and may cause cracking.

The magnitude of the daily cycle can be evaluated on an average monthly basis, but the power law nature of crack growth means that the few above average cycles will have a disproportionate damaging effect, for which correction factors can be developed, SECTION 2.3.

Crack-opening movements will also be affected by restraint of thermal warping due to self-weight forces, SECTION 2.4, and sub-base friction restraint SECTION 2.5.

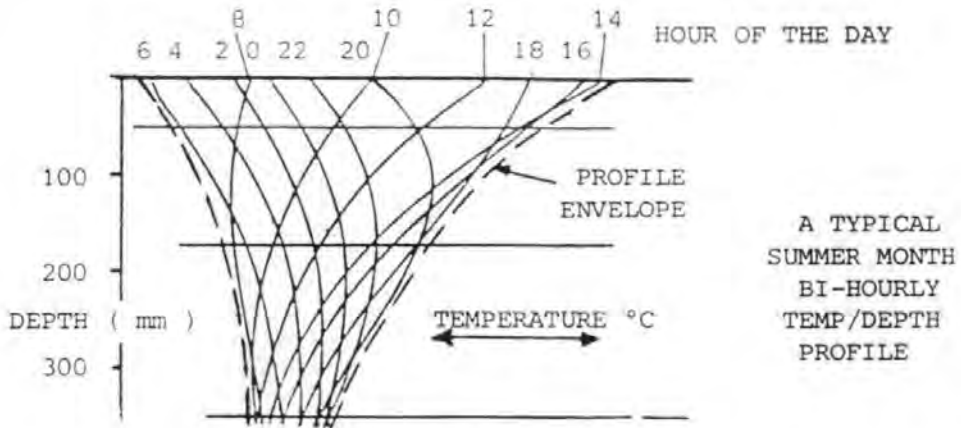
Self-weight restraint of warping is almost absolute and the small percentage of the slab that is unrestrained can be estimated. The actual crack-opening can then be estimated between upper and lower bound values.

The upper bound estimate of crack opening (warping unrestrained) corresponds to the daily cycle of temperature at the upper surface of the roadbase.

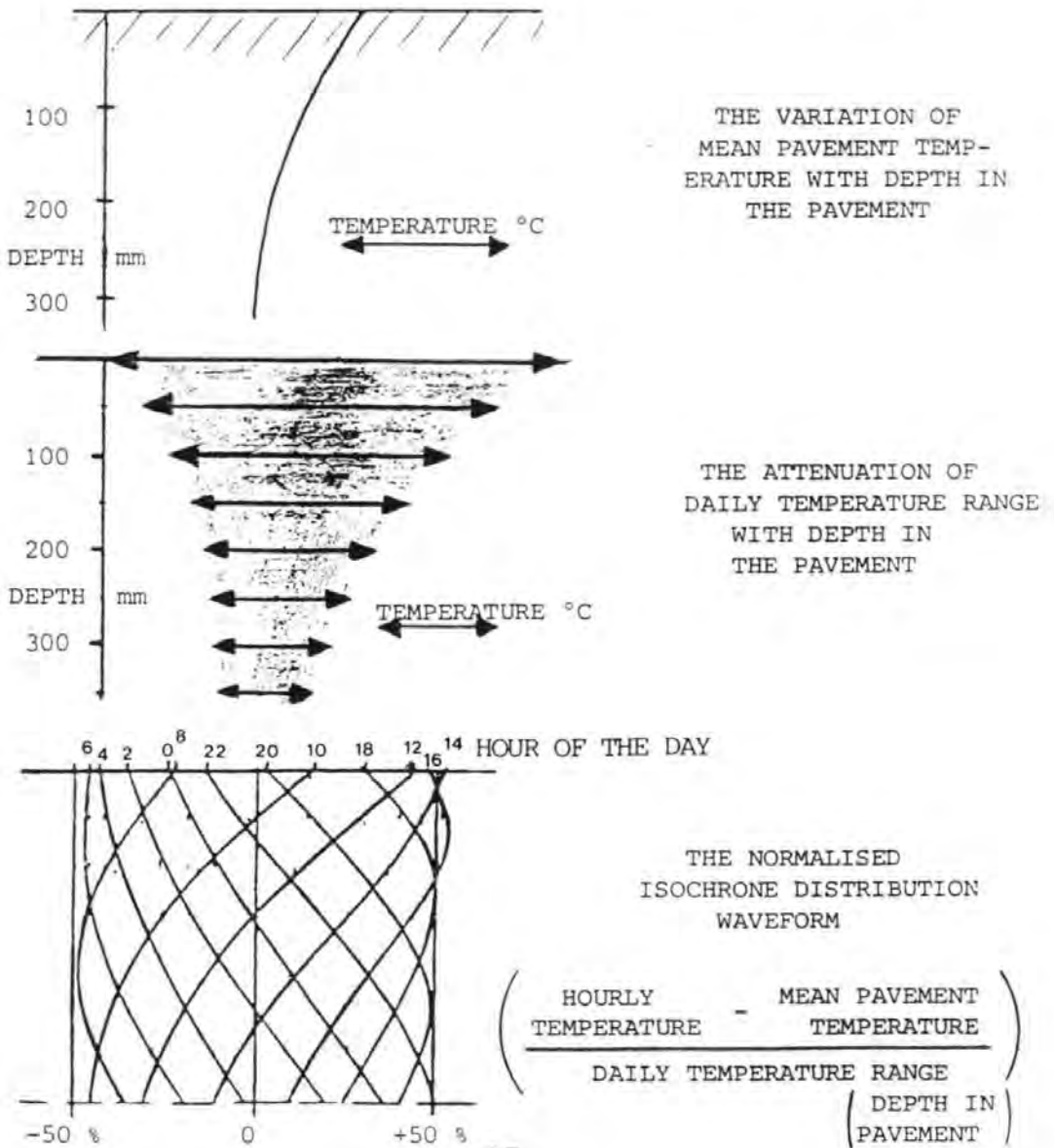
The lower bound estimate of crack opening (warping restraint absolute) corresponds to the daily cycle of mean temperature for the roadbase depth. This can be evaluated by plotting hourly profiles of temperature with depth in the pavement, FIG 2.1.

FIG 2 . 1

PAVEMENT HOURLY TEMPERATURE / DEPTH PROFILES .



TEMPERATURE / DEPTH PROFILES HAVE THREE INDEPENDANT COMPONENTS



No extensive data on temperature variations in composite pavements is available for U.K. conditions, but extensive data for a 12 month period, 1969-70, at several depths in the pavement, is available for full-depth bituminous or concrete pavements¹¹.

This bituminous and concrete pavement data can be used to estimate daily temperature ranges at any depth in a composite pavement and also hourly temperature/depth profiles.

The composite pavement "Temperature Model" can be formulated for each month of the year and for a range of surfacing thicknesses from 100 to 200mm.

2.2 A Temperature Model for Composite Pavements

The information represented by the profiles can be split into 3 components, FIG 2.1, and each component can be separately evaluated for a composite pavement and re-combined.

The most important component is the attenuation of daily temperature range with depth and this can be found by considering the "swept area" of the profiles which is analogous to the heat gain of the pavement during the daytime, and this is a combination of surface absorption and convection loss effects.

The variation of mean pavement temperature with depth in composite pavements is found using data from a TRRL survey³⁵ that compared mean temperatures in bituminous and composite pavements.

The "normalised" isochrone distribution is more a function of the time of year than of the pavement material and so for each month of the year, an isochrone distribution that resembles that in a bituminous pavement at depths $0 \rightarrow 100$ mm and resembles that in a concrete pavement at depths $100 \rightarrow 300$ mm, can be used to "fill in" the profiles for a composite pavement.

The development of this temperature model is explained in detail, APPENDIX, and the results for a 100 mm surfacing composite pavement are summarised, TABLE 2.1/2 and FIG 2.2.

TABLE 2 . 1

MEAN MONTHLY TEMPERATURES FOR THE AIR & BITUMINOUS , CONCRETE AND
COMPOSITE PAVEMENTS AT DEPTHS 0 TO 300 mm .

(°C)

| DEPTH IN PAVEMENT (mm) | JAN | FEB | MAR | APR | MAY | JUN | JUL | AUG | SEP | OCT | NOV | DEC |
|-----------------------------------|---|-----|-----|------|------|------|------|------|------|------|-----|-----|
| | AIR TEMPERATURE (LONG TERM MEAN , CENTRAL ZONE) | | | | | | | | | | | |
| | 3.0 | 3.3 | 5.3 | 8.2 | 11.1 | 14.3 | 15.9 | 15.4 | 13.7 | 9.8 | 6.2 | 4.1 |
| | BITUMINOUS PAVEMENT TEMPERATURE | | | | | | | | | | | |
| 0 | 4.8 | 5.3 | 8.3 | 13.2 | 18.9 | 24.4 | 24.6 | 21.6 | 17.9 | 12.2 | 8.0 | 5.8 |
| 100 | 4.7 | 5.3 | 8.1 | 12.4 | 17.5 | 23.1 | 23.9 | 20.7 | 16.8 | 11.6 | 7.6 | 5.5 |
| 150 | 4.8 | 5.3 | 8.0 | 12.1 | 17.0 | 22.6 | 23.6 | 20.5 | 16.6 | 11.6 | 7.7 | 5.6 |
| 250 | 4.9 | 5.4 | 7.9 | 11.7 | 16.3 | 21.8 | 22.9 | 20.2 | 16.9 | 12.1 | 8.3 | 6.0 |
| 300 | 5.1 | 5.5 | 7.9 | 11.5 | 16.0 | 21.5 | 22.6 | 20.2 | 17.2 | 12.5 | 8.6 | 6.3 |
| | CONCRETE PAVEMENT TEMPERATURE | | | | | | | | | | | |
| 0 | 2.2 | 2.9 | 5.5 | 9.4 | 13.4 | 17.8 | 20.7 | 19.5 | 15.4 | 9.9 | 5.3 | 3.1 |
| 100 | 2.3 | 3.0 | 5.5 | 9.2 | 13.2 | 17.4 | 19.1 | 18.0 | 15.0 | 10.1 | 5.9 | 3.6 |
| 150 | 2.4 | 3.0 | 5.5 | 9.2 | 13.2 | 17.3 | 18.9 | 17.8 | 15.0 | 10.2 | 6.1 | 3.7 |
| 250 | 2.5 | 3.2 | 5.7 | 9.3 | 13.2 | 17.2 | 19.0 | 18.2 | 15.3 | 10.5 | 6.3 | 3.8 |
| 300 | 2.5 | 3.2 | 5.8 | 9.3 | 13.2 | 17.2 | 19.2 | 18.5 | 15.5 | 10.6 | 6.4 | 3.9 |
| | COMPOSITE PAVEMENT (100 mm SURFACING) | | | | | | | | | | | |
| 0 | 3.4 | 4.0 | 6.8 | 11.1 | 15.9 | 21.3 | 22.7 | 20.6 | 16.6 | 10.9 | 6.5 | 4.3 |
| 100 | 3.9 | 4.6 | 7.2 | 11.3 | 16.2 | 22.0 | 22.9 | 20.1 | 16.2 | 11.1 | 7.0 | 4.9 |
| 150 | 4.1 | 4.6 | 7.1 | 11.1 | 15.8 | 21.8 | 22.9 | 20.1 | 16.1 | 11.2 | 7.3 | 4.9 |
| 250 | 4.0 | 4.6 | 7.1 | 10.8 | 15.2 | 21.1 | 22.4 | 20.0 | 16.3 | 11.5 | 7.5 | 5.2 |
| 300 | 4.1 | 4.6 | 7.1 | 10.8 | 15.0 | 20.9 | 22.2 | 20.0 | 16.4 | 11.7 | 7.7 | 5.3 |
| | COMPOSITE PAVEMENT (150 mm SURFACING) | | | | | | | | | | | |
| 0 | 3.9 | 4.4 | 7.3 | 11.8 | 16.8 | 22.4 | 23.4 | 20.9 | 17.0 | 11.3 | 7.0 | 4.8 |
| 100 | 4.3 | 4.9 | 7.6 | 11.8 | 16.7 | 22.6 | 23.5 | 20.5 | 16.5 | 11.3 | 7.3 | 5.1 |
| 150 | 4.4 | 4.9 | 7.6 | 11.6 | 16.3 | 22.3 | 23.3 | 20.3 | 16.3 | 11.4 | 7.4 | 5.3 |
| 250 | 4.4 | 4.9 | 7.4 | 11.2 | 15.6 | 21.6 | 22.7 | 20.1 | 16.6 | 11.8 | 7.9 | 5.5 |
| 300 | 4.5 | 5.0 | 7.4 | 11.0 | 15.4 | 21.3 | 22.4 | 20.1 | 16.9 | 12.1 | 8.1 | 5.8 |
| | COMPOSITE PAVEMENT (200 mm SURFACING) | | | | | | | | | | | |
| 0 | 4.2 | 4.7 | 7.6 | 12.3 | 17.6 | 23.2 | 23.9 | 21.2 | 17.3 | 11.7 | 7.4 | 5.2 |
| 100 | 4.5 | 5.1 | 7.9 | 12.1 | 17.1 | 22.9 | 23.7 | 20.6 | 16.6 | 11.5 | 7.4 | 5.3 |
| 150 | 4.6 | 5.1 | 7.8 | 11.8 | 16.7 | 22.5 | 23.5 | 20.5 | 16.5 | 11.5 | 7.6 | 5.4 |
| 250 | 4.6 | 5.1 | 7.6 | 11.4 | 15.9 | 21.7 | 22.8 | 20.2 | 16.7 | 11.9 | 8.1 | 5.7 |
| 300 | 4.8 | 5.2 | 7.6 | 11.2 | 15.7 | 21.4 | 22.6 | 20.2 | 17.0 | 12.3 | 8.3 | 6.0 |

TABLE 2 . 2

MEAN MONTHLY DAILY TEMPERATURE RANGES FOR THE AIR & BITUMINOUS ,
CONCRETE AND COMPOSITE PAVEMENTS AT DEPTHS 0 TO 300 mm .

(°C)

| DEPTH IN PAVEMENT (mm) | JAN | FEB | MAR | APR | MAY | JUN | JUL | AUG | SEP | OCT | NOV | DEC |
|-----------------------------------|---|-----|------|------|------|------|------|------|------|-----|-----|-----|
| | DAILY RANGE OF AIR TEMPERATURE | | | | | | | | | | | |
| | 4.0 | 4.6 | 6.4 | 8.3 | 9.5 | 9.8 | 9.2 | 8.8 | 8.6 | 7.5 | 6.0 | 4.5 |
| | DAILY RANGE OF BITUMINOUS PAVEMENT TEMPERATURE | | | | | | | | | | | |
| 0 | 2.4 | 5.8 | 10.8 | 15.5 | 20.3 | 23.3 | 19.5 | 15.5 | 11.6 | 8.0 | 4.3 | 2.0 |
| 100 | 1.3 | 3.2 | 6.6 | 9.7 | 12.0 | 13.1 | 11.2 | 9.1 | 7.0 | 5.0 | 3.1 | 1.5 |
| 150 | 1.0 | 2.4 | 4.9 | 7.3 | 8.8 | 9.6 | 8.3 | 6.8 | 5.3 | 3.8 | 2.5 | 1.2 |
| 250 | 0.6 | 1.2 | 2.4 | 3.7 | 4.6 | 5.1 | 4.5 | 3.6 | 2.8 | 2.0 | 1.5 | 0.7 |
| 300 | 0.4 | 0.9 | 1.6 | 2.5 | 3.1 | 3.6 | 3.1 | 2.5 | 2.0 | 1.4 | 1.0 | 0.5 |
| | DAILY RANGE OF CONCRETE PAVEMENT TEMPERATURE | | | | | | | | | | | |
| 0 | 3.5 | 4.3 | 6.6 | 9.0 | 11.2 | 12.2 | 10.9 | 9.2 | 7.5 | 5.9 | 4.5 | 3.5 |
| 100 | 2.2 | 2.7 | 3.9 | 5.8 | 7.3 | 7.7 | 6.8 | 5.6 | 4.4 | 3.3 | 2.6 | 2.1 |
| 150 | 1.8 | 2.1 | 3.1 | 4.7 | 5.8 | 6.1 | 5.4 | 4.5 | 3.5 | 2.7 | 2.1 | 1.7 |
| 250 | 1.2 | 1.4 | 2.0 | 3.1 | 3.7 | 3.9 | 3.7 | 3.2 | 2.6 | 2.1 | 1.6 | 1.3 |
| 300 | 1.0 | 1.2 | 1.8 | 2.5 | 3.0 | 3.3 | 3.2 | 2.9 | 2.4 | 1.9 | 1.5 | 1.2 |
| | DAILY RANGE , COMPOSITE PAVEMENT (100 mm SURFACING) | | | | | | | | | | | |
| 0 | 4.2 | 6.4 | 10.0 | 14.5 | 19.5 | 19.8 | 19.0 | 15.2 | 11.3 | 7.8 | 4.9 | 3.3 |
| 100 | 2.3 | 3.5 | 5.5 | 9.1 | 11.5 | 12.7 | 10.8 | 9.0 | 6.8 | 4.9 | 3.5 | 2.5 |
| 150 | 1.9 | 2.7 | 4.3 | 7.4 | 9.0 | 10.1 | 8.6 | 7.2 | 5.5 | 4.0 | 2.9 | 2.0 |
| 250 | 1.3 | 1.9 | 2.9 | 4.8 | 5.9 | 6.6 | 5.9 | 5.2 | 4.0 | 3.1 | 2.2 | 1.6 |
| 300 | 1.0 | 1.5 | 2.4 | 3.9 | 4.7 | 5.4 | 5.1 | 4.7 | 3.8 | 2.8 | 2.1 | 1.4 |
| | DAILY RANGE , COMPOSITE PAVEMENT (150 mm SURFACING) | | | | | | | | | | | |
| 0 | 3.7 | 6.1 | 9.9 | 14.4 | 19.4 | 19.6 | 19.2 | 15.7 | 11.5 | 7.9 | 4.6 | 2.9 |
| 100 | 2.0 | 3.4 | 6.0 | 9.1 | 11.5 | 12.5 | 10.9 | 9.3 | 6.9 | 4.9 | 3.3 | 2.2 |
| 150 | 1.6 | 2.5 | 4.5 | 6.8 | 8.3 | 9.2 | 8.3 | 6.9 | 5.3 | 3.8 | 2.7 | 1.7 |
| 250 | 1.0 | 1.7 | 2.9 | 4.5 | 5.2 | 5.9 | 5.6 | 4.9 | 3.9 | 3.0 | 2.0 | 1.3 |
| 300 | 0.9 | 1.4 | 2.6 | 3.6 | 4.3 | 4.9 | 4.8 | 4.6 | 3.6 | 2.6 | 1.9 | 1.2 |
| | DAILY RANGE , COMPOSITE PAVEMENT (200 mm SURFACING) | | | | | | | | | | | |
| 0 | 3.5 | 6.0 | 10.0 | 14.5 | 19.0 | 20.0 | 19.4 | 16.1 | 11.8 | 8.0 | 4.4 | 2.6 |
| 100 | 1.9 | 3.3 | 6.1 | 9.1 | 11.2 | 12.8 | 11.1 | 9.5 | 7.1 | 5.0 | 3.2 | 2.0 |
| 150 | 1.5 | 2.5 | 4.5 | 6.8 | 8.2 | 9.4 | 8.3 | 7.1 | 5.4 | 3.8 | 2.6 | 1.6 |
| 200 | 1.0 | 1.7 | 3.2 | 4.9 | 6.1 | 6.0 | 6.0 | 5.2 | 3.9 | 2.8 | 2.1 | 1.3 |
| 250 | 0.9 | 1.4 | 2.5 | 4.1 | 4.9 | 4.8 | 5.0 | 4.5 | 3.4 | 2.6 | 1.8 | 1.2 |
| 300 | 0.7 | 1.2 | 2.3 | 3.3 | 4.0 | 4.0 | 4.3 | 4.2 | 3.1 | 2.3 | 1.7 | 1.1 |

FIG 2 . 2

BI-HOURLY TEMPERATURE / DEPTH PROFILES FOR BITUMINOUS , CONCRETE AND COMPOSITE PAVEMENTS , JANUARY AND APRIL .

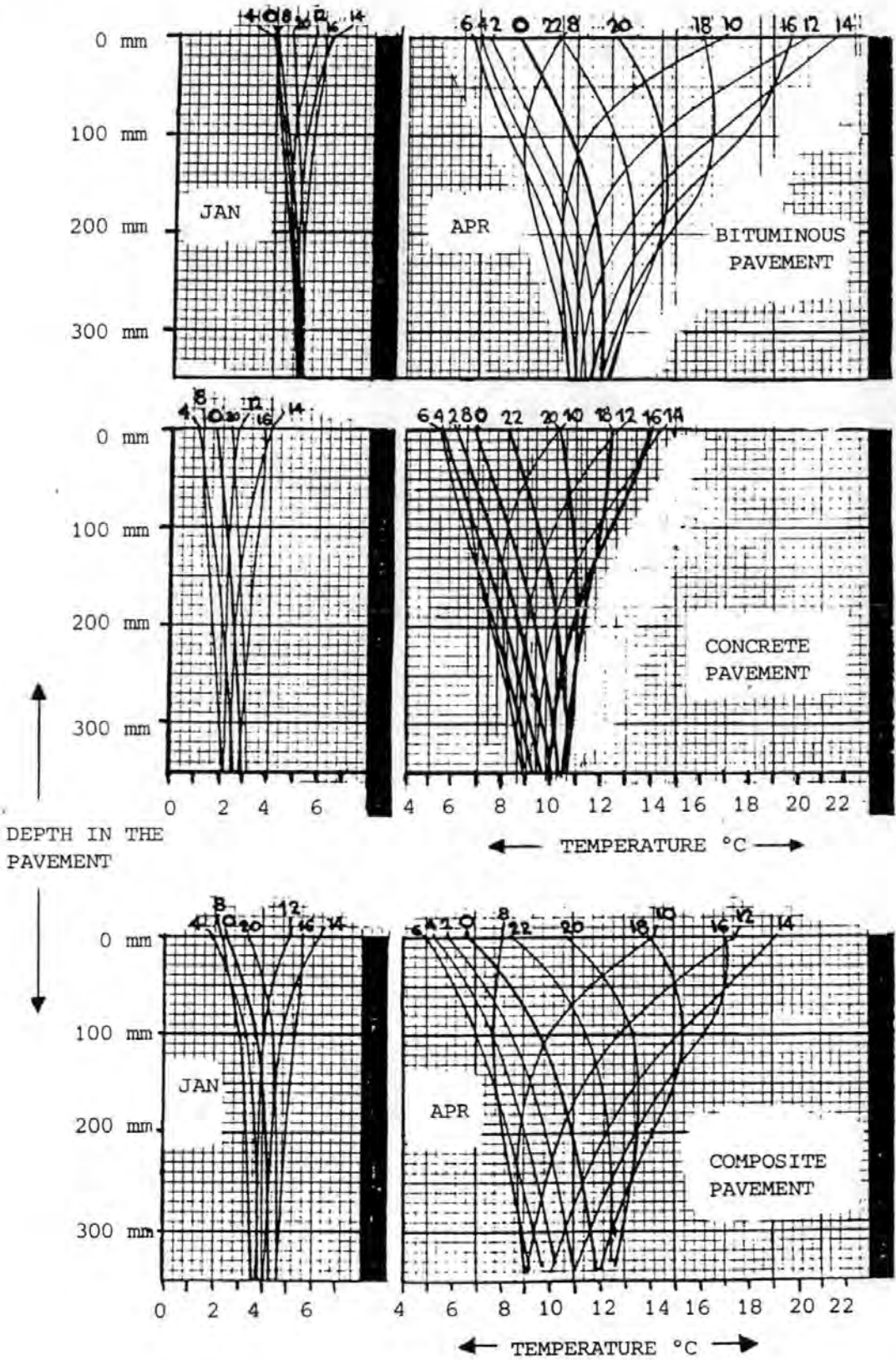
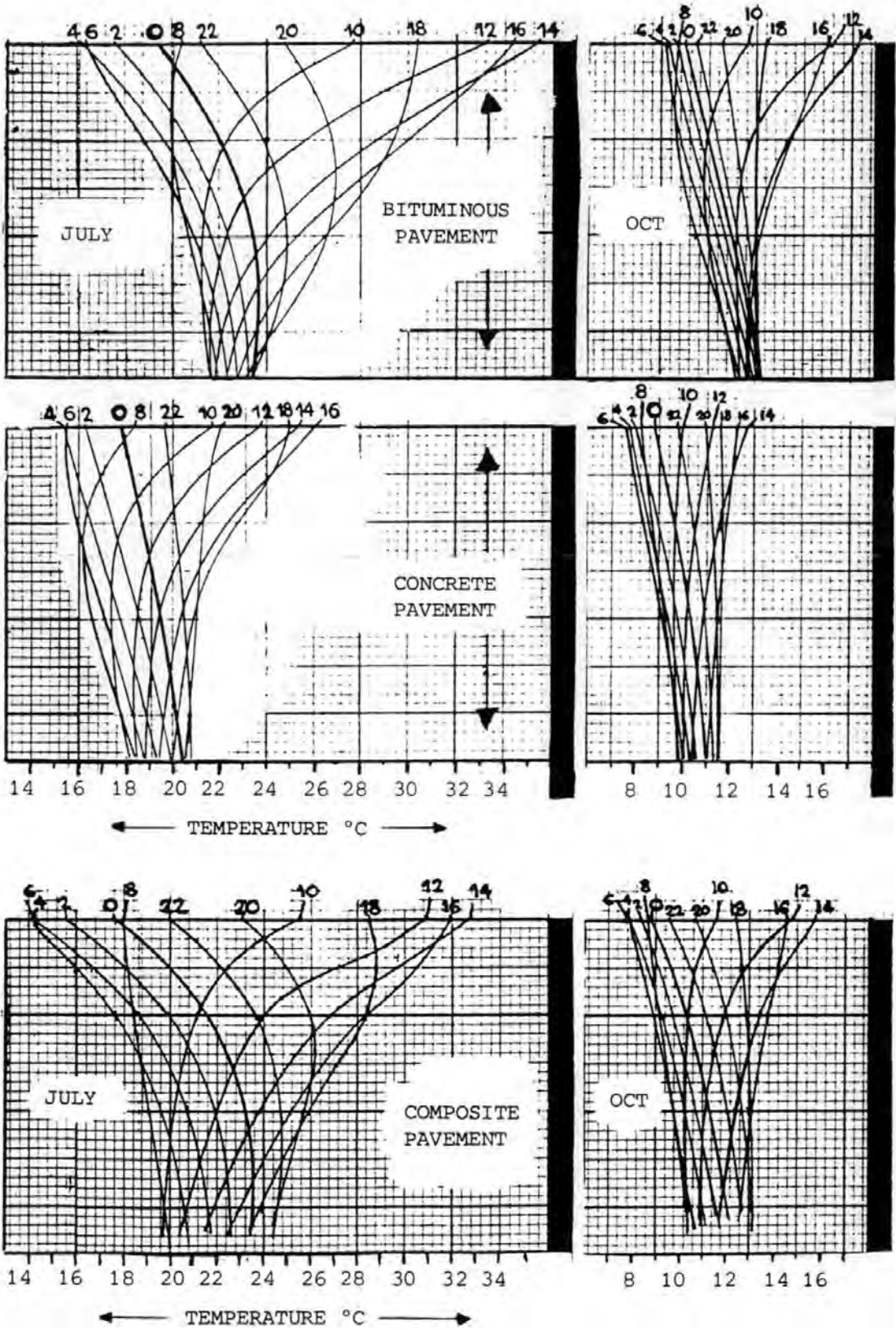


FIG 2 . 2 CONTINUED

BI- HOURLY TEMPERATURE / DEPTH PROFILES FOR BITUMINOUS , CONCRETE AND COMPOSITE PAVEMENTS , JULY AND OCTOBER .



The procedures for estimating composite pavement temperature/depth profiles are only approximate, but separate evaluation of the 3 components does reduce cumulative errors. Errors cannot be assessed in absolute terms but they must be considerably smaller than the differences in temperature range, between bituminous and concrete pavements, which are approximately -30%.

The temperature model is related to monthly mean air temperatures and daily air temperature ranges, and so can be adapted for any site where this type of data concerning air temperatures is available.

The daily temperature ranges at roadbase depth are consistently greater (17% JAN → 86% AUG) than is implied by the results of an early TRRL survey at Harmondsworth³⁶, that compared temperatures in exposed and asphalt covered concrete slabs.

The site at Harmondsworth was, however, flanked by low buildings to the north and an orchard to the south. These will have influenced shadow and shelter from wind at the site.

The temperature model described relates to temperature measurements taken from two sites, located at Alconbury and Long Berrington on Trunk Road A1, that are exposed in all directions.

Therefore these recent studies and the earlier work at Harmondsworth are not directly comparable.

2.3 The 6th Power Effect

The growth rate of reflected cracking in visco-elastic materials is proportional to approximately 6th power of crack opening movements^{26,27,32}, and these are linearly related to daily temperature ranges.

Thus the "equivalent crack growth mean" daily temperature range will be the approximate 6th power mean of the actual daily temperature ranges, and this is about 25% greater than the linear average value for a one month period (30 days).

The difference between 6th power and linear mean daily temperature ranges can be evaluated for all months of the year for concrete pavements using the TRRL data¹¹, and for bituminous pavements for four 20 day periods using other TRRL data³⁶, TABLE 2.3

TABLE 2 . 3

COMPARISON OF MEAN AND 6TH POWER MEAN DAILY TEMPERATURE RANGES

INDIVIDUAL DAILY TEMPERATURE RANGES FOR MONTHLY PERIODS AT DEPTH 127 mm IN A CONCRETE PAVEMENT AND FOR 20 DAY PERIODS AT EITHER 40 mm OR 100 mm IN A BITUMINOUS PAVEMENT (*)

| | JAN | FEB | JAN FEB | MAR | APR | MAR APR | MAY | JUN | MAY JUN | JUL | AUG | JUL AUG | SEP | OCT | NOV | DEC |
|---|------|------|------------|------|------|------------|------|------|------------|------|------|------------|------|-----|------|-----|
| (°C) | 1 | 1 | * | 2 | 4 | * | 8 | 6 | * | 4 | 7 | * | 2 | 4 | 3 | 2 |
| | 1 | 2 | 5 | 2 | 4 | 14 | 3 | 6 | 15 | 6 | 3 | 13 | 3 | 3 | 3 | 2 |
| | 2 | 2 | 7 | 0 | 8 | 11 | 7 | 2 | 15 | 8 | 4 | 13 | 8 | 3 | 0 | 3 |
| | 2 | 2 | 3 | 2 | 8 | 11 | 3 | 5 | 7 | 8 | 5 | 9 | 3 | 3 | 6 | 2 |
| | 3 | 2 | 4 | 3 | 8 | 7 | 1 | 7 | 9 | 2 | 5 | 13 | 4 | 3 | 3 | 2 |
| | 3 | 3 | 7 | 6 | 8 | 13 | 5 | 10 | 16 | 1 | 7 | 15 | 4 | 3 | 3 | 2 |
| | 2 | 4 | 8 | 5 | 6 | 10 | 9 | 12 | 15 | 2 | 7 | 18 | 2 | 3 | 3 | 2 |
| | 2 | 4 | 5 | 6 | 6 | 11 | 4 | 9 | 10 | 4 | 7 | 12 | 7 | 2 | 2 | 2 |
| | 3 | 3 | 8 | 3 | 7 | 5 | 5 | 9 | 12 | 6 | 4 | 15 | 5 | 5 | 2 | 1 |
| | 2 | 4 | 8 | 3 | 3 | 14 | 3 | 9 | 13 | 2 | 3 | 17 | 3 | 5 | 2 | 2 |
| | 3 | 4 | 6 | 3 | 3 | 14 | 4 | 9 | 7 | 3 | 6 | 17 | 4 | 3 | 4 | 1 |
| | 3 | 2 | 3 | 1 | 5 | 15 | 5 | 9 | 12 | 8 | 6 | 16 | 5 | 1 | 3 | 1 |
| | 1 | 2 | 8 | 2 | 6 | 18 | 3 | 9 | 16 | 8 | 4 | 10 | 1 | 3 | 3 | 2 |
| | 2 | 4 | 10 | 2 | 5 | 17 | 3 | 9 | 14 | 9 | 4 | 13 | 1 | 2 | 2 | 3 |
| | 2 | 5 | 3 | 3 | 4 | 18 | 3 | 9 | 11 | 9 | 3 | 13 | 1 | 3 | 2 | 1 |
| | 3 | 4 | 5 | 2 | 4 | 9 | 5 | 7 | 16 | 9 | 5 | 13 | 2 | 2 | 2 | 1 |
| | 3 | 3 | 8 | 1 | 4 | 11 | 4 | 8 | 16 | 7 | 4 | 16 | 3 | 3 | 3 | 2 |
| | 1 | 3 | 2 | 1 | 5 | 10 | 4 | 4 | 15 | 8 | 4 | 15 | 2 | 2 | 5 | 2 |
| | 1 | 3 | | 0 | 7 | 8 | 6 | 6 | | 5 | 2 | 16 | 6 | 2 | 2 | 0 |
| | 1 | 3 | | 2 | 4 | 9 | 9 | 3 | | 4 | 5 | | 7 | 3 | 3 | 0 |
| | 1 | 4 | | 2 | 4 | 20 | 9 | 4 | | 6 | 4 | | 4 | 1 | 2 | 4 |
| | 3 | 4 | | 2 | 5 | | 6 | 9 | | 7 | 3 | | 5 | | 4 | 3 |
| | 4 | 3 | | 2 | 5 | | 5 | 3 | | 8 | 3 | | 6 | | 1 | 2 |
| | 1 | 2 | | 2 | 4 | | 7 | 5 | | 4 | 5 | | 4 | | 2 | 2 |
| | 1 | 1 | | 2 | 6 | | 5 | 6 | | 8 | 3 | | 3 | 2 | 2 | 2 |
| | 2 | 3 | | 2 | 3 | | 4 | 6 | | 7 | 4 | | 3 | 2 | 2 | 3 |
| | 1 | 3 | | 5 | 5 | | 5 | 6 | | 9 | 4 | | 4 | 3 | 2 | 2 |
| | 2 | 2 | | 7 | 3 | | 7 | 6 | | 4 | 2 | | 4 | 1 | 4 | 1 |
| | 2 | | | 7 | 5 | | 7 | 7 | | 2 | 2 | | 4 | 2 | 3 | 1 |
| | 2 | | | 4 | 7 | | 3 | 7 | | 7 | 2 | | 5 | 2 | 2 | 2 |
| 1 | | | 4 | | | 3 | | | 9 | 2 | | | 1 | | 1 | |
| MEAN | 2.0 | 2.9 | 5.9 | 2.9 | 5.2 | 12.3 | 5.0 | 6.9 | 12.8 | 5.9 | 4.2 | 14.1 | 3.8 | 2.6 | 2.7 | 1.8 |
| 6th POWER MEAN | 2.7 | 3.5 | 7.2 | 4.5 | 6.2 | 14.7 | 6.6 | 8.3 | 14.0 | 7.4 | 5.3 | 15.0 | 5.3 | 3.4 | 3.7 | 2.5 |
| RATIO | 1.32 | 1.23 | | 1.41 | 1.20 | | 1.29 | 1.09 | | 1.26 | 1.06 | | 1.36 | | 1.39 | |
| AVERAGE RATIO FOR COMPOSITE PAVEMENT | | 1.28 | | 1.31 | | | 1.19 | | | 1.16 | | | 1.26 | | 1.29 | |

The ratio 6th power mean/linear mean is a measure of climatic variability and appears slightly larger for concrete than bituminous pavements, but this could be due to using 30 not 20 day periods. For composite pavements, the average of these bituminous and concrete pavement values can be used to convert mean daily temperature ranges, TABLE 2.2, into 6th power mean values which compensate for the increased damaging effect of the few above average daily temperature ranges in each month.

2.4 Warping Restraint Effects

The magnitude of the warping restraint factor (EQN 1) when self-weight restraint of warping is absolute, is shown, TABLE 2.4. Actual values will be between 0.70 and 1.00.

This comparison of upper and lower bound estimates of crack-opening movements can be made for 4 key months where temperature/depth profiles have been plotted for a 100mm surfacing composite pavement, FIG 2.2.

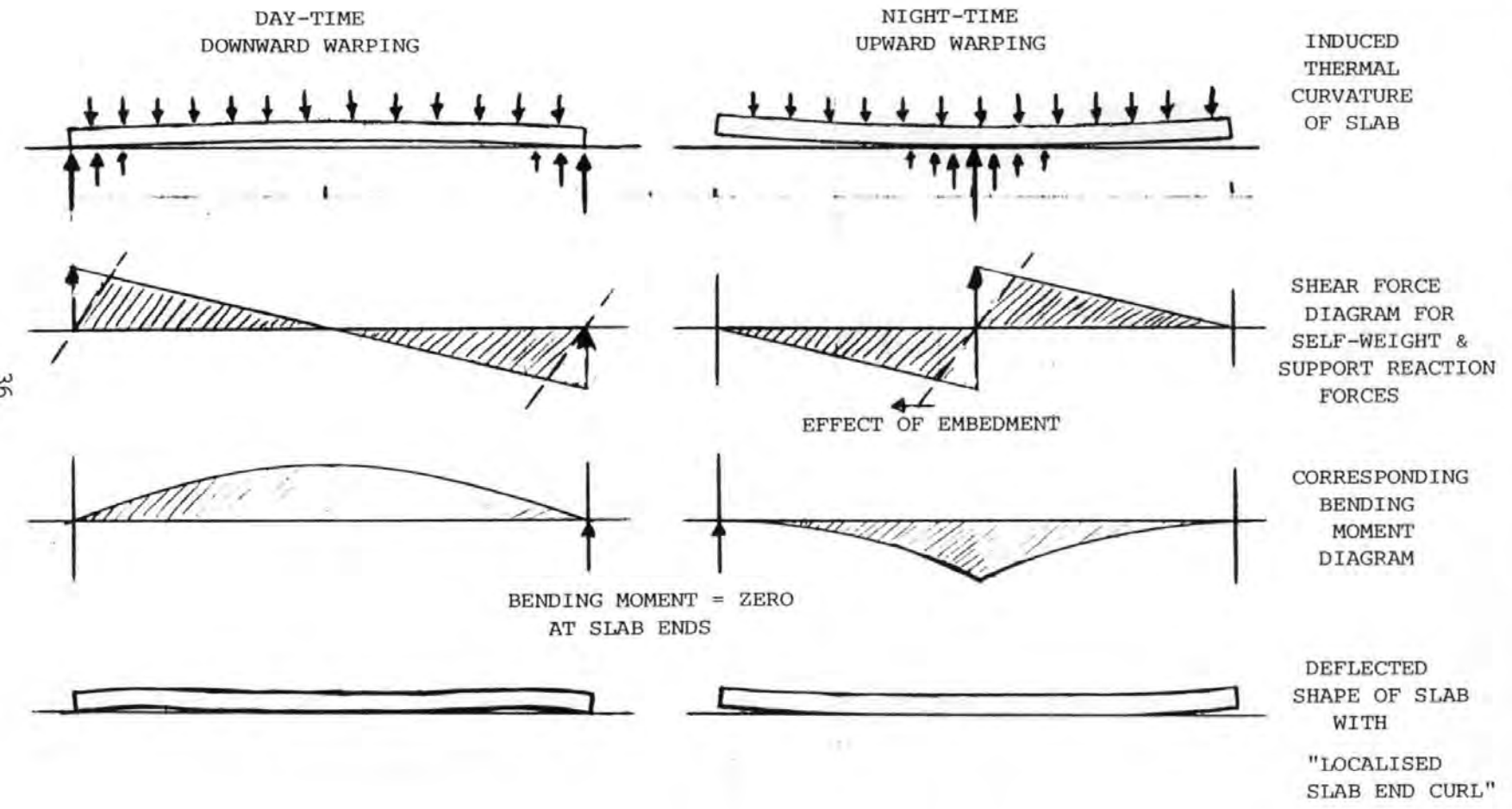
TABLE 2.4 Comparison of upper and lower bound estimates for the daily temperature range that causes crack-opening

| MONTH | Warping Unrestrained | Absolute Restraint | Absolute Restraint Warping Restraint Factor, w. (EQN 1) |
|-------|----------------------------------|--|---|
| | Daily Temp' Range at Depth 100mm | Daily Range Mean 'Temp' Over Depth of Roadbase | |
| JAN | 2.3 °C | 1.7 °C | 0.74 |
| APR | 9.1 °C | 6.5 °C | 0.71 |
| JUL | 10.8 °C | 7.6 °C | 0.70 |
| OCT | 4.9 °C | 3.7 °C | 0.76 |

A simplified analysis of the shear forces and bending moments that are generated by thermal warping is illustrated, FIG 2.3.

A SIMPLIFIED ANALYSIS OF SELF-WEIGHT RESTRAINT OF THERMAL WARPING .

FIG 2 . 3



It can be seen from FIG 2.3 that the bending moments are greatest at the slab centres and decrease to zero at the slab ends. Thus there must be some unrestrained warping at the slab ends. This "slab end curl" is controlled by the build-up of self-weight induced bending moment inward from the slab ends, FIG 2.3, which is equal for any length of slab of a given thickness and density.

Thus slab end curl is related to temperature gradients but is not dependent on slab length.

The extent of slab end curl can be evaluated by considering the approximate limit to self-weight restraint of warping, given by the equation

$$\begin{array}{l} \text{Thermally Induced} \\ \text{Lift at Slab Ends} \end{array} = \begin{array}{l} \text{Self Weight Induced} \\ \text{Deflection at Slab Ends} \end{array} \quad (\text{EQN 3})$$

These self-weight forces are mobilised because the support reaction forces become concentrated at the slab centre with upward warping or at the slab ends with downward warping. In practice, with a non-rigid foundation there will be embedment of these portions of the slabs and the full self-weight forces will not be mobilised.

Equations can be formulated for:-

$$\begin{array}{l} \text{Thermally Induced Lift} \\ \text{At Slab Ends} \end{array} = \frac{dT \alpha L^2}{8h} \quad (\text{EQN 4})$$

$$\begin{array}{l} \text{Slab End Deflection} \\ \text{For 100\% Mobilised} \\ \text{Self-Weight Forces} \end{array} = \frac{WL^4}{128 EI} \quad (\text{EQN 5})$$

where

dT = Temperature difference across slab, °C

α = Thermal coefficient of expansion, °C⁻¹

h = Thickness of slab, m

L = Slab length, m

W = Distributed self-weight forces, N/m

E = Youngs modulus (lean concrete), N/m²

I = 2nd moment of area (concrete slab), m⁴

The following "typical values" can be used:-

$$\begin{aligned}\alpha &= 10^{-5}/^{\circ}\text{C} & h &= 0.2\text{m} \\ E &= 3 \times 10^{10} \text{ N/m}^2 & I &= 6.67 \times 10^{-4} \text{ m}^4 \\ W &= 6,870 \text{ N/m (slab + surfacing).}\end{aligned}$$

(EQN 3) now reduces to:-

$$dT = \frac{h W L^2}{16 EI \alpha} = 0.429L^2 \quad (\text{EQN 6})$$

The temperature difference vs slab length curve, FIG 2.4, is only approximate because of the effects of embedment. The slab lengths indicated, FIG 2.4, will still have slab-end curl because the full self-weight forces are not mobilised.

The relationship between embedment and mobilised self-weight forces can be evaluated if the shape of the embedment profile is known. Upward thermal curvature produces an embedment profile of the form $y = \gamma (u-x^2)$, where $x = 0$ is the slab centre. The effect of those "distributed" support forces in reducing the self-weight deflection at the slab ends, is expressed in terms of the % embedment vs % mobilised self-weight deflection, FIG.2.5, which is independent of slab length.

The thermal lift deflection and self-weight deflection at points along the slab can also be expressed in forms that are independent of slab length, FIG 2.6.

If deflections are equal and opposite at the slab ends, FIG 2.4, then the extent of embedment and mobilised self-weight deflection can be deduced.

The interaction of % mobilised self-weight deflection and the thermal lift deflection, determines the extent of embedment, which in turn implies the % mobilised self-weight deflection. The equilibrium of these quantities is found by using FIG 2.5 (mobilised self-weight deflection = 75% and extent of embedment = 60%).

FIG 2 . 4

THE LIMITING TEMPERATURE DIFFERENCE FOR SELF-WEIGHT RESTRAINT OF UPWARD WARPING IN THE IDEALISED SITUATION WHERE A 200 mm THICK SLAB IS SUPPORTED BY A RIGID FOUNDATION .

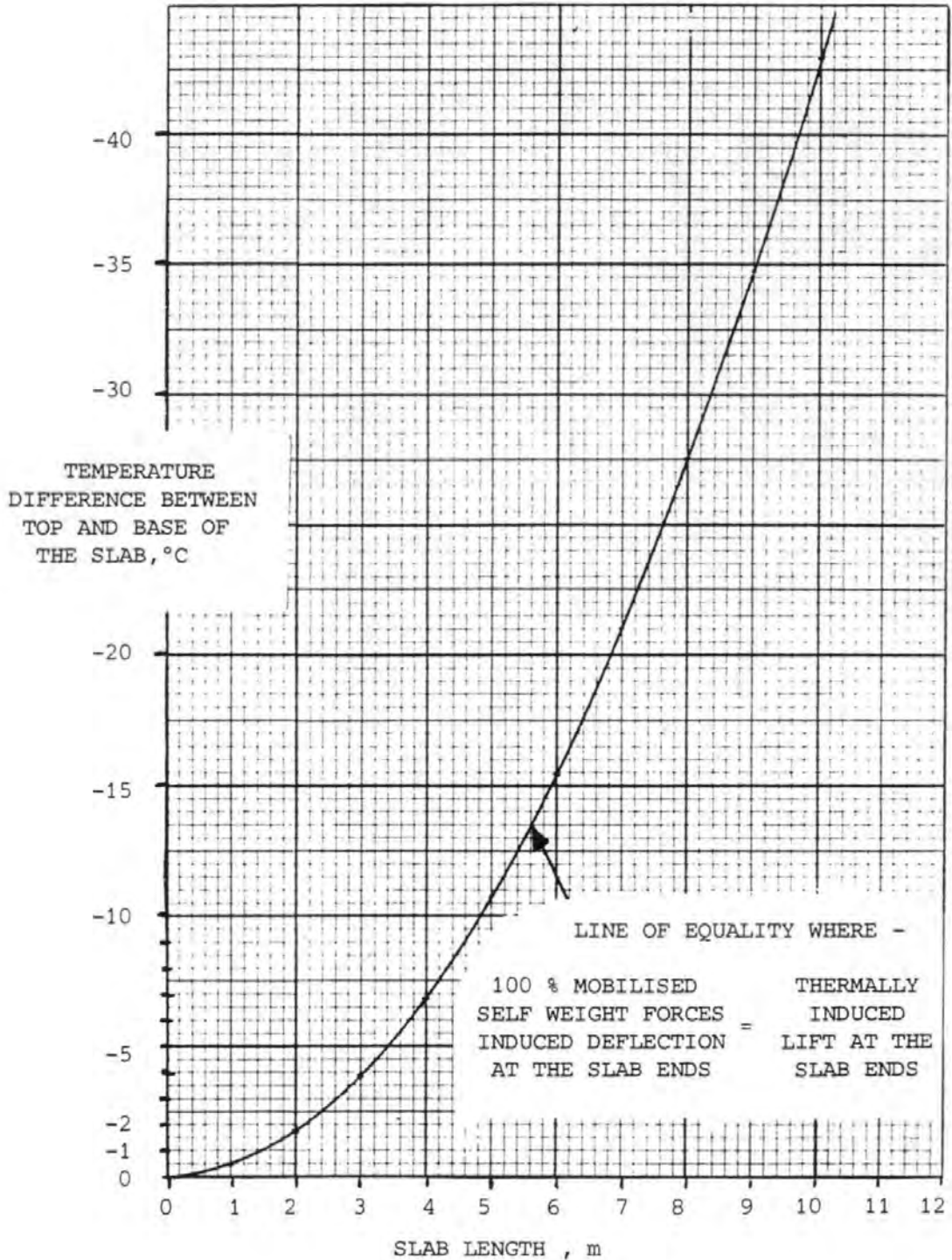


FIG 2 . 5

THE EFFECT OF EMBEDMENT AT THE SLAB CENTRE AND DISTRIBUTION OF THE SUPPORT REACTION FORCES , IN REDUCING THE POTENTIAL SELF-WEIGHT INDUCED DEFLECTION AT THE SLAB ENDS .

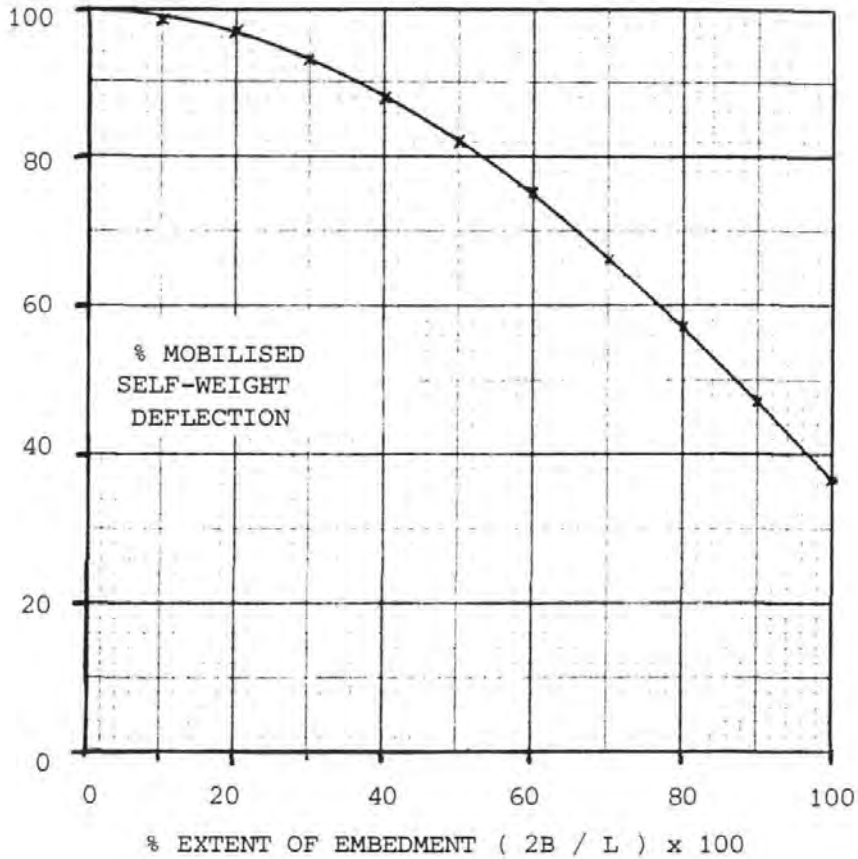
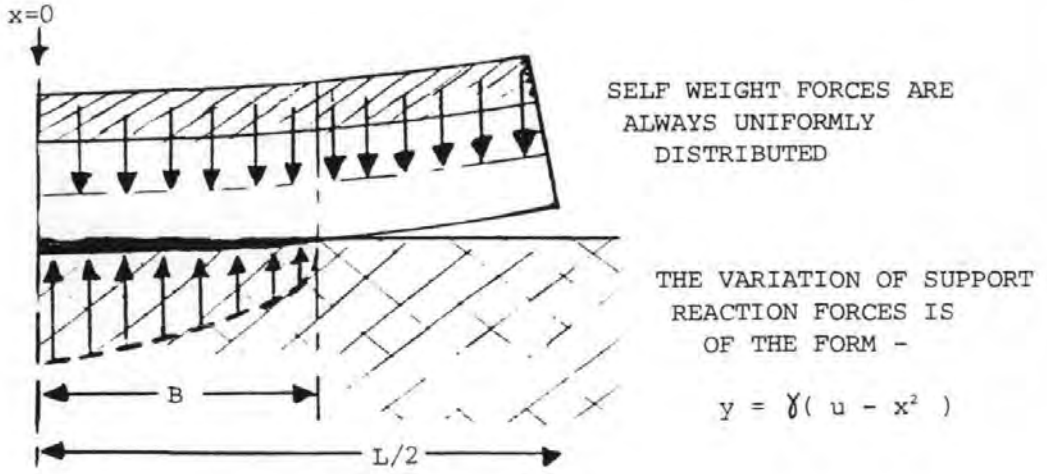
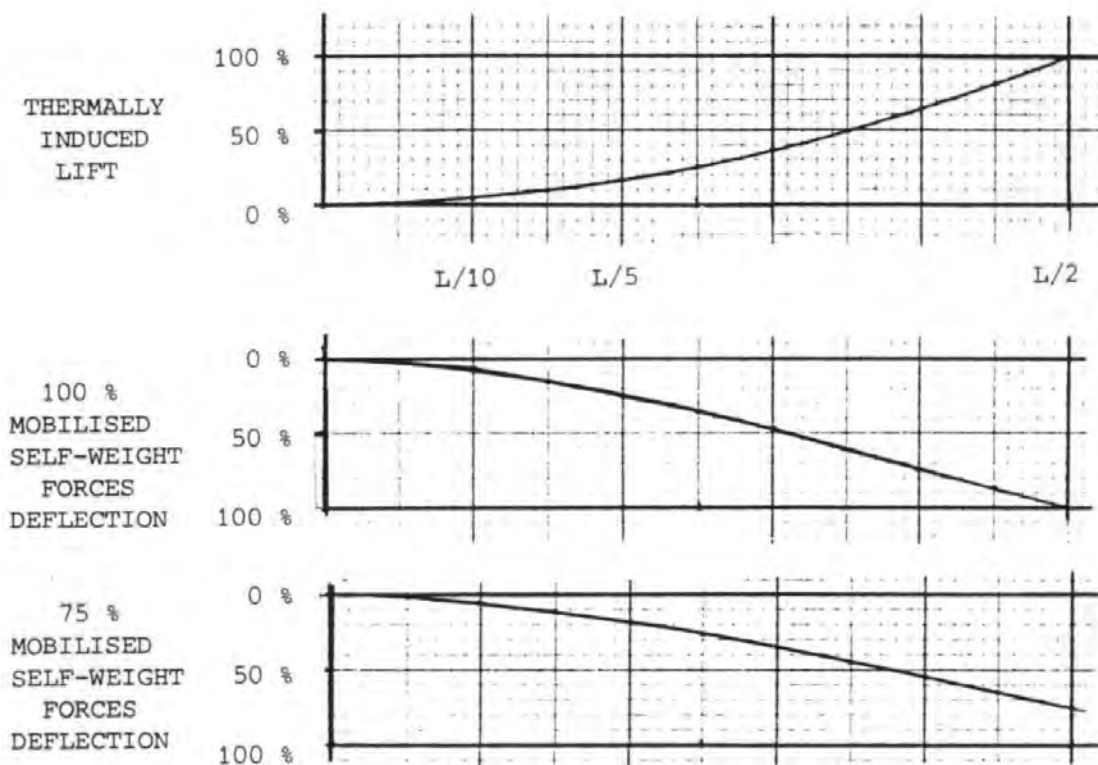


FIG 2 . 6

THE VARIATION OF THERMAL AND POTENTIAL SELF-WEIGHT INDUCED DEFLECTIONS ALONG THE SLAB , AS A % OF THE SLAB END DEFLECTION .



THE INTERACTION OF THERMAL LIFT

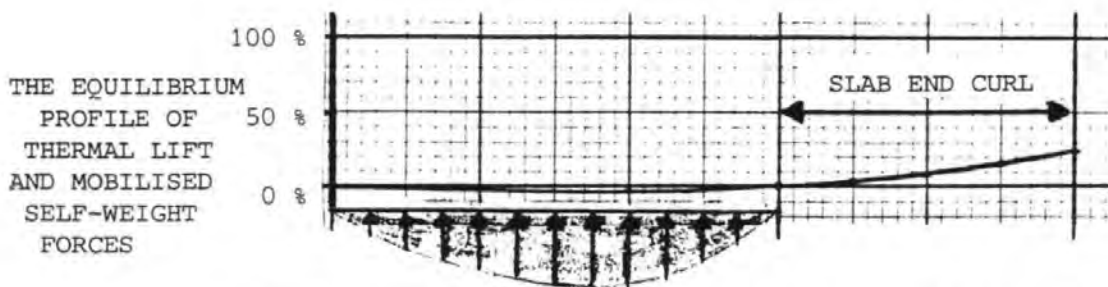
AND 75 % MOBILISED
SELF-WEIGHT FORCES

⇒ 60 % EMBEDMENT

AND 60 % EMBEDMENT

⇒ 75% MOBILISED SELF-WEIGHT
FORCES

⇒ EQUILIBRIUM .



THE PRECISE EXTENT AND DEPTH OF EMBEDMENT WILL DEPEND ON THE STIFFNESS OF THE FOUNDATION , BUT THE " CENTROID " OF THE SUPPORT REACTION FORCES WILL NOT MOVE SIGNIFICANTLY.

The final embedment profile, FIG 2.6, is different to that in FIG 2.5, but its main feature, the concentration of support forces near the slab centre, is still valid.

Thus slab end curl (unrestrained warping) will extend for 40% of the slab lengths indicated, FIG 2.4, at relevant temperature differences.

The temperature differences of the UK climate, for the roadbase of a 100mm surfacing composite pavement, can be found from the hourly temperature profiles, FIG 2.2, and are summarised, TABLE 2.5.

TABLE 2.5

TEMPERATURE DIFFERENCES ACROSS THE ROADBASE AT THE MAXIMUM AND MINIMUM POINTS OF THE DAILY CYCLE AT DEPTH 100mm IN A COMPOSITE PAVEMENT

| MONTH | TEMPERATURE (°C) | | TIME (hrs) | | TEMP DIFFERENCE | |
|-------|------------------|------|------------|--------|-------------------|---------------------|
| | MIN | MAX | AT MIN | AT MAX | AT MIN | AT MAX |
| JAN | 3.0 | 5.3 | 07.00 | 16.00 | -0.65 | +0.8 |
| APR | 7.1 | 16.3 | 06.00 | 16.00 | -2.45 | +4.5 |
| JUL | 17.8 | 28.6 | 06.00 | 17.00 | -2.8 | +5.1 |
| OCT | 8.9 | 13.8 | 07.00 | 15.00 | -1.6 | +1.4 |
| | | | | | UPWARD WARPING | DOWNWARD WARPING |

The temperature differences are greater when warping of the slab ends is downward, but the bending moments of the self-weight forces are also greater, FIG. 2.3, and so the length of slab end curl can be considered as about the same in both cases.

The temperature differences of the UK climate are sufficiently small, TABLE 2.5, that the slab end curl only constitutes a small % of slab length and so the appropriate warping restraint factors, TABLE 2.6, are nearer absolute restraint, TABLE 2.4, than unrestrained warping.

TABLE 2.6 ESTIMATION OF SLAB END CURL
AND WARPING RESTRAINT FACTORS

| MONTH | TEMPERATURE DIFFERENCE ACROSS SLAB | SLAB LENGTH WITH 60% EMBEDMENT FIG 2.4 | EXTENT OF SLAB END CURL (20% EACH END) | | | |
|---|------------------------------------|--|--|------|------|--|
| | °C | m | m | | | |
| JAN | 0.65 | 1.3 | 0.26 | | | |
| APR | 2.45 | 2.35 | 0.47 | | | |
| JUL | 2.8 | 2.5 | 0.50 | | | |
| OCT | 1.6 | 1.9 | 0.38 | | | |
| PROPORTION OF SLAB LENGTH THAT WILL CURL = PROPORTION OF UNRESTRAINED WARPING | MONTH | SLAB LENGTH (m) | | | | |
| | | 5 | 10 | 15 | 20 | |
| | JAN | 0.10 | 0.05 | 0.03 | 0.02 | |
| | APR | 0.19 | 0.09 | 0.06 | 0.05 | |
| | JUL | 0.20 | 0.10 | 0.07 | 0.05 | |
| OCT | 0.15 | 0.08 | 0.05 | 0.04 | | |
| APPROPRIATE WARPING RESTRAINT FACTOR (w) | JAN | 0.77 | 0.75 | 0.75 | 0.75 | |
| | APR | 0.76 | 0.74 | 0.73 | 0.72 | |
| | JUL | 0.76 | 0.73 | 0.72 | 0.72 | |
| | OCT | 0.80 | 0.78 | 0.77 | 0.77 | |

These warping restraint factors, w , are used in conjunction with ΔT , the daily temperature range at the upper surface of the roadbase in (EQN 1) to calculate cyclic crack opening movements, TABLE 2.8. (w) values for the other months are interpolated.

2.5 Sub-base Friction Restraint Effects

Sub-base friction forces could restrain the expansion and contraction of roadbase slabs and thus affect crack opening.

This can be evaluated using the average foundation restraint stress data¹¹ where the shear stress rises linearly with displacement to a

value of $6 \times 10^3 \text{ N/m}^2$ at 1.36 mm, and then remains constant for displacements greater than 1.36 mm.

A slab end displacement of 1.36 mm corresponds to crack opening of 2.72 mm, which will hardly ever occur under U.K. climatic conditions and so only the initial rising portion of the restraint stress curve need be considered.

The restraint stress data¹¹ refers to a 150 mm slab; for a 300 mm (slab and surfacing) the restraint stress will be doubled to approximately $(8.8 \times 10^3 \text{ N/m}^2)/\text{mm}$ displacement.

For a long thin slab, these shear stresses on the underside can be considered to act as horizontal tensile stresses within the slab. These tensile stresses determine the restraint to contraction of the slab ends. The ratio -

$$\frac{\text{Restraint to contraction of slab ends}}{\text{Unrestrained contraction of slab ends}} \quad (\text{EQN 6})$$

can be used to determine correction factors for sub-base friction restraint effects, TABLE 2.7.

For a slab of length L, taking 1 m width of pavement and $x = 0$ at the slab centre.

$$\text{Restraint Stress at } x = 8.8 \times 10^6 \cdot \Delta T \cdot \alpha \cdot x \quad \text{N/m}^2$$

$$\text{Tensile Force in Slab at } x = 8.8 \times 10^6 \Delta T \cdot \alpha \int_x^{L/2} x \cdot dx \quad \text{N}$$

$$\text{Restraint to contraction at Slab End} = \frac{8.8 \times 10^6 \Delta T \cdot \alpha}{E \cdot h} \int_0^{L/2} x \cdot dx \quad \text{m}$$

$$\text{Unrestrained contraction at Slab End} = \Delta T \cdot \alpha \cdot \frac{L}{2} \quad \text{m}$$

$$\text{Restraint Ratio (EQN 6)} = \frac{7.33 \times 10^5}{E \cdot h} L^2$$

$$h = 0.2 \text{ m}$$

$$E = 3 \times 10^{10} \text{ N/m}^2$$

$$\text{Restraint Ratio (EQN 6)} = 1.22 \times 10^{-4} L^2$$

TABLE 2.7 CORRECTION FACTORS FOR CRACK OPENING FOR SUBBASE FRICTION EFFECTS

| SLAB LENGTH (m) | 5 | 10 | 15 | 20 |
|-------------------------------------|------|------|------|------|
| RESTRAINT RATIO | .003 | .012 | .027 | .049 |
| CORRECTION FACTOR FOR CRACK OPENING | 1.00 | 0.99 | 0.97 | 0.95 |

2.6 The Magnitude of Crack-Opening Movements

The magnitude of daily crack-opening cycles is determined by -

Roadbase slab length

Roadbase coefficient of thermal expansion

Thickness of Surfacing

Month of the year

Daily crack opening movements for a range of conditions are tabulated, TABLE 2.8. These values are based on the daily temperature ranges at the upper surface of the roadbase, TABLE 2.2, and have been corrected for -

The approx. 6th power mean effect, TABLE 2.3

Warping restraint effects, TABLE 2.6

Subbase friction restraint effects, TABLE 2.7

These horizontal crack-opening movements (1-2 mm) will be used in a program of simulative testing to determine the resistance of U.K. surfacing mixes to thermal reflection cracking.

TABLE 2 . 8

DAILY CYCLIC CRACK OPENING MOVEMENTS IN THE ROADBASE , CORRECTED FOR 6th POWER MEAN , WARPING RESTRAINT & SUBBASE FRICTION RESTRAINT EFFECTS. THESE VALUES OF CYCLIC CRACK OPENING (mm) ARE FOR LEAN CONCRETE WITH THERMAL COEFFICIENT , $\alpha = 10^{-5} / ^\circ\text{C}$, FOR OTHER VALUES OF α THE CYCLIC CRACK OPENING WILL BE PROPORTIONALLY GREATER .

| SLAB LENGTH (m) | JAN | FEB | MAR | APR | MAY | JUN | JUL | AUG | SEP | OCT | NOV | DEC |
|---------------------------------------|-----|-----|------|------|------|------|------|------|------|-----|-----|-----|
| COMPOSITE PAVEMENT , 100 mm SURFACING | | | | | | | | | | | | |
| 5 | .11 | .17 | .27 | .45 | .52 | .57 | .48 | .40 | .34 | .25 | .18 | .13 |
| 10 | .22 | .33 | .53 | .87 | 1.00 | 1.09 | .91 | .78 | .64 | .48 | .34 | .24 |
| 15 | .32 | .48 | .78 | 1.25 | 1.45 | 1.59 | 1.31 | 1.12 | .93 | .69 | .50 | .36 |
| 20 | .42 | .63 | 1.00 | 1.63 | 1.87 | 2.07 | 1.71 | 1.47 | 1.22 | .90 | .65 | .47 |
| COMPOSITE PAVEMENT , 150 mm SURFACING | | | | | | | | | | | | |
| 5 | .08 | .12 | .22 | .34 | .38 | .41 | .37 | .31 | .27 | .19 | .14 | .09 |
| 10 | .15 | .24 | .43 | .65 | .72 | .79 | .70 | .60 | .50 | .37 | .26 | .16 |
| 15 | .22 | .34 | .64 | .96 | 1.05 | 1.15 | 1.01 | .86 | .72 | .54 | .39 | .24 |
| 20 | .29 | .45 | .82 | 1.22 | 1.35 | 1.50 | 1.31 | 1.13 | .95 | .70 | .50 | .32 |
| COMPOSITE PAVEMENT , 200 mm SURFACING | | | | | | | | | | | | |
| 5 | .05 | .08 | .16 | .24 | .28 | .27 | .27 | .23 | .20 | .14 | .11 | .07 |
| 10 | .10 | .16 | .31 | .47 | .53 | .51 | .51 | .45 | .37 | .27 | .20 | .12 |
| 15 | .14 | .23 | .45 | .69 | .77 | .75 | .73 | .65 | .53 | .39 | .30 | .19 |
| 20 | .18 | .30 | .58 | .88 | .99 | .98 | .95 | .85 | .70 | .51 | .39 | .24 |

It is accepted that there will also be a small amount of warping at the slab ends, FIG 2.6, but this will be of secondary importance and can be considered in the conclusions to this project.

Crack-opening movements could also be estimated for other climates by increasing them in direct proportion with monthly mean daily air temperature ranges, relative to those shown, TABLE 2.2.

3.0 TEST AND ANALYTICAL METHODOLOGY

3.1 Introduction to Simulative Testing

A thorough investigation of the effect of thermal stresses would involve heating and cooling sections of composite pavement. This approach is impractical because of the time involved to make and test a sufficiently wide range of materials.

The simulation of thermally induced movements (horizontal crack opening) in the surfacing is the most realistic form of testing.

These reflection cracking fatigue tests can be accelerated from a 24 hr. cycle to 0.1 Hz, SECTION 3.2.

The results of these "fatigue" tests can be developed into a predictive model for thermal reflection cracking by the application of fracture mechanics concepts, SECTION 3.3. The fatigue crack growth constants (A,n) can be determined for U.K. type asphalt surfacing materials with the aid of finite element analyses of the test samples, SECTION 3.4, that determine stress intensity factors (K_1) and crack growth rates (dc/dN) throughout each test.

These material constants (A,n) form the basis of a predictive model for thermal reflection cracking, in conjunction with the equivalent mean stress intensity factor during crack growth (\bar{K}_1) which is also evaluated from the finite element results, SECTION 3.4, and depends on the value of n.

A master curve, SECTION 3.4, enables \bar{K}_1 to be determined and fatigue life predicted, for the range of values of crack opening, Effective Young's Modulus of the surfacing and thickness of the surfacing that are likely to be encountered in the U.K.

It can also be seen from the loads involved in the finite element analyses, SECTION 3.5, that the surfacing will offer negligible restraint to crack opening in the roadbase.

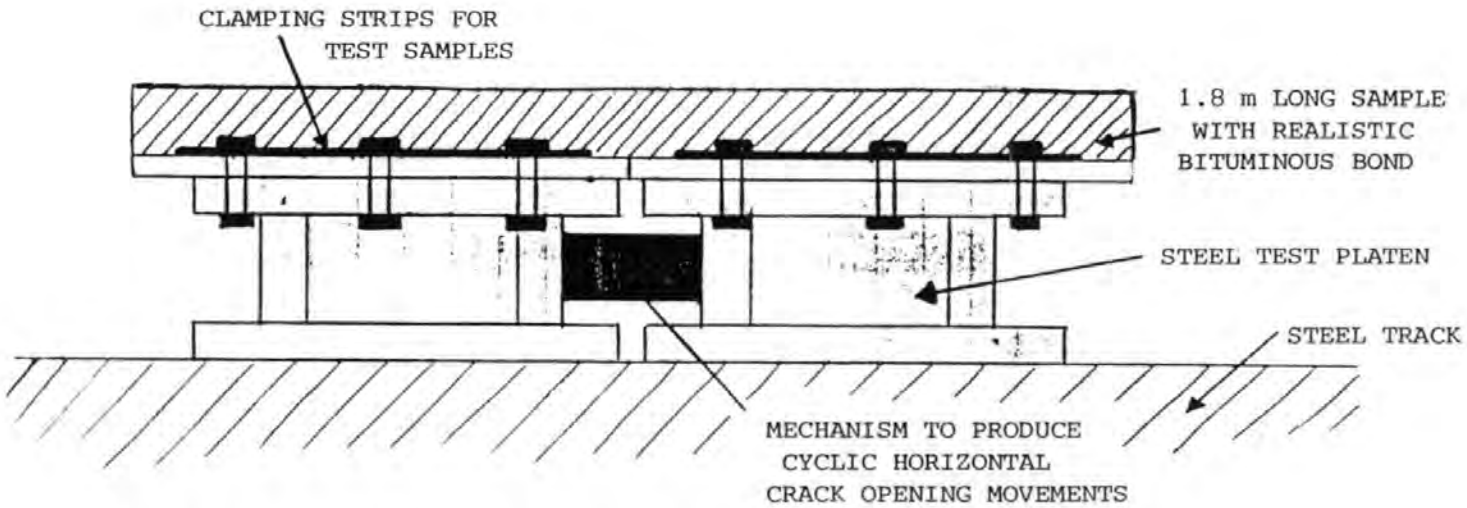
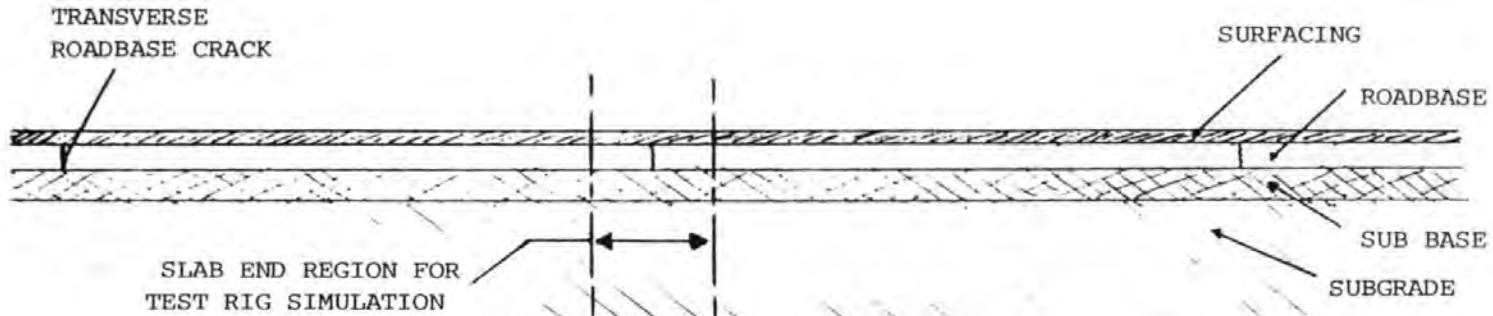
Ideally, a simulative test rig should apply this constant cyclic crack opening to asphalt surfacing samples, throughout each test. However, this is not a serious constraint to testing because adequate values of (K_1) and (dc/dN) for fracture mechanics analysis, can still be obtained with a test rig that does yield slightly in the initial stages of each test when the surfacing is uncracked and the loads will be very high and indeterminate.

The simulative testing relates to longitudinal thermal movements about transverse cracks in the cement-bound roadbase layer. A longitudinal section of a composite pavement is shown, FIG 3.1, together with the basic design for the simulative test rig.

Simulative testing is desirable for study of the effects of certain mechanisms associated with reflection cracking.

- (i) The possibility of bond break or yield at the interface between the asphalt surfacing and the lean concrete roadbase.
- (ii) The tendency of asphaltic materials to multiple cracking especially with "applied displacement" type loading. This effect causes problems because the application of fracture mechanics theory to test results is practical only when there is a single crack which follows a straight path.
The likelihood of multiple, convoluted cracking means that empirical testing is necessary for validation of the application of fracture mechanics concepts to reflection cracking.
- (iii) The need for later modification of the test regime to study the combined influence of thermal and traffic movements, the interaction of which may not be predictable by any other means.

FIG 3 . 1
A LONGITUDINAL SECTION OF A COMPOSITE PAVEMENT AND THE BASIC DESIGN
FOR THE SIMULATIVE TEST RIG FOR ASPHALT SURFACING SAMPLES .



The slab-end region modelled by "composite" samples with a realistic bituminous membrane bond, must be at least 1.8 m to allow bond break or yield to develop and yet leave sufficient bond intact to prevent an unrepresentative failure by debonding.

A considerable amount of material is required for such large samples. The undamaged portions of these samples can be re-used as short (0.45 m) samples. These short samples will require an epoxy resin bond to prevent debonding.

A comparison of fatigue lives of the two types of samples does confirm how representative the short, epoxy resin bonded samples are. It is considered that internal shear within the short samples has a similar stress relieving effect as yield of the bituminous bond in long samples and so both are representative of conditions in the road.

It must be mentioned that the use of bituminous emulsion as a curing membrane for lean concrete, although widespread, is not mandatory.

The alternatives permitted in the specification⁴ are an aluminised curing compound containing metal flakes, or polythene sheets that are subsequently removed. The bond between the lean concrete and the surfacing will be less reliable when these treatments are used, and so the likelihood of thermal reflection cracking will be reduced compared to when the bituminous emulsion, BS 434,³⁸ is used.

The test samples model surfacings that are "well bonded" to the concrete layer, as this is believed to represent the usual situation.

A surfacing that is not bonded may be more susceptible to other types of deterioration and so this is not advisable.

3.2 Reasons for Accelerated Testing

In order to be able to test a range of samples, testing must be accelerated from a 24 hr. cycle in the pavement to approximately 0.1 Hz with the test rig.

With an elastic material acceleration of testing presents no problems, but with a visco-elastic material some consideration of time and temperature is necessary because of stress relaxation effects, which become more significant at higher temperatures and slow loading rates.

The beneficial effects of stress relaxation can be seen from controlled strain fatigue tests on a sandsheet mix, Pell 1962²⁸, FIG 3.2.

An increase in test temperature from 0 → 40°C at 25 Hz increases the fatigue life by a factor of 1,000 at a strain of 5×10^{-4} .

A slowing down of test frequency from 10^{-1} Hz to 10^{-5} Hz would give a similar increase in fatigue life, also due to stress relaxation.

The aim of accelerated testing is to balance the reduced stress relaxation at a higher frequency, with increased stress relaxation from using a higher test temperature, or a softer grade of bitumen. The determination of equivalent temperatures for accelerated testing is covered in SECTION 4.

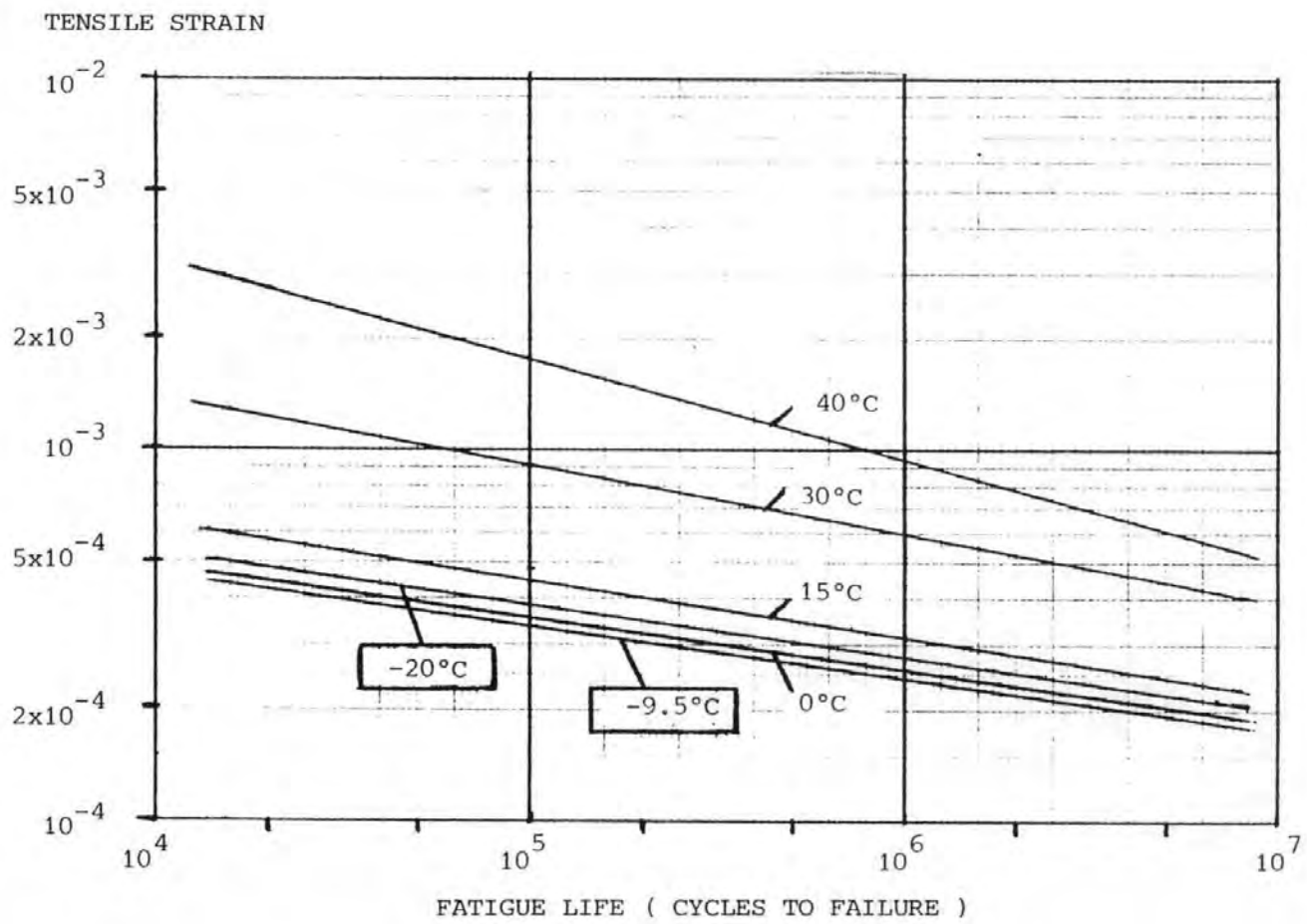
3.3 Fracture Mechanics

An introduction to the fatigue crack growth equation, $dc/dN = AK_1^n$ (EQN 2), is given in SECTION 1.8.

(EQN 2) is an empirical equation that refers to the phase of steady macroscopic crack growth that follows microscopic crack initiation and precedes unstable fracture. This is the only relevant phase of crack growth with thermal reflection cracking.

"FATIGUE LINES" FOR CONTROLLED STRAIN FATIGUE TESTING OF A SANDSHEET
MIX AT 25 Hz AND VARIOUS TEMPERATURES , PELL 28 , 1962

FIG 3 . 2



The crack initiation must be almost immediate because of the high localised stresses when the surfacing is uncracked and it is well bonded to the concrete. Also the unstable fracture will not occur until the crack has reached the very last "threads" of material and this will be undetectable.

Three geometrical modes of crack growth (opening mode, in-plane shear and transverse shear) were defined by Irwin²². Only the first (opening mode) is relevant to thermal reflection cracking and the crack tip stresses can be characterised by the opening mode stress intensity factor K_1 .

Irwin²² noted that the crack tip stress field has the same shape for all crack tips regardless of the shape of the component and the magnitude of the stresses, i.e. the stresses are inversely proportional to \sqrt{r} where r is the distance into the material ahead of the crack tip. Thus $\sigma_{(r)} \cdot \sqrt{r}$ is a constant and this constant is the opening mode stress intensity factor, which has the value K_1 where -

$$K_1 = \sigma_{(r)} \sqrt{2\pi r} \quad (\text{EQN 7})$$

(EQN 7) was developed from analysis of an infinite sheet, Westergaard²¹, and is only valid for real components in the limit as $r \rightarrow 0$.

(EQN 7) is also strictly only valid for ideal linear elastic or linear visco-elastic materials. Its application to real materials where there is usually a small crack-tip yield zone, is only held to be valid if the average stress in the uncracked section of the component is less than 80% of the yield stress³⁹.

In general, K_1 is determined by plotting $\sigma_{(r)} \sqrt{2\pi r}$ vs r ahead of the crack path and extrapolating to $r = 0$ where the curve should level out.

Structures such as cracked composite pavements require repeated finite element analysis with a range of crack lengths, SECTION 3.4,

to determine crack tip stresses (σ_r) and K_1 as a function of crack length. Once the variation of K_1 vs crack length is known, the material constants A, n can be determined from crack growth rates during fatigue tests.

Even for a linear visco-elastic material, A and n can be expected to vary with test conditions of temperature and frequency, although there may be regions where n is almost constant.

Schapery's original theory of crack growth in linear visco-elastic materials²⁷ relates A and n to visco-elastic material properties -

$$A = \frac{\Pi}{6\sigma_m^2 I^2} \left(\frac{(1-\nu^2)D}{2\Gamma} \right)^{\frac{1}{m}} \left(\Delta+ \int_0^{\Delta+} w(+)^{2(1+\frac{1}{m})} dt \right) \quad (\text{EQN 8})$$

$$n = 2\left(1 + \frac{1}{m}\right) \quad (\text{EQN 9})$$

where: σ_m = tensile strength

I = an unknown factor between 1 and 2

ν = Poisson's ratio

D = creep compliance at time = 1 second

Γ = fracture energy per unit area of crack surface produced

m = slope of a log-log plot of creep compliance vs time

$\Delta+$ = period of 1 cycle of loading

w(+)= wave shape of the stress intensity factor vs time

Schapery's equations (EQNS 8 & 9) have the potential to make fatigue testing redundant because A and n are related to the results of static tests. However, the creep compliance, fracture energy and tensile strength will all vary with time and temperature and so extensive testing would still be necessary.

Previous researchers who have investigated Schapery's equations,^{18 32} have found the difference between experimental and predicted A values to be rarely less than a factor of 10.

Schapery's equation for n (EQN 9) is probably more useful, but it is only valid for conditions of linear visco-elasticity which implies low strains and high fatigue lives.

Molenaar³² noted that the error factor between experimental and theoretical n values was related to the air void content of the mix, FIG 3.3. This relationship implied that Schapery's equation for n was valid for mixes with void contents less than 3%. This is probably so because mixes with lower % void contents can take higher strains before the onset of yield and non-linearity.

Schapery's theory has recently been extended⁴⁰ to apply to non-linear visco-elastic materials, but a different parameter, the J-Integral³⁹, is required to characterise crack-tip stresses because K_1 relates to the inverse \sqrt{r} stress intensity which only happens with linear elasticity or linear visco-elasticity.

Schapery's extended theory will not be necessary for U.K. Type rolled asphalt surfacing mixes, because the air voids content will be around 3% and Schapery's original equation for n (EQN 9) can be considered to be valid³².

For these mixes where the air void content is 3% or less, tensile creep tests and (EQN 9) can be used to determine theoretical n values which greatly assist in the evaluation of A which can vary dramatically with test conditions (frequency and temperature).

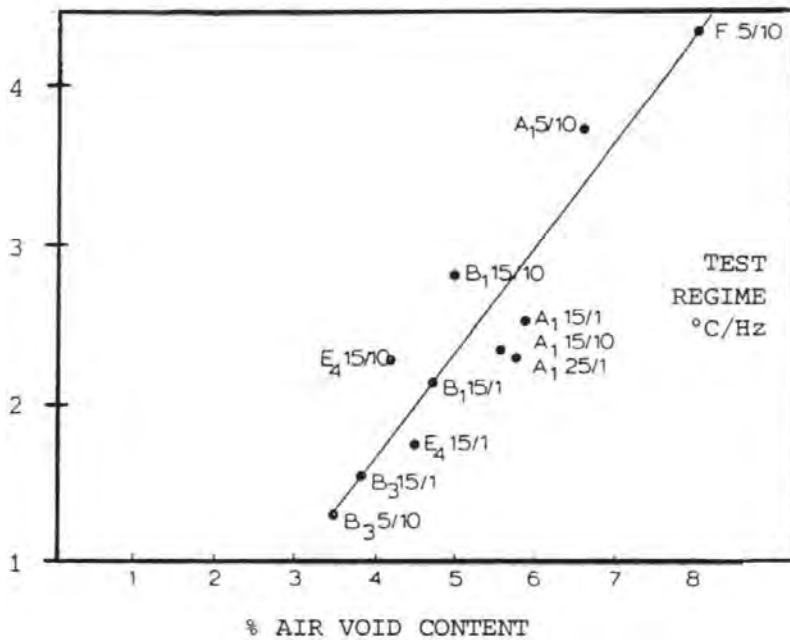
This fracture mechanics "approach" enables the prediction of thermal reflection cracking fatigue lives, when the variation of K_1 with crack length is known, by the integral form of (EQN 2);

$$N_f = \int_0^h \frac{1}{AK_1^n} dc \quad (\text{EQN 10})$$

FIG 3 . 3

THE RATIO BETWEEN EXPERIMENTALLY DETERMINED "n" VALUES AND THEORETICAL VALUES PREDICTED BY SCHAPERY'S THEORY , EXPRESSED AS A FUNCTION OF THE AIR VOID CONTENT OF THE MIX, MOLENAAR³², 1983 .

$$\text{RATIO : } \frac{\text{"n" THEORETICAL}}{\text{"n" EXPERIMENTAL}}$$



KEY TO MIX TYPES AND % ADDED BITUMEN

- A₁ GRAVEL-SAND ASPHALT , 5% 50PEN
- B₁ OPEN GRADED ASPHALTIC CONCRETE , 5% 100PEN
- B₃ OPEN GRADED ASPHALTIC CONCRETE , 5% 50PEN
- E₄ DENSE GRADED ASPHALTIC CONCRETE , 6.4% 100PEN
- F COLD ASPHALT , 7.5% (100PEN + FLUXOIL)

where N_f = fatigue life (cycles to failure)

h = surfacing thickness

c = crack length

In thermal reflection cracking, the surfacing is subjected to cycles of crack opening movement, which induce cycles of alternating tensile and compressive stresses.

Thus the cycle of K_1 at a given crack length must alternate from +ive to -ive.

Although the exact mechanism of crack growth is uncertain, only the +ive pulse of K_1 will be considered to cause cracking.

3.4 Finite Element Analysis

Finite element analysis of the test samples is necessary to determine K_1 values during crack growth, for fracture mechanics analysis of test results and prediction of fatigue life.

The PAFEC 75 FINITE ELEMENT PACKAGE, which incorporates a crack-tip "module", was used for the analysis.

The test samples investigated were approximately 100mm thickness of U.K. type rolled asphalt two-course surfacing comprising 60mm basecourse + 40mm wearing course. This is representative of the more lightly trafficked end of the design spectrum where thermal effects are more likely to be significant.

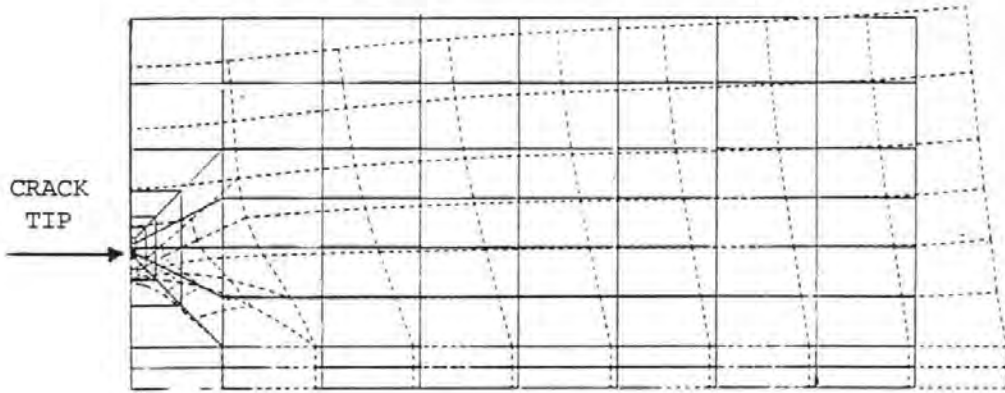
The finite element model used was a half-sample, with half the actual crack opening displacement applied to the test platen and "in-plane" restraints for the test platen base and the crack plane.

Six different but related meshes were used to model different crack lengths, of which three are illustrated, FIG 3.4.

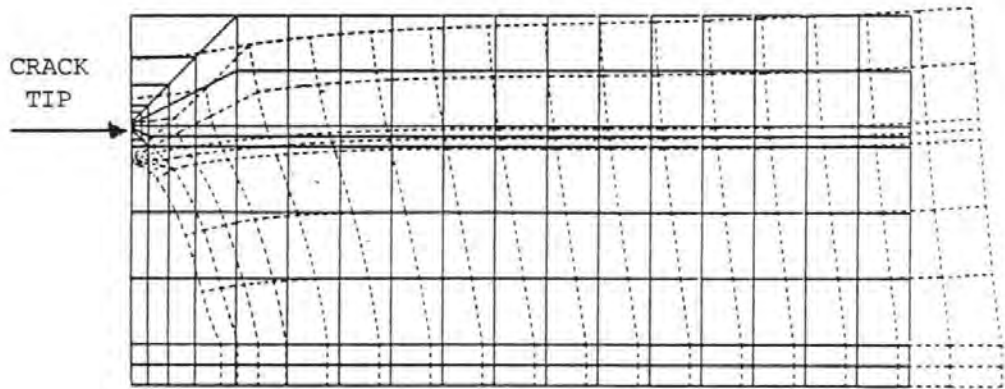
FIG 3 . 4

THREE EXAMPLES OF THE " PAFEC " FINITE ELEMENT MESH FOR HALF A 450 mm x 95 mm SURFACING SAMPLE BONDED TO 12 mm THICK STEEL PLATES . THE DEFORMED SHAPE OF THE SAMPLES IS SHOWN BY THE DOTTED LINES .

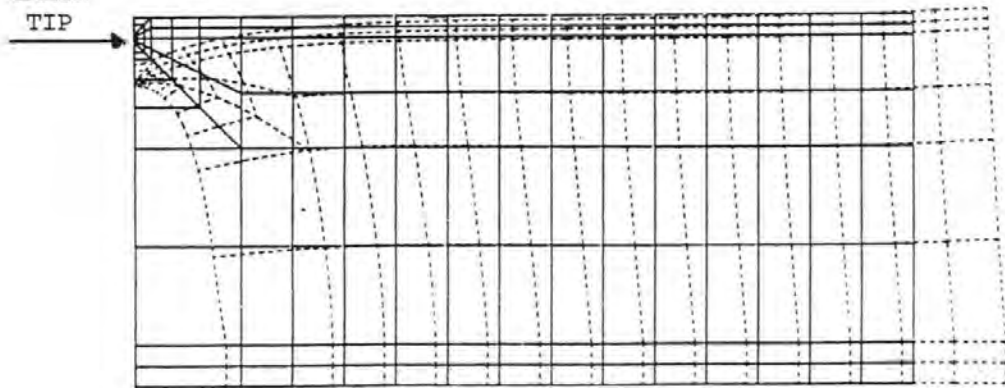
CRACK RATIO (c/h) = 0.284



CRACK RATIO (c/h) = 0.652



CRACK RATIO (c/h) = 0.926



The basic parameters for the analysis were:-

crack opening cycle, CO = 1mm

thickness of surfacing, h = 95mm

Effective Youngs Modulus (basecourse), $E'_B = 10^8 \text{ N/m}^2$

The analysis was repeated for three ratios of Effective Modulus (basecourse : wearing course) i.e. 1:1, 2:1 and 3.5:1. The Effective Modulus of the basecourse is usually higher because of the lower bitumen content.

Also, the analysis was performed in the plain strain mode with $\nu = 0.45$, Poisson's ratio has been observed to tend to 0.5 for visco-elastic materials at slow loading rates or at high temperatures⁴¹.

The dimensions of the smallest element at the crack tip were, 0.3mm in the basecourse and 0.2mm in the wearing course. This was considered to give more than sufficient precision, as changing the size of the crack tip element from 0.3mm to 1.5mm gave the same value of K_1 within 1%, using the procedure for calculating K_1 from (EQN 7) extrapolated to $r=0$.

The values of K_1 obtained from the analysis are peak-to-peak values corresponding to a crack-opening cycle of 1.0mm.

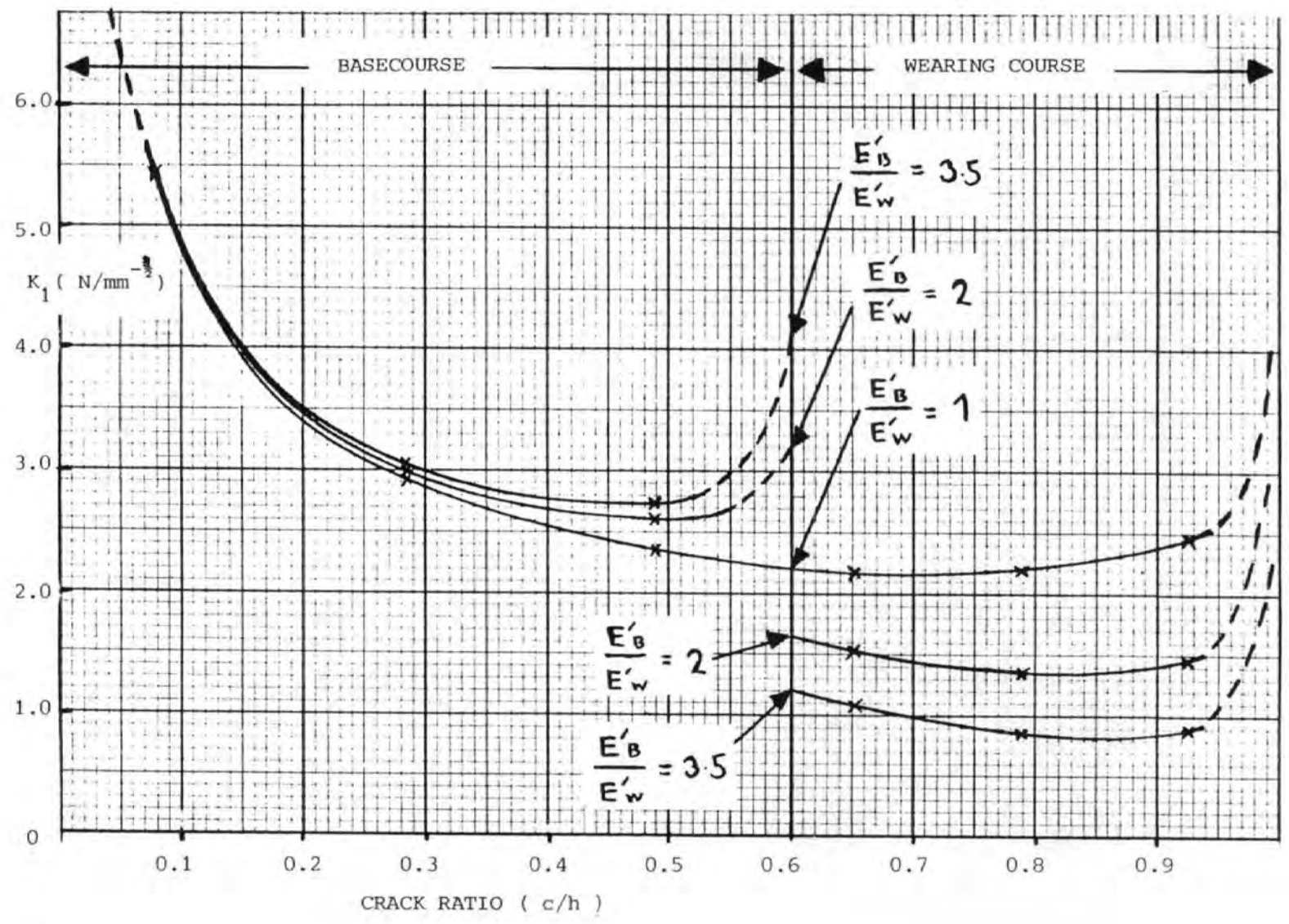
The peak positive values of K_1 can be assumed to be half these values because the cycle of applied strain is sinusoidal and this will induce a sinusoidal cycle of stress with a time lag, in a visco-elastic material.

The peak positive values of K_1 can be expressed as $K_1 = f(\text{crack length})$, FIG 3.5.

FIG 3.5 is, in effect, a master curve that can be used to determine K_1 vs c/h for other situations.

By virtue of the theory of elasticity, K_1 vs c/h , will increase in direct proportion to both crack opening and the Effective Modulus

FIG 3 . 5
 THE VARIATION OF PEAK POSITIVE K_1 (K_1 IS CYCLIC) WITH CRACK RATIO .
 95 mm TWO-COURSE SURFACING
 1 mm CYCLIC CRACK OPENING
 10^8 N/m² EFFECTIVE MODULUS OF THE BASECOURSE (E'_B)



of the basecourse.

K_1 vs c/h , can also be determined for any thickness of surfacing where the ratio of basecourse to wearing course thickness is still 60:40.

Consider the two surfacing samples, FIG 3.6. The stress distribution will be identical in both samples when the crack-opening in SAMPLE II is $h/95$ mm.

The stress intensity factor, K_1 , is related to the crack-tip stress field by (EQN 7) -

$$K_1 = \sigma(r) \sqrt{2\pi r} \text{ as } r \rightarrow 0$$

In SAMPLE II, $\sigma(r)$ will occur at a shorter distance from the crack tip than in SAMPLE I by a factor $h/95$. Thus:-

$$K_1 (\text{SAMPLE II}) = \sqrt{\frac{h}{95}} K_1 (\text{SAMPLE I}) \quad (\text{EQN 11})$$

When crack opening is equal in both samples:-

$$\begin{aligned} K_1 (\text{SAMPLE II}) &= \sqrt{\frac{h}{95}} K_1 (\text{SAMPLE I}) \cdot \frac{95}{h} \\ \Rightarrow K_1 (\text{SAMPLE II}) &= \sqrt{\frac{95}{h}} K_1 (\text{SAMPLE I}) \quad (\text{EQN 12}) \end{aligned}$$

Thus for surfacings of thickness h (mm), where crack opening, Effective Modulus and crack length ratio are the same, the value of K_1 in FIG 3.5 is multiplied by $\sqrt{95/h}$.

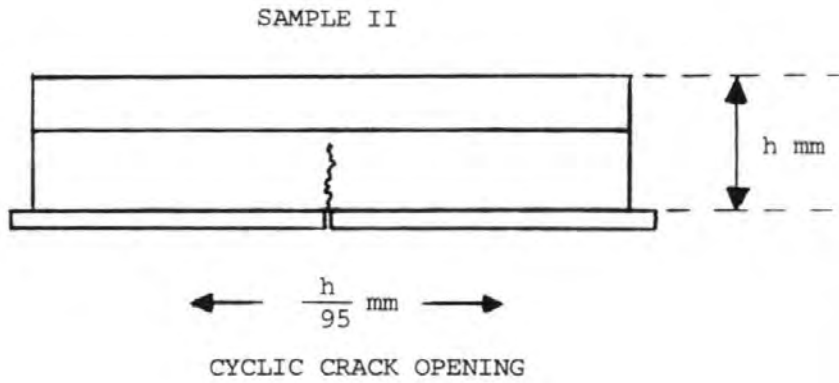
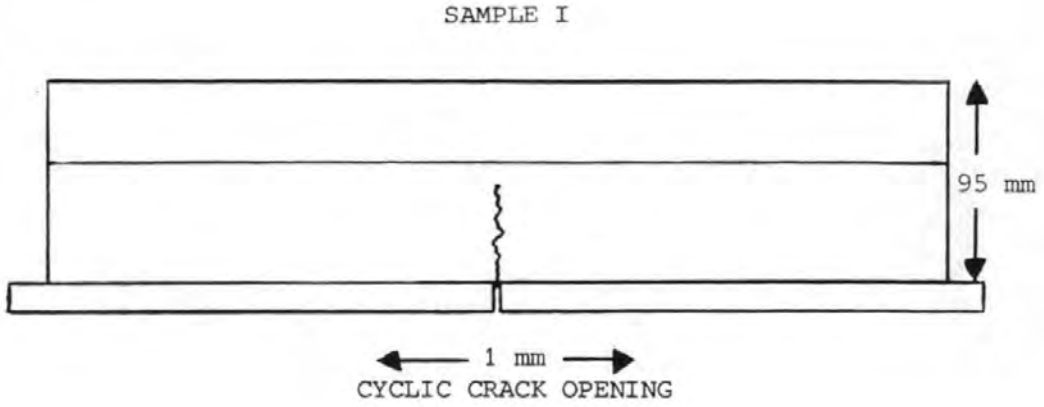
The use of $K_1 = f(\text{crack length})$ for the determination of fatigue life (EQN 10) is simplified by defining an equivalent mean K_1 (\bar{K}_1) that gives the same fatigue life as the range of K_1 vs crack length:-

$$Nf = \frac{h}{A\bar{K}_1^n} \quad (\text{EQN 13})$$

$$\text{where } \bar{K}_1 = \left(\frac{1}{h} \int_0^h \frac{1}{K_1^n} dc \right)^{-\frac{1}{n}} \quad (\text{EQN 14})$$

FIG 3 . 6

TWO SAMPLES OF DIFFERENT THICKNESSES WITH IDENTICAL STRESS DISTRIBUTIONS AT THE SAME CRACK RATIO (c/h) .



The equivalent \bar{K}_1 for a given range of K_1 vs crack length will vary slightly with the actual value of n . Thus \bar{K}_1 must be evaluated for a range of n ($n=4, 6$ & 8) and values can then be interpolated for other values of n .

Also, \bar{K}_1 values have to be evaluated separately for the basecourse and wearing course when a two-course surfacing is used.

31 increments of h and numerical integration were used and the results are presented in the form of a "master curve", FIG 3.7.

3.5 Consistency of Crack Opening Movements

The final assumption involved in the analysis of thermal stresses, SECTION 1.7, was that the stiffness of the surfacing is sufficiently low that it will offer negligible resistance to cyclic crack opening in the lean concrete so this will be constant regardless of crack length ratio (c/h).

The forces required to produce crack-opening in an asphaltic surfacing were also determined by the finite element analysis, TABLE 3.1.

TABLE 3.1 FORCE PER METRE WIDTH, TO PRODUCE 1mm CRACK OPENING IN 95mm SURFACING WHERE $E'_B = 10^8$ N/m² AND $E'_B/E'_W = 2$.

| CRACK LENGTH RATIO (c/h) | FORCE PER METRE WIDTH (N) |
|--------------------------|---------------------------|
| 0.079 | 6444 |
| 0.283 | 3843 |
| 0.489 | 2657 |
| 0.652 | 1828 |
| 0.789 | 1268 |
| 0.926 | 960 |

These "surfacing restraint" forces can be considered to act over the entire length of the concrete slabs. The forces are generated in the slab end regions and so they must act over at least 95-99%

FIG 3 . 7

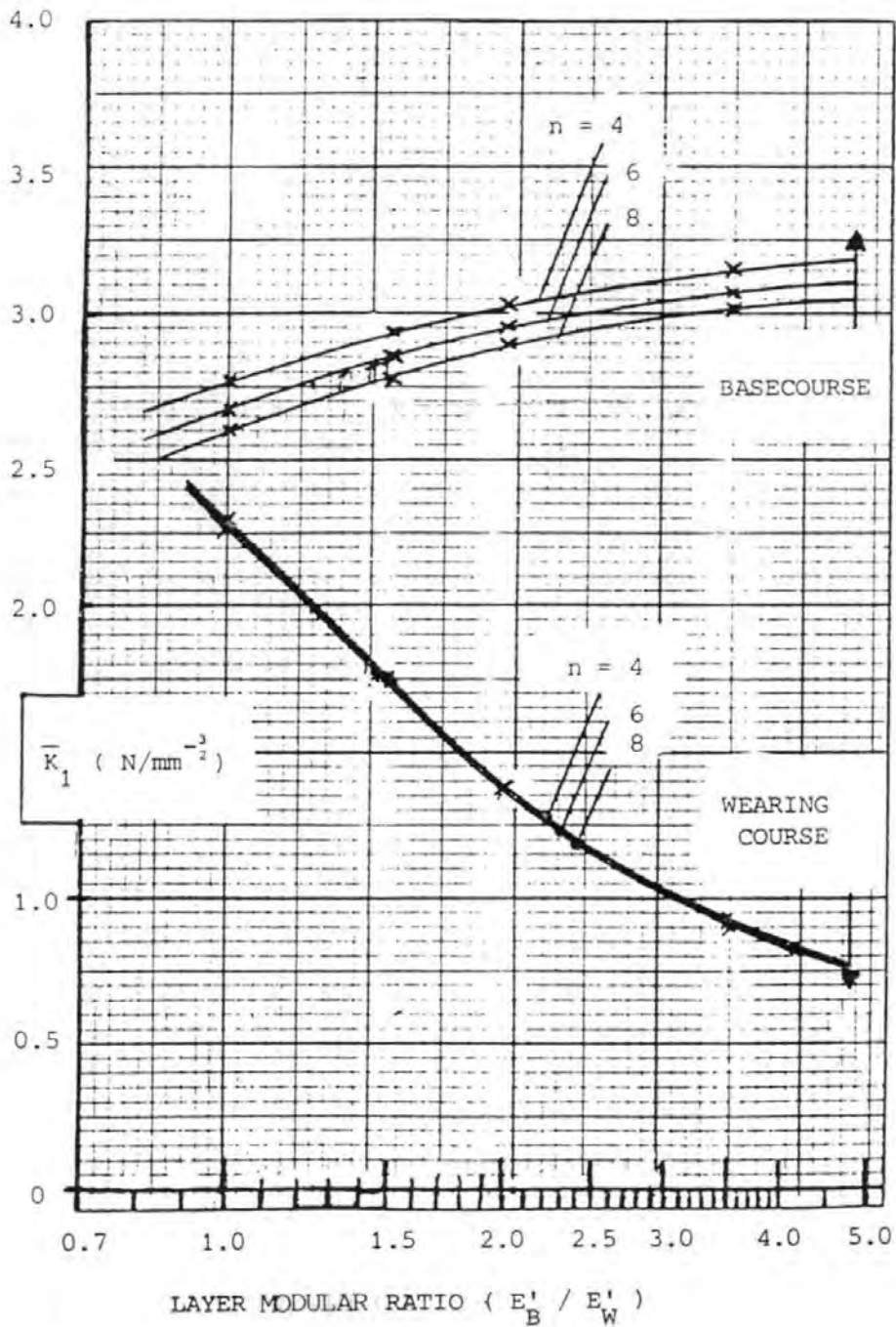
MASTER CURVE OF EQUIVALENT MEAN K_1 (\bar{K}_1) FOR THE DETERMINATION OF FATIGUE LIFE -

$$N_F = \frac{h}{A \cdot \bar{K}_1^n}$$

CYCLIC CRACK OPENING (CO) = 1 mm , $\bar{K}_1 \propto CO$

EFFECTIVE MODULUS, BASECOURSE (E'_B) = 10^8 N/m² , $\bar{K}_1 \propto E'_B$

THICKNESS OF SURFACING (h) = 95 mm , $\bar{K}_1 \propto \frac{95}{h}$



of slab length, so this assumption will only slightly over-estimate surfacing restraint effects.

A restraint ratio (R) similar to that used for sub-base restraint effects, SECTION 2.5, is defined to assist in the calculation:-

$$R = \frac{\text{Restraint to contraction of slab ends (mm)}}{\text{Unrestrained contraction of slab ends (mm)}} \quad (\text{EQN 15})$$

Restrained crack opening is then given by:-

$$CO_{\text{RESTRAINED}} = CO_{\text{UNRESTRAINED}} \left(\frac{1}{1+R} \right) \quad (\text{EQN 16})$$

R(EQN 15) can be evaluated for 0.2m thick roadbase slabs where $E_{\text{LEAN CONCRETE}} = 3 \times 10^{10} \text{ N/m}^2$ and slab length (L) = 10m = 10^4 mm , taking 1m width of pavement:-

$$\begin{aligned} R &= (\text{Strain in slab} \times L) / CO \\ \Rightarrow R &= \left(\frac{\text{Force per mm CO} \times CO \times 10^4}{\text{CSA SLAB} \times E_{\text{LEAN CONCRETE}}} \right) / CO \\ \Rightarrow R &= 1.67 \times 10^{-6} (\text{Force per mm CO}) \quad (\text{EQN 17}) \end{aligned}$$

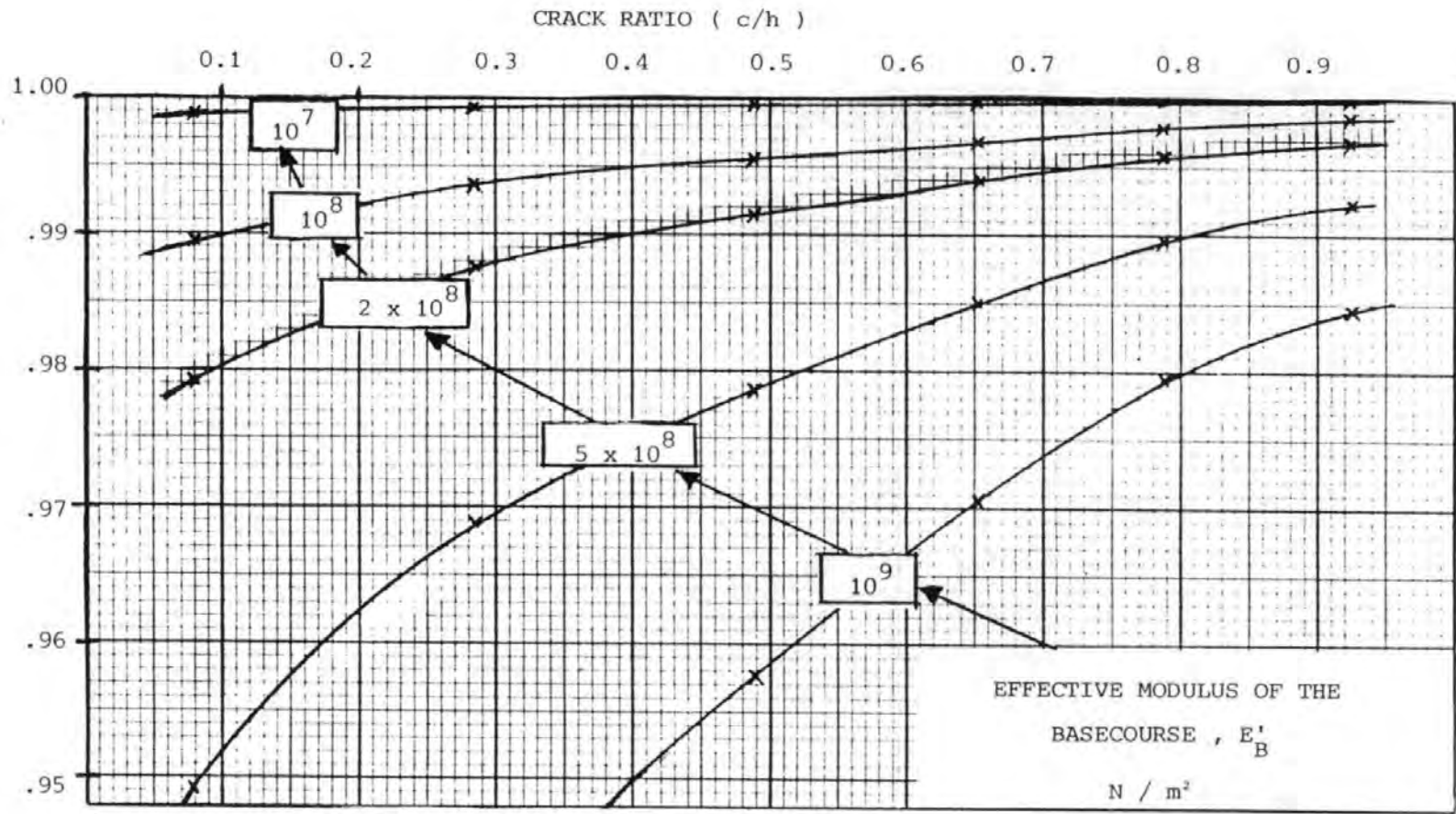
The restrained crack opening can be evaluated using (EQN 17), (EQN 16) and TABLE 3.1, for a range of values of E_B^1 , and is illustrated, FIG 3.8.

The Effective Modulus of the basecourse (E_B^1) will rarely exceed $2 \times 10^8 \text{ N/m}^2$, so crack-opening will only vary by 1-2% which is negligible. Also crack-opening will be assisted by small internally generated tensile stresses in the surfacing.

RESTRAINT OF CYCLIC CRACK OPENING BY SURFACING, AS A FUNCTION OF THE EXTENT OF CRACKING IN THE SURFACING (c/h) AND THE EFFECTIVE MODULUS OF THE BASECOURSE (E'_B)

FIG 3 . 8

LAYER MODULUS RATIO, (E'_B / E'_M) = 2.0
 SURFACING THICKNESS, $h = 95 \text{ mm}$



RATIO : $\frac{\text{CRACK OPENING WITH SURFACING RESTRAINT}}{\text{UNRESTRAINED CRACK OPENING}}$

4.0 BITUMEN STIFFNESS AS A REDUCED PARAMETER IN ACCELERATED TESTING

4.1 Introduction to Accelerated Testing

The need for accelerated testing has been summarised, SECTION 3.2. Accelerated tests can be performed with equal cyclic crack opening (CO) and equal cyclic bitumen stiffness.

In these accelerated tests, the mix stiffness and consequently both stress and strain will be reproduced. More importantly, fatigue crack growth per cycle will also be reproduced because it is related to bitumen stiffness-mix stiffness.

Thermal reflection cracking resulting from thermal movements in cracked cement-bound roadbase, occurs under low frequency loading, conditions far removed from those applied in conventional fatigue testing to simulate traffic loading.

Low frequency and/or high temperature produces low stiffness conditions. Under these low stiffness conditions, brittle fracture does not happen and crack growth is a result of severe localised deformation at the crack-tip. Fracture or deformation of the aggregate particles is unlikely and so it seems reasonable to expect the crack growth rate to be determined by bitumen stiffness.

This hypothesis is supported by observations of the fracture process in bitumen and bituminous mixes. Heukelom⁴², Majidzadeh and Herrin⁴³ and Schapery²⁷, SECTION 4.2.

In the determination of cyclic bitumen stiffness, some consideration of the non-sinusoidal nature of crack opening and the temperature ranges over which it occurs is necessary in order to determine monthly 24 hour sinusoidal cycles at constant temperature that produce the same crack growth as the actual cycles, SECTION 4.3 and 4.4.

A limited amount of stress-relaxation data has been published for a typical U.K. Hot Rolled Asphalt Basecourse mix⁴⁴. This data is used, SECTION 4.3, to compare the cycles of stress produced by 24 increments of crack opening of actual and sinusoidal cycles of equal amplitude.

Typical values for the crack growth constants A, n from the test results are used, together with the fracture mechanics criterion of equal ΣAK_1^n for the positive increments of K_1 , which implies equal crack growth per cycle, SECTION 4.3.

Monthly 24 hour sinusoidal cycles, so defined, can be accelerated to approx 0.1hz by using either a higher temperature or a softer grade of bitumen, and the criterion of equal bitumen stiffness defined by Van der Poel's monograph³⁴.

The test conditions of bitumen stiffness for two 50 PEN bitumens, and equi-stiffness test temperatures for testing with 50 and 200 PEN bitumen, are determined, SECTION 4.5.

Bitumen stiffness can be referred to as a "reduced parameter" for fatigue testing because it combines the influences of three variables:-

Test Temperature, Test Frequency and Bitumen Grade.

4.2 Observations of the Influence of Bitumen Stiffness in the Fracture Process

The stiffness of bitumen³⁴ was found by Heukelom⁴² to be a useful indicator of the variation of the tensile strength of bitumen and bituminous mixes, FIG 4.1, with test conditions of temperature, loading rate and bitumen grade.

It is the opinion of the author that the same is true for the fatigue of bituminous mixes because fatigue and tensile fracture are the same process; fracture = fatigue (NF=1).

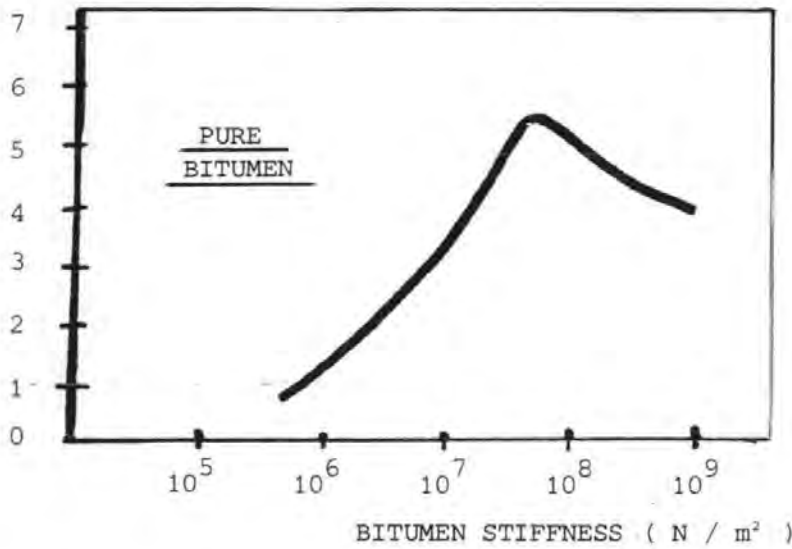
Heukelom⁴² also reported fatigue tests on pure bitumen, where the relationships between both stress and strain and NF could be correlated in terms of bitumen stiffness.

In later wheel-tracking fatigue tests of bituminous mixes reported by Van Dijk⁴⁵, fatigue life (NF) vs stress and strain data were

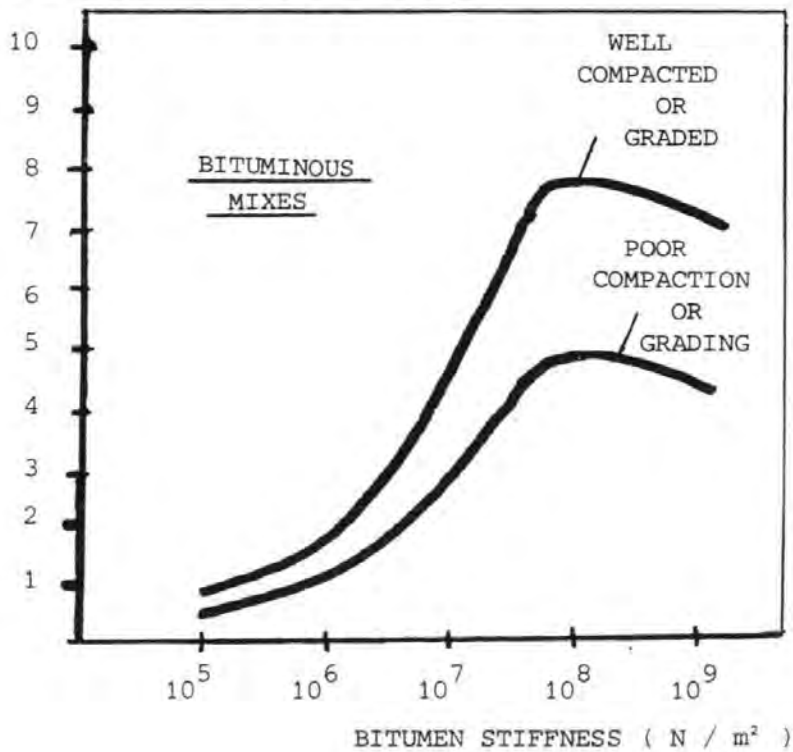
FIG 4 . 1

THE RELATIONSHIP BETWEEN THE TENSILE STRENGTH OF BOTH PURE BITUMEN AND BITUMEN / AGGREGATE MIXES AND BITUMEN STIFFNESS, HEUKELOM⁴², 1966 .

TENSILE STRENGTH (N / m²) x 10⁶



TENSILE STRENGTH (N / m²) x 10⁶



correlated in terms of mix stiffness and total energy dissipated during the test.

When evaluating the fatigue life of a specific mix, either bitumen stiffness (S_{BIT}) or mix stiffness (S_{MIX}) can be used to correlate with NF because $S_{MIX} \iff S_{BIT}$.

This is evident from the SHELL nomograph⁴⁶, FIG 4.2, which is valid for any mix for S_{BIT} greater than 10^7 N/m².

Creep tests⁴⁷, FIG 4.3, are required for individual mixes to evaluate the S_{BIT} vs S_{MIX} relationship for S_{BIT} lower than 10^7 N/m². These creep tests⁴⁷ were carried out in compression for correlation with a rutting model.

Creep tests can be carried out in either tension or compression, tension is more relevant for application to fracture and fatigue.

The work of SHELL investigators^{34,42,45,46}, is related to fracture and fatigue under rapid loading and moderate to low temperatures corresponding to high bitumen stiffness.

Thermal reflection cracking occurs at much lower levels of bitumen stiffness where the fracture process is even more likely to be controlled by bitumen stiffness, because crack growth is more likely to be through the bitumen films.

The work of Majidzadeh and Herrin⁴³ relates to the tensile fracture of thin films of bitumen at conditions of low bitumen stiffness more relevant to thermal reflection cracking. The basic failure mechanism observed by these researchers was hydrostatic failure, FIG 4.4.

This failure mechanism was observed to break down if moderate stresses developed during applied loading, leading to fracture by tensile rupture and if high stresses developed during loading, leading to brittle fracture. These observations of Majidzadeh and Herrin are illustrated, FIG 4.5, in terms of zones of fracture mode on a plot of test conditions of bitumen stiffness (72 PEN BITUMEN; PI Unknown; Assumed PI + 0.35) vs the aspect ratio (diameter:thickness) of the films.

FIG 4 . 2

THE " SHELL " NOMOGRAPH RELATING MIX STIFFNESS AND BITUMEN STIFFNESS AT HIGH STIFFNESS CONDITIONS , CLAESSEN et al⁴⁶ , 1977 .

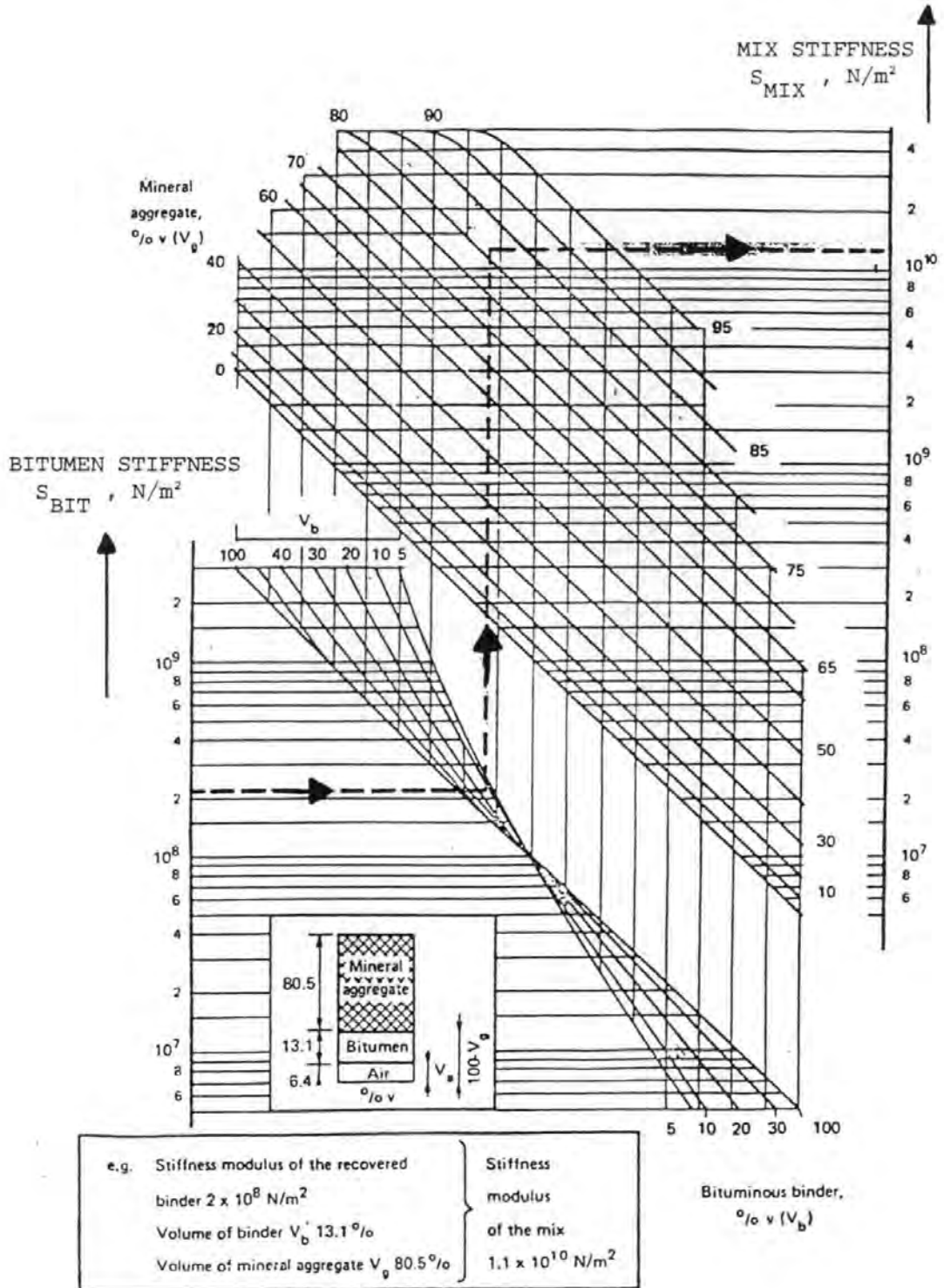
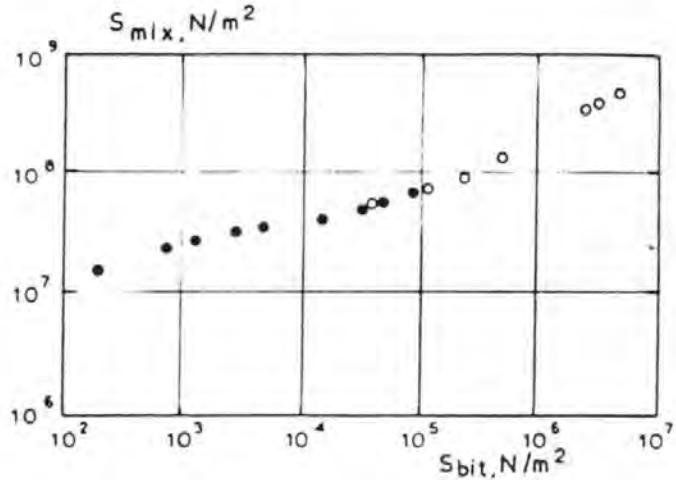


FIG 4 . 3

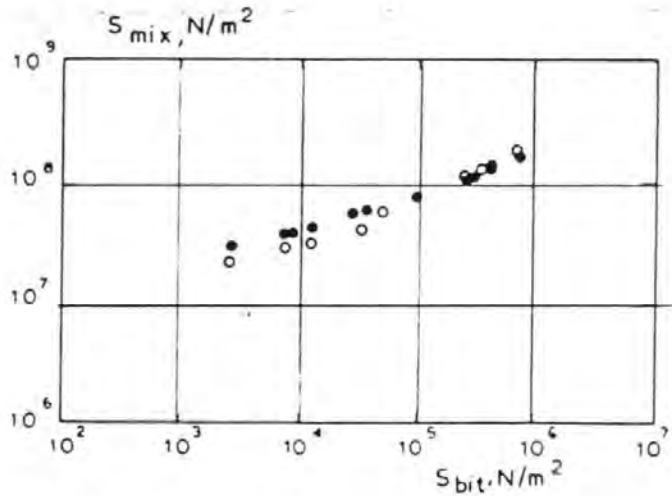
CREEP TESTS TO RELATE MIX STIFFNESS TO BITUMEN STIFFNESS FOR INDIVIDUAL MIXES AT LOW STIFFNESS CONDITIONS, HILLS, BRIEN & VAN DE LOO⁴⁷, 1974 .

"COMPRESSIVE CREEP"

SANDSHEET MIX WITH
CRUSHED SAND,
7% BITUMEN,
10% AIR VOIDS.
TESTED AT TWO
TEMPERATURES,
10°C & 30°C
AND STRESS LEVEL
0.4 MN/m²



SANDSHEET MIX WITH
CRUSHED SAND,
7% BITUMEN,
10% AIR VOIDS.
TESTED AT TWO
STRESS LEVELS,
0.1 & 0.8 MN/m²
AND TEMPERATURE
20°C



RICH ASPHALTIC
CONCRETE MIX,
5.8% BITUMEN,
2.5% AIR VOIDS.
TESTED WITH TWO
BITUMEN GRADES,
50/60 & 180/200 PEN,
TEMPERATURE 20°C
AND STRESS LEVEL
0.1 MN/m²

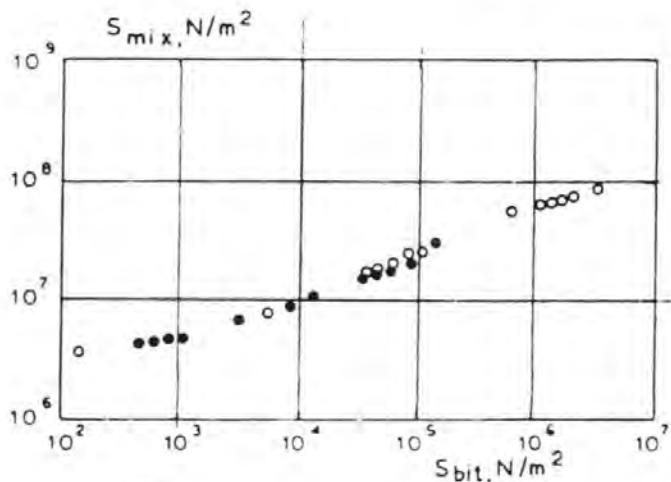


FIG 4 . 4

THE THREE MODES OF TENSILE FRACTURE OF THIN (0.02 - 2 mm) FILMS OF BITUMEN (72 PEN), TESTED AT A RANGE OF TEMPERATURES (0 - 45 °C) AND LOADING RATES (0.005 - 1 in/minute) ,
 MAJIDZADEH & HERRIN⁴³ , 1965 .

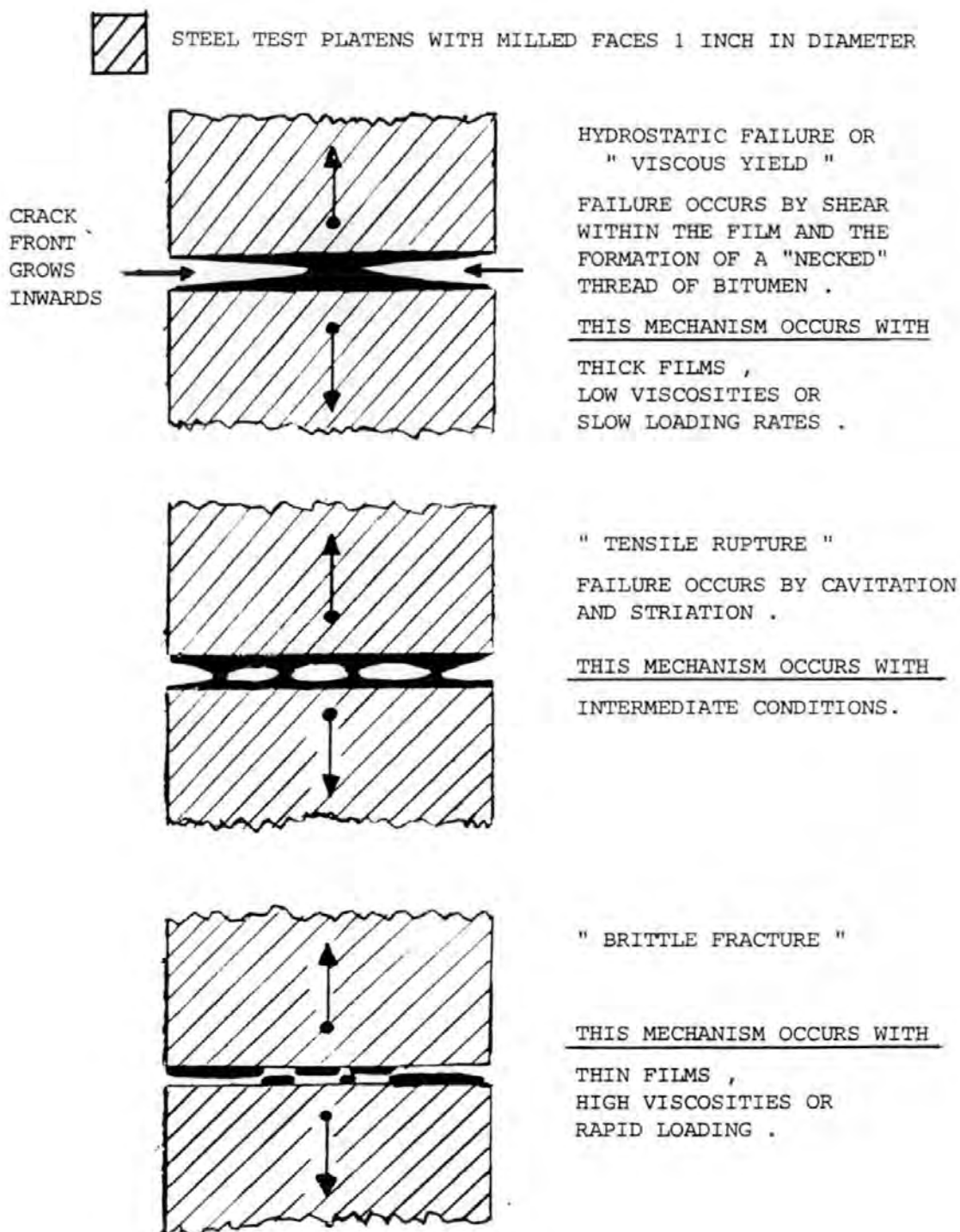
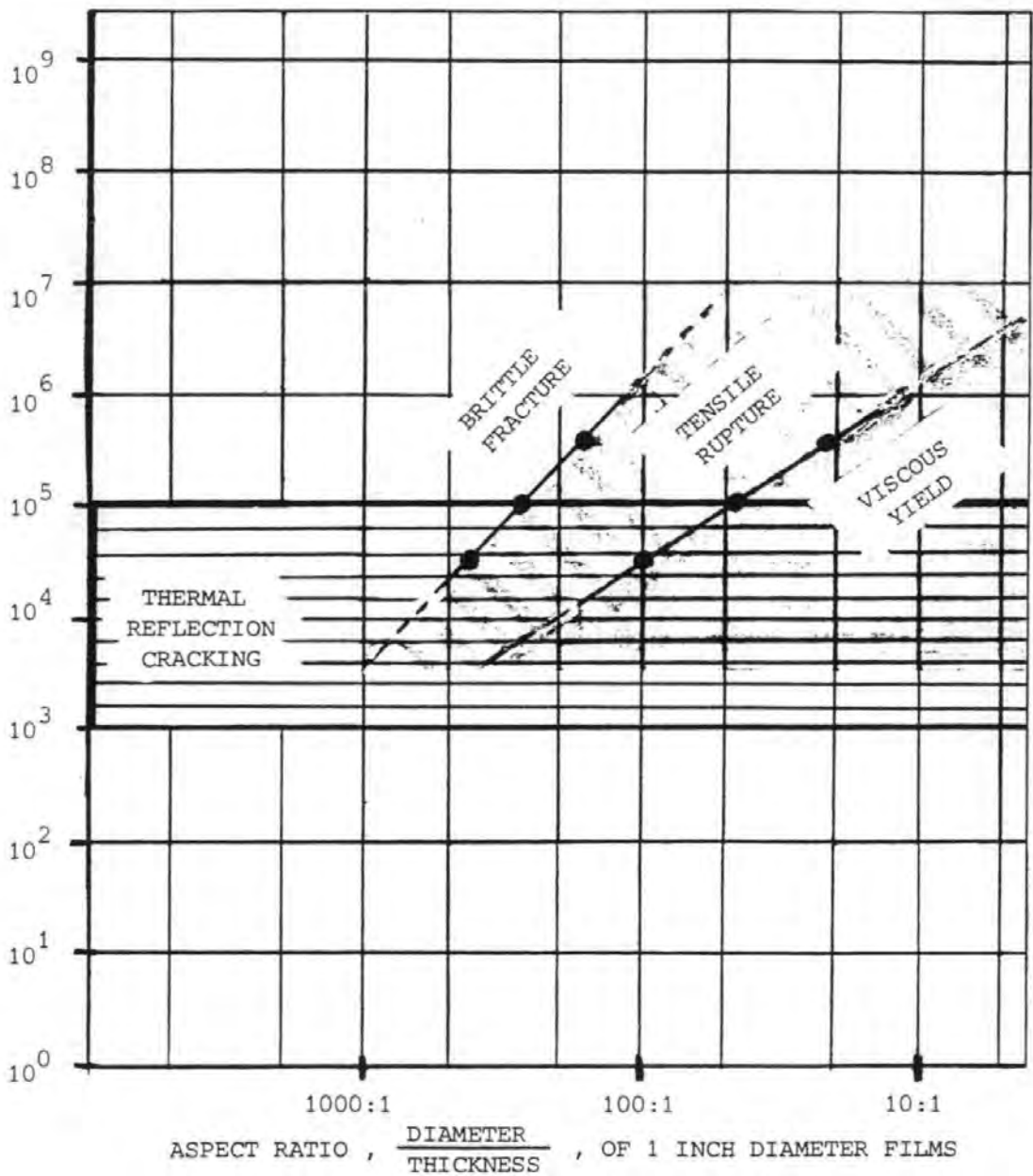


FIG 4 . 5

THE RELATIONSHIP BETWEEN THE MODE OF TENSILE FRACTURE OF THIN FILMS OF BITUMEN AND THE TEST CONDITIONS OF BITUMEN STIFFNESS ,
 "ADAPTED FROM" MAJIDZADEH & HERRIN⁴³ ,1965.

TEST CONDITIONS OF
 BITUMEN STIFFNESS N/m^2



It can be seen from FIG 4.5 that for the low stiffness conditions associated with thermal reflection cracking, brittle fracture will only occur if the aspect ratio of bitumen films within a mix is thinner than 300:1. The formation of such wide, thin films in bituminous mixes is unlikely because of the irregular surfaces of the aggregate and the presence of air voids.

Majidzadeh and Herrin⁴³ observed that for non-brittle fracture, the peak stress occurs during the early stages of the flow and the "classical" intermolecular fracture only happens much later across the thin necked "thread" or "threads" of bitumen at a much reduced load. This implies that the fracture strength (peak stress) is not related to the electrostatic surface energy, but is determined by the resistance of films of bitumen to transverse contraction and necking i.e. bitumen stiffness.

Fatigue crack growth under cyclic loading can be described as the repeated fracture of a crack-tip element of material with consequent advancement of the crack-tip. Thus fatigue crack growth and constants A, n should also be determined by test conditions of bitumen stiffness of the individual loading cycles.

Further evidence that fatigue crack growth is determined by bitumen stiffness can be deduced from Schapery's equations for A & n (EQNs 8 & 9).

Schapery's equations²⁷ relate A and n to three material properties. Of these, two have been shown by SHELL investigators to be functions of bitumen stiffness i.e.:-

$$\text{Tensile Strength} \propto S_{\text{BIT}}^{42}$$

$$\text{Creep Compliance} = 1/S_{\text{MIX}}; S_{\text{MIX}} \propto S_{\text{BIT}}^{46,47}$$

The third material property (τ) the fracture surface energy is also probably related to bitumen stiffness as described below, Crack growth in ductile steel has been described as a mechanism of void coalescence ahead of the crack front³⁹, which is analogous to the tensile rupture, FIG 4.4, observed by Majidzadeh and Herrin⁴³ in thin films of bitumen.

Orowan⁴⁸ observed that in the fracture of ductile steel, the plastic work portion of fracture surface energy was three orders of magnitude greater than the "free surface" energy portion and so the latter could be neglected in this "non-brittle" fracture.

Thus the fracture surface energy of bituminous mixes should also be dominated by the plastic work term which is bitumen stiffness related.

Thus Schapery's theory also implies that A & n can be correlated in terms of test conditions of bitumen stiffness, and so accelerated testing is viable.

4.3 Temperature Compensation for the Non-Sinusoidal Daily Cycle

The daily cycles of crack-opening in the roadbase are non-sinusoidal and occur over a range of temperatures during the day.

The simulative testing has to use sinusoidal cycles at constant temperature, which must produce the same fatigue crack growth as the actual cycles.

The fatigue crack growth per cycle is dependant upon the wave shape of the stress intensity factor²⁷ which is determined by the wave shape of the crack opening cycle.

Fatigue crack growth per cycle can be evaluated for both the actual cycles and sinusoidal cycles at constant temperatures, by considering hourly increments, TABLES 4.1/2. The equivalent sinusoidal daily cycles produce the same crack growth per cycle when the temperature is a few °C warmer than the mean of the actual cycle.

The daily cycle of pavement temperature was considered in SECTION 2 , and hourly temperature-depth profiles were plotted for four typical months for each season of the year, FIG 2.2, from which daily cycles of mean temperature can be determined for the roadbase and surfacing, FIG 4.6.

The near absolute restraint of thermal warping in the roadbase means that the crack opening cycle is determined by the cycle of depth-averaged mean roadbase temperature, FIG. 4.6.

TABLE 4 . 1

EVALUATION OF CRACK GROWTH PER CYCLE FOR ACTUAL DAILY CYCLES

CO = HOURLY CRACK OPENING T_s = MEAN SURFACING TEMPERATURE

K_1 = STRESS INTENSITY FACTOR $A_1 K_1^n$ = INCREMENTAL CRACK GROWTH

| HOURLY INTERVAL | JANUARY | | | | APRIL | | | | JULY | | | | OCTOBER | | | |
|-----------------|-----------------------------|-------|--------------|-------------|----------------------------|-------|--------------|-------------|-----------------------------|-------|--------------|-------------|-----------------------------|-------|--------------|-------------|
| | CO | T_s | K_1 | $A_1 K_1^n$ | CO | T_s | K_1 | $A_1 K_1^n$ | CO | T_s | K_1 | $A_1 K_1^n$ | CO | T_s | K_1 | $A_1 K_1^n$ |
| | mm | °C | $Nmm^{-3/2}$ | mm | mm | °C | $Nmm^{-3/2}$ | mm | mm | °C | $Nmm^{-3/2}$ | mm | mm | °C | $Nmm^{-3/2}$ | mm |
| | $\times 10^{-13}$ | | | | $\times 10^{-9}$ | | | | $\times 10^{-12}$ | | | | $\times 10^{-12}$ | | | |
| 12 - 13 | -.048 | 4.8 | | | -.183 | 15.7 | | | -.182 | 28.2 | | | -.112 | 13.7 | | |
| 13 - 14 | -.050 | 5.3 | | | -.177 | 16.7 | | | -.165 | 29.3 | | | -.103 | 14.3 | | |
| 14 - 15 | -.056 | 5.6 | | | -.121 | 17.4 | | | -.139 | 30.1 | | | -.079 | 14.6 | | |
| 15 - 16 | -.035 | 5.5 | | | -.085 | 17.3 | | | -.104 | 30.3 | | | -.043 | 14.4 | | |
| 16 - 17 | .019 | 5.1 | .081 | .43 | -.048 | 16.3 | | | -.052 | 29.8 | | | .019 | 13.8 | .015 | |
| 17 - 18 | .021 | 4.6 | .101 | 1.03 | .019 | 15.1 | .012 | | -.017 | 29.0 | | | .032 | 13.0 | .028 | .02 |
| 18 - 19 | .025 | 4.2 | .128 | 3.54 | .077 | 14.0 | .056 | .01 | .052 | 27.6 | .005 | | .043 | 12.3 | .045 | .17 |
| 19 - 20 | .023 | 3.9 | .126 | 2.36 | .100 | 12.8 | .092 | .04 | .087 | 25.7 | .009 | .03 | .053 | 11.7 | .060 | 1.06 |
| 20 - 21 | .025 | 3.7 | .141 | 4.59 | .119 | 11.6 | .140 | .20 | .121 | 23.8 | .016 | .66 | .060 | 11.1 | .077 | 3.11 |
| 21 - 22 | .023 | 3.5 | .135 | 3.11 | .137 | 10.5 | .200 | .87 | .130 | 22.4 | .021 | 2.02 | .062 | 10.6 | .088 | 4.58 |
| 22 - 23 | .023 | 3.3 | .141 | 3.12 | .142 | 9.5 | .252 | 1.77 | .130 | 21.2 | .026 | 3.81 | .066 | 10.1 | .103 | 9.11 |
| 23 - 24 | .023 | 3.1 | .145 | 3.59 | .132 | 8.6 | .279 | 1.69 | .130 | 20.1 | .031 | 6.15 | .066 | 9.8 | .109 | 9.87 |
| 0 - 1 | .023 | 3.0 | .149 | 3.60 | .113 | 7.9 | .273 | .88 | .121 | 19.1 | .034 | 6.47 | .060 | 9.4 | .109 | 7.81 |
| 1 - 2 | .023 | 2.9 | .151 | 4.08 | .100 | 7.4 | .267 | .52 | .104 | 18.2 | .034 | 3.49 | .053 | 9.2 | .098 | 3.23 |
| 2 - 3 | .021 | 2.7 | .145 | 2.41 | .083 | 7.0 | .240 | .17 | .113 | 17.5 | .042 | 7.80 | .051 | 8.9 | .102 | 2.99 |
| 3 - 4 | .023 | 2.6 | .160 | 4.19 | .073 | 6.7 | .227 | .10 | .104 | 16.8 | .043 | 6.15 | .047 | 8.7 | .098 | 2.06 |
| 4 - 5 | .017 | 2.5 | .124 | .76 | .063 | 6.4 | .211 | .05 | .095 | 16.2 | .045 | 5.10 | .034 | 8.5 | .073 | .23 |
| 5 - 6 | .017 | 2.5 | .124 | .76 | .056 | 6.1 | .202 | .03 | .078 | 16.0 | .038 | 1.43 | .028 | 8.4 | .062 | .08 |
| 6 - 7 | .008 | 2.5 | .054 | .01 | .035 | 6.3 | .117 | | .043 | 16.3 | .019 | .03 | .019 | 8.5 | .039 | |
| 7 - 8 | .004 | 2.6 | .027 | | -.044 | 7.3 | | | -.043 | 17.4 | | | -.024 | 8.7 | | |
| 8 - 9 | -.006 | 2.7 | | | -.102 | 9.2 | | | -.087 | 19.4 | | | -.060 | 9.3 | | |
| 9 - 10 | -.039 | 2.9 | | | -.138 | 11.2 | | | -.156 | 22.1 | | | -.075 | 10.3 | | |
| 10 - 11 | -.044 | 3.4 | | | -.171 | 13.0 | | | -.182 | 24.7 | | | -.094 | 11.6 | | |
| 11 - 12 | -.042 | 4.1 | | | -.181 | 14.5 | | | -.182 | 26.7 | | | -.100 | 12.8 | | |
| $A_1 K_1^n$ | SUM = 3.7×10^{-12} | | | | SUM = 6.3×10^{-9} | | | | SUM = 4.3×10^{-11} | | | | SUM = 4.4×10^{-11} | | | |

TABLE 4 . 2

EVALUATION OF CRACK GROWTH PER CYCLE FOR EQUIVALENT SINUSOIDAL DAILY CYCLES AT CONSTANT TEMPERATURE

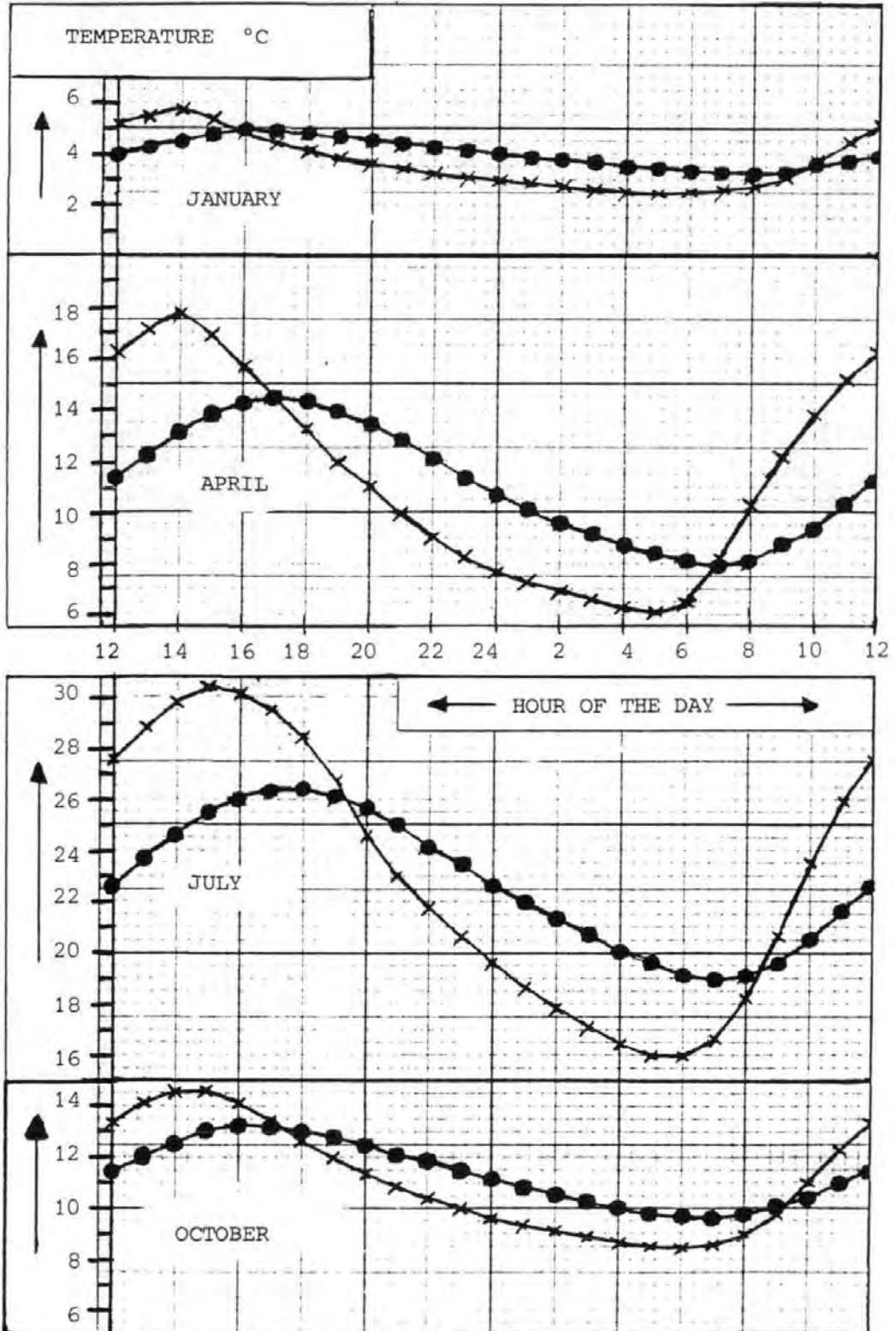
CO = HOURLY CRACK OPENING
 K_1 = STRESS INTENSITY FACTOR
 T_s = MEAN SURFACING TEMPERATURE
 $A_1 K_1^n$ = INCREMENTAL CRACK GROWTH

| HOURLY INTERVAL | JANUARY | | | | APRIL | | | | JULY | | | | OCTOBER | | | |
|-----------------|-------------------------------|-------|---------------------|-------------|------------------------------|-------|---------------------|-------------|-------------------------------|-------|---------------------|-------------|-------------------------------|-------|---------------------|-------------|
| | CO | T_s | K_1 | $A_1 K_1^n$ | CO | T_s | K_1 | $A_1 K_1^n$ | CO | T_s | K_1 | $A_1 K_1^n$ | CO | T_s | K_1 | $A_1 K_1^n$ |
| | mm | °C | Nmm ^{-3/2} | mm | mm | °C | Nmm ^{-3/2} | mm | mm | °C | Nmm ^{-3/2} | mm | mm | °C | Nmm ^{-3/2} | mm |
| | | | x10 ⁻¹³ | | | | x10 ⁻⁹ | | | | x10 ⁻¹¹ | | | | x10 ⁻¹¹ | |
| 12 - 13 | | | | | | | | | | | | | | | | |
| 13 - 14 | | | | | | | | | | | | | | | | |
| 14 - 15 | -ive | | | | -ive | | | | -ive | | | | -ive | | | |
| 15 - 16 | | | | | | | | | | | | | | | | |
| 16 - 17 | | | | | | | | | | | | | | | | |
| 17 - 18 | | | | | | | | | | | | | | | | |
| 18 - 19 | .006 | 8.9 | .011 | | .021 | 11.6 | .025 | | .023 | 22.2 | .003 | | .011 | 13.8 | .009 | |
| 19 - 20 | .015 | 8.9 | .033 | 0.02 | .061 | 11.6 | .073 | | .066 | 22.2 | .010 | | .034 | 13.8 | .026 | |
| 20 - 21 | .025 | 8.9 | .052 | 0.42 | .100 | 11.6 | .115 | 0.06 | .104 | 22.2 | .017 | 0.05 | .055 | 13.8 | .041 | 0.05 |
| 21 - 22 | .033 | 8.9 | .067 | 2.22 | .129 | 11.6 | .150 | 0.35 | .135 | 22.2 | .023 | 0.24 | .071 | 13.8 | .053 | 0.21 |
| 22 - 23 | .039 | 8.9 | .079 | 6.17 | .150 | 11.6 | .175 | 0.93 | .158 | 22.2 | .028 | 0.91 | .083 | 13.8 | .062 | 0.62 |
| 23 - 24 | .042 | 8.9 | .085 | 9.74 | .161 | 11.6 | .187 | 1.40 | .170 | 22.2 | .029 | 1.35 | .090 | 13.8 | .068 | 1.08 |
| 0 - 1 | | | | 9.74 | | | | 1.40 | | | | 1.35 | | | | 1.08 |
| 1 - 2 | | | | 6.17 | | | | 0.93 | | | | 0.91 | | | | 0.62 |
| 2 - 3 | " | " | " | 2.22 | " | " | " | 0.35 | " | " | " | 0.24 | " | " | " | 0.21 |
| 3 - 4 | | | | 0.42 | | | | 0.06 | | | | 0.05 | | | | 0.05 |
| 4 - 5 | | | | 0.02 | | | | | | | | | | | | |
| 5 - 6 | | | | | | | | | | | | | | | | |
| 6 - 7 | | | | | | | | | | | | | | | | |
| 7 - 8 | | | | | | | | | | | | | | | | |
| 8 - 9 | -ive | | | | -ive | | | | -ive | | | | -ive | | | |
| 9 - 10 | | | | | | | | | | | | | | | | |
| 10 - 11 | | | | | | | | | | | | | | | | |
| 11 - 12 | | | | | | | | | | | | | | | | |
| $A_1 K_1^n$ | SUM = 3.7 x 10 ⁻¹² | | | | SUM = 5.5 x 10 ⁻⁹ | | | | SUM = 5.1 x 10 ⁻¹¹ | | | | SUM = 3.9 x 10 ⁻¹¹ | | | |

FIG 4 . 6

THE DAILY CYCLES OF SURFACING AND ROADBASE TEMPERATURE FOR A 100 mm SURFACING COMPOSITE PAVEMENT .

* * * * * MEAN TEMPERATURE IN THE SURFACING , 0 - 100 mm
 ● ● ● ● ● MEAN TEMPERATURE IN THE ROADBASE , 100 - 300 mm



The comparison of fatigue crack growth per cycle is made here for these four months, FIG 4.6, and the following conditions:-

Roadbase slab length (15m), thermal coefficient of expansion ($10^{-5}/^{\circ}\text{C}$) and surfacing thickness (100mm).

The amplitude of the crack opening cycle has been evaluated, TABLE 2.8, (January 0.32mm, April 1.25mm, July 1.31mm & October 0.69mm) and hourly crack-opening increments can be determined from hourly variations in the roadbase temperature cycle, FIG 4.6, for each month.

The relaxation modulus data for a UK Type H.R.A. basecourse mix⁴⁴ can then be used to determine 24 point cycles of K_1 from these hourly "constant rate of strain" crack opening movements, TABLE 4.1/2. The relaxation modulus, FIG 4.7,⁴⁴ relates to instantaneous applied strain with a high initial stress that subsequently relaxes:-

$$\text{Relaxation Modulus} \quad \text{RM (time, Temp)} = \frac{\text{Residual Stress (time, Temp)}}{\text{Initial Strain}} \quad (\text{EQN 18})$$

The effective modulus for constant rate of strain type loading is greater than the relaxation modulus (EQN 18) but is related to it. The constant rate of strain modulus, γ , (EQN 19) is given by the sum of residual stresses from increments of strain equally spaced over the preceding time interval:-

$$\gamma(\text{It, Temp}) = \left(\frac{1}{\text{It}} \right) \int_0^{\text{It}} \text{RM (time, Temp)} \, dt \quad (\text{EQN 19})$$

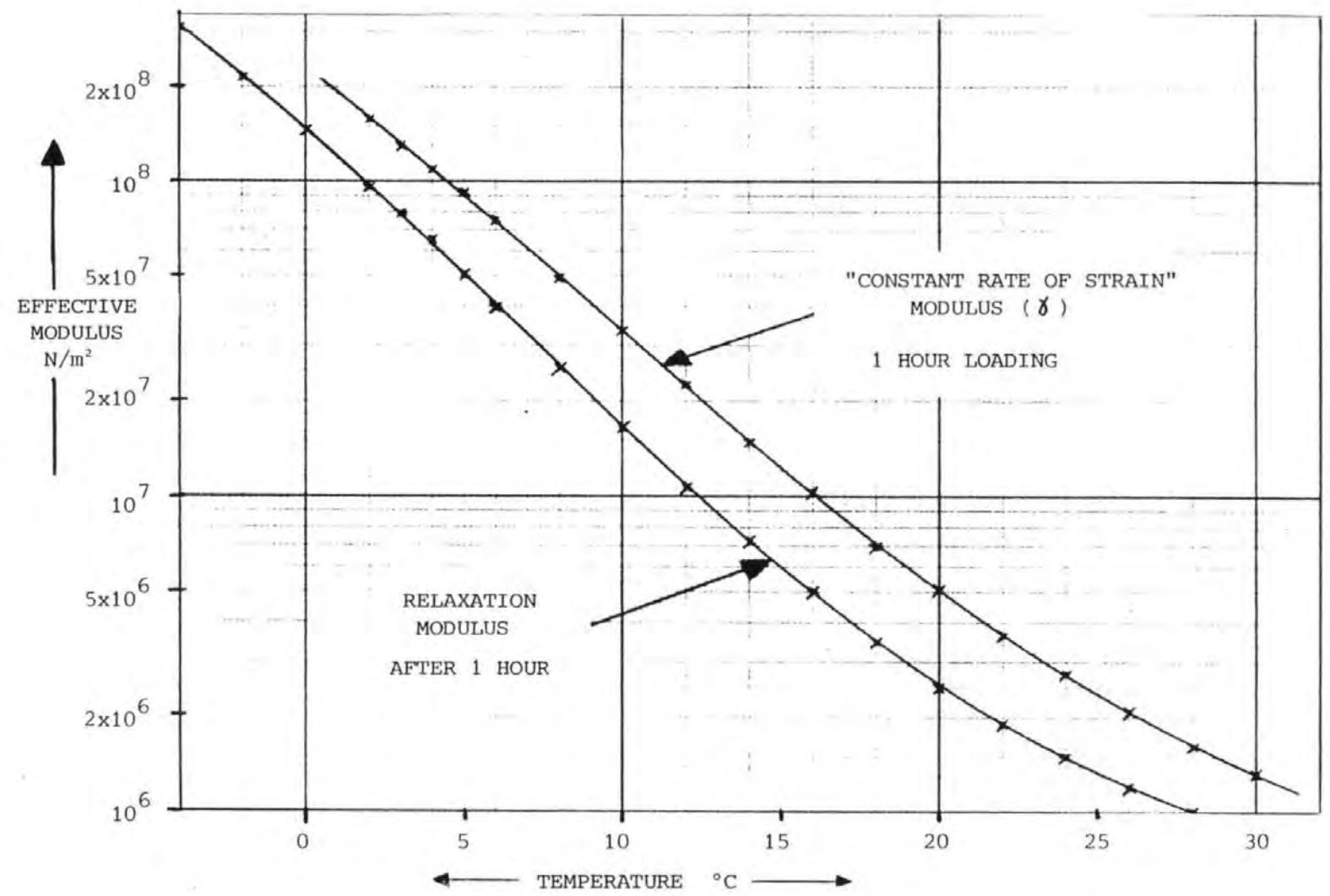
Where It = the incremental time interval.

$\gamma(1 \text{ Hour})$, FIG 4.7, was evaluated for a range of temperatures ($2+30^{\circ}\text{C}$) by re-plotting the relaxation modulus data, FIG 4.7, to a linear time axis and using the trapezium rule to estimate the value of the integral (EQN 19).

At the end of an hourly interval of constant crack opening movement, the magnitude of the crack tip stress intensity factor (\bar{K}_1) is determined by the finite element results, FIG 3.7, and is a function

RELAXATION MODULUS AND "CONSTANT RATE OF STRAIN" MODULUS (δ) FOR A ROLLED ASPHALT BASECOURSE MATERIAL, "ADAPTED FROM" STILL 44, 1972.

FIG 4.7



of the hourly crack opening and the effective modulus (γ) for a 1 hour interval, i.e.

$$\bar{K}_1 = 4.8 (\text{HOURLY CO}_{\text{mm}}) \frac{\gamma}{10^8} \text{N/mm}^{3/2} \quad (\text{EQN 20})$$

The quantity \bar{K}_1 (EQN 20) is the equivalent mean value for crack propagation in a 100mm single course surfacing (EQN 13).

At the lower end (2+10°C) of the temperature range considered, a slight correction to (EQN 20) is necessary to account for additional unrelaxed stresses from the previous hourly interval:-

$$\bar{K}_1 = 4.8 (\text{HOURLY CO}_{\text{mm}}) \left(\frac{\gamma}{10^8} \right) \left(1 + \frac{\text{RM (1 HOUR)}}{\text{RM}_0} \right) \text{N/mm}^{3/2} \quad (\text{EQN 21})$$

where RM_0 = (the relaxation modulus at time =0) which is difficult to measure accurately, but was estimated as $4 \times 10^9 \text{ N/m}^2$ ⁴⁴. Fortunately the value of $(\text{RM (1 HOUR)}/\text{RM}_0)$ at 2°C and above, is less than 2% and so the effect of uncertainty in estimating RM_0 will be negligible.

The evaluation of fatigue crackgrowth for the actual and equivalent sinusoidal daily cycles is detailed TABLE 4.1/2.

The fatigue crack growth per cycle is evaluated as the sum of the crack growth per increment ($A_1 K_1^n$) during the hourly increments of constant loading of the positive pulse of K_1 .

The crack growth constant for 1 hour loading increments (A_1) is different to that for the complete cycle (A) because the loading time is different. However crack growth for a cycle split into increments is still the same because A and A_1 are determined by bitumen stiffness which compensates for the difference in loading time.

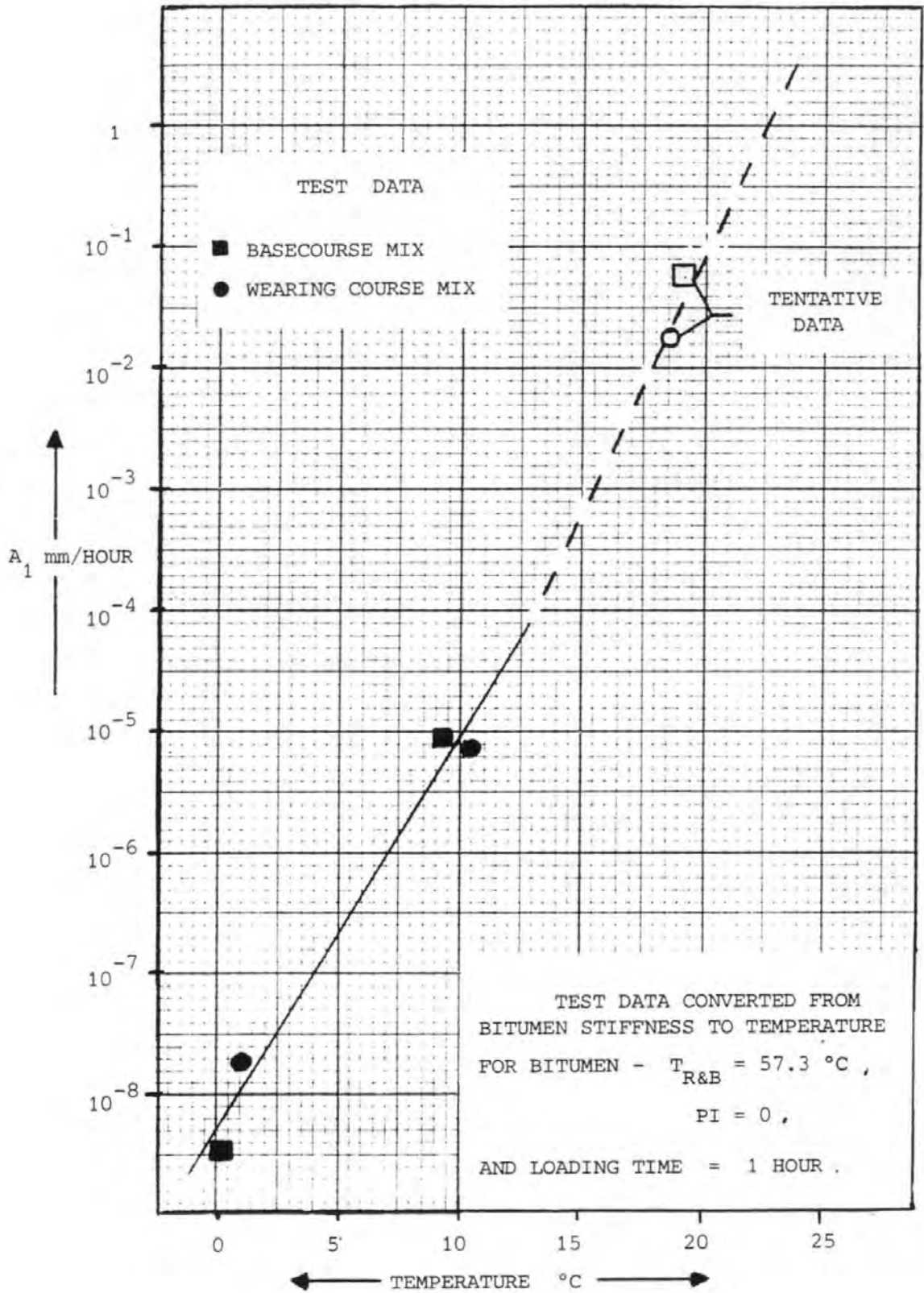
Average values for A_1 and n, FIG 4.8, from the test results, FIG 6.9, are used here to evaluate hourly increments of fatigue crack growth ($A_1 K_1^n$) and fatigue crack growth per cycle (AK_1^n).

Fatigue crack growth per cycle is not exactly the same for some months, TABLE 4.1/2. This is because of rounding-off errors in the calculations and because the equivalent sinusoidal cycle temperature could only be assessed to the nearest 0.1°C.

FIG 4 . 8

THE VARIATION WITH TEMPERATURE OF THE FATIGUE CRACK GROWTH CONSTANT, A_1 , FOR 1 HOUR LOADING AT CONSTANT K_1 .

" n " = CONSTANT = 6.45



The fatigue crack growth per cycle is very sensitive to variations in temperature. A_1 increases with temperature and \bar{K}_1 decreases. The combined variation ($A_1 \bar{K}_1^n$) produces a decrease in crack growth rate as temperature rises by a factor of 1.64 per °C, over the range 0+15°C, but "levelling off", FIG 4.7, above 15°C .

This factor of 1.64 per °C relating crack growth rate and temperature can be used to determine temperature corrections for the variation of mean daily temperature within each month, SECTION 4.4.

Values of fatigue crack growth, TABLES 4.1/2 are meaningful in relative terms but not in absolute terms because they were obtained by combining crack growth constants from the test mixes with K_1 values determined using relaxation modulus data from a different mix.

It is also possible that the cycles of crack-opening movement could be of a "stick-slip" nature due to the restraining effects of sub-base friction. This would result in very uneven cycles of (\bar{K}_1) and ($A_1 \bar{K}_1^n$) with spikes that would be very difficult to analyse. It is probable that the high frequency vibration effects of traffic loading will help to overcome friction during thermal contraction and so the crack-opening movements can be assumed to occur at constant rates over hourly intervals.

4.4 Temperature Corrections for the Variation of Mean Daily Temperature within each Month.

The equivalent temperature for each month of the year is also affected by the variation of mean daily temperature within each month.

The frequency distribution of the individual daily values about the monthly mean, TABLE 4.3, is taken from the variation of median (\approx mean) daily temperature at depth 127mm in a concrete pavement,¹¹. This distribution is a measure of climatic variability and is the same for all types of pavement.

The differences between equivalent monthly temperatures and the mean monthly values, TABLE 4.3, vary from -0.6°C to -2.4°C. The calculated difference for the year taken as a whole is -1.4°C.

TABLE 4 . 3
TEMPERATURE CORRECTIONS FOR THE DAILY VARIATION OF MEAN PAVEMENT
TEMPERATURE WITHIN EACH MONTH

| | | MONTHLY FREQUENCY DISTRIBUTIONS OF INDIVIDUAL DAILY MEAN TEMPERATURES ABOUT THE MONTHLY MEAN VALUE (° C) | | | | | | | | | | | | | | | TEMPERATURE SHIFT FROM MEAN GROWTH (°C) | | | | | | | | | | | | | | | | |
|-----------------------------|---|---|-----|-----|-----|-----|-----|-----|-----|-----|-----|-----|-----|-----|-----|-----|--|----------------------|------|------|------|------|------|------|------|------|------|-------|-------|-------|-------|------|------|
| | | +8 | +7 | +6 | +5 | +4 | +3 | +2 | +1 | 0 | -1 | -2 | -3 | -4 | -5 | -6 | NET CRACK GROWTH | FROM MEAN (°C) | | | | | | | | | | | | | | | |
| JAN | | | | | | | 1 | 7 | 3 | 3 | 1 | 3 | 1 | 3 | 1 | 2 | 1 | 2 | 1 | 1 | 1 | 3.08 | -2.3 | | | | | | | | | | |
| FEB | | | | | | | 2 | 1 | 3 | 2 | 1 | 4 | 4 | 1 | 1 | 3 | 5 | 1 | | | | 1.54 | -0.9 | | | | | | | | | | |
| MAR | | | | | 1 | 1 | | 1 | 2 | 4 | 4 | 8 | 4 | 5 | | 1 | | | | | | 1.31 | -0.6 | | | | | | | | | | |
| APR | | | | | 1 | 2 | 2 | 2 | 2 | 2 | 2 | 3 | 3 | 6 | 3 | 1 | 1 | | | | | 1.41 | -0.7 | | | | | | | | | | |
| MAY | | | | | | 2 | 6 | 1 | 4 | 2 | 2 | 2 | 4 | 4 | 3 | | 1 | | | | | 1.51 | -0.8 | | | | | | | | | | |
| JUN | | | | 2 | 1 | 3 | 2 | 2 | 3 | 1 | 3 | 1 | 1 | 3 | 2 | 2 | 2 | 1 | | | 1 | 2.68 | -2.0 | | | | | | | | | | |
| JUL | | | 1 | 1 | 1 | | 3 | 1 | 3 | 2 | 5 | 1 | 3 | 1 | | 1 | 1 | 1 | 2 | | 4 | 3.55 | -2.4 | | | | | | | | | | |
| AUG | | | | 1 | 2 | 1 | 3 | 1 | 4 | 3 | 1 | 2 | 2 | 1 | 1 | 2 | 1 | 3 | 2 | 1 | | 1.79 | -1.2 | | | | | | | | | | |
| SEP | | | | | 1 | 2 | 4 | 3 | 3 | 3 | 3 | 2 | 3 | 2 | 1 | 1 | | 1 | | 1 | | 1.54 | -0.9 | | | | | | | | | | |
| OCT | | | | | | | 3 | 2 | 5 | 2 | 6 | 1 | 2 | 2 | 2 | 1 | 2 | | | | | 1.49 | -0.8 | | | | | | | | | | |
| NOV | 1 | 1 | | | 1 | 2 | | 1 | 2 | 3 | 3 | 2 | 1 | 2 | 2 | 1 | 2 | 1 | 3 | | 1 | 1 | 3.09 | -2.3 | | | | | | | | | |
| DEC | | | | | 1 | 1 | 1 | 3 | 2 | 1 | 4 | 2 | 1 | 6 | 3 | 4 | 2 | | | | | | 1.47 | -0.8 | | | | | | | | | |
| TOTAL | 1 | 1 | 0 | 0 | 0 | 1 | 2 | 3 | 3 | 3 | 11 | 10 | 21 | 26 | 24 | 30 | 34 | 33 | 25 | 27 | 26 | 22 | 17 | 11 | 11 | 8 | 1 | 2 | 5 | 1 | 3 | 2.02 | -1.4 |
| RELATIVE CRACK GROWTH | | .02 | .02 | .03 | .04 | .05 | .06 | .08 | .11 | .14 | .18 | .23 | .29 | .37 | .49 | .61 | .78 | 1.00 | 1.28 | 1.64 | 2.10 | 2.69 | 3.46 | 4.43 | 5.68 | 7.28 | 9.33 | 11.95 | 15.32 | 19.63 | 25.16 | | |

It was decided to use the average of -1.4°C and the calculated monthly values, because there was no clear trend over the year.

Constant temperatures for a sinusoidal daily cycle have been interpolated, TABLE 4.4, for all months of the year by comparing the calculated values, TABLE 4.2, with the monthly mean temperatures for depths 0-100mm in a composite pavement, TABLE 2.1.

The interpolated sinusoidal daily cycle temperatures, TABLE 4.4, are then adjusted to compensate for disproportionate damaging effect of the few colder than average cycles in each month.

4.5 Cyclic Conditions of Bitumen Stiffness and Suitable Test Temperatures.

The determination of equivalent temperatures for a sinusoidal daily cycle used data from test mixes and a HRA basecourse mix⁴⁴, containing bitumen of an average temperature susceptibility ($PI=0$).

The equivalent temperatures, TABLE 4.4, only represent small deviations from the mean monthly pavement temperatures and so they are reasonable as base temperatures for the acceleration of testing of mixes containing road bitumens where $PI = (-1 \rightarrow +1)$.

Suitable frequencies and raised temperatures for accelerated testing are defined by the criterion of equal bitumen stiffness, as defined by the Van der Poel Nomograph³⁴, FIG 4.9.

Values of bitumen stiffness predicted by the Nomograph have a possible error of a factor of two, but the accuracy of the time-temperature shift for a given grade of bitumen would be expected to reduce the size of the factor.

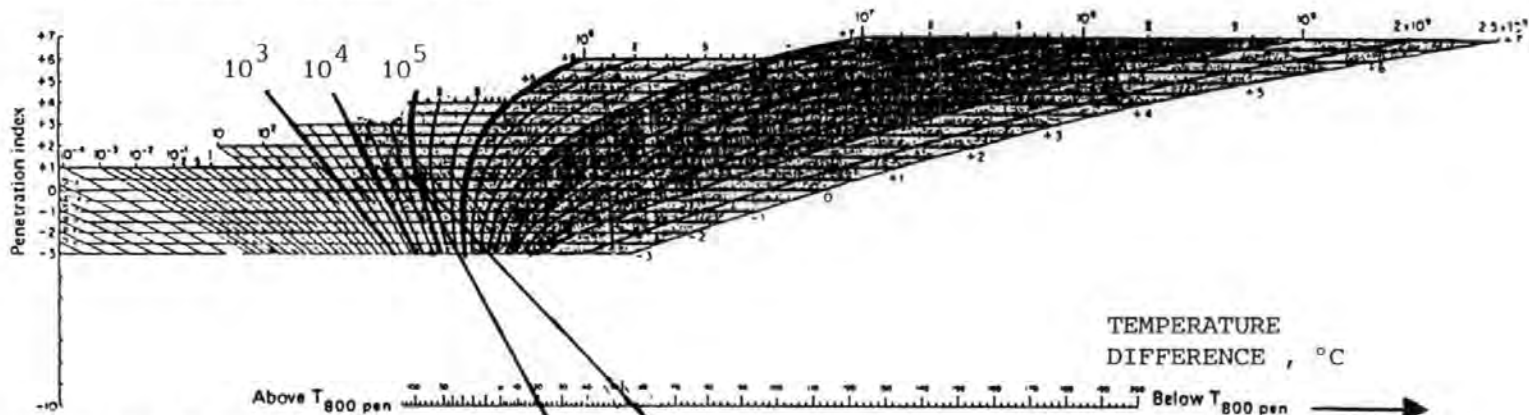
The appropriate loading time for sinusoidal cyclic loading to give the same crack growth as a pulse of constant loading, depends upon the value of the exponent n in the crack growth equation AK_1^n . When $n = 5 \rightarrow 6$, the positive pulse of a sinusoidal cycle does produce the same crack growth as a pulse of constant loading at the peak stress, of duration $1/(2\pi \times \text{frequency})$. So this loading time convention is appropriate.

DETERMINATION OF EQUIVALENT MONTHLY TEMPERATURES (°C) FOR A
 SINUSOIDAL DAILY CYCLE AT CONSTANT TEMPERATURE .

TABLE 4 . 4

| | MEAN SURFACING TEMPERATURE , DEPTH 0-100 mm, FOR THE ACTUAL DAILY CYCLE | CALCULATED TEMPERATURES FOR EQUIVALENT SINUSOIDAL DAILY CYCLES | INTERPOLATED DIFFERENCES FOR EQUIVALENT SINUS- OIDAL AND ACTUAL DAILY CYCLES | INTERPOLATED TEMPERATURES FOR EQUIVALENT SINUSOIDAL DAILY CYCLES | TEMPERATURE SHIFTS FOR VARIABILITY OF MEAN DAILY TEMPERATURE | EQUIVALENT TEMPERATURES FOR SINUSOIDAL DAILY CYCLES |
|-----|---|--|--|--|--|---|
| JAN | 3.7 | 8.9 | | | - 1.9 | 7.0 |
| FEB | 4.3 | | + 3.6 | 7.9 | - 1.2 | 6.7 |
| MAR | 7.0 | | + 2.0 | 9.0 | - 1.0 | 8.0 |
| APR | 11.2 | 11.6 | | | - 1.1 | 10.5 |
| MAY | 16.1 | | + 0.1 | 16.2 | - 1.1 | 15.1 |
| JUN | 21.7 | | - 0.3 | 21.4 | - 1.7 | 19.7 |
| JUL | 22.8 | 22.2 | | | - 1.9 | 20.3 |
| AUG | 20.3 | | + 0.5 | 20.8 | - 1.3 | 19.5 |
| SEP | 16.4 | | + 1.7 | 18.1 | - 1.2 | 16.9 |
| OCT | 11.0 | 13.8 | | | - 1.1 | 12.7 |
| NOV | 6.8 | | + 3.6 | 10.4 | - 1.9 | 8.5 |
| DEC | 4.6 | | + 4.4 | 9.0 | - 1.1 | 7.9 |

BITUMEN STIFFNESS , N/m²



The stiffness modulus, defined as the ratio $\sigma/\epsilon = \text{stress/strain}$, is a function of time of loading (frequency), temperature difference with $T_{800 \text{ pen}}$ and N .

$T_{800 \text{ pen}}$ is the temperature at which the penetration would be 800.

This is obtained by extrapolating the experimental log penetration versus temperature line to the penetration value 800.

At low temperatures and/or high frequencies the stiffness modulus of all bitumens asymptotes to a limit of approx. $3 \times 10^9 \text{ N/m}^2$

Units:

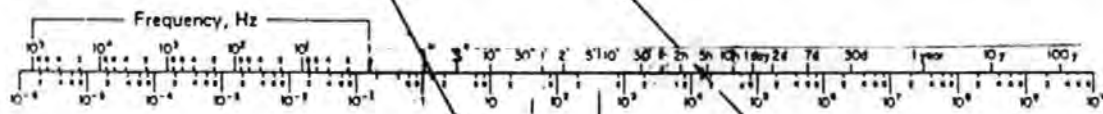
$1 \text{ N/m}^2 = 10 \text{ dyn/cm}^2 = 1.02 \times 10^{-6} \text{ kgt/cm}^2 = 1.45 \times 10^{-4} \text{ lb/sq. in.}$

$1 \text{ N s/m}^2 = 10 \text{ P}$

TEMPERATURE DIFFERENCE , °C

Above $T_{800 \text{ pen}}$ Below $T_{800 \text{ pen}}$

ACCELERATED TESTING,
TEMPERATURE INCREASED,
LOADING TIME REDUCED.



LOADING TIME (s)

THE VAN DER POEL NOMOGRAPH FOR DETERMINATION OF BITUMEN STIFFNESS 34

FIG 4 . 9

The test conditions of bitumen stiffness are illustrated, TABLE 4.5, for two 50 PEN bitumens. Equi-stiffness temperatures for accelerated testing are illustrated for testing with either 50 or 200 PEN bitumen. The use of 200 PEN bitumen enables lower test temperatures to be used.

Also the repetition of tests with 50 and 200 PEN bitumen at the same value of bitumen stiffness does provide some measure of validation of the use of bitumen stiffness as a reduced parameter for fatigue testing of specific mixes.

The simulative reflection cracking fatigue tests can be performed on a limited range of mixes at a range of fixed values of crack opening and bitumen stiffness. The variation of the crack growth constants (A,n) can then be expressed in terms of bitumen stiffness. Fatigue crack growth can then be evaluated over the range of monthly conditions of crack opening and bitumen stiffness, a process analogous to the application of Miner's Law⁴⁹.

Miner's Law has been shown to be valid for bituminous material when there are no rest periods⁵⁰. These daily thermal cycles, although slow, are continuous with no rest periods.

TABLE 4 . 5

CONDITIONS OF CYCLIC BITUMEN STIFFNESS FOR TWO TYPES OF 50 PEN BITUMEN & EQUISTIFFNESS TEST TEMPERATURES FOR TESTING WITH EITHER -

50 PEN BITUMEN ($T_{R\&B}$ 56½ °C , PI + 0.6) OR -
 200 PEN BITUMEN ($T_{R\&B}$ 42½ °C , PI + 0.3) .

| DAILY CYCLE TEMPERATURE (°C) (TABLE 4.4) | CONDITIONS OF CYCLIC BITUMINOUS STIFFNESS (N / m ²) x 10 ³ | | EQUI - STIFFNESS TEST TEMPERATURES FOR TESTING AT FREQUENCY , 0.12 Hz (°C) | | | |
|--|---|--|---|-----------------|------------------------------|-----------------|
| | NORMAL 50 PEN BITUMEN $T_{R\&B}$ 58 °C PI + 0.37 | HARDENED 50 PEN BITUMEN $T_{R\&B}$ 66 °C PI + 0.58 | TESTING WITH 50 PEN BITUMEN | | TESTING WITH 200 PEN BITUMEN | |
| | | | NORMAL 50 PEN | HARDENED 50 PEN | NORMAL 50 PEN | HARDENED 50 PEN |
| JAN 7.0 | 32 | 172 | 42 | 32 | 28 | 19 |
| FEB 6.7 | 34 | 187 | 41½ | 31½ | 27½ | 18½ |
| MAR 8.0 | 25 | 138 | 43½ | 33½ | 29½ | 20 |
| APR 10.5 | 13.4 | 75 | 47 | 36½ | 33 | 23 |
| MAY 15.1 | 4.4 | 25 | | 43½ | 40 | 29½ |
| JUN 19.7 | 1.40 | 8.2 | | 50 | 48½ | 36 |
| JUL 20.3 | 1.22 | 7.2 | | 51 | 49½ | 37 |
| AUG 19.5 | 1.48 | 8.6 | | 50 | 48 | 35½ |
| SEP 16.9 | 2.8 | 16.1 | | 46 | 43 | 32 |
| OCT 12.7 | 7.8 | 44 | 50½ | 40 | 36½ | 26½ |
| NOV 8.5 | 22 | 121 | 44 | 34 | 30 | 20½ |
| DEC 7.9 | 25 | 140 | 43½ | 33 | 29½ | 20 |

5.0 TEST PROCEDURES

5.1 Asphalt Mix Proportions and Preparation of Test Samples

Dense impermeable mixes are normally used for two-course surfacings in the U.K.

For major roads designed for traffic levels greater than 2.5 MSA, only hot rolled asphalt to BS 594⁵ is permitted for the wearing course, and a choice of hot rolled asphalt to BS 594⁵ and dense bitumen macadam to BS 4987⁶ is permitted for the basecourse.

50 PEN bitumen is normally used for the hot rolled asphalt (HRA) which is a gap-graded mix similar to a stone filled sandsheet mix.

A softer grade of bitumen, usually 100 PEN is used for the dense bitumen macadam (DBM) because this type of mix obtains more stability from its aggregate grading, and also because DBM type mixes tend to have higher air void contents and are consequently more susceptible to bitumen hardening by oxidation. DBM mixes are similar to the asphaltic concrete mixes used in the USA and other countries.

The range of mixes in the test program was limited to hot rolled asphalt basecourse and wearing course mixes, made with two bitumen grades (50 & 200 PEN) and a range of nominal sizes for the coarse aggregate (20, 28 & 40mm in the basecourse and 14 & 20mm in the wearing course). It had been hoped to test a wider range of mixes including DBM basecourse but the need to obtain test results for a wide range of values of cyclic crack opening and temperature (bitumen stiffness) meant that only a limited range of mixes could be tested.

The constituents of the test mixes and the mix proportions are summarised TABLE 5.1.

TABLE 5.1 MIX PROPERTIES AS % WT MIX

| CONSTITUENTS | BASECOURSE MIXES | | WEARING COURSE MIXES | |
|---|------------------|------|----------------------|------|
| | BC | BCS | WC | WCS |
| COARSE AGGREGATE MDORCROFT LIMESTONE | 65.0 | 65.0 | 30.0 | 30.0 |
| FINE AGGREGATE, SAND ROCKBEAR QUARTZITE | 29.3 | 29.3 | 54.8 | 54.8 |
| LIMESTONE FILLER | - | - | 7.3 | 7.3 |
| | | | | |
| 50 PEN BITUMEN T _{R&B} 56½ °C PI+0.6 | 5.7 | - | 7.9 | - |
| 200 PEN BITUMEN T _{R&B} 42½ °C PI + 0.3 | - | 5.7 | - | 7.9 |
| | | | | |
| % AIR VOIDS IN COMPACTED MIX | 0+1 | 0+1 | 0+4 | 0+2 |

Aggregate grading curves for the test mixes are illustrated, FIG 5.1, in relation to the specification limits, BS 594⁵. The hot rolled asphalt wearing course mix is the 1973 standard recipe mix 1A for crushed rock aggregate⁵.

The bitumen content of the wearing course mixes, TABLE 5.1, is lower than the optimum, 8.3 + 9.4%, implied by TRRL wheel tracking test, whole mix Marshall Tests, and the results from full scale trial surfacings at the A33 Winchester by Pass⁵¹, (The Rockbear sand was included in trials of rolled asphalt wearing courses with eight types of fine aggregate).

The bitumen properties, TABLE 5.1, were obtained from 100cc samples of bitumen taken immediately before mixing. The aggregate was at least 10°C cooler by the time the bitumen was added to it, and it was considered that further hardening of the bitumen after the start of mixing, would be negligible.

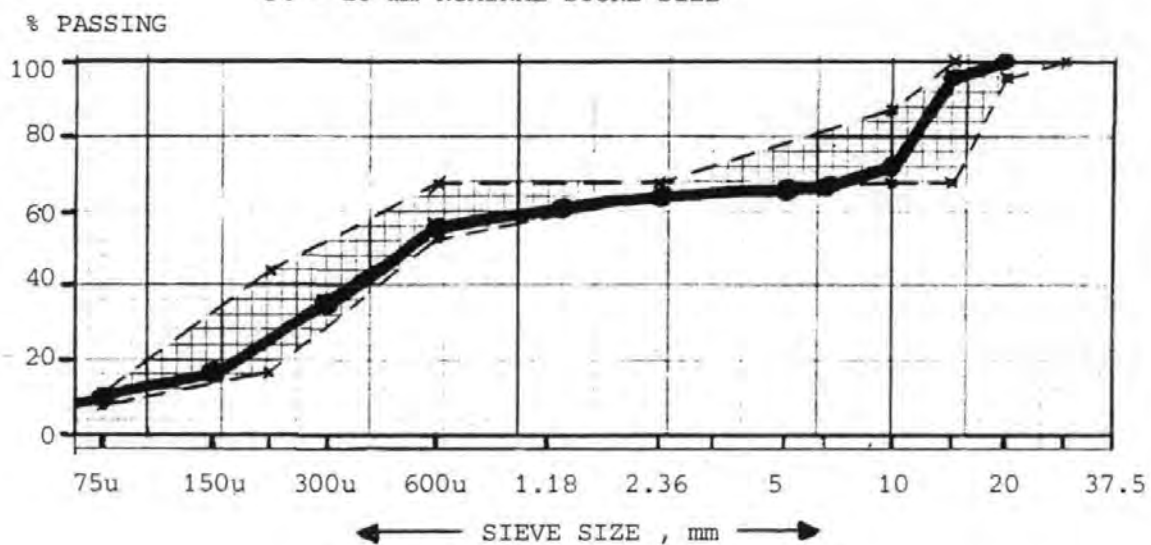
FIG 5 . 1

AGGREGATE GRADING CURVES FOR THE TEST MIXES IN RELATION TO THE SPECIFICATION , BS 594⁵ .

— * — — = SPECIFICATION LIMITS
 — * — — = SPECIFICATION LIMITS

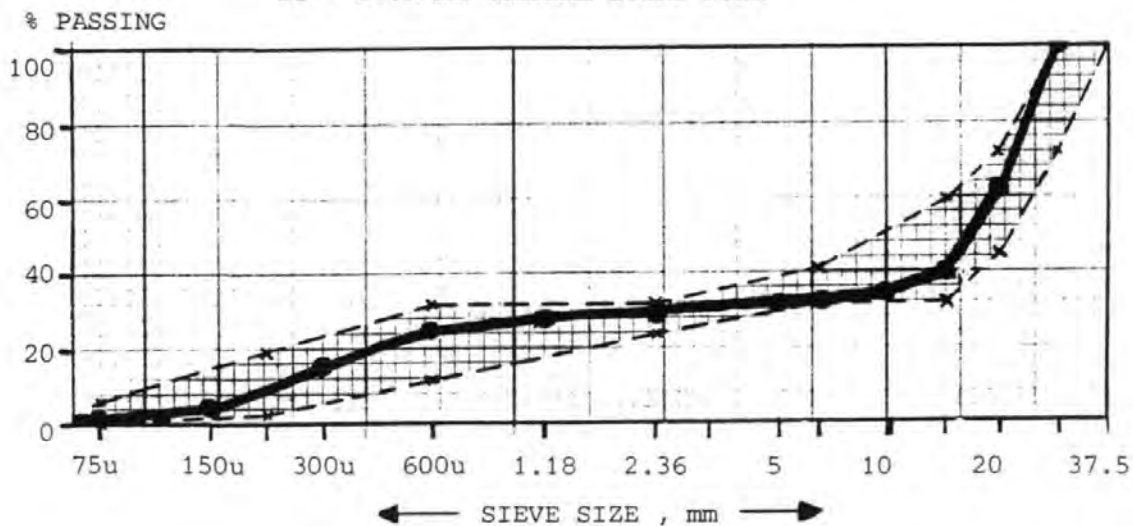
HOT ROLLED ASPHALT WEARING COURSE RECIPE MIX 1A .

14 - 20 mm NOMINAL STONE SIZE



HOT ROLLED ASPHALT BASECOURSE MIX

28 - 37.5 mm NOMINAL STONE SIZE



For all the 50 PEN and the 200 PEN samples, the required volume of bitumen was obtained from two heated 5 gallon batches, then kept in sealed tins at room temperature until use. This ensured identical bitumen properties for all samples.

The void contents of the test mixes, TABLE 5.1, were determined from the measured mix density and the theoretical mix density with zero voids, BS 594⁶.

They are low because of the unusual compaction method used for the samples.

Rolling compaction was not possible because a roller of sufficient deadweight was not available and so a Kango Hammer with a 75mm x 100mm pre-heated foot was used to compact the test samples.

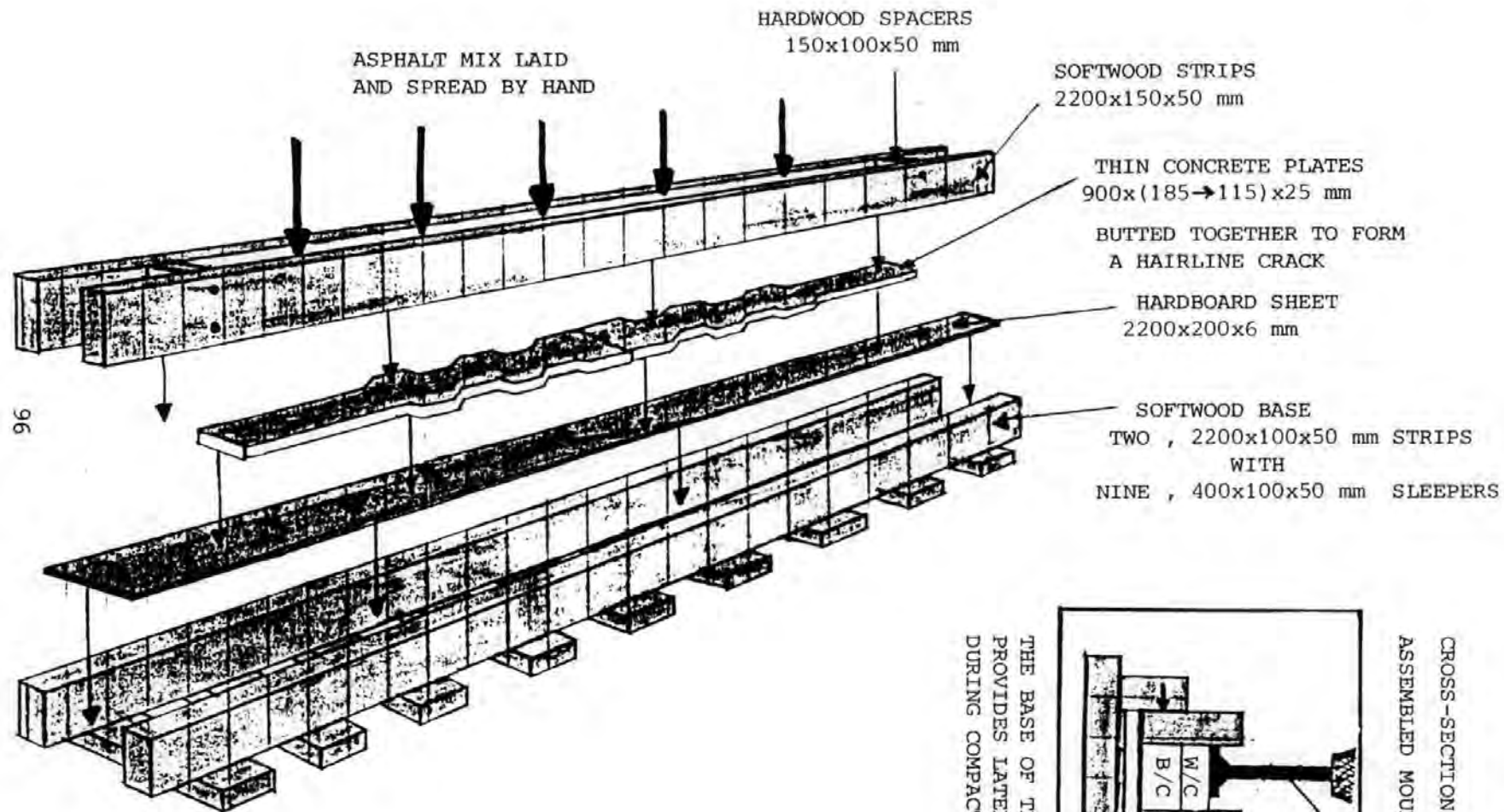
The base course and wearing course were laid and compacted over pairs of thin concrete plates in a specially designed wooden mould 1800mm long x 100mm wide, FIG 5.2.

Equal compactive effort was used for all the test samples. The foot of the Kango Hammer was moved around the inside edge of the mould in a continuous cyclic motion, for a fixed period of time and by the same operator. This process was observed to produce a "re-moulding" of the asphalt during compaction similar to that which occurs with rolling compaction.

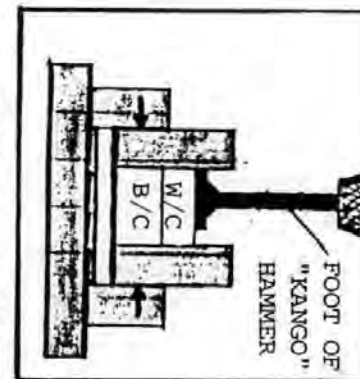
The duration of compaction was approximately equal to the maximum time available after mixing and spreading the asphalt, before it cooled to the minimum rolling temperature (30 minutes for the base-course and 15 minutes for the wearing course).

This compacting time was realised to be possibly too long because of the low void contents produced, TABLE 5.1, although no reliable data is available for realistic void contents of hot rolled asphalt compacted over lean concrete.

A Hobart mixer with a workable maximum batch size of 0.0075m³ was used for the test samples. For each batch the required amounts of bitumen and aggregates were heated separately in an oven for 16 hours at the maximum mixing temperature⁶. The mixer bowl and



THE BASE OF THE MOULD PROVIDES LATERAL SUPPORT DURING COMPACTION



CROSS-SECTION OF ASSEMBLED MOULD

"EXPLODED" VIEW OF WOODEN MOULD FOR COMPACTION OF TEST SAMPLES .

FIG 5 . 2

mixing hook were also pre-heated in this manner.

For each sample, two batches were required for the basecourse and these were mixed in quick succession and compacted together. Only one batch was required for the wearing course and coated chippings were added halfway through compaction. All materials were mixed until the aggregate was completely and uniformly covered. In practice this took about 8 minutes.

The concrete plates, FIG 5.2, were designed to simulate the fine texture of the top 25mm of a lean concrete roadbase and were at least 7 days old when used. The concrete was a 50/50 mix of grit and sand with aggregate/cement ratio of 4:1 and a water/cement ratio of 0.575. A high strength mix was required for such thin plates. The concrete plates were also reinforced by two 6mm diameter steel rods running the length of the plates, supporting a $\frac{1}{2}$ inch square, 1mm wire mesh that covered the area of the plates.

A bituminous curing emulsion was used at the minimum specified rate of 0.5 gal/yd² 38. The interaction of the residue of this emulsion and the hot asphalt during laying, produces a realistic bond in these 1.8m long samples.

Seven 1800mm long samples were produced with a range of nominal stone sizes in the basecourse and wearing course, TABLE 5.2.

TABLE 5.2 NOMINAL STONE SIZES IN THE TEST MIXES

| MIX DESIGNATION NUMBER | BITUMEN GRADE PEN | NOMINAL STONE SIZE mm | |
|------------------------|----------------------|-----------------------|------------|
| | | WEARING COURSE | BASECOURSE |
| 1 s | 200 | 14+10 | 20+14 |
| 2 s | 200 | 14+10 | 28+20 |
| 3 s | 200 | 14+10 | 40+28 |
| 4 s | 200 | 20+14 | 28+20 |
| 1 | 50 | 14+10 | 20+14 |
| 2 | 50 | 14+10 | 28+20 |
| 4 | 50 | 20+14 | 28+20 |

A 50 PEN Sample with 40+28mm Stone in the basecourse was not produced because of difficulties with the larger stones jamming the mixer and being ejected.

These 1,800mm samples were tested at room temperature and the undamaged 900mm long portions of surfacing were detached from the concrete plates and re-bonded over a series of four (250 x 200 x 12mm) steel plates with 125g of ARALDITE 2005. A further 42 tests were then performed at elevated temperatures with these "half" and "quarter" samples. These short epoxy resin bonded samples comprised the bulk of the test program.

5.2 Details of the Test Rig

The test rig was designed around a steel frame that was available in the laboratory.

1.8m long samples had to be tested at ambient temperatures but samples shorter than 1.5m could be tested at elevated temperatures with the aid of a detachable thermal cabinet, FIG 5.3.

Air is not an ideal medium for temperature control and the test samples had to be left for at least 2 hours and often overnight before a constant temperature was attained.

However, the short samples also required 24 hours for the Araldite bond to cure and so the curing and pre-heating periods for each sample were timed to coincide.

The test platens were constructed from 3 layers of 25mm thick steel plate, which provided a smooth top surface for the attachment of samples and enabled the lever-arm mechanism to be bolted through from underneath. The lever-arm mechanism transmits the crack-opening movements and is illustrated, Fig 5.4. The movements are generated by an adjustable eccentric on a flywheel plate, driven by a geared down, shunt wound, electric motor.

Further detail of the test-rig is illustrated by PLATES 5.1 & 5.2, such as the side plates and track clamps which constrain the test platens to permit only crack-opening movement and the portal frame

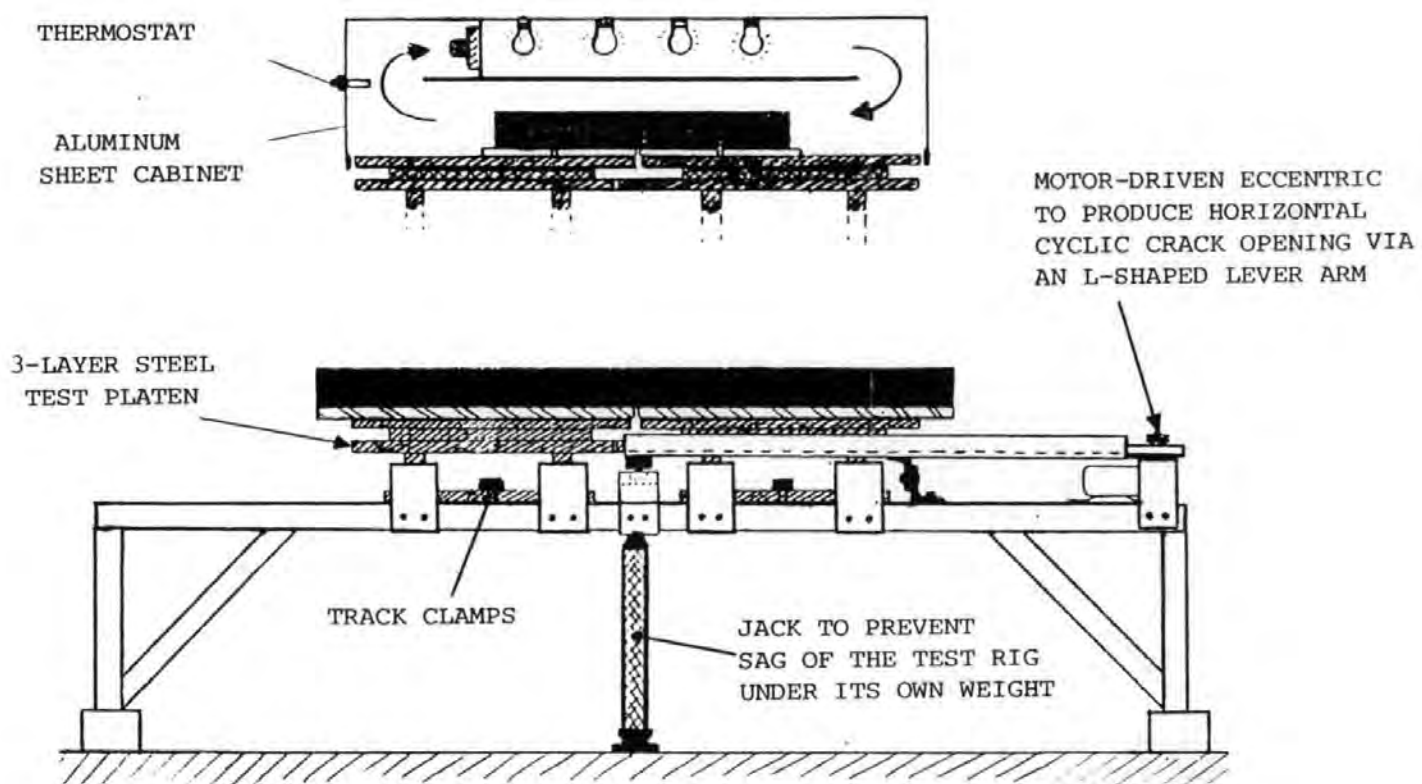


FIG 5 . 3

SCALE 1 : 16

SIDE ELEVATION OF TEST RIG WITH 1800 mm LONG TEST SAMPLE AND SECTION OF "CLOSED CIRCUIT AIR FLOW" THERMAL CABINET FOR TESTING SHORTER EPOXY RESIN BONDED SAMPLES AT ELEVATED TEMPERATURES .

DETAIL OF THE TEST-RIG MECHANISM THAT PRODUCES CYCLIC CRACK OPENING .

FIG 5 . 4

PLAN VIEW SHOWING
THE LEVER-ARM ATTACHED
TO THE UNDERSIDE OF
THE LOWER LAYER OF
THE 3-LAYER STEEL
TEST PLATENS .

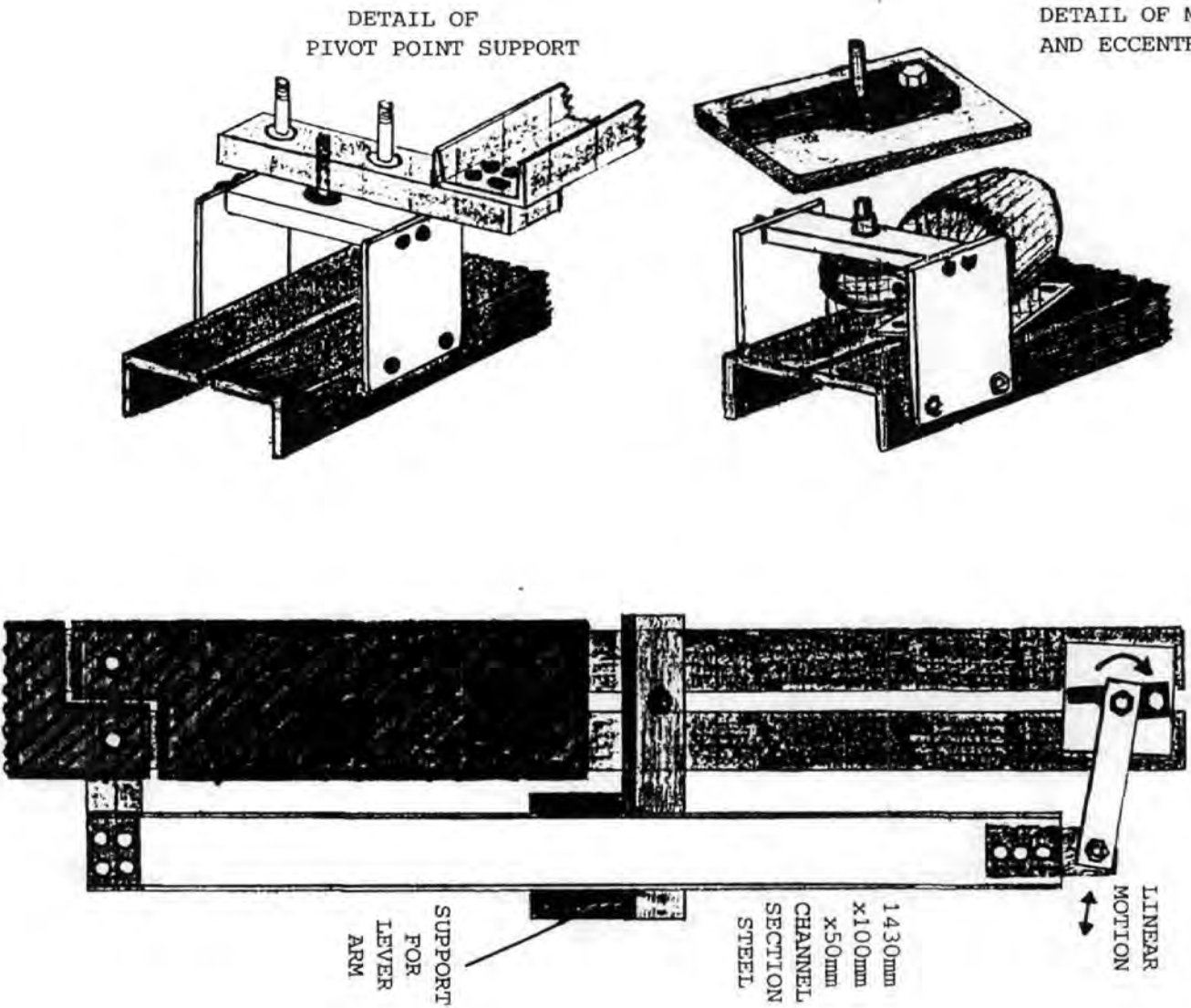


PLATE 5 . 1

APPROX SIDE VIEW OF TEST RIG WITH DETACHABLE TEMPERATURE CONTROL
CABINET IN FOREGROUND

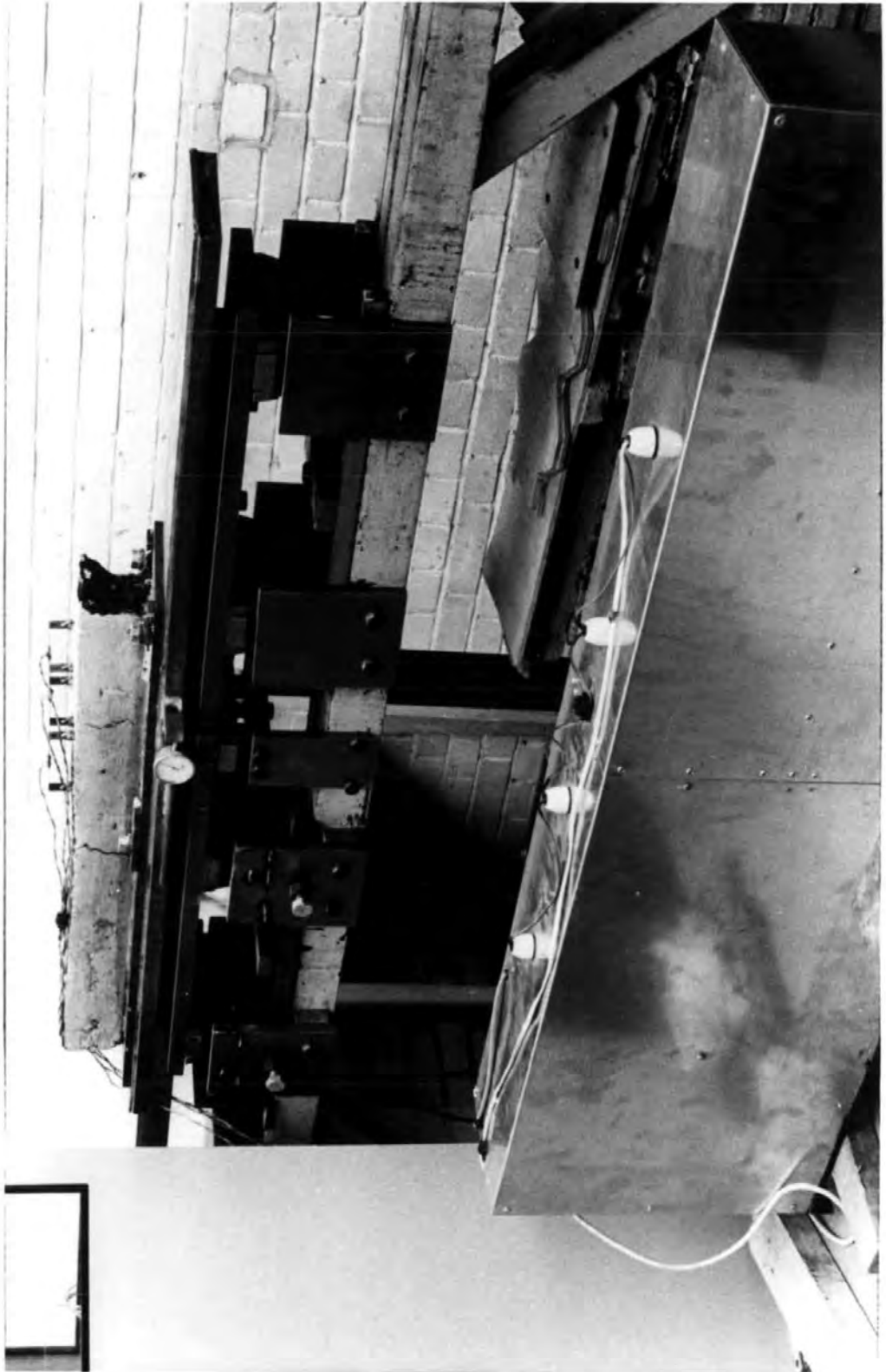
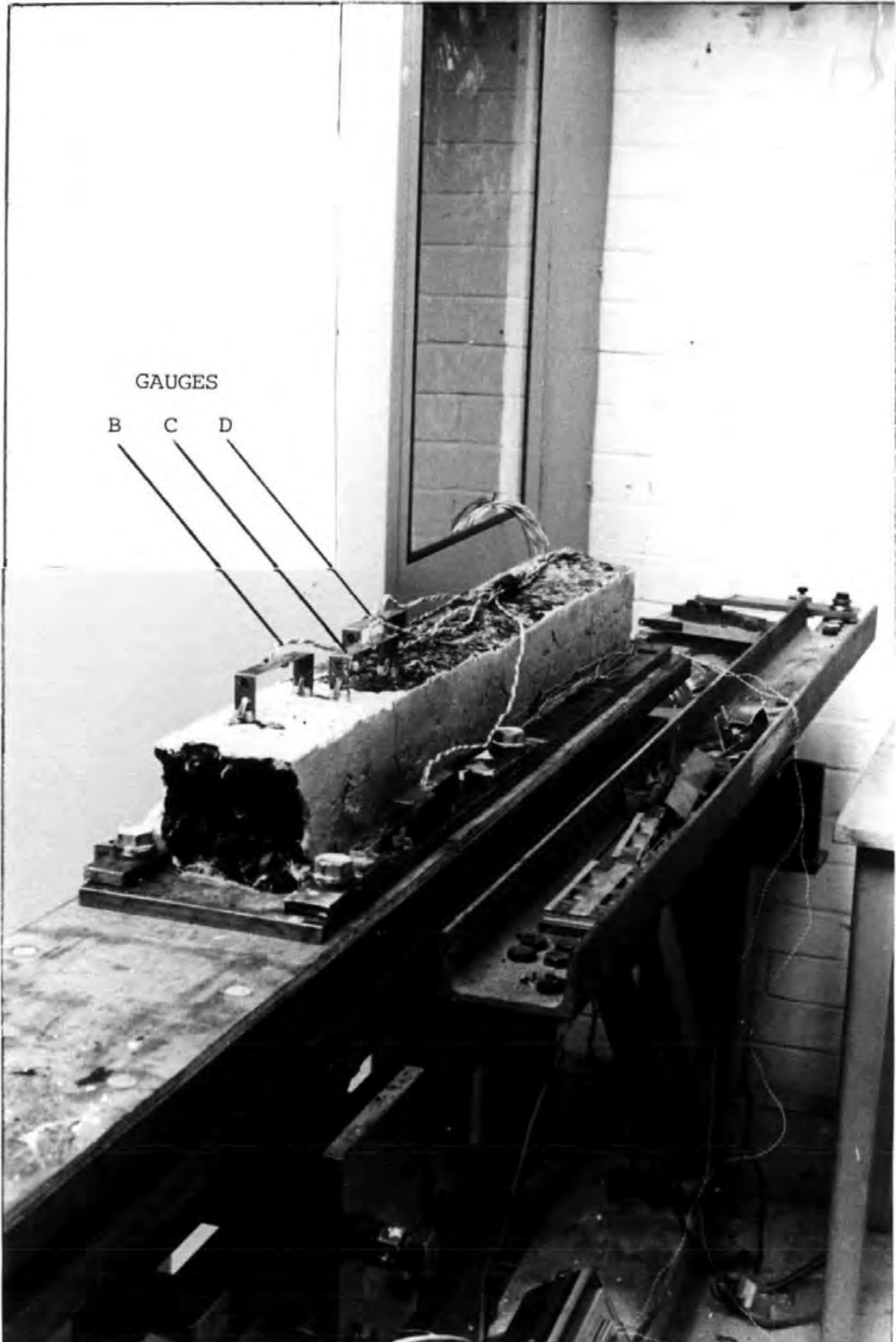


PLATE 5 . 2

APPROX END VIEW OF TEST RIG TO ILLUSTRATE PORTAL FRAME GAUGES AND
LEVER ARM MECHANISM



mounted strain gauges that monitor displacements throughout each test.

5.3 Measurement of Crack Growth During Testing

Portal frame type displacement gauges, FIG 5.5, were developed for the test programme. These gauges were re-usable and generated negligible reaction force when measuring cyclic displacements ($<1N/mm$).

A single gauge was used to monitor the cyclic crack opening movement (CO) applied to the base of the test samples (GAUGE A) and three gauges were mounted in a line on top of the test samples (GAUGES B, C & D), PLATES 5.1 & 5.2.

GAUGES A, B, C & D were calibrated with the aid of a dial gauge mounted on the side of the test rig, PLATE 5.1. The gauge outputs were amplified and recorded throughout each test, on a U-V type multi-channel chart recorder.

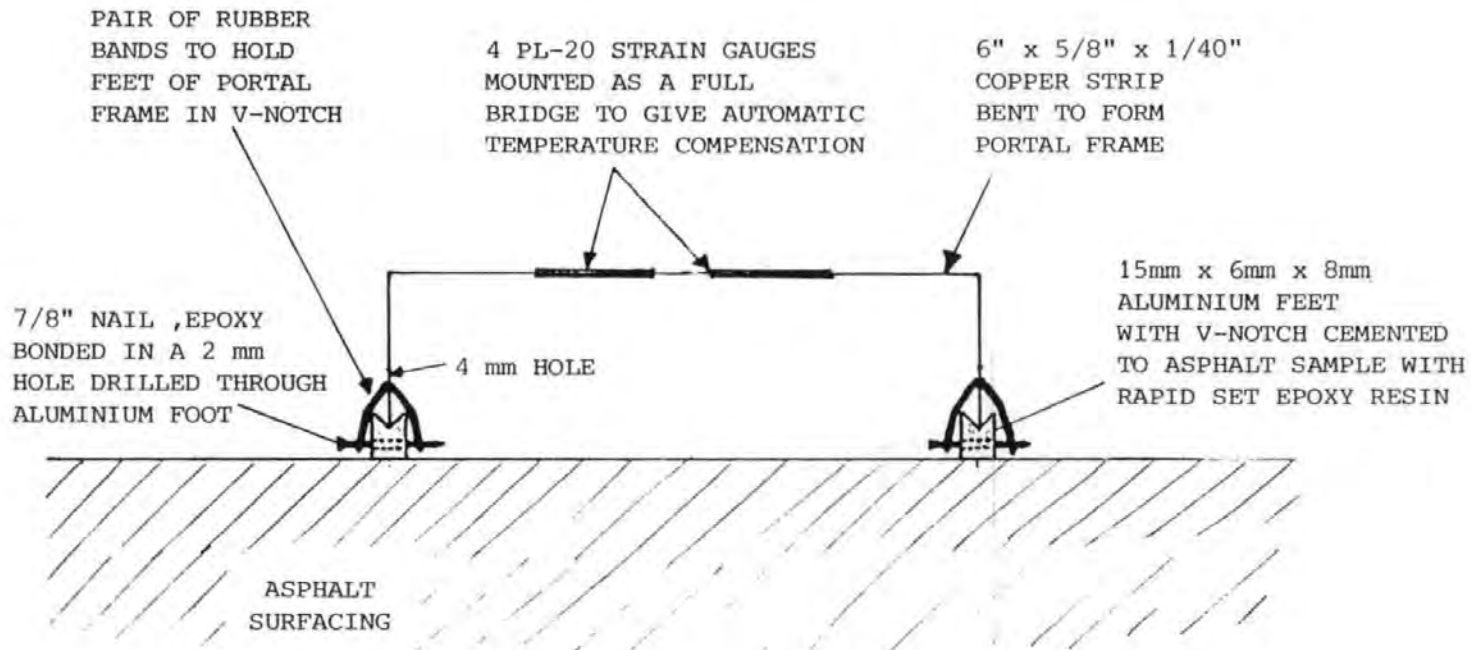
In all tests, the transverse crack rose up through the central 100mm of the samples monitored by GAUGE C.

The cyclic displacements recorded from GAUGE C increased steadily during each test from approx. 15% CO to approx 100% CO. It was realised that the ratio of the displacements recorded from GAUGE C and GAUGE A was physically related to the height of the crack front within the samples and could be used to determine crack growth rates during testing and the failure point of each test.

The displacement ratio C/A vs crack length curves for a 95mm sample, FIG 5.6, were determined from the finite element results, SECTION 3.4.

5.4 Tensile Creep Tests to Determine the Effective Modulus of Materials during Testing

The Effective Modulus (mix stiffness) of both the basecourse and the wearing course, at the test conditions of temperature and frequency (bitumen stiffness), had to be ascertained:-



RE-USABLE PORTAL FRAME DISPLACEMENT GAUGES TO MONITOR CYCLIC CRACK OPENING AND CYCLIC DISPLACEMENTS OVER A 100 mm GAUGE LENGTH .

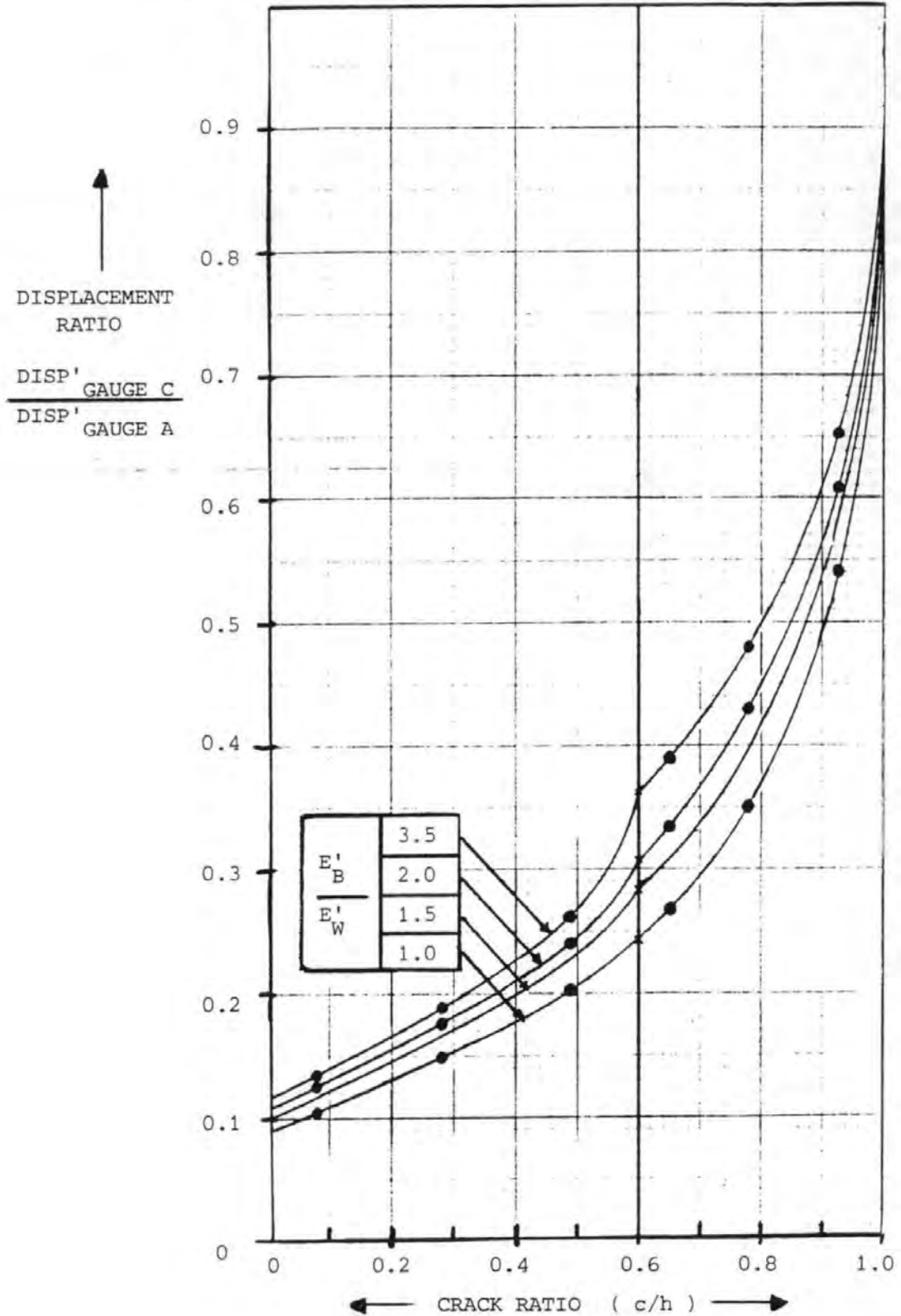
FIG 5 . 5

FIG 5 . 6

CURVES TO DETERMINE THE CRACK RATIO (c/h) OF PARTIALLY CRACKED SAMPLES FROM THE RATIO OF THE CYCLIC DISPLACEMENTS AT THE TOP AND BASE OF THE SAMPLES , 95 mm SURFACING .

E'_B = EFFECTIVE MODULUS OF THE BASECOURSE

E'_W = EFFECTIVE MODULUS OF THE WEARING COURSE



- i) To enable crack growth rates (dc/dN) during testing to be determined from, FIG 5.6,
- ii) to enable stress intensity factors (K_1) during crack growth to be determined from, FIG 3.5.

These experimental values of (dc/dN) and (K_1) enable experimental values for fatigue crack growth constants A, n to be determined.

Hills et al⁴⁷ have shown that the results of creep tests at different temperatures and stress levels, with bitumen grades, could all be combined as plots of S_{MIX} vs S_{BIT} for that specific mix. These plots define the Effective Modulus (S_{MIX}) for a range of test conditions (S_{BIT}).

These creep tests results also enable theoretical values of the crack growth constant n to be determined from Schapery's Theory²⁷ where n is related to the slope of a LOG-LOG plot of creep compliance ($1/S_{MIX}$) vs time.

Tensile creep tests were performed on pieces approx (100 x 100 x 40)mm that were cut from samples after testing and had been used for void content analysis. The tensile creep test apparatus is illustrated, FIG 5.7.

24 samples of basecourse and wearing course with coated chippings, were tested at ambient temperatures (15-18°C) and stress levels of approx 0.1MN/m² and the S_{MIX} vs S_{BIT} curves are illustrated, FIG 5.8. There was no discernable difference between the 14 and 20mm stone size wearing course mixes and the 20, 28 and 40mm stone size basecourse mixes and the mean curves are illustrated, FIG 5.9. These curves were found to be reasonably consistent, when extrapolated, with the SHELL data⁴⁶ for bitumen stiffness $10^7 + 10^9$ N/m² that is valid for all mixes.

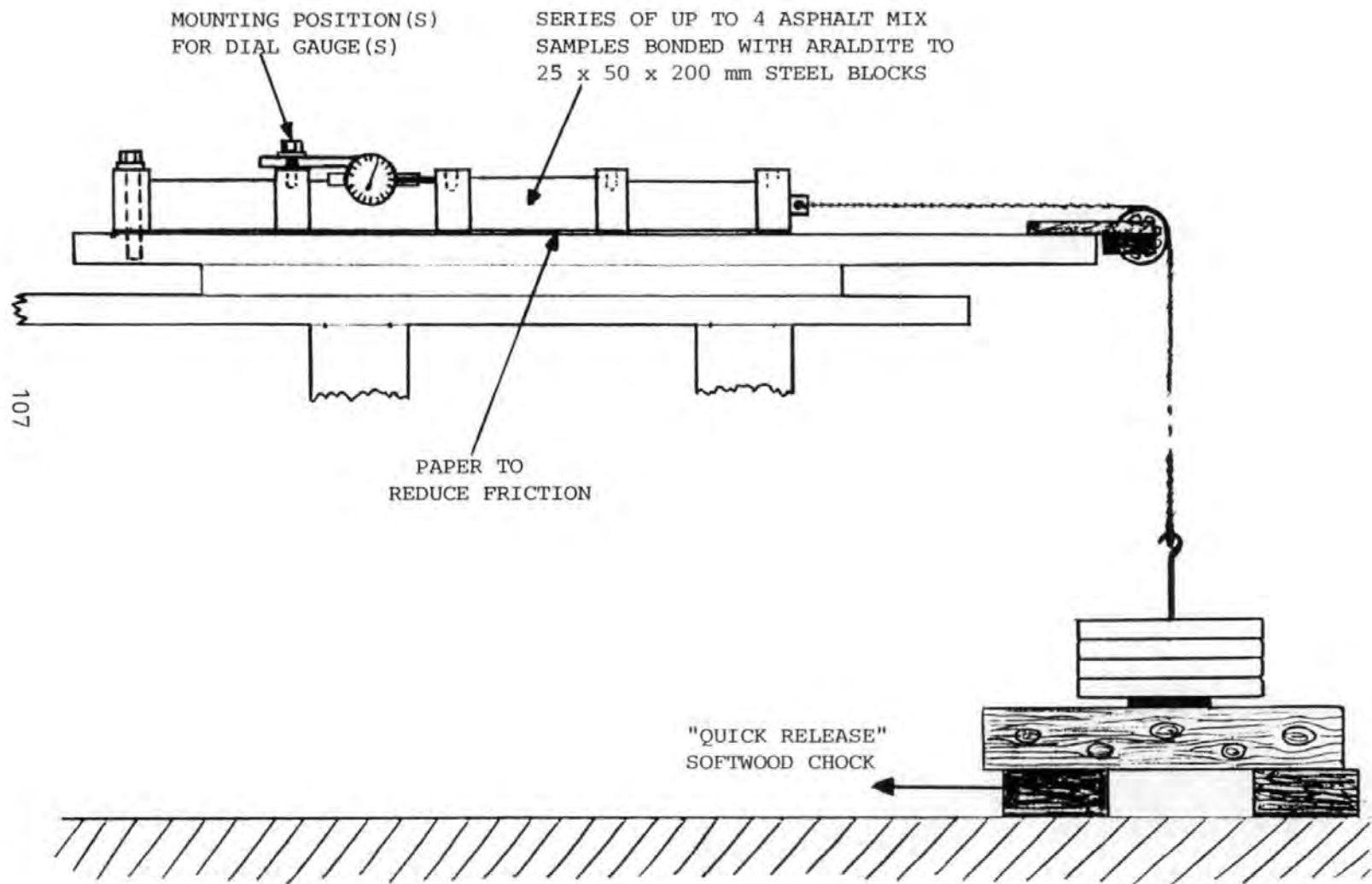


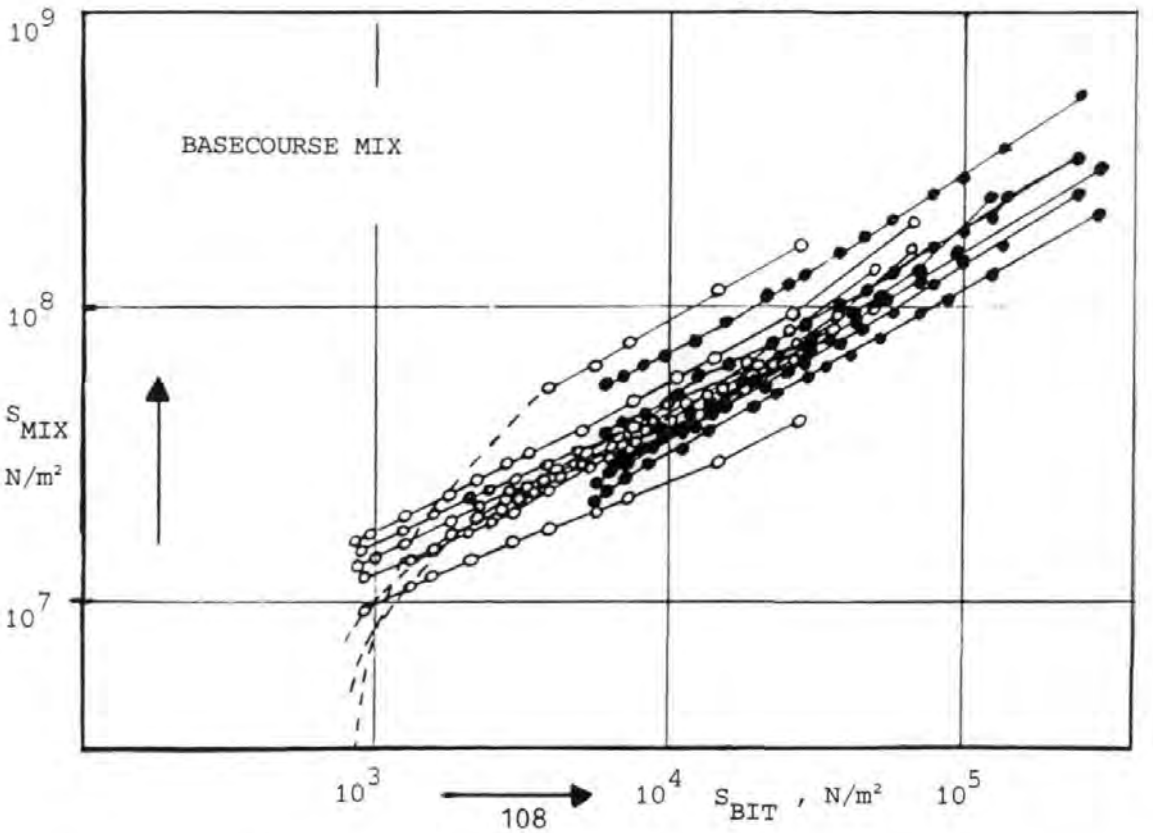
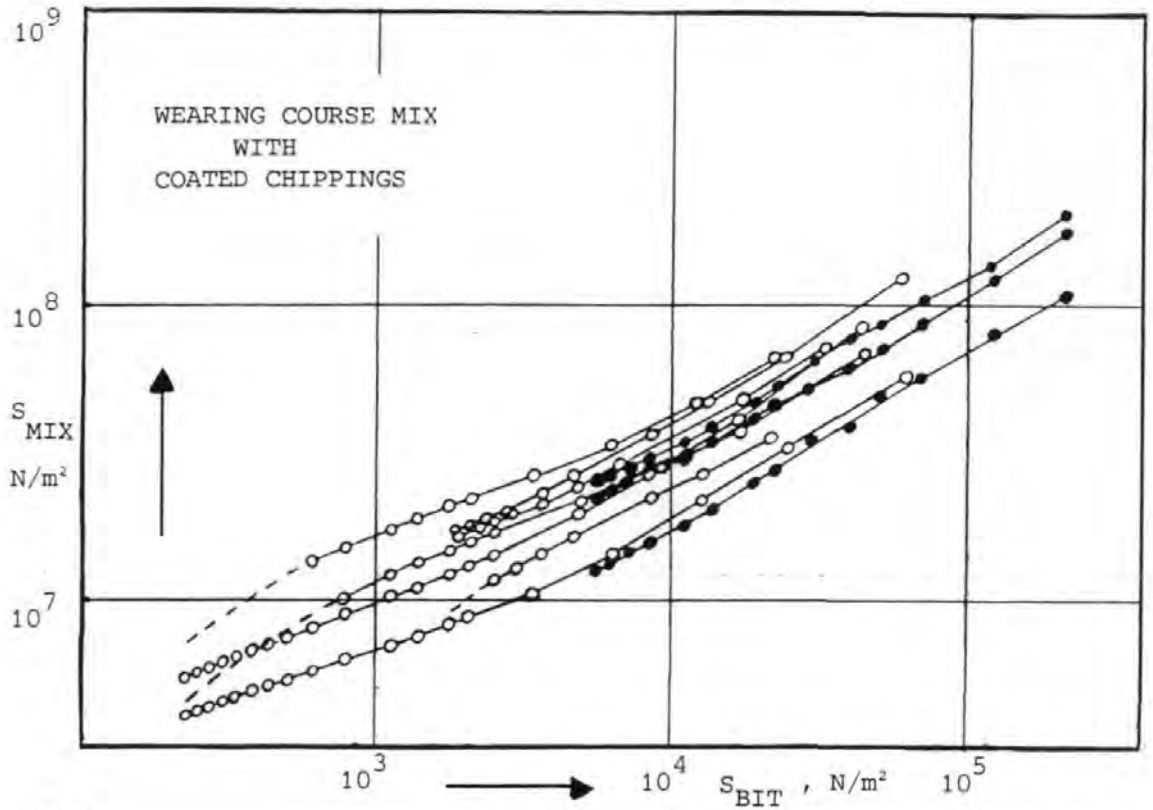
FIG 5 . 7

APPARATUS ATTACHED TO THE TEST RIG FOR SIMULTANEOUS TENSILE CREEP TESTING OF UP TO 4 , 100 x 100 x 40 mm SAMPLES .

FIG 5 . 8

CREEP CURVES DERIVED FROM TESTING 100 x 100 x 40 mm SAMPLES CUT FROM THE TEST MIXES AFTER TESTING .

- 50 PEN SAMPLES
- 200 PEN SAMPLES



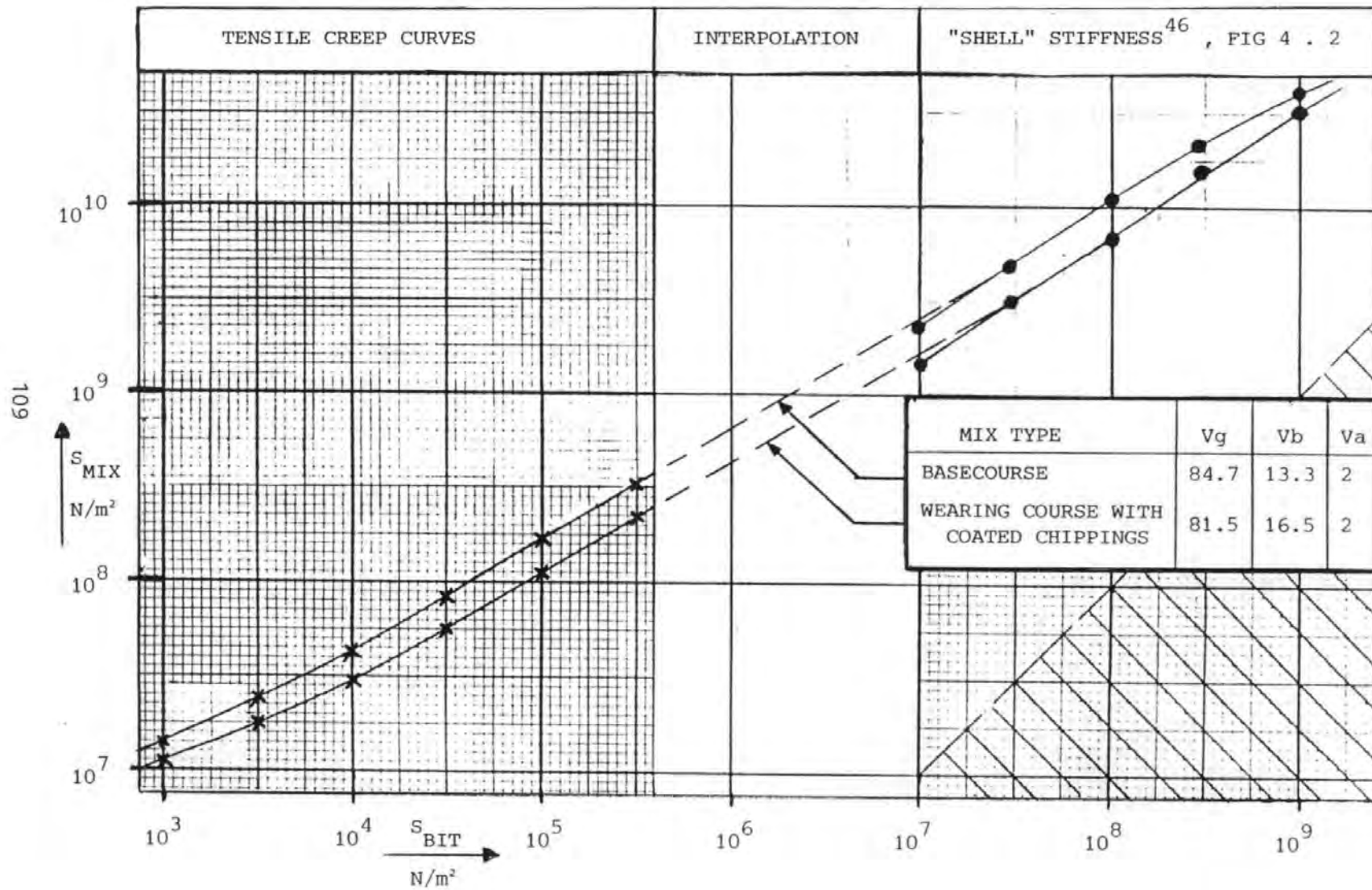


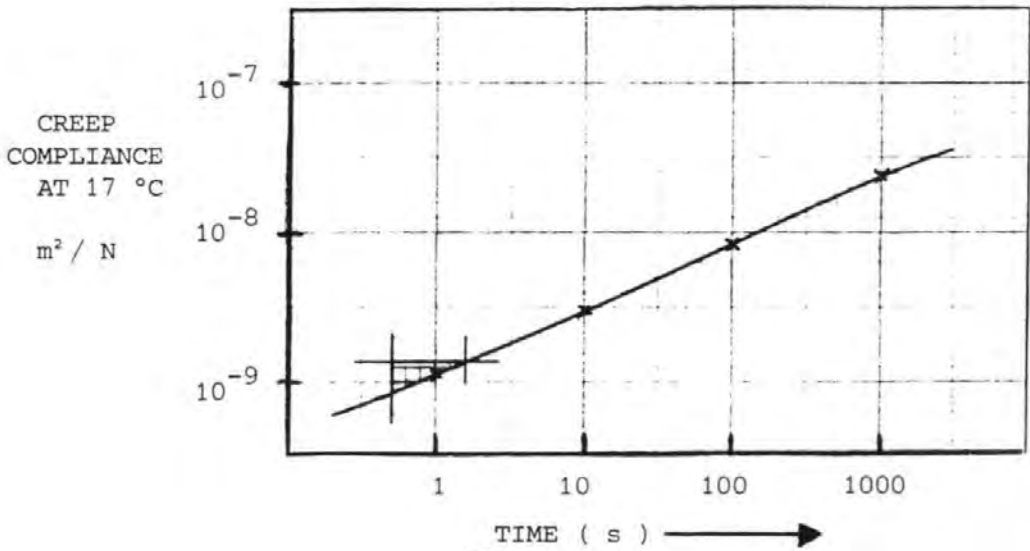
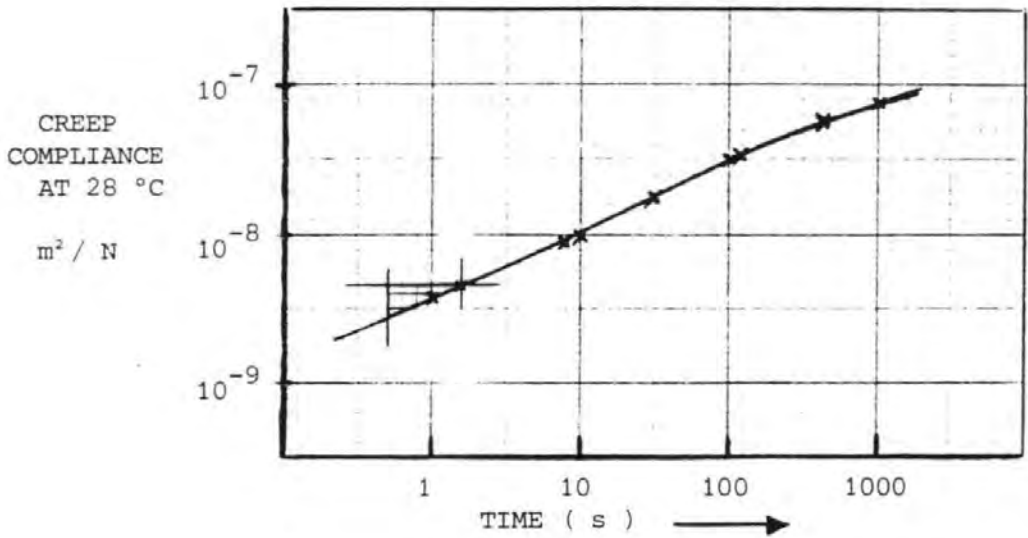
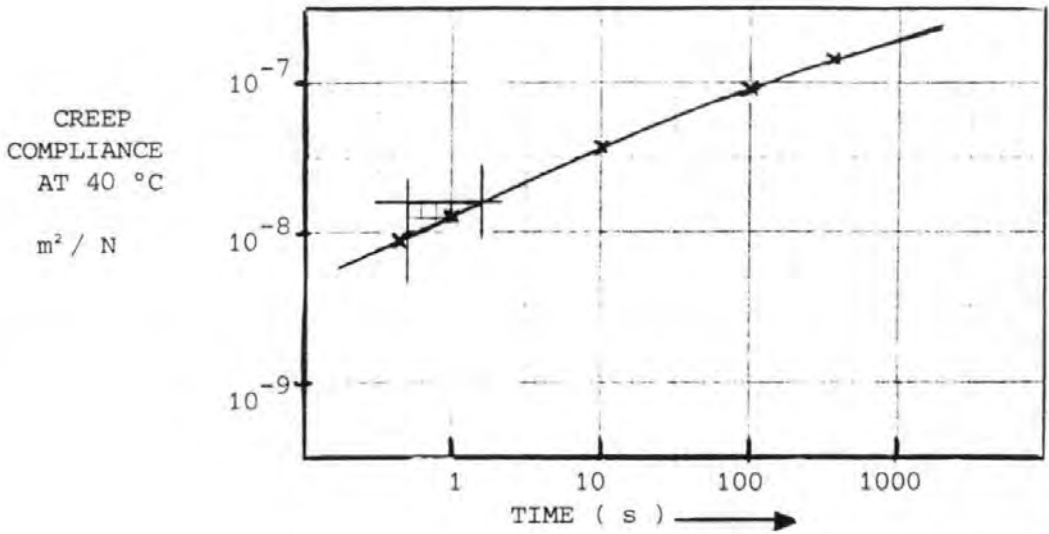
FIG 5 . 9
COMPARISON OF THE TENSILE CREEP CURVES FOR THE TEST MIXES WITH THE "SHELL" STIFFNESS RELATIONSHIP AT HIGH BITUMEN STIFFNESS.

The mean curves, FIG 5.9, were replotted as LOG-LOG plots of creep compliance vs time at a range of temperatures. According to Schapery's Theory²⁷, theoretical n values for testing at 0.12Hz are determined by the slope of the curves between 0.443 and 1.33 seconds.

Creep compliance curves for the wearing course mix with 50 PEN bitumen are illustrated, FIG 5.10, and the calculation of theoretical n values is summarised, TABLE 5.3.

FIG 5 . 10

LOG - LOG PLOTS OF CREEP COMPLIANCE vs TIME, FOR THE WEARING COURSE MIX WITH COATED CHIPPINGS, CONTAINING 50 PEN BITUMEN .



DETERMINATION OF THEORETICAL n VALUES FOR THE TEST MIXES FROM
 SCHAPERY'S THEORY²⁷ (TESTING AT 0.12 Hz)

TABLE 5 . 3

| MIX TYPE | BITUMEN GRADE | TEMPERATURE (°C) | EFFECTIVE MODULUS (CREEP COMPLIANCE) ⁻¹ AT TIME = 1 SECOND (N / m ²) | SLOPE m AT TIME 1 SECOND | n | MEAN VALUE FOR n EXCLUDING 200 PEN AT 43 °C | |
|---|---|--|--|--------------------------|------|---|------|
| WEARING COURSE WITH COATED CHIPPINGS | 50 PEN T _{R&B} 56½°C PI + 0.6 | 17 | 8.91 x 10 ⁸ | 0.43 | 6.65 | 6.57 | |
| | | 28 | 2.63 x 10 ⁸ | 0.42 | 6.76 | | |
| | | 40 | 7.76 x 10 ⁷ | 0.46 | 6.35 | | |
| | 200 PEN T _{R&B} 42½°C PI + 0.3 | 17 | 2.09 x 10 ⁸ | 0.45 | 6.44 | 6.45 | |
| | | 26 | 7.94 x 10 ⁷ | 0.46 | 6.35 | | |
| | | 37 | 2.88 x 10 ⁷ | 0.41 | 6.88 | | |
| | | 43 | 1.91 x 10 ⁷ | 0.37 | 7.41 | | |
| | BASE COURSE | 50 PEN T _{R&B} 56½°C PI + 0.6 | 17 | 1.45 x 10 ⁹ | 0.44 | 6.54 | 6.33 |
| | | | 28 | 4.07 x 10 ⁸ | 0.43 | 6.65 | |
| | | | 40 | 1.17 x 10 ⁸ | 0.49 | 6.08 | |
| 200 PEN T _{R&B} 42½°C PI + 0.3 | | 17 | 3.31 x 10 ⁸ | 0.47 | 6.26 | 6.33 | |
| | | 26 | 1.20 x 10 ⁸ | 0.48 | 6.17 | | |
| | | 37 | 4.17 x 10 ⁷ | 0.47 | 6.26 | | |
| | | 43 | 2.63 x 10 ⁷ | 0.41 | 6.88 | | |

6.0 TEST RESULTS

6.1 Observations

Simulative thermal reflection cracking tests have been performed at 0.12hz and 3 temperature levels corresponding to 3 levels of bitumen stiffness for each bitumen grade.

The test results are detailed, TABLE 6.1/2/3/4, and can be used to plot fatigue lines, FIG 6.1.

The 46 test results were only just sufficient to establish the position of the fatigue lines. The slope of the fatigue lines, FIG 6.1, is $-(1/n)$ predicted by creep tests and Schapery's equation, TABLE 5.3, for the wearing course material.

The scatter of the test data was such that experimental values for the slope of fatigue lines could not be determined. This scatter of the test data is a combination of inherent scatter and scatter due to variations of $\pm 5\text{mm}$ in sample surfacing thickness and $\pm 3^\circ\text{C}$ in test temperature.

Major problems were encountered when the 200 PEN Samples were tested at approx 40°C ; TABLE 6.4. The 4s mix samples were the first to be tested and these were observed to slump laterally after approximately 5000 cycles, but the fatigue lives for these tests could be estimated from the crack growth up to 5000 cycles.

Mix samples denoted as 1s, 2s and 3s were tested at higher temperatures and an n-SECTION Steel Collar was fitted over the test sample to restrain lateral slump during testing.

This Steel Collar had minimal clearance to either side of the test samples and a silicone grease was used to reduce friction.

Unfortunately the test samples still became stuck to the Steel Collar and this appeared to prevent further vertical cracking. Horizontal cracking did develop in the basecourse of these samples towards the end of the tests, but this was probably caused by the Steel Collar and not a realistic effect.

Five of these tests became stuck between 50 and 5000 cycles and the fatigue lives could be estimated from the peaks of the crack growth vs cycles curves. The remaining tests became stuck after 2 to 5 cycles

| STONE SIZE IN MIX | TEST SAMPLE DIMENSIONS (mm) | | CYCLIC CRACK OPENING (mm) | | TEST TEMPERATURE (°C) | | TEST CONDITIONS OF BITUMEN STIFFNESS (N / m ²) | | FATIGUE LIFE (CYCLES) FOR 100 % CRACKING | % CRACKED IN TESTS WITH NO FAILURE |
|-------------------|-------------------------------|--------|-----------------------------|-------------|-------------------------|-------------|---|---------------------|--|------------------------------------|
| | TABLE 5.2 | LENGTH | HEIGHT | BASE COURSE | WEARING COURSE | BASE COURSE | WEARING COURSE | BASE COURSE | | |
| 2 | 1800 | 100 | | 0.89 | 16½ | 16½ | 2.8x10 ⁶ | 2.8x10 ⁶ | 3,400 | |
| 1 | 1800 | 100 | | 0.95 | 17 | 17 | 2.0x10 ⁶ | 2.0x10 ⁶ | 3,000 | |
| 4 | 1800 | 100 | | 0.99 | 17½ | 17½ | 2.4x10 ⁶ | 2.4x10 ⁶ | 2,400 | |
| 2 | 450 | 95 | 0.82 | 0.86 | 27½ | 29 | 4.0x10 ⁵ | 3.1x10 ⁵ | 51,000 EST | 57 |
| 2 | 900 | 95 | 0.89 | 0.96 | 26½ | 27½ | 4.6x10 ⁵ | 3.9x10 ⁵ | 3,650 | |
| 4 | 450 | 94 | 0.93 | 0.97 | 25 | 26½ | 6.5x10 ⁵ | 4.9x10 ⁵ | 4,150 | |
| 1 | 450 | 97 | 1.05 | 1.06 | 28½ | 30 | 3.2x10 ⁵ | 2.2x10 ⁵ | 4,200 | |
| 2 | 450 | 98 | 1.01 | 1.14 | 26½ | 27½ | 4.7x10 ⁵ | 4.0x10 ⁵ | 3,360 | |
| 4 | 450 | 94 | 1.06 | 1.14 | 25½ | 26½ | 5.6x10 ⁵ | 4.6x10 ⁵ | 2,440 | |
| 1 | 900 | 93 | 1.21 | 1.28 | 29½ | 31 | 2.8x10 ⁵ | 2.2x10 ⁵ | 2,600 | |
| 4 | 900 | 92 | 1.22 | 1.35 | 24½ | 25½ | 6.8x10 ⁵ | 5.6x10 ⁵ | 2,220 | |
| 1 | 450 | 90 | 1.43 | 1.52 | 26 | 27½ | 5.1x10 ⁵ | 3.8x10 ⁵ | 1,450 | |

EST = FATIGUE LIFE ESTIMATED FROM PEAK % CRACKED AT END OF TEST

TEST RESULTS FOR SAMPLES WITH 50 PEN BITUMEN AT APPROXIMATELY 17 °C AND 27 °C AT 0.12 Hz .

TABLE 6 . 1

TEST RESULTS FOR SAMPLES WITH 50 PEN BITUMEN AT APPROXIMATELY 40 °C AND 0.12 Hz .

TABLE 6 . 2

| STONE SIZE IN MIX | TEST SAMPLE DIMENSIONS (mm) | | CYCLIC CRACK OPENING (mm) | | TEST TEMPERATURE (°C) | | TEST CONDITIONS OF BITUMEN STIFFNESS (N / m ²) | | FATIGUE LIFE (CYCLES) FOR 100 % CRACKING | % CRACKED IN TESTS WITH NO FAILURE |
|-------------------|-------------------------------|--------|-----------------------------|-------------|-------------------------|-------------|---|-------------------|--|------------------------------------|
| | TABLE 5.2 | LENGTH | HEIGHT | BASE COURSE | WEARING COURSE | BASE COURSE | WEARING COURSE | BASE COURSE | | |
| 2 | 450 | 94 | 1.03 | 1.07 | 35 | 37 | 1.1×10^5 | 7.9×10^4 | 22,000 | |
| 2 | 450 | 90 | 1.25 | 1.27 | 36 | 38 | 8.9×10^4 | 6.2×10^4 | 2,320 | |
| 1 | 450 | 99 | 1.34 | 1.36 | 37½ | 39½ | 6.8×10^4 | 4.8×10^4 | 250,000 EST | 77 |
| 4 | 450 | 91 | 1.37 | 1.38 | 41 | 43½ | 3.9×10^4 | 2.5×10^4 | 3,400 | |
| 2 | 900 | 93 | 1.43 | 1.50 | 36½ | 39 | 8.3×10^4 | 5.4×10^4 | 2,050 | |
| 1 | 900 | 97 | 1.60 | 1.60 | 38½ | 41½ | 5.9×10^4 | 3.5×10^4 | 14,400 | |
| 4 | 450 | 96 | 1.72 | 1.76 | 39 | 41½ | 5.2×10^4 | 3.4×10^4 | 10,750 | |
| 4 | 900 | 89 | 1.75 | 1.84 | 40½ | 43 | 4.0×10^4 | 2.6×10^4 | 11,250 | |
| 1 | 450 | 98 | 1.86 | 1.92 | 39 | 41 | 5.4×10^4 | 3.8×10^4 | 18,150 | |

EST = FATIGUE LIFE ESTIMATED FROM % CRACKED AT END OF TEST

TEST RESULTS FOR SAMPLES WITH 200 PEN BITUMEN AT APPROXIMATELY
17 °C AND 27 °C AT 0.12 Hz .

TABLE 6 . 3

| STONE SIZE IN MIX | TEST SAMPLE DIMENSIONS (mm) | | CYCLIC CRACK OPENING (mm) | | TEST TEMPERATURE (°C) | | TEST CONDITIONS OF BITUMEN STIFFNESS (N / m ²) | | FATIGUE LIFE (CYCLES) FOR 100 % CRACKING | % CRACKED IN TESTS WITH NO FAILURE |
|-------------------------|-------------------------------------|--------|-----------------------------------|----------------|-------------------------------|----------------|---|---------------------|---|--|
| | TABLE 5.2 | LENGTH | HEIGHT | BASE COURSE | WEARING COURSE | BASE COURSE | WEARING COURSE | BASE COURSE | | |
| 1s | 1800 | 100 | | 0.96 | 16½ | 16½ | 2.6x10 ⁵ | 2.6x10 ⁵ | 30,000 | |
| 4s | 1800 | 100 | | 1.00 | 17½ | 17½ | 1.9x10 ⁵ | 1.9x10 ⁵ | 25,000 | |
| 1s | 450 | 95 | 1.19 | 1.19 | 24 | 25 | 7.2x10 ⁴ | 6.0x10 ⁴ | 25,000 | |
| 3s | 450 | 95 | 1.22 | 1.22 | 24½ | 26 | 6.3x10 ⁴ | 4.9x10 ⁴ | 30,900 | |
| 4s | 450 | 98 | 1.20 | 1.29 | 21½ | 22½ | 1.1x10 ⁵ | 9.1x10 ⁴ | 7,800 | |
| 2s | 450 | 96 | 1.36 | 1.36 | 26 | 27½ | 4.9x10 ⁴ | 3.7x10 ⁴ | 27,600 | |
| 3s | 900 | 93 | 1.41 | 1.41 | 24½ | 26 | 6.0x10 ⁴ | 4.7x10 ⁴ | 18,900 | |
| 1s | 900 | 93 | 1.45 | 1.49 | 25 | 26 | 5.5x10 ⁴ | 4.7x10 ⁴ | 3,900 | |
| 4s | 900 | 93 | 1.57 | 1.67 | 23 | 23½ | 7.9x10 ⁴ | 7.1x10 ⁴ | 2,600 | |
| 1s | 450 | 96 | 1.68 | 1.68 | 25 | 26½ | 5.6x10 ⁴ | 4.4x10 ⁴ | 3,660 | |
| 3s | 450 | 92 | 1.68 | 1.68 | 26 | 28 | 4.5x10 ⁴ | 3.2x10 ⁴ | 22,500 | |
| 2s | 900 | 97 | 1.72 | 1.72 | 25½ | 27 | 4.8x10 ⁴ | 3.7x10 ⁴ | 14,950 | |
| 2s | 450 | 97 | 1.82 | 1.85 | 27 | 29 | 3.8x10 ⁴ | 2.6x10 ⁴ | 7,800 | |
| 4s | 450 | 93 | 1.97 | 2.05 | 23½ | 24½ | 7.1x10 ⁴ | 5.9x10 ⁴ | 825 | |

TEST RESULTS FOR SAMPLES WITH 200 PEN BITUMEN AT APPROXIMATELY
40 °C AND 0.12 Hz .

TABLE 6 . 4

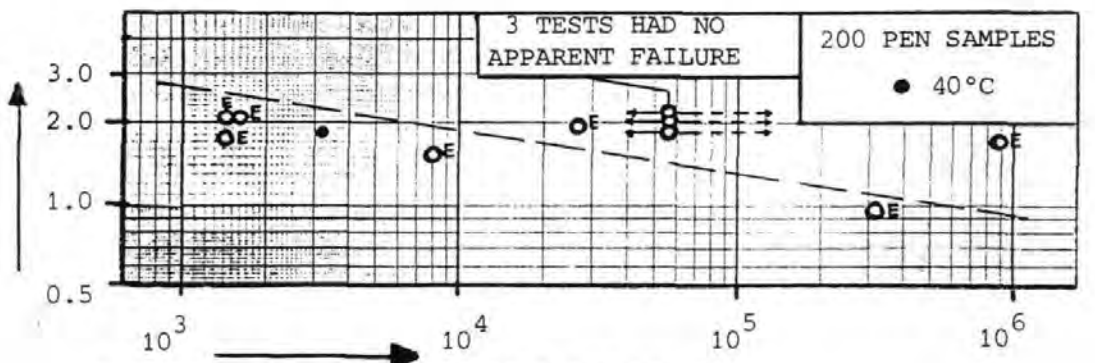
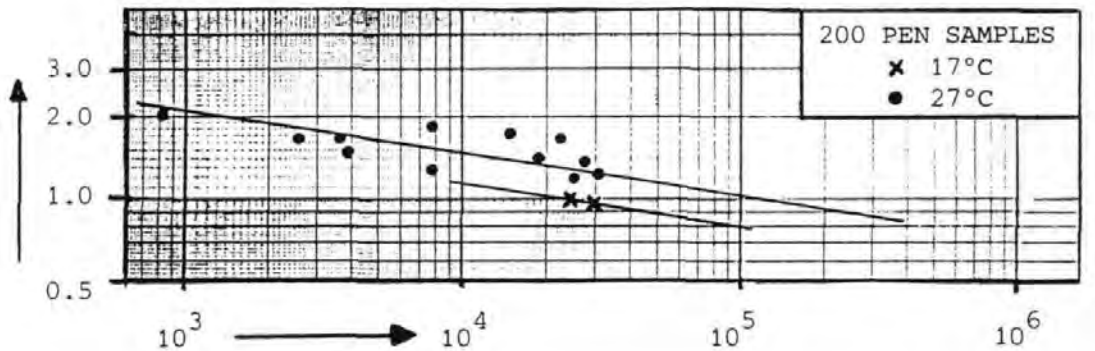
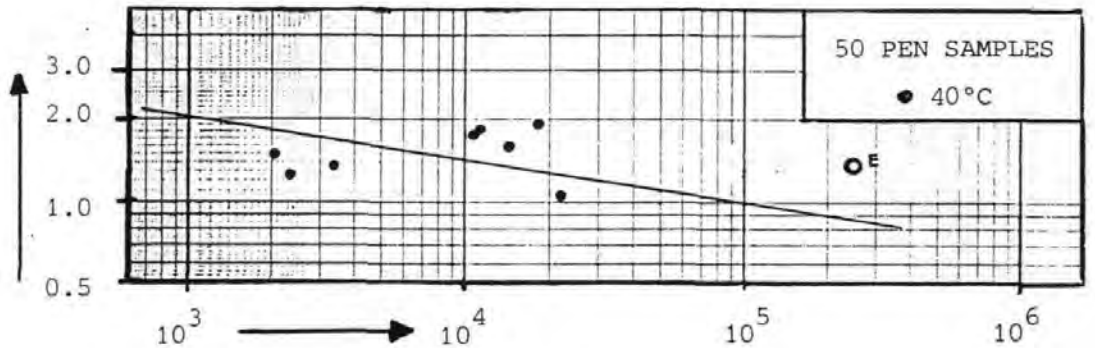
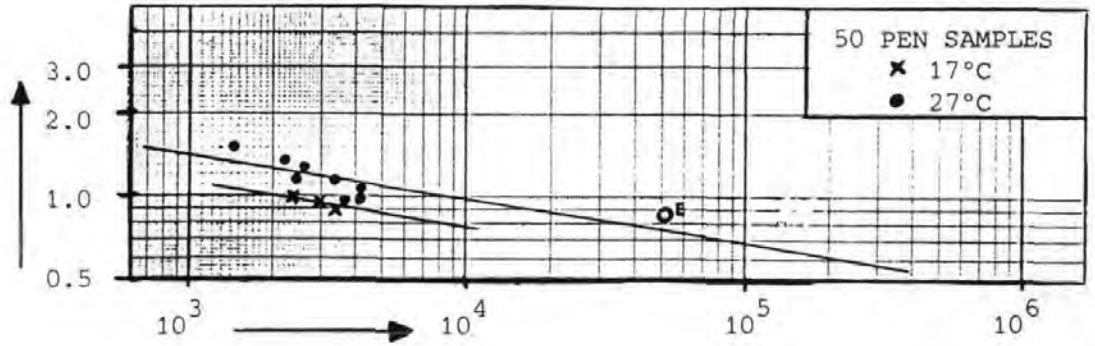
| STONE SIZE IN MIX | TEST SAMPLE DIMENSIONS (mm) | | CYCLIC CRACK OPENING (mm) | | TEST TEMPERATURE (°C) | | TEST CONDITIONS OF BITUMEN STIFFNESS (N / m ²) | | FATIGUE LIFE (CYCLES) FOR 100 % CRACKING | % CRACKED IN TESTS WITH NO FAILURE |
|-------------------------|-------------------------------------|--------|-----------------------------------|----------------|-------------------------------|----------------|---|---------------------|---|--|
| | TABLE 5.2 | LENGTH | HEIGHT | BASE COURSE | WEARING COURSE | BASE COURSE | WEARING COURSE | BASE COURSE | | |
| 4s | 900 | 92 | 0.96 | 0.96 | 38½ | 41½ | 4.8x10 ³ | 3.1x10 ³ | 420,000 EST | 62½ |
| 4s | 450 | 92 | 1.52 | 1.52 | 35 | 37 | 9.8x10 ³ | 6.3x10 ³ | 8,100 EST | 90½ |
| 4s | 450 | 92 | 1.93 | 1.93 | 34½ | 36½ | 1.0x10 ⁴ | 7.4x10 ³ | 26,000 EST | 82½ |
| 1s | 900 | 97 | 1.69 | 1.70 | 36 | 38 | 7.9x10 ³ | 5.8x10 ³ | 900,000 EST | 62 |
| 2s | 450 | 89 | 1.75 | 1.75 | 39 | 41 | 5.4x10 ³ | 4.0x10 ³ | 1,420 EST | 72½ |
| 1s | 450 | 95 | 1.83 | 1.83 | 34½ | 36½ | 1.2x10 ⁴ | 8.3x10 ³ | 3,200 | |
| 3s | 900 | 91 | 1.84 | 1.84 | 43 | 46 | 3.0x10 ³ | 2.0x10 ³ | | 49 |
| 2s | 900 | 91 | 2.05 | 2.05 | 40½ | 43 | 4.0x10 ³ | 2.8x10 ³ | | 49 |
| 3s | 450 | 93 | 2.08 | 2.09 | 41½ | 44½ | 3.9x10 ³ | 2.5x10 ³ | 1,600 EST | 74 |
| 1s | 450 | 97 | 2.08 | 2.10 | 36 | 38 | 8.3x10 ³ | 6.0x10 ³ | 1,430 EST | 69½ |
| 2s | 450 | 94 | 2.13 | 2.14 | 38½ | 40½ | 5.9x10 ³ | 4.4x10 ³ | | 44 |
| 3s | 450 | 90 | 2.25 | 2.25 | 55 | 60 | 6.8x10 ² | 4.0x10 ² | | 82 |

EST = FATIGUE LIFE ESTIMATED FROM PEAK % CRACKED DURING TEST

FIG 6 . 1

"FATIGUE LINES" FOR 95 mm TWO-COURSE SURFACING , DERIVED FROM THE TEST RESULTS .

CYCLIC CRACK OPENING , mm



FATIGUE LIFE (CYCLES TO 100% CRACKED)

and fatigue lives and can only be regarded as tentative.

The tests with no failure point were usually terminated at 40,000 cycles (4 days testing). The fatigue life could then be estimated by comparing the peak of crack growth, with the median crack growth vs % fatigue life curve for all test samples with that bitumen grade at that temperature, FIG 6.2. The curves for 50 and 200 PEN samples tested at 40°C were combined. These 40°C results were distorted by an approximate 5°C temperature difference between the top and bottom of the samples which tended to slow down crack growth in the wearing course.

Of the curves for samples tested at 27°C, where the temperature difference between top and bottom of the samples was only 2½°C, only those for the 200 PEN samples are truly representative. The results for the 50 PEN samples were distorted because high loads reduced crack opening movements applied by the test rig in the early stages of the tests and this tended to slow down crack growth in the base-course.

The crack ratio (c/h) during each test was determined from displacements in the sample and, FIG 5.6, which is valid for a sharp-tipped crack in an ideal elastic material. At realistic values of crack opening a correction is necessary to account for the presence of a yielded zone around the crack-tip.

Just sufficient of the creep tests exhibited non-linearity (dotted lines on FIG 5.8) to establish the median yield strain as 0.6% for the basecourse mix and 1% for the wearing course mix.

These values enabled a correction curve for crack length, FIG 6.3, to be plotted for various values of crack opening and an elastic-plastic material. However, yield in bituminous materials is not elastic-plastic but gradual and so the average of uncorrected and corrected, FIG 6.3, crack length was considered the best estimate and used to plot crack growth, FIG 6.2.

FIG 6 . 2

MEDIAN LINES (O) FOR THE CRACK GROWTH vs % FATIGUE LIFE EXPIRED RELATIONSHIP FOR THOSE TESTS WHERE 100 % CRACKING OCCURRED .

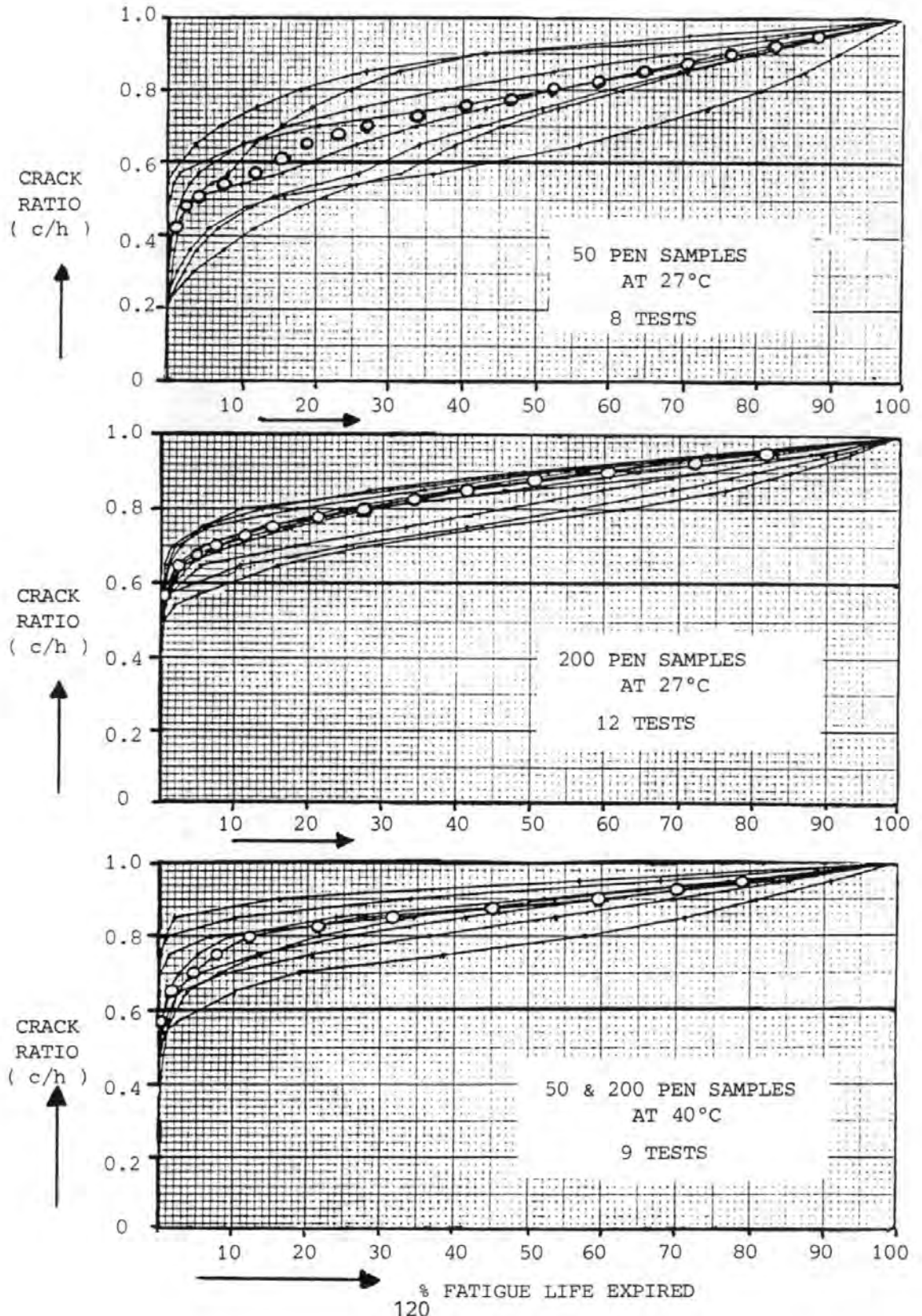


FIG 6 . 3

CORRECTION CURVES FOR THE CRACK RATIO (c/h) DETERMINED BY THE GAUGE DISPLACEMENTS , TO ACCOUNT FOR THE INFLUENCE OF A PLASTIC ZONE AT THE CRACK TIP .

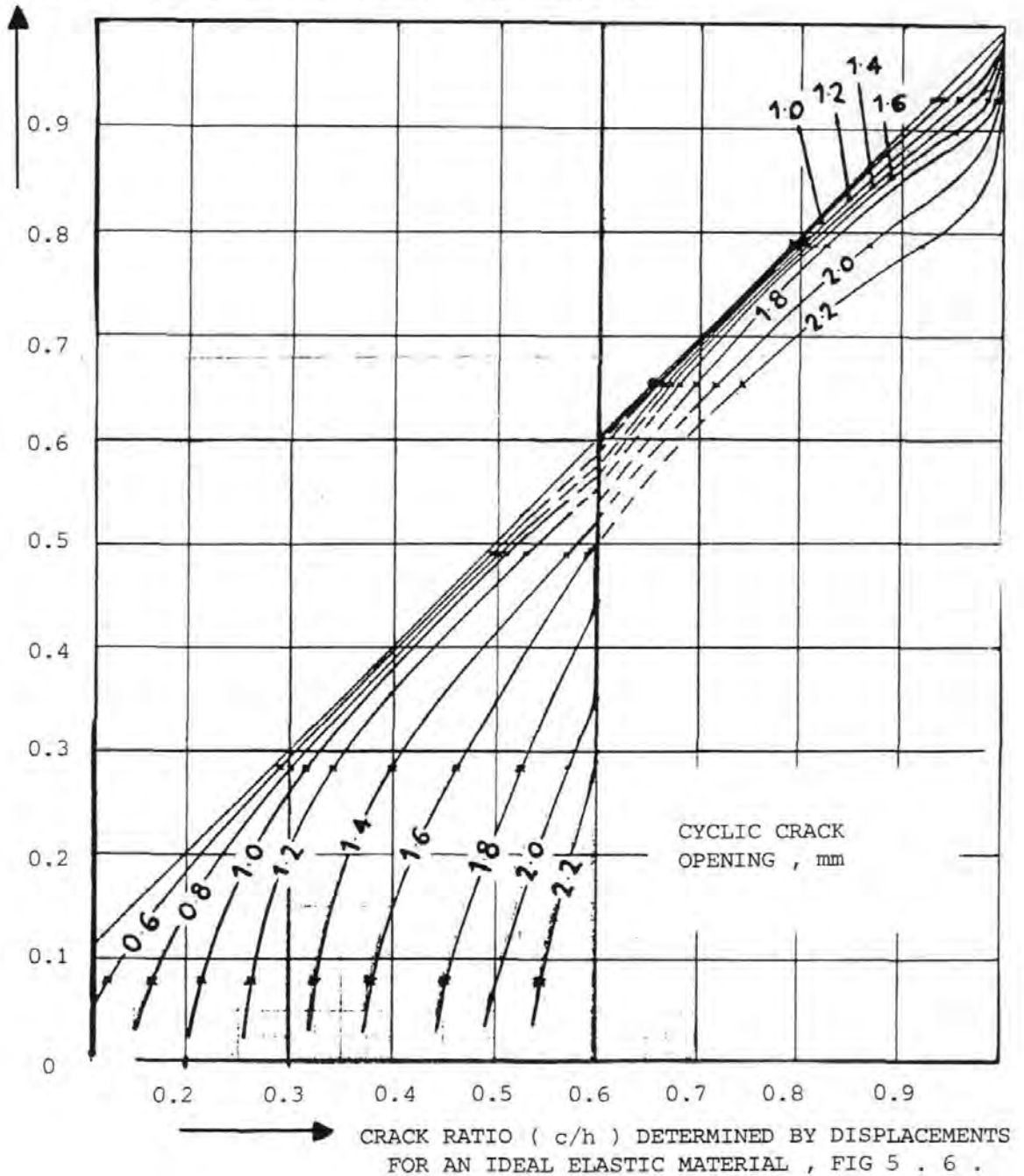
95 mm SURFACING

BASECOURSE YIELD STRAIN = 0.6 %

WEARING COURSE YIELD STRAIN = 1.0 %

CYCLIC CRACK OPENING , 0.6/0.8/1.0/1.2/1.4/1.6/1.8/2.0/2.2 mm

ACTUAL CRACK RATIO (c/h) FOR AN ELASTIC-PLASTIC MATERIAL
WHERE THE CRACK TIP DETERMINED BY DISPLACEMENTS IS
THE TIP OF A YIELD ZONE AHEAD OF THE CRACK TIP



6.2 Bitumen Stiffness Interpretation of Test Results

The cyclic conditions of bitumen stiffness for a 24 hour thermal cycle were evaluated, TABLE 4.5, for two 50 PEN bitumens that represent the probable upper and lower limits of hardness (Softening Point, Temp, °C) for 50 PEN bitumens recovered from asphalt surfacing after approximately 10 years.

The ranges of bitumen stiffness for thermal reflection cracking fatigue are, TABLE 4.5,:

$$\begin{aligned} 1.22 \times 10^3 & \rightarrow 3.4 \times 10^4 \text{ N/m}^2 \text{ for } T_{R\&B} \text{ } 58^\circ\text{C} \\ 7.2 \times 10^3 & \rightarrow 1.87 \times 10^5 \text{ N/m}^2 \text{ for } T_{R\&B} \text{ } 66^\circ\text{C} \end{aligned}$$

The mean levels of bitumen stiffness for which test results were obtained were, TABLE 6.1/2/3/4:

$$\begin{aligned} (5.8 \times 10^3, 5.6 \times 10^4 \text{ \& } 2.2 \times 10^5) \text{ N/m}^2 & \text{ for 200 PEN} \\ (5.6 \times 10^4, 4.4 \times 10^5 \text{ \& } 2.4 \times 10^6) \text{ N/m}^2 & \text{ for 50 PEN.} \end{aligned}$$

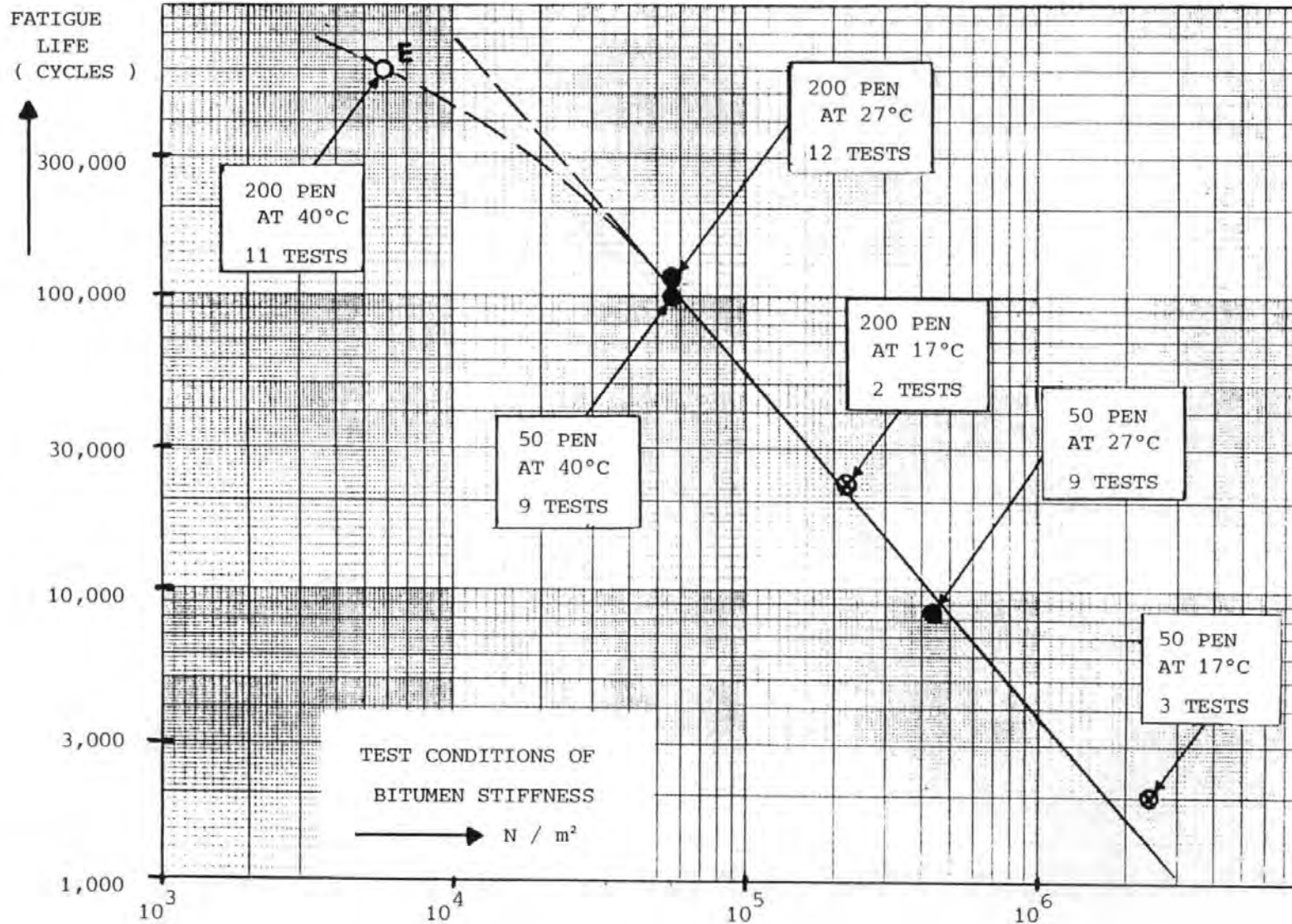
A single test was performed with a 200 PEN sample at a bitumen stiffness lower than 10^3 N/m^2 , TABLE 6.4, but the sample slumped too early for the fatigue life to be estimated. Also the temperature variations with a sample at such elevated temperatures ($55 \rightarrow 60^\circ\text{C}$) were unrealistic and so no further tests were attempted.

The variation of thermal reflection cracking fatigue life with test conditions of bitumen stiffness is illustrated, FIG 6.4, by plotting the intercepts of the fatigue lines, FIG 6.1, at cyclic crack opening = 1mm, versus the mean level of bitumen stiffness for the series of tests, TABLES 6.1/2/3/4.

The virtual coincidence of the data points, FIG 6.4, for 50 and 200 PEN samples at bitumen stiffness $5.6 \times 10^4 \text{ N/m}^2$ gives some measure of validation of this bitumen stiffness "fatigue criterion" for testing at different temperatures and presumably at different frequencies.

FIG 6 . 4
 THERMAL REFLECTION CRACKING FATIGUE LIFE , EXPRESSED AS A FUNCTION OF
 BITUMEN STIFFNESS .

95 mm TWO-COURSE SURFACING
 1 mm CYCLIC CRACK OPENING



The bitumen stiffness "fatigue criterion" is thus valid for bitumens of normal temperature susceptibility ($PI \approx +0.5$) over the range of bitumen stiffness $10^4 \rightarrow 10^6 \text{ N/m}^2$.

The variation of fatigue life, FIG 6.4, with bitumen stiffness appears to be linear on a LOG-LOG basis for $S_{BIT} > 2 \times 10^4 \text{ N/m}^2$, with a "kink" in the line near $2 \times 10^4 \text{ N/m}^2$ which is probably related to the "kink" in the creep test curves, FIG 5.7/8, which represents a "work hardening" mechanism.

The data point for 50 PEN samples at 17°C lies above the line because the test rig was unable to apply constant crack opening movement to such stiff samples when only slightly cracked and this increased the fatigue life in these 3 tests.

Also, the virtual collinearity, FIG 6.4, of the test results for long bituminous bonded samples at 17°C and short epoxy resin bonded samples at $27 \& 40^\circ\text{C}$, indicates that the use of the latter in simulative tests is acceptable.

6.3 Fracture Mechanics Interpretation of Test Results

The purpose of fracture mechanics analysis of fatigue test results is to determine the material constants (A, n) that relate crack growth rates (dc/dN) to crack-tip stress intensity factors (K_1) in the crack growth eqn,

$$dc/dN = A K_1^n \quad (\text{EQN 2})$$

The exponent n is evaluated at the slope of a LOG-LOG plot of dc/dN vs K_1 and the constant A is given by the intercept of dc/dN at $K_1 = 1$.

These fatigue constants (A, n) enable crack growth rates and thus fatigue lives to be predicted from K_1 values determined by finite element analyses.

dc/dN and K_1 were evaluated from test results at 6 points in the basecourse and 5 points in the wearing course and the pairs of values

were plotted to logarithmic axes, FIG 6.5/6, to determine experimental A & n values.

dc/dN and K_1 values from some of the tests performed were not included. Results from the two "stiffest" and the two "softest" tests of the three "successful" test series, i.e. tests performed on 50 PEN Samples at (27 & 40°C) and 200 PEN samples at 27°C, TABLES 6.1/2/3, were rejected in order to reduce the scatter of data, FIGS 6.5/6, by only using data from a $\pm 1\frac{1}{2}$ °C temperature band.

However, all the dc/dN and K_1 values that could be evaluated from tests with 200 PEN samples at 40°C, were used; because in most of these tests the crack did not propagate to the full height.

The basic fracture mechanics interpretation of the test results FIGS 6.5/6 produces experimental n values that are 1.25 and 2.1 times greater than values predicted by creep tests and Schapery's theory, TABLE 5.3.

However the presence of slight (± 2 °C) temperature differences between the top and base of each layer of the test samples will have tended to increase these experimental n values and so they are not necessarily reliable.

Also the indirect method by which K_1 values were calculated, using the mean mix stiffness from creep tests, FIGS 5.8/9, implies that these K_1 values have a possible error of a factor of 1.57 (wearing course) and 1.87 (basecourse).

This uncertainty in K_1 is illustrated, FIGS 6.7/8, and indicates that theoretical n values, TABLE 5.3, are reasonable and that n can be considered constant over the range of interest.

(A) values are dependant upon the choice of slope (n value) of the line through the data points, FIG 6.5/6/7/8. The corresponding variation of A values, when theoretical n values are used is illustrated, FIG 6.9.

The collinearity of the data points for 50 PEN samples at 40°C and 200 PEN samples at 27°C, FIGS 6.5/6/7/8 indicates that the variation of A with bitumen grade and test conditions, can indeed be considered to be a function of bitumen stiffness, FIG 6.9.

FIG 6 . 5

FRACTURE MECHANICS INTERPRETATION OF THE TEST RESULTS , BASECOURSE MIX,
 EXPERIMENTAL "n" VALUE = 13.3 .

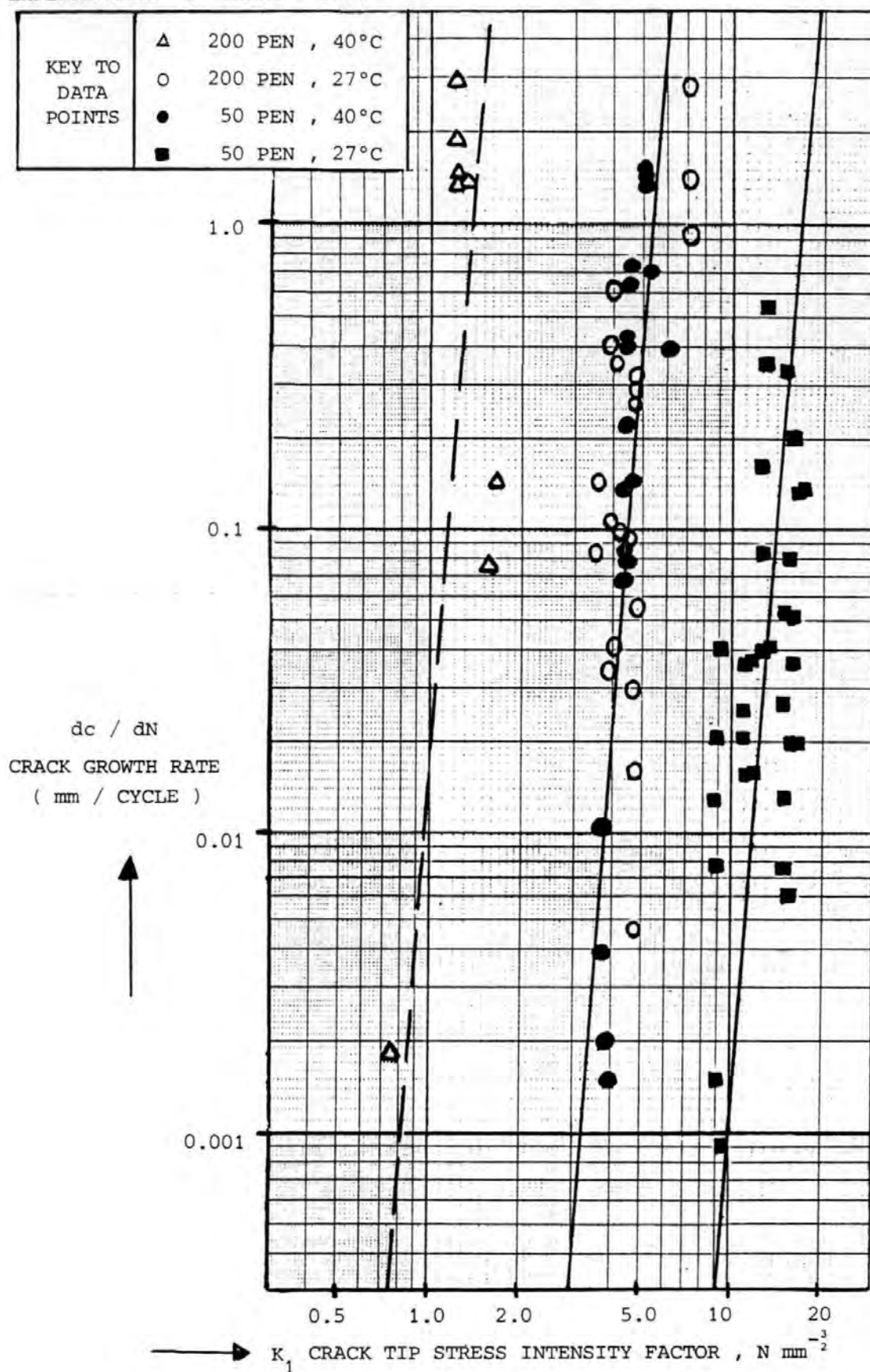


FIG 6 . 6

FRACTURE MECHANICS INTERPRETATION OF TEST RESULTS , WEARING COURSE MIX
 EXPERIMENTAL "n" VALUE = 8.2

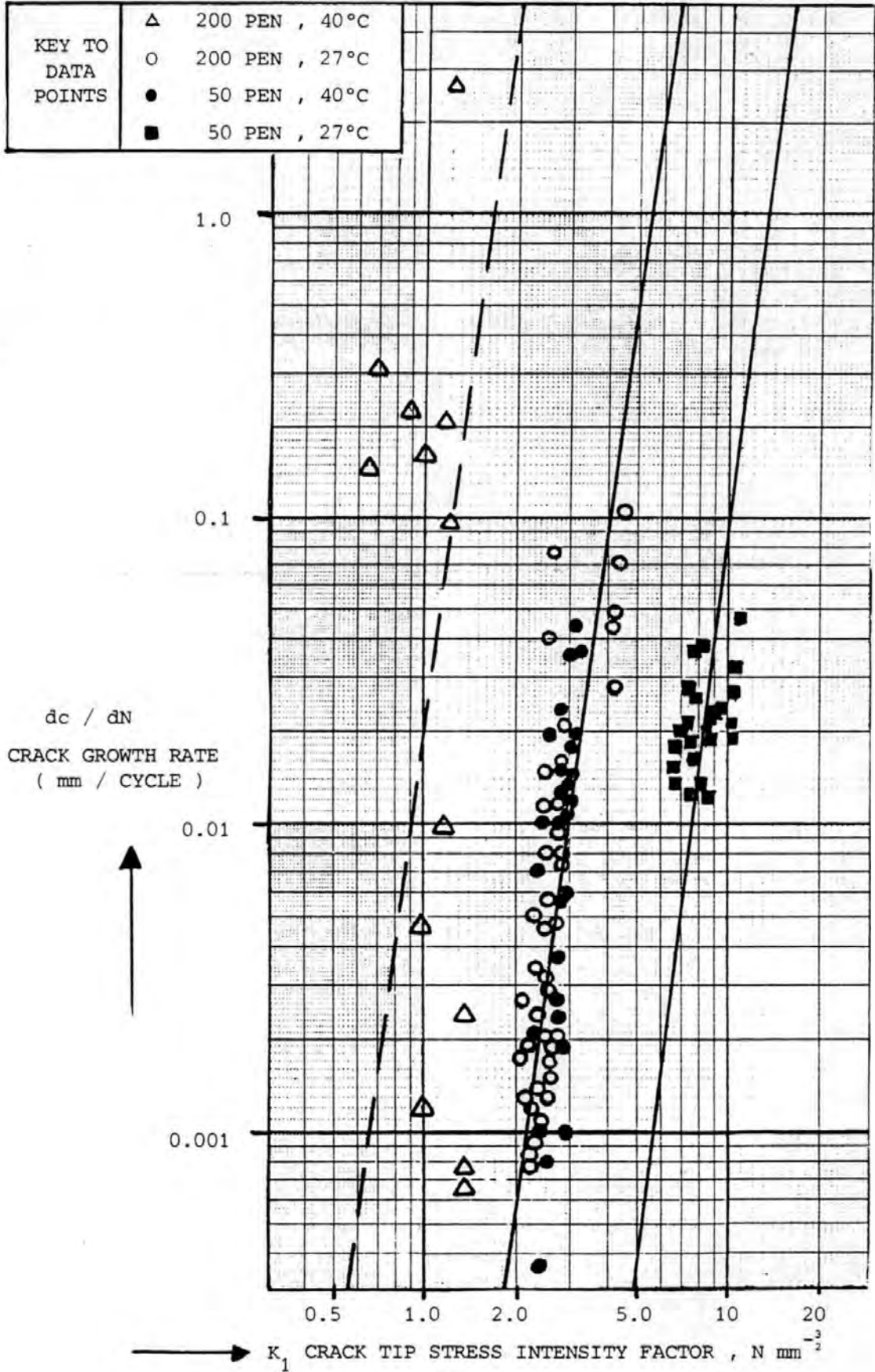


FIG 6 . 7

SCHAPERY'S THEORY INTERPRETATION OF THE TEST RESULTS , BASECOURSE MIX
THEORETICAL "n" VALUE = 6.33 .

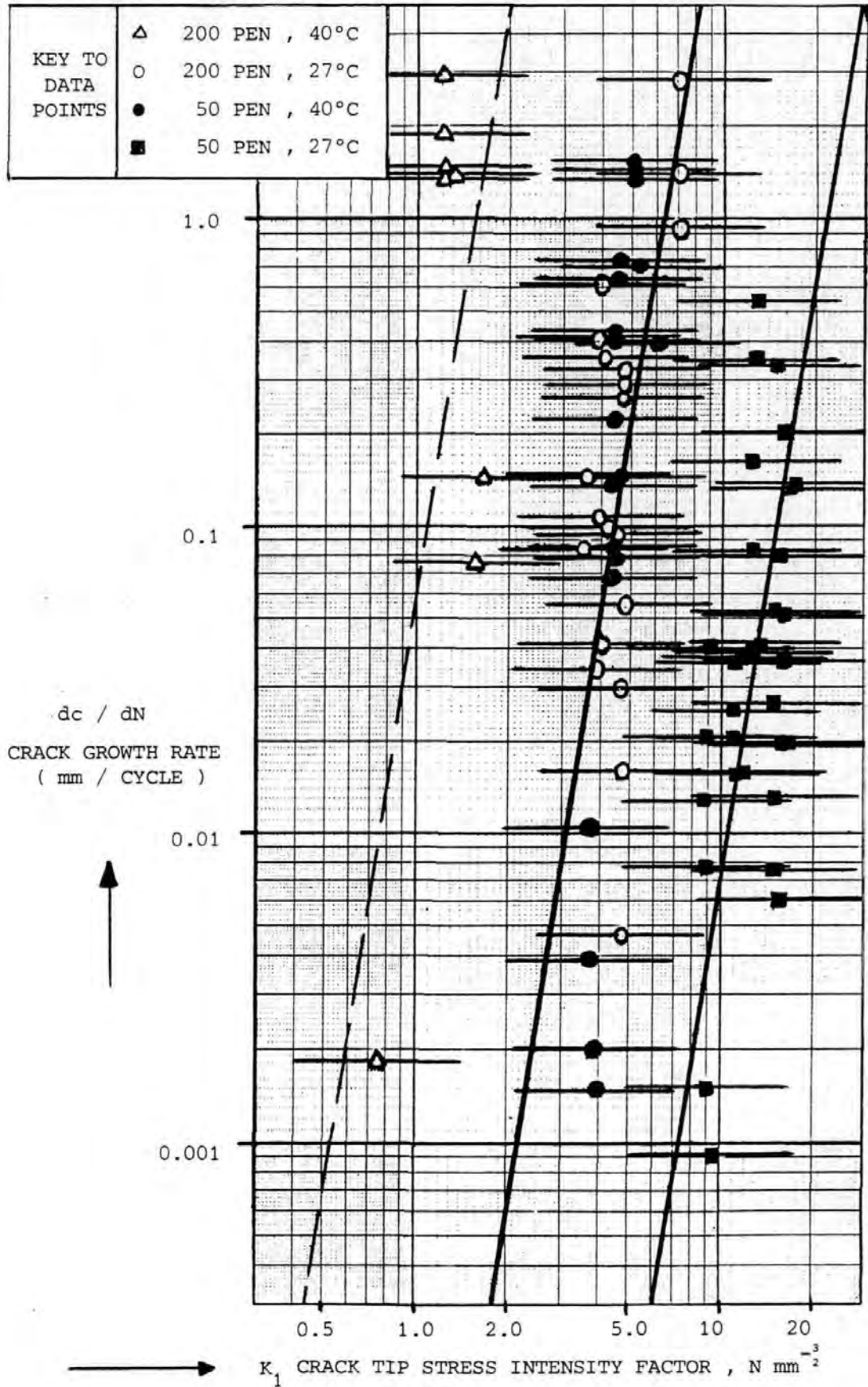


FIG 6 . 8

SCHAPERY'S THEORY INTERPRETATION OF TEST RESULTS , WEARING COURSE MIX
THEORETICAL "n" VALUE = 6.57 .

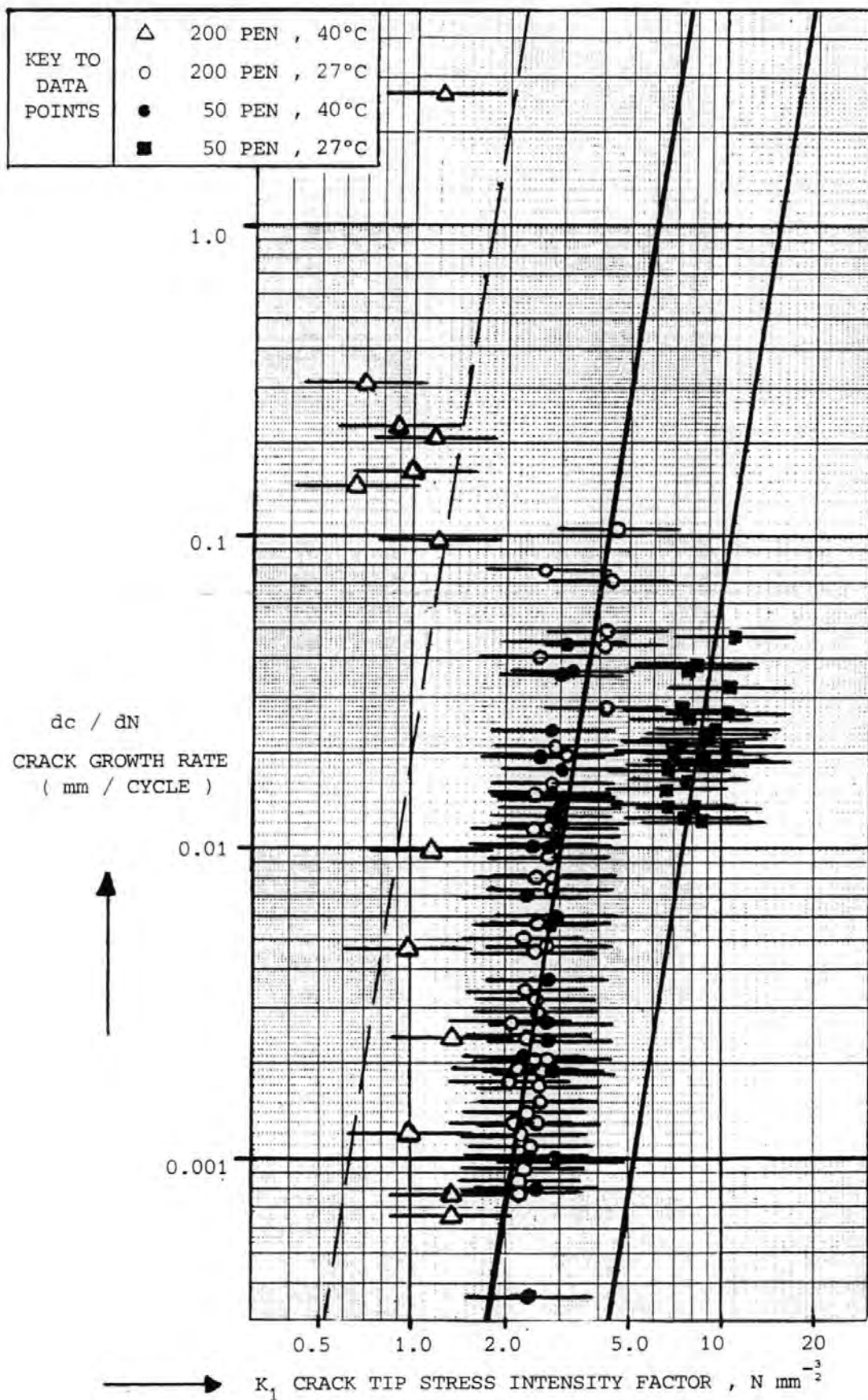
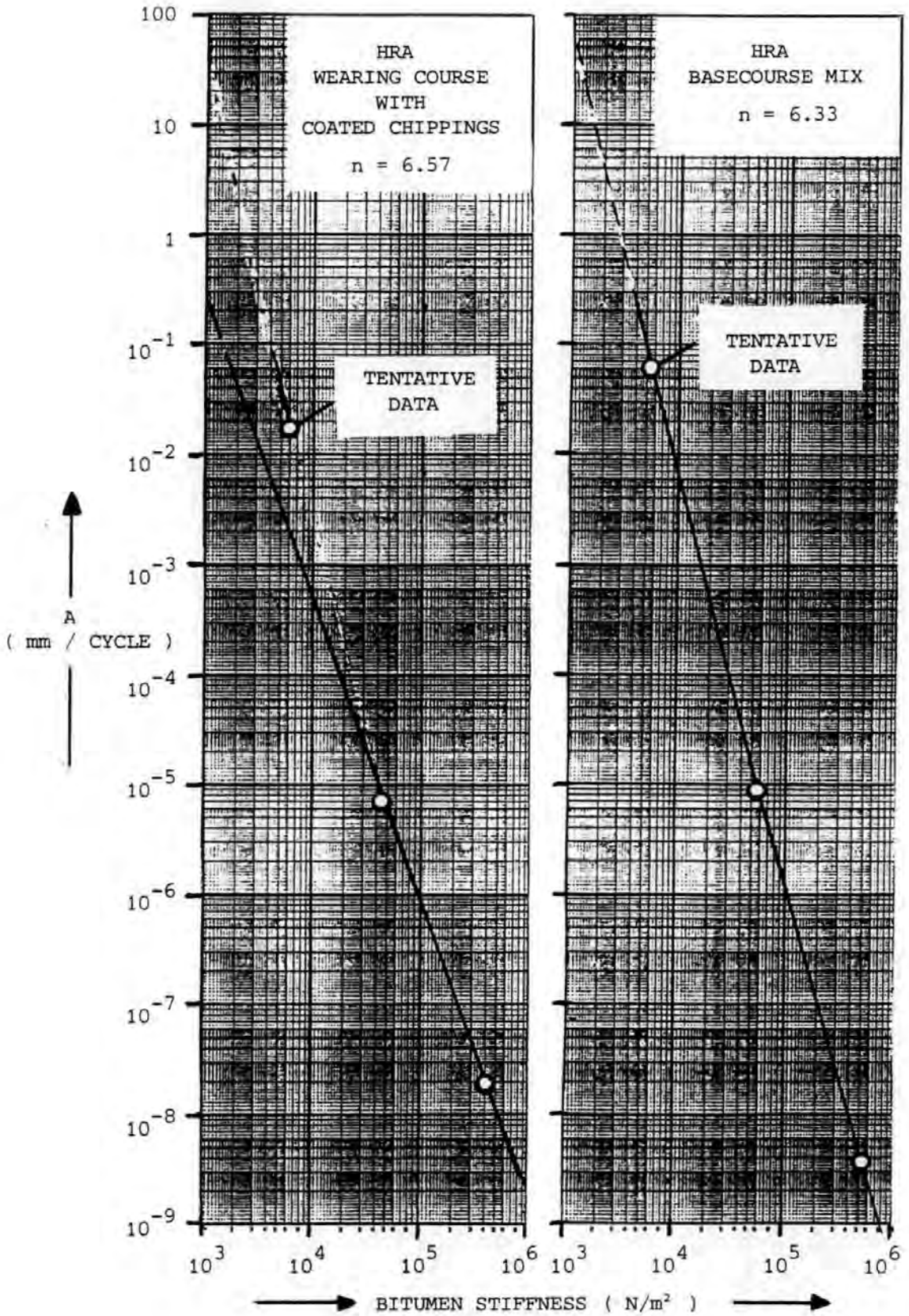


FIG 6 . 9

THE RESULTS OF SIMULATIVE TESTS TO DETERMINE FATIGUE CONSTANTS A , n FOR THE TEST MIXES .



(A) values determined at the lowest bitumen stiffness level ($6 \times 10^3 \text{ N/m}^2$) are only tentative because some of the tests had no tendency to fail and so the (A) values obtained represent those tests with above average crack growth rates. Consequently, the tentative data point for the wearing course mix, FIG 6.9, lies above the line. The slopes of the LOG A vs LOG S_{BIT} lines, FIG 6.9, are not equal. The steeper slope for the basecourse mix is considered to be because of this mix's lower filler content and greater tendency towards open grading which results in proportionally greater crack growth at low stiffness conditions.

7.0 A PREDICTIVE MODEL FOR THERMAL REFLECTION CRACKING DEVELOPED FROM SIMULATIVE TESTING

7.1 Introduction

Observations of reflection cracking at the surface of roads with high strength lean concrete roadbases indicate that the roadbase crack spacing is usually greater than 5m. Reflection cracking at long spacings can be caused by thermal movements in the roadbase. The first stage of this project was the characterisation of the external parameters (roadbase and climate) that determine daily cyclic crack opening movements in the roadbase and surfacing temperatures (on a monthly basis). This information is then combined with material testing and finite element results to give the predictive model for thermal reflection cracking that was summarised by the flowchart, FIG 1.9.

There are four design parameters in the predictive model:-

- i) surfacing mix type (basecourse + wearing course)
- ii) state of compaction (basecourse + wearing course)
- iii) bitumen properties (basecourse + wearing course)
- iv) thickness of surfacing

the predictive model also requires the determination of the following parameters for proposed mixes, by a variety of methods

- v) Cyclic bitumen stiffness (S_{BIT}), SECTION 4
- vi) Mix Stiffness (S_{MIX} or E'), SECTION 5
- vii) Fatigue constants (A, n), SECTION 6
- viii) Stress intensity factor (\bar{K}_1), SECTION 3

At present the predictive model can only be used for the mixes tested where mix stiffness and fracture properties (v/vi/vii) have been evaluated. However thermal reflection cracking fatigue life can be predicted for these mixes with a range of bitumen properties ($T_{R\&B}$, PI) and a range of thickness of surfacing (100 - 200mm) when there is a 60/40 thickness ratio of basecourse/wearing course.

Further investigations to develop procedures for estimating the fatigue constants A, n for specified mixes are continuing. Early results from these investigations relating the fatigue constants A, n to bitumen stiffness and void content, have been published⁵².

7.2 The External Parameters (Roadbase and Climate)

The external parameters involved in thermal reflection cracking are:

- Roadbase transverse crack spacing
- Roadbase thermal coefficient of expansion
- Monthly, daily temperature range (top of roadbase)
- Monthly mean temperature in surfacing.

The first three of these parameters combine to determine daily cyclic crack opening movements in the roadbase, TABLE 7.1, that may cause thermal reflection cracking of the surfacing above.

The mean temperature in the surfacing is used to determine equivalent constant temperatures for each month, for a sinusoidal crack opening cycle, TABLE 7.2. These temperatures define monthly values of bitumen stiffness for cyclic loading which, in turn, indicate appropriate monthly values for the other material properties in the predictive model.

Roadbase transverse crack spacing, L

Research by Taylor and Williams¹² has shown that the roadbase transverse crack spacing is determined by the roadbase tensile strength, coefficient of thermal expansion and temperature fall in the 1st or 2nd night after laying. These three factors combine to determine a critical slab length of roadbase that will crack at the centre. However, slabs only slightly shorter than this critical slab length will not crack and so when all factors are constant, the roadbase transverse crack spacing can still vary by a factor of two. Tensile strength, thermal coefficient and temperature fall can all vary by a factor of two approximately, which indicates that lean concrete roadbase crack spacing could possibly vary by a factor of

TABLE 7 . 1
 DAILY CYCLIC CRACK OPENING MOVEMENTS IN THE ROADBASE FOR (5th ,
 25th , 50th , 75th & 95th) PERCENTILE VALUES OF THE ESTIMATED
 NORMAL DISTRIBUTION OF ROADBASE TRANSVERSE CRACK SPACING (FIG 7.1) .
 (mm)

| MONTH | | JAN | FEB | MAR | APR | MAY | JUN | JUL | AUG | SEP | OCT | NOV | DEC |
|-----------------------------|------|-----|-----|------|------|------|------|------|------|------|-----|-----|-----|
| 100 mm BITUMINOUS SURFACING | | | | | | | | | | | | | |
| TRANSVERSE | 5.8 | .12 | .18 | .29 | .46 | .56 | .60 | .50 | .41 | .35 | .26 | .18 | .14 |
| ROADBASE | 10.4 | .21 | .32 | .51 | .81 | .96 | 1.04 | .87 | .75 | .61 | .46 | .33 | .23 |
| CRACK | 13.5 | .27 | .41 | .65 | 1.04 | 1.21 | 1.32 | 1.09 | .94 | .79 | .58 | .42 | .29 |
| SPACING | 16.9 | .33 | .50 | .80 | 1.29 | 1.49 | 1.64 | 1.35 | 1.15 | .95 | .71 | .52 | .37 |
| (m) | 21.8 | .41 | .63 | 1.00 | 1.63 | 1.86 | 2.04 | 1.69 | 1.45 | 1.20 | .90 | .65 | .46 |
| 150 mm BITUMINOUS SURFACING | | | | | | | | | | | | | |
| TRANSVERSE | 5.8 | .08 | .13 | .22 | .35 | .40 | .42 | .38 | .32 | .29 | .20 | .16 | .09 |
| ROADBASE | 10.4 | .15 | .23 | .41 | .63 | .70 | .75 | .67 | .58 | .48 | .35 | .26 | .16 |
| CRACK | 13.5 | .18 | .29 | .53 | .79 | .88 | .95 | .85 | .72 | .61 | .44 | .32 | .20 |
| SPACING | 16.9 | .22 | .35 | .65 | .98 | 1.08 | 1.18 | 1.03 | .89 | .74 | .56 | .40 | .25 |
| (m) | 21.8 | .28 | .44 | .81 | 1.22 | 1.33 | 1.49 | 1.29 | 1.12 | .96 | .69 | .50 | .32 |
| 200 mm BITUMINOUS SURFACING | | | | | | | | | | | | | |
| TRANSVERSE | 5.8 | .05 | .08 | .16 | .26 | .29 | .28 | .28 | .24 | .21 | .16 | .12 | .07 |
| ROADBASE | 10.4 | .09 | .15 | .29 | .44 | .52 | .50 | .49 | .43 | .35 | .26 | .19 | .12 |
| CRACK | 13.5 | .12 | .19 | .37 | .58 | .65 | .63 | .62 | .54 | .45 | .33 | .25 | .15 |
| SPACING | 16.9 | .14 | .23 | .44 | .70 | .79 | .79 | .75 | .66 | .55 | .40 | .30 | .19 |
| (m) | 21.8 | .17 | .29 | .57 | .87 | .98 | .98 | .95 | .83 | .70 | .50 | .39 | .24 |

TABLE 7 . 2

MEAN AND EQUIVALENT MEAN MONTHLY VALUES FOR -
 THE DAILY TEMPERATURE RANGE AT THE TOP OF THE ROADBASE &
 THE MEAN TEMPERATURE IN THE SURFACING

(° C)

| MONTH | | JAN | FEB | MAR | APR | MAY | JUN | JUL | AUG | SEP | OCT | NOV | DEC |
|--|-----|-----|-----|-----|------|------|------|------|------|------|------|-----|-----|
| MEAN DAILY TEMPERATURE RANGE AT TOP OF ROADBASE LAYER (°C) | | | | | | | | | | | | | |
| THICKNESS OF SURFACING (mm) | 100 | 2.3 | 3.5 | 5.5 | 9.1 | 11.5 | 12.7 | 10.8 | 9.0 | 6.8 | 4.9 | 3.5 | 2.5 |
| | 150 | 1.6 | 2.5 | 4.5 | 6.8 | 8.3 | 9.2 | 8.3 | 6.9 | 5.3 | 3.8 | 2.7 | 1.7 |
| | 200 | 1.0 | 1.7 | 3.2 | 4.9 | 6.1 | 6.0 | 6.0 | 5.2 | 3.9 | 2.8 | 2.1 | 1.3 |
| EQUIVALENT MEAN DAILY TEMPERATURE RANGE AT TOP OF ROADBASE LAYER FOR CALCULATION OF DAILY CYCLIC CRACK OPENING MOVEMENTS (°C) | | | | | | | | | | | | | |
| THICKNESS OF SURFACING (mm) | 100 | 2.2 | 3.3 | 5.2 | 8.3 | 9.7 | 10.6 | 8.7 | 7.5 | 6.3 | 4.6 | 3.4 | 2.3 |
| | 150 | 1.4 | 2.3 | 4.2 | 6.3 | 7.0 | 7.6 | 6.8 | 5.8 | 4.9 | 3.5 | 2.6 | 1.6 |
| | 200 | 1.0 | 1.5 | 3.0 | 4.6 | 5.4 | 5.4 | 5.3 | 4.3 | 3.6 | 2.6 | 2.0 | 1.2 |
| MEAN TEMPERATURE IN THE SURFACING (°C) | | | | | | | | | | | | | |
| THICKNESS OF SURFACING (mm) | 100 | 3.7 | 4.3 | 7.0 | 11.2 | 16.1 | 21.7 | 22.8 | 20.3 | 16.4 | 11.0 | 6.8 | 4.6 |
| | 150 | 4.2 | 4.7 | 7.5 | 11.7 | 16.7 | 22.4 | 23.4 | 20.6 | 16.6 | 11.4 | 7.2 | 5.0 |
| | 200 | 4.5 | 5.0 | 7.8 | 12.1 | 17.1 | 22.9 | 23.7 | 20.7 | 16.7 | 11.6 | 7.4 | 5.3 |
| EQUIVALENT MEAN CONSTANT TEMPERATURE IN THE SURFACING FOR A SINUSOIDAL CYCLE (°C) , FOR DETERMINATION OF BITUMEN STIFFNESS | | | | | | | | | | | | | |
| THICKNESS OF SURFACING (mm) | 100 | 7.0 | 6.7 | 8.0 | 10.5 | 15.1 | 19.7 | 20.3 | 19.5 | 16.9 | 12.7 | 8.5 | 7.9 |
| | 150 | 7.5 | 7.1 | 8.5 | 11.0 | 15.7 | 20.4 | 20.9 | 19.8 | 17.1 | 13.1 | 8.9 | 8.3 |
| | 200 | 7.8 | 7.4 | 8.8 | 11.4 | 16.1 | 20.9 | 21.2 | 19.9 | 17.2 | 13.3 | 9.1 | 8.6 |

16 at different sites, but only a factor of 4 at specific sites where only the night-time temperature fall will vary.

Crack surveys have been carried out at 6 sites in order to determine typical roadbase crack spacings (slab lengths). These surveys indicated that roadbase crack spacings do vary by a factor of 4. In all, 10.8Km of carriageway were surveyed of which 6.2Km contained reflection cracks at spacings illustrated by FIG 7.1.

It was considered that most of the observed 20m + crack spacings probably contained unreflected transverse cracks and so the observed frequency distribution, FIG 7.1, was re-interpreted with 65% of the 20m+ spacings taken to be double spacings, which does give a more "normal" shaped distribution with a mean value of 13.5m and a 90% scatter band of 5.8 → 21.8m which corresponds to the factor of 4 expected for similar roadbases.

This variability of crack spacing will be "carried through" the analysis of thermal reflection cracking by considering five crack spacings that span 90% of the estimated "normal" roadbase crack spacing distribution, FIG 7.1, i.e. (5th, 25th, 50th, 75th & 95th % values)

Roadbase thermal coefficient of expansion, α

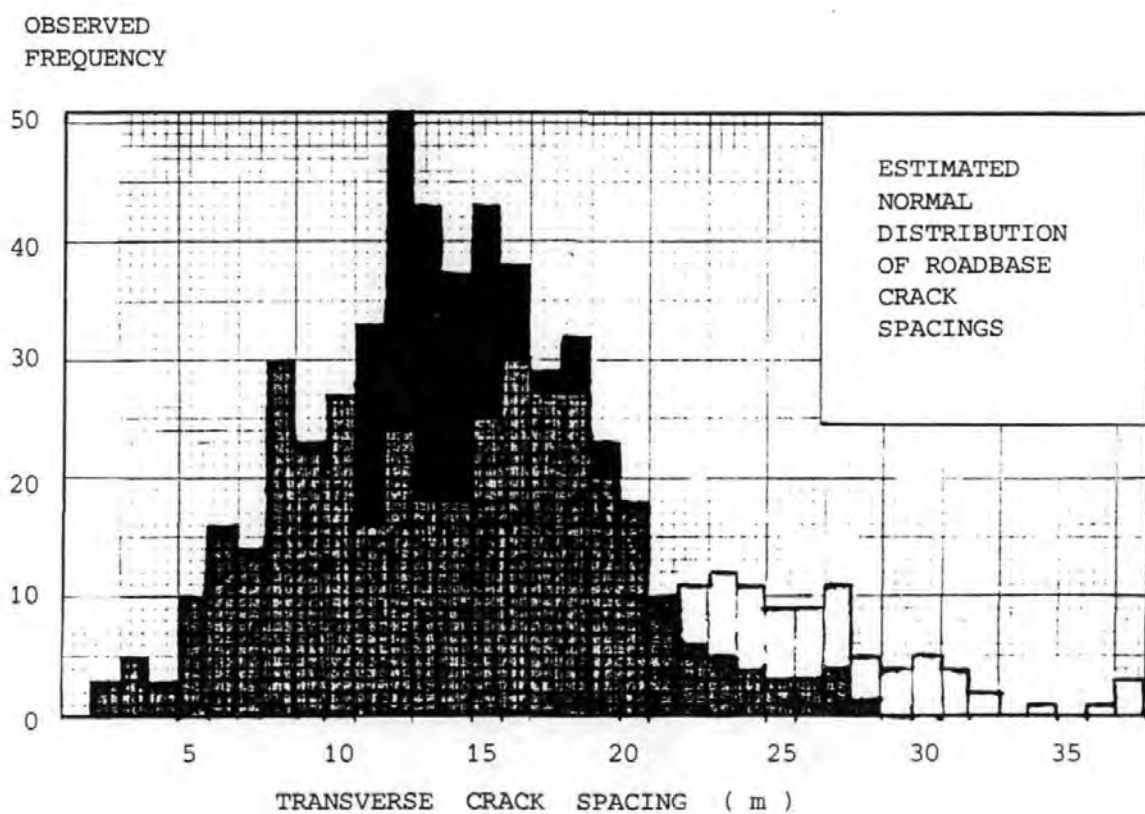
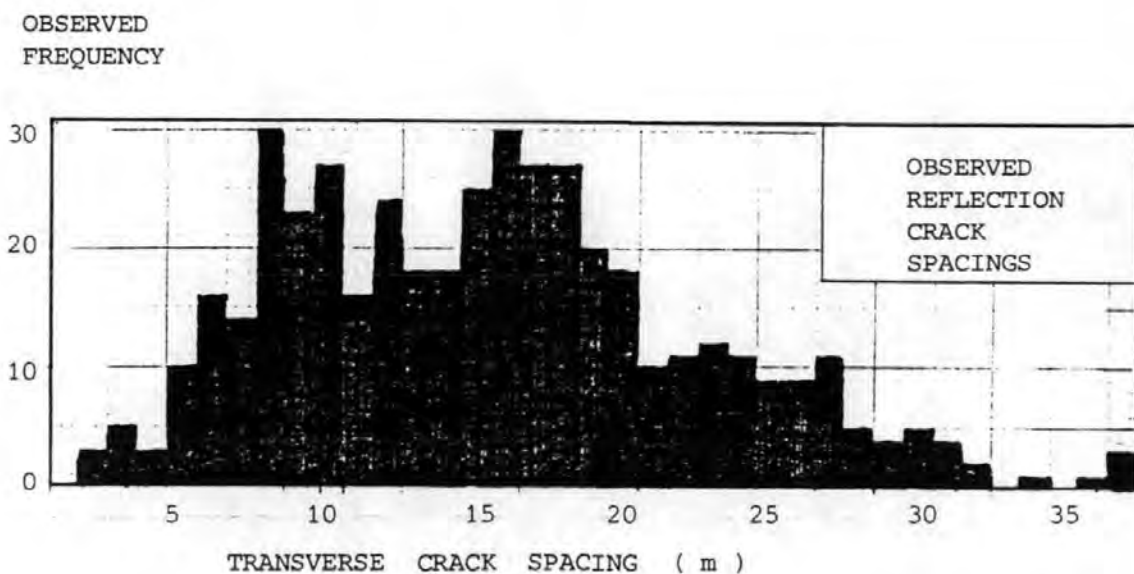
The coefficient of thermal expansion of concrete made with different aggregates was summarised, TABLE 1.2, ^{12,14}. The 6 sites in Devon where crack surveys were carried out contain lean concrete made with a range of aggregates:-

| | | |
|-----------------|---|--------------------------------------|
| A30 Honiton | - | Quartzite |
| A30 Ide | - | Limestone |
| A30 Fingle Glen | - | Limestone and Non Cementitious Fines |
| A30 Launceston | - | Granite |
| A38 Plympton | - | Limestone + China Clay Sand Fines |
| M5 Willand | - | Limestone + Quartzite Fines |

- for which, TABLE 1.2, indicates an average value of $9.25 \times 10^{-6}/^{\circ}\text{C}$ for α . This value of α determines the magnitude of cyclic crack opening movements, TABLE 7.1, produced by the observed roadbase crack spacing distribution, FIG 7.1.

FIG 7 . 1

FREQUENCY DISTRIBUTIONS OF OBSERVED REFLECTION CRACK SPACINGS AND PROBABLE ROADBASE CRACK SPACINGS AT 6 SITES IN DEVON .



The cyclic crack opening movements determined, TABLE 7.1, are also valid for the same % of roadbase crack spacings in lean concrete roadbases of similar strength with any value of α -

The magnitude of cyclic crack opening movements in the roadbase is dependant upon roadbase strength but is in fact independant of α . This is because for a given roadbase strength the crack spacing will be inversely proportional to α , but subsequent cyclic crack opening movements are directly proportional to both crack spacing and α , and so the influence of α is cancelled out.

Daily temperature range (top of roadbase), ΔT

Daily temperature ranges at various depths in composite pavements were evaluated, TABLE 2.2, and the daily temperature range at the top of the roadbase is summarised for 100, 150 & 200mm surfacing, TABLE 7.2.

Monthly values for cyclic crack opening movements are given by, $CO = L.\alpha.\Delta T$, (EQN 1) but have to be adjusted to compensate for:-

- i) self-weight restraint of warping in the roadbase,
- ii) sub-base friction restraint,
- iii) the disproportionate damaging effect of the few extreme daily temperature ranges in each month.

Equivalent mean monthly values of ΔT have been determined, TABLE 7.2, that compensate for the above factors. These equivalent mean monthly values of ΔT combine with $\alpha = 9.25 \times 10^{-6}/^{\circ}\text{C}$ and roadbase crack spacings, FIG 7.1, in (EQN 1) to give the cyclic crack opening movements indicated, TABLE 7.1.

Monthly mean temperature in the surfacing

Monthly mean temperatures at various depths in composite pavements were evaluated, TABLE 2.1, and monthly mean temperature in the surfacing is summarised for 100, 150 & 200mm surfacing, TABLE 7.2.

In order to be able to relate the results of simulative testing using sinusoidal cycles and constant temperatures, equivalent monthly mean

surfacing temperatures had to be evaluated, TABLE 7.2, that compensated for two factors:-

- i. actual daily cycles are not sinusoidal and do not occur at a constant temperature
- ii. the few colder than average days in each month have a disproportionate damaging effect.

The "decaying exponential" type cooling at varying temperature of the daily thermal cycles is less severe in terms of fatigue crack growth per cycle than a sinusoidal cycle at constant temperature especially in winter.

Fatigue life in a controlled strain type process usually increases with temperature and so the actual daily cycles are equivalent to sinusoidal cycles at constant temperatures up to 5°C higher than the mean of the actual cycle.

The disproportionate damaging effects of the few colder than average days in each month has also been investigated and was found to "drop" the equivalent monthly temperatures by approximately 1.4°C.

Thus equivalent mean monthly surfacing temperatures for a sinusoidal cycle, TABLE 7.2, are on average slightly higher but less extreme than the mean values.

7.3 The Design Parameters

In the design of bituminous surfacings to resist reflection cracking, either the mix design or the thickness can be varied.

The format of this predictive model is that for specified surfacing mixes (basecourse + wearing course) at a specified state of compaction (air void content) the thermal reflection cracking fatigue life will be plotted as a function of bitumen properties and surfacing thickness.

Surfacing Mix Type

The necessary material properties for the predictive model have so far only been evaluated for standard hot rolled asphalt (HRA)

basecourse and wearing course (recipe mix 1A) to BS 594⁵. The mix proportions and aggregate gradings of these mixes are summarised TABLE 5.1, FIG 5.1.

The use of hot rolled asphalt for the wearing course is almost universal but dense bitumen macadam (DBM) TO BS 4987⁶ is probably used more frequently than HRA for the basecourse because it is cheaper.

The material properties of DBM basecourse and other non-standard mixes are currently being evaluated at Plymouth Polytechnic in a "follow-up" project to this, the results of which will be available in the near future. Results from HRA mixes are sufficient to satisfy the present need to explain the occurrence of reflection cracking. Only then can improved mixes be developed with confidence.

Air Void Content

Equal compactive effort was used for all the test samples and this produced very low void contents. The void content was calculated by comparison of the actual mix density (obtained by weighing in air and water) with the theoretical mix density.

The average air void content of 28 100 x 100 x 40mm pieces cut from the test samples was 0.5%.

It is probable that similarly low void contents are obtained in practice in bituminous surfacings over lean concrete because the lean concrete acts as a stiff base for compaction.

The prediction of thermal reflection cracking fatigue life can thus only be made for HRA mixes with air void contents of approximately 1%.

The possible effect of higher void contents being obtained in practice is uncertain because mix stiffness would be reduced. However fatigue crack growth at these low stiffness conditions is by void coalescence ahead of the crack tip and so it is probable that higher void contents would reduce fatigue life.

Bitumen Properties

The main variable considered in the predictive model is bitumen stiffness which is determined by temperature, loading frequency and the bitumen properties ($T_{R\&B}$ and PI),³⁴.

50 PEN bitumen is normally used in HRA mixes. Typical bitumen properties for 50 PEN grade bitumen before mixing have been shown to lie within the ranges ($T_{R\&B}$ 52 → 56°C) and (PI 0 → +0.5).

The bitumen usually undergoes some oxidation at the mixing plant which increases its stiffness⁵³.

Oxidation is likely to be greater with wearing course mixes because the higher rolling temperature specified⁵ means that higher mixing temperatures are more likely to be used. Also any further oxidation after laying, would develop from the surface.

The predictive model will consider 50 PEN bitumen at 3 levels of oxidation (25, 35 and 45 PEN). This represents the range of recovered penetration obtained in practice from mixes with 50 PEN bitumen⁵³.

Recovered penetration alone (unlike $T_{R\&B}$ °C) does give a reasonable estimate of bitumen stiffness at 7 → 22°C because it is measured at a similar temperature. Probable combinations of bitumen properties ($T_{R\&B}$, PI) that correspond to 25, 35 and 45 recovered penetration are:

(66°C, +0.58), (62°C, +0.57) & (58°C, + 0.37)

These bitumen properties are required to determine bitumen stiffness from the van der Poel nomograph³⁴.

Thickness of surfacing

The thicknesses of bituminous surfacing in the predictive model are not strictly equivalent to those currently in use in the UK.

The predictive model is based on finite element analyses with a 60/40 thickness ratio of basecourse : wearing course, whilst in practice a 40mm wearing course is invariably used and the remaining thickness

is made up of basecourse mix or basecourse and roadbase mix for surfacings thicker than 160mm.

7.4 Material Properties and Stress Intensity Factors

Bitumen Stiffness

This is the first material property that has to be evaluated for the predictive model. It also serves to determine appropriate values for mix stiffness (S_{MIX}) and the fatigue constants A,n.

Bitumen stiffness for cyclic loading is determined according to the convention, loading time = $1/2\pi f$ (where f = frequency). For 24 hourly cyclic loading the appropriate loading time is 13,751 seconds.

Bitumen stiffness determined by the nomograph³⁴ is illustrated, FIG 7.2, for oxidised 50 PEN bitumen (recovered penetrations 25, 35 and 45) and the equivalent sinusoidal cycle temperatures, TABLE 7.1.

Mix Stiffness

The relationship between mix stiffness and bitumen stiffness can be determined from creep tests⁴⁷.

The relationship is not necessarily the same in compression and tension. It is the mix stiffness in tension that is of interest here because cracking occurs during the tensile half of the loading pulse. The $S_{MIX} - S_{BIT}$ relationships for the HRA mixes, FIG 7.3, were determined from tensile creep tests on araldite end-bonded, 100 x 100 x 40mm samples at stress levels of approximately 0.1 MN/m^2 .

Fatigue Constants A, n

The crack-tip stress intensity factor (K_1) and the fatigue crack growth per cycle (dc/dN) are related by the equation- $dc/dN = AK_1^n$ (EQN 2) - where A,n are the fatigue constants.

The fatigue constants for the HRA mixes were determined from simulative thermal reflection cracking fatigue tests. n values were found to be approximately constant over the range of interest and A values were found to vary with bitumen stiffness.

FIG 7 . 2

CYCLIC BITUMEN STIFFNESS FOR 50 PEN BITUMEN AT 3 LEVELS OF OXIDATION ,
 AFTER VAN DER POEL³⁴

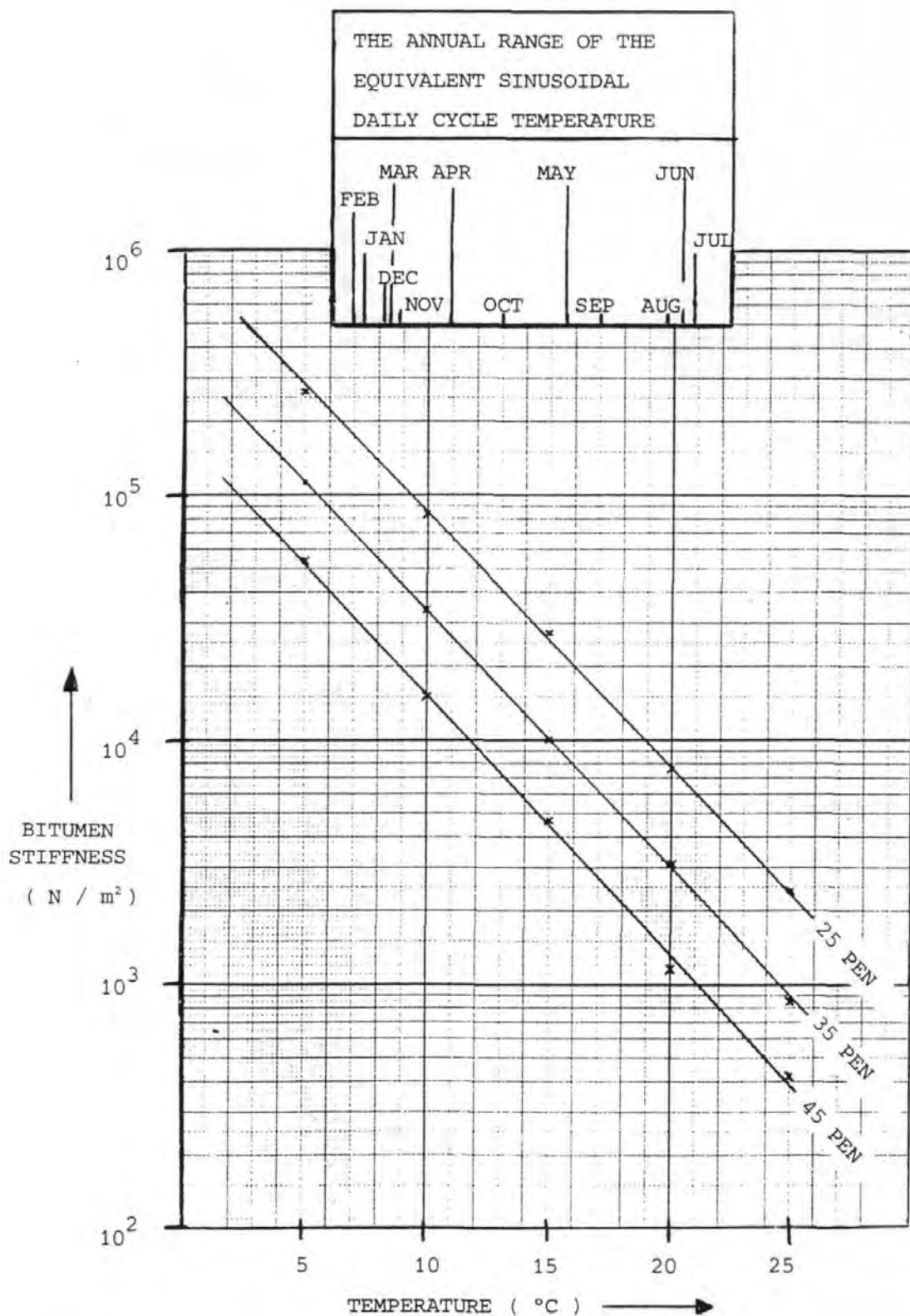
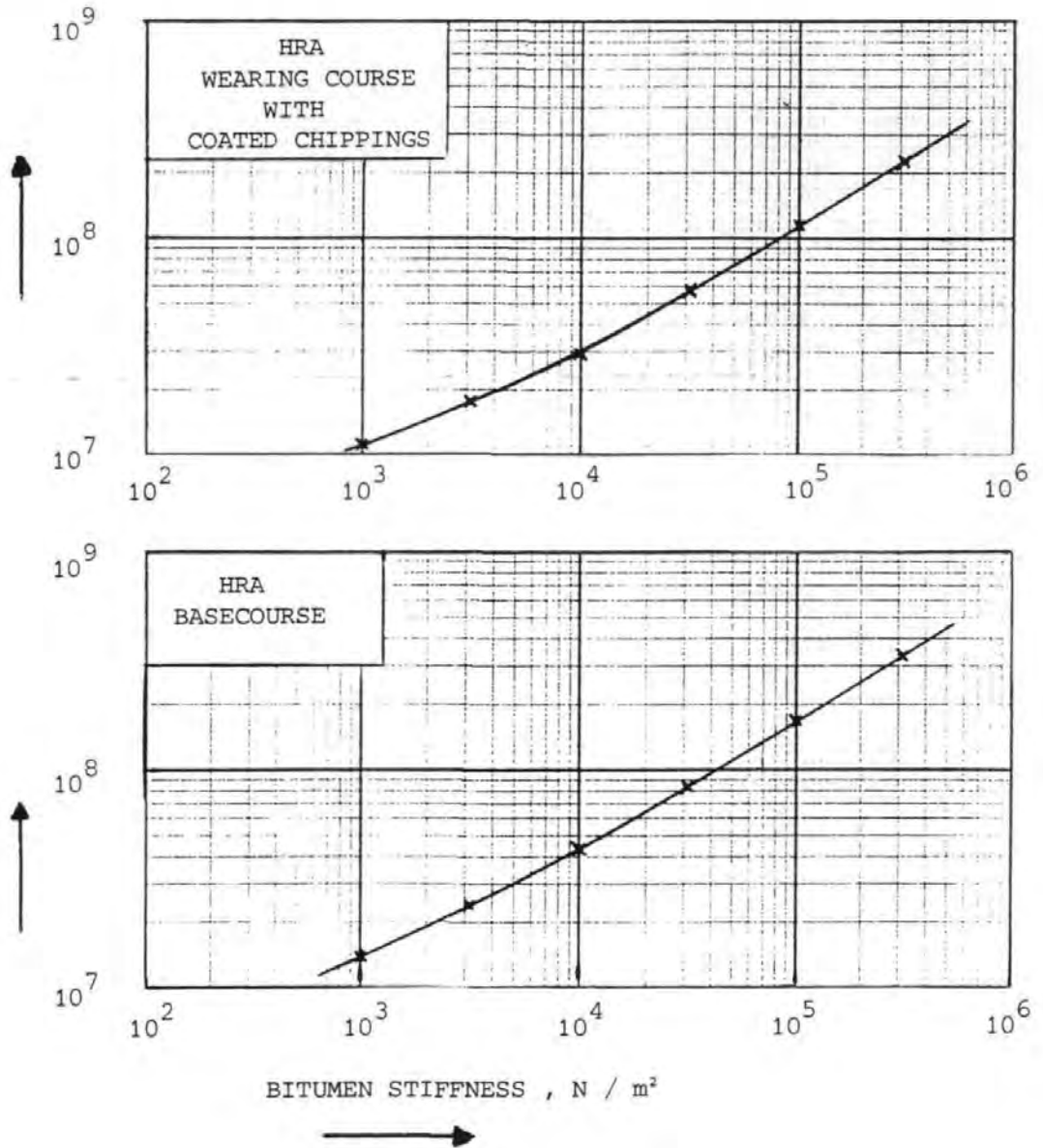


FIG 7 . 3

THE RESULTS OF TENSILE CREEP TESTS TO DETERMINE MIX STIFFNESS AS A FUNCTION OF BITUMEN STIFFNESS .

MIX STIFFNESS , N / m²



Values for n predicted by Schapery's Theory²⁷ and creep tests, were considered to be acceptable. These n values and the corresponding variations of A with bitumen stiffness are illustrated, FIG 6.9, for HRA mixes. A values, FIG 6.9, were calculated from regression analysis of 300 data points of crack growth rate (dc/dN) and stress intensity factor (K_1), obtained from 26 of the 42 tests performed. Some test results had to be rejected because of inadequate temperature (bitumen stiffness) control.

Cyclic displacements astride the crack path at the top and base of the samples were monitored continuously and used to determine crack length and thus (dc/dN) by comparison with finite element analysis of partially cracked samples.

Crack-Tip Stress Intensity Factors, (K_1), (\bar{K}_1)

Crack-Tip Stress Intensity Factors (K_1) for evaluation of fatigue constants (A, n), have been calculated, FIG 3.5, using a finite element model of half a 450mm long laboratory sample bonded to 12mm thick steel plates. The 2D mesh used 100 + 180 elements (8 nodes per element) loaded in the applied displacement & plane strain modes.

Fatigue Life (N_f) is given by integrating (EQN 2):-

$$N_f = \int_0^h \frac{1}{AK_1^n} dc \quad (\text{EQN 10})$$

where h = surfacing layer thickness

and c = height of crack within surfacing.

K_1 is a function of the crack length (c/h), FIG 3.5, and the prediction of fatigue life is greatly simplified by defining an equivalent mean K_1 (\bar{K}_1) such that

$$N_f = \frac{h}{A\bar{K}_1^n} \quad (\text{EQN 13})$$

A "master curve" of \bar{K}_1 has been developed, FIG 7.4, to determine both \bar{K}_1 (basecourse) and \bar{K}_1 (wearing course). \bar{K}_1 varies slightly with n and \bar{K}_1 values have to be interpolated, FIG 7.4, between $n = 4, 6, 8$.

7.5 Prediction of Thermal Reflection Cracking

Thermal reflection cracking fatigue life, N_F , (EQN 13) has to be evaluated separately for the basecourse and the wearing course. N_F is evaluated for each month of the year and the equivalent annual N_F is determined from the 12 monthly values by Miner's Law⁴⁹:-

$$N_F = \left(\frac{1}{12} \left(\frac{1}{N_{F1}} + \frac{1}{N_{F2}} + \dots + \frac{1}{N_{F12}} \right) \right)^{-1}$$

Equivalent annual values of N_F have been evaluated for BS Standard⁵ hot rolled asphalt basecourse and wearing course mixes with the following parameters:-

- Bitumen (25, 35 & 45 PEN) Recovered Penetration
- Surfacing Thickness (100, 150 & 200)mm
- Roadbase Crack Spacing (5.8, 10.4, 13.5, 16.9 & 21.8)m

The evaluation of N_F is illustrated, TABLE 7.3, for 25 PEN bitumen, 100mm surfacing and 13.5m roadbase crack spacing (the 50% value of the "estimated normal" roadbase crack spacing distribution, FIG 7.1). The variation of N_F with bitumen oxidation, surfacing thickness and roadbase crack spacing is illustrated, FIG 7.5.

These results, FIG 7.5, predict that the roadbase crack spacing has to be at least 21.8m for thermal stresses to crack through a 90-100mm surfacing in less than 20 Years.

Thermal reflection cracks have been observed on an untrafficked extension to a By-pass at Camborne in Cornwall. The road was constructed in 1975 and 3 reflection cracks were observed on the 100m untrafficked section in 1982.

FIG 7 . 4

MASTER CURVE OF EQUIVALENT MEAN K_1 (\bar{K}_1) FOR THE DETERMINATION OF FATIGUE LIFE -

$$N_F = \frac{h}{A \cdot \bar{K}_1^n}$$

CYCLIC CRACK OPENING (CO) = 1 mm

, $\bar{K}_1 \propto CO$

MIX STIFFNESS ,BASECOURSE, $S_{MIX_B} = 10^8$ N/m²

, $\bar{K}_1 \propto S_{MIX_B}$

THICKNESS OF SURFACING (h) = 95 mm

, $\bar{K}_1 \propto \frac{95}{h}$

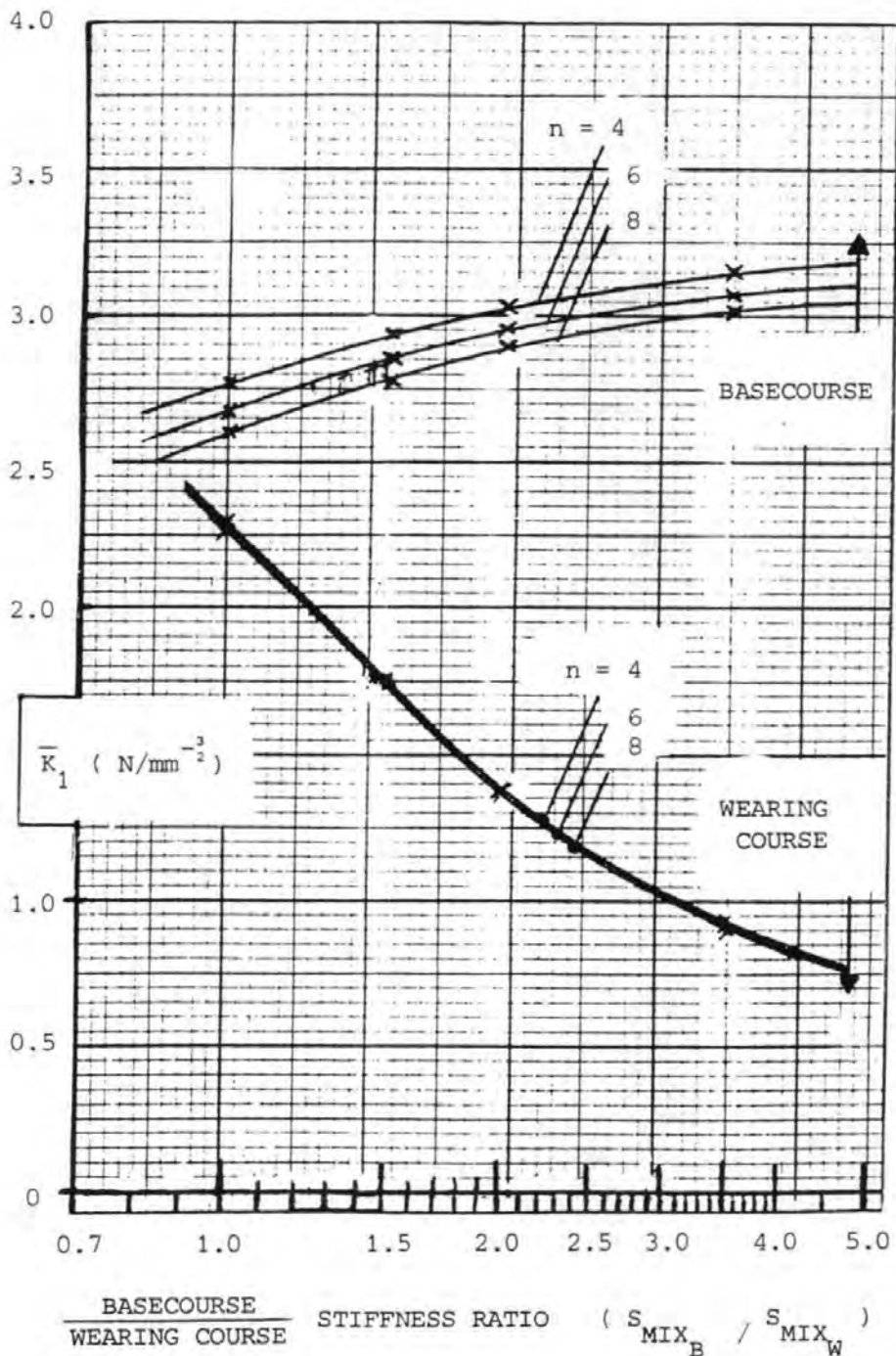


TABLE 7 . 3

THE EVALUATION OF EQUIVALENT ANNUAL FATIGUE LIFE $\{ N_F \}$ FOR 100 mm SURFACING , OXIDISED BITUMEN (25 PEN) & 13.5m ROADBASE TRANSVERSE CRACK SPACING

| MONTH | BITUMEN STIFFNESS ($N/m^2 \times 10^3$) | MIX STIFFNESS ($N/m^2 \times 10^8$) | BASE : WEARING COURSE STIFFNESS RATIO | CYCLIC CRACK OPENING (mm) | STRESS INTENSITY FACTOR ($N / (mm^2)$) | | FATIGUE CRACK GROWTH CONSTANT , A (mm / CYCLE) | FATIGUE LIFE FOR LAYER (CYCLES) | FATIGUE LIFE FOR SURFACING (CYCLES) | NET DAMAGE PER CYCLE (1 / FATIGUE LIFE) | | |
|---|--|--|--|--------------------------------|--|--------------------|--|---|---|---|-----|-----|
| | | | | | W/C | B/C | | | | | W/C | B/C |
| | | | | | W/C | B/C | | | | | W/C | B/C |
| JAN | 172 | 1.60 2.32 | 1.45 | .27 | 1.09 1.72 | 2.05E-7 1.8 E-7 | 110760000 10760000 | 121 500 000 | .000 000 01 | | | |
| FEB | 187 | 1.65 2.42 | 1.47 | .41 | 1.70 2.74 | 1.8 E-7 1.25E-7 | 6804000 813000 | 7 617 000 | .000 000 13 | | | |
| MAR | 138 | 1.38 2.00 | 1.45 | .65 | 2.26 3.57 | 3.8 E-7 3.4 E-7 | 496000 56000 | 552 000 | .000 001 81 | | | |
| APR | 75 | .96 1.40 | 1.46 | 1.04 | 2.51 4.00 | 2.2 E-6 3.0 E-6 | 43000 3090 | 46 100 | .000 021 69 | | | |
| MAY | 25 | .50 .73 | 1.46 | 1.21 | 1.53 2.44 | 4.5 E-5 2.0 E-4 | 54400 1060 | 55 500 | .000 018 02 | | | |
| JUN | 8 | .27 .39 | 1.44 | 1.32 | .90 1.42 | 1.0 E-3 1.3 E-2 | 81100 500 | 81 600 | .000 012 55 | | | |
| JUL | 7 | .25 .37 | 1.48 | 1.09 | .70 1.11 | 1.48E-3 2.3 E-2 | 292000 1350 | 293 000 | .000 003 41 | | | |
| AUG | 9 | .28 .40 | 1.43 | .94 | .66 1.03 | 9.5 E-4 1.1 E-2 | 672000 4500 | 676 500 | .000 001 48 | | | |
| SEP | 16 | .39 .57 | 1.46 | .79 | .78 1.24 | 1.7 E-4 1.0 E-3 | 1190000 15400 | 1 205 000 | .000 000 83 | | | |
| OCT | 44 | .70 1.02 | 1.46 | .58 | 1.03 1.63 | 9.5 E-6 2.3 E-5 | 3470000 118000 | 3 590 000 | .000 000 28 | | | |
| NOV | 121 | 1.29 1.86 | 1.44 | .42 | 1.36 2.15 | 5.5 E-7 5.4 E-7 | 9650000 874000 | 10 520 000 | .000 000 10 | | | |
| DEC | 144 | 1.40 2.04 | 1.46 | .29 | 1.03 1.63 | 3.4 E-7 3.3 E-7 | 96900000 8250000 | 105 100 000 | .000 000 01 | | | |
| MINERS LAW EQUIVALENT ANNUAL FATIGUE LIFE (N_F) | | | | | | | | 199 000 | .000 005 03 | | | |
| JAN | 172 | | | .72 | SINGLE COMBINATIONS OF BITUMEN STIFFNESS AND CYCLIC CRACK OPENING THAT ARE EQUIVALENT TO THE 12 MONTHLY PAIRS OF VALUES | | | | | | | |
| APR | 75 | | | .83 | | | | | | | | |
| OCT | 44 | | | .90 | | | | | | | | |
| JUL | 7 | | | 1.16 | | | | | | | | |

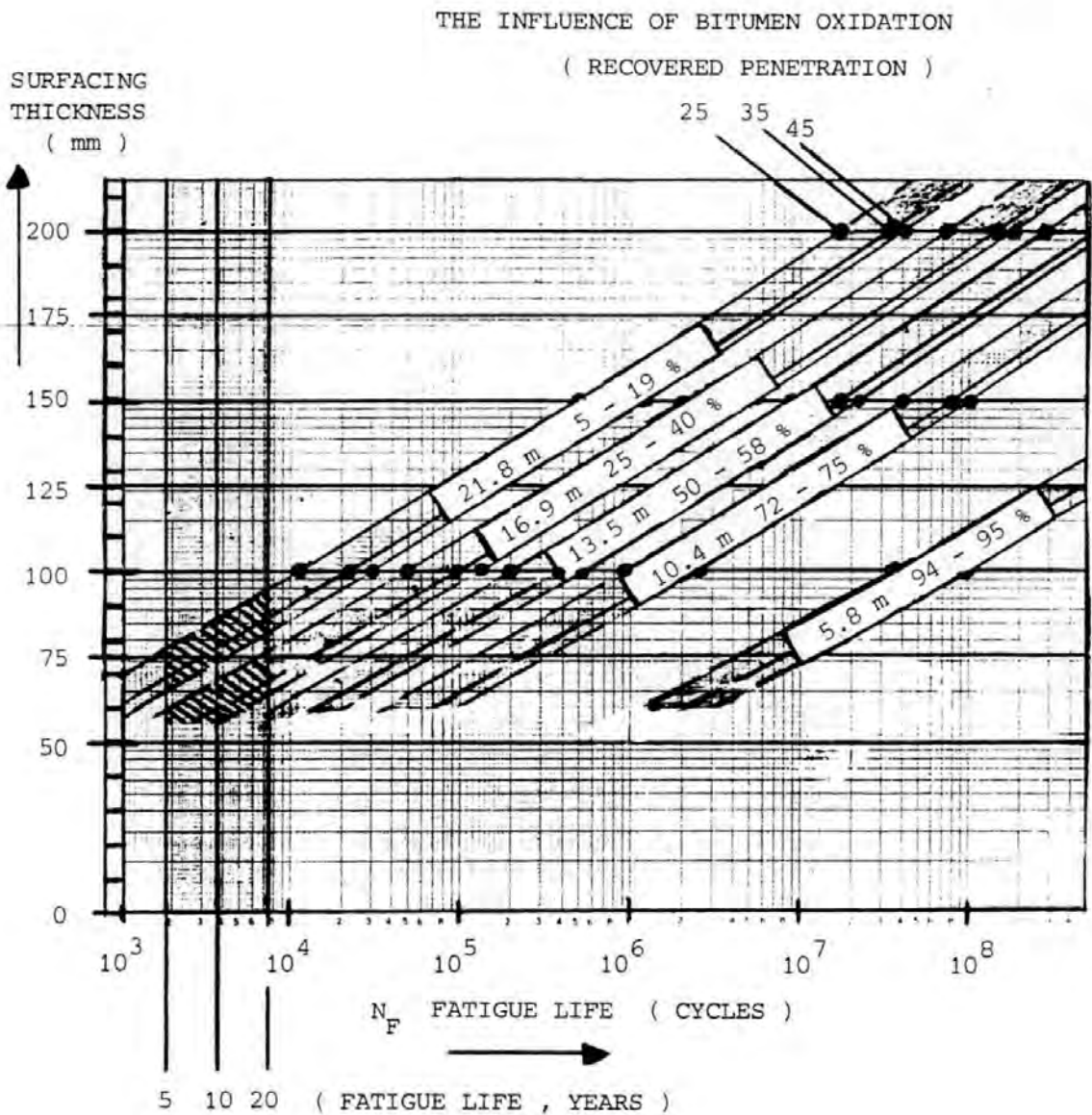
FIG 7 . 5

THE VARIATION OF THERMAL REFLECTION CRACKING FATIGUE LIFE WITH OXIDATION OF THE BITUMEN , AND SURFACING THICKNESS , FOR 5 ROADBASE CRACK SPACINGS -

21.8 , 16.9 , 13.4 , 10.4 , 5.8 m

AND ROADBASE THERMAL COEFFICIENT , $= 9.25 \times 10^{-6} / ^\circ\text{C}$

THESE CRACK SPACINGS CORRESPOND TO INDICATED %s OF THE " ESTIMATED NORMAL " AND THE OBSERVED DISTRIBUTIONS OF CRACK SPACINGS , FIG 7 . 1



These reflection cracks were not sufficiently regular for the roadbase transverse crack spacings to be deduced. Spacings may be equal to the 33m observed and are likely to be greater than the 23m indicated by FIG 7.5 to cause thermal reflection cracking after 7 years with the 90mm surfacing used at this site.

A limited number of simulative tests have been performed with mixes other than standard HRA basecourse and wearing course, TABLE 8.1. Two test results were obtained for surfacing samples with DBM basecourse and HRA wearing course (incorporating crushed rock fine aggregate), that were cut from the road at Camborne. These test results indicated that fatigue life for the surfacing at Camborne is lower than that for standard mixes, FIG 7.5, by a factor of 2. This reduces the required crack spacing, to cause thermal reflection cracking after 7 years, from 23m to 20.5m.

These observations at Camborne do partially validate this predictive model for thermal reflection cracking fatigue life. However, observations of reflection cracking on trafficked roads at spacings much lower than 20m indicate that this roadbase thermal crack opening mechanism does not provide an adequate predictive model for all reflection cracking and other mechanisms must also be considered, i.e.:

- i. traffic stresses,
- ii. thermal warping,
- iii. shrinkage of roadbase or surfacing
- iv. settlement.

Simulative testing and prediction of thermal reflection cracking can also be greatly simplified by the use of equivalent annual values of bitumen stiffness and cyclic crack opening, TABLE 7.3. These produce the same fatigue life (with standard mixes) as the 12 monthly combinations of bitumen stiffness and cyclic crack opening.

This research project is to be continued and the test rig, FIG 5.3/4, is to be developed to apply a combined simulation of thermal and

traffic stresses to surfacing samples.

The use of equivalent annual values of bitumen stiffness and crack opening, to simulate thermal stresses in these tests, will eliminate the need for further simulative testing at a range of monthly values of bitumen stiffness, FIG 7.2, which was one of the most time-consuming aspects of this project.

8.0 SUMMARY AND RECOMMENDATIONS FOR FURTHER WORK

8.1 Mix Design

A large number of simulative tests have been performed on 90-100mm two-course surfacing samples containing UK type hot rolled asphalt mixes with standard bitumen contents (7.9% wt mix in the wearing course and 5.7% wt mix in the basecourse) and low void contents of approximately 1%.

Simulative tests were performed at a range of values of cyclic crack opening (CO) and bitumen stiffness (S_{BIT}) and the median fatigue life for all tests is illustrated as a function of CO and S_{BIT} , FIG 6.4 and FIG 6.1.

A slight influence of the nominal stone size on fatigue life was apparent from test results. Test samples containing 20mm or 40mm coarse aggregate in the basecourse gave fatigue lives 25% longer than the average and test samples containing 28mm coarse aggregate in the basecourse gave fatigue lives 20% shorter than the average.

Also, this N_F vs (CO & S_{BIT}) relationship for standard mixes enabled the relative fatigue life for other mixes to be determined from simulative testing at any value of (CO & S_{BIT}) by comparison with FIG 6.4.

14 simulative tests have been performed with other mixes, mainly to investigate whether the alternative DBM basecourse mix⁶ will influence thermal reflection cracking fatigue life, but also to investigate the effects of high and low filler contents or crushed rock fine aggregate, in the HRA wearing course. The tests used (450 x 100 x 100)mm samples of two-course surfacing (60mm basecourse + 40mm wearing course) bonded with epoxy resin to steel plates. The same method of compaction was used, FIG 5.2, and this again resulted in very low void contents. The results of these "mix design" tests are summarised, TABLE 8.1, and the following observations have been made:-

TABLE 8 . 1

RELATIVE FATIGUE LIVES FOR SURFACINGS WITH DBM BASECOURSES AND VARIOUS HRA TYPE WEARING COURSES .
 * (DBM BASECOURSE NORMALLY USES 100 PEN BITUMEN AND SO THE BITUMEN STIFFNESS IS LOWER THAN IN THE WEARING COURSE) .

| MIX WEARING COURSE | TYPE BASE COURSE | CYCLIC CRACK OPENING (mm) | WEARING COURSE * BITUMEN STIFFNESS N /m ² | FATIGUE LIFE , N _F CORRECTED FOR 95 mm SURFACING | N _F FOR 95 mm STANDARD MIX AT THE SAME CRACK OPENING AND BITUMEN STIFFNESS | RELATIVE FATIGUE LIFE FOR MIX | |
|---|------------------------|--------------------------------------|--|---|--|----------------------------------|------------------------------------|
| | | | | | | FOR EACH TEST | GEOMETRIC MEAN VALUE FOR MIX |
| LOW FILLER CONTENT HRA WITH 7 % PASSING 75µm | DBM | 0.99 | 5.9 x10 ⁵ | 1,900 | 7,400 | 0.26 | 0.55 |
| | | 0.99 | 4.8 x10 ⁵ | 380 | 9,400 | 0.04 | |
| | | 1.63 | 2.3 x10 ⁵ | 830 | 825 | 1.01 | |
| | | 1.55 | 6.9 x10 ⁵ | 2,720 | 320 | 8.5 | |
| STANDARD HRA WITH 9 % PASSING 75µm | DBM | 0.89 | 7.3 x10 ⁵ | 7,020 | 11,600 | 0.61 | 0.92 |
| | | 0.93 | 7.3 x10 ⁵ | 12,000 | 8,700 | 1.38 | |
| HIGH FILLER CONTENT HRA WITH 11 % PASSING 75µm | DBM | 1.32 | 5.8 x10 ⁵ | 470 | 1,130 | 0.42 | 0.56 |
| | | 1.22 | 7.1 x10 ⁵ | 405 | 1,490 | 0.27 | |
| | | 1.36 | 8.3 x10 ⁵ | 675 | 625 | 1.08 | |
| | | 1.34 | 8.7 x10 ⁵ | 504 | 635 | 0.79 | |
| V HIGH FILLER CONTENT HRA WITH 13 % PASSING 75µm | DBM | 0.99 | 3.7 x10 ⁵ | 510 | 12,800 | 0.04 | 0.18 |
| | | 0.99 | 5.5 x10 ⁵ | 6,860 | 8,000 | 0.86 | |
| CRUSHED ROCK FINES HRA | DBM | 0.78 | 1.6 x10 ⁵ | 24,700 | 159,000 | 0.15 | 0.47 |
| | | 1.00 | 3.2 x10 ⁵ | 21,000 | 14,400 | 1.45 | |

- i. The use of the alternative DBM basecourse mix does not appear to reduce fatigue life significantly.
- ii. The 9% filler content used in the standard HRA wearing course mix appears to be the optimum.
- iii. The use of crushed rock fine aggregate in the HRA wearing course appears to reduce fatigue life by a factor of two approximately.

These observations of relative fatigue lives are still only tentative because tests were performed at bitumen stiffness conditions slightly outside the range at which thermal reflection cracking usually occurs, FIG 7.2, and also there was considerable scatter, in the relative fatigue life, between tests. More tests are probably necessary to obtain precise values of relative fatigue life for these mixes.

The influences of 3 mix parameters:-

- i. Bitumen grade and oxidation (Bitumen Stiffness)
- ii. Nominal stone size in mix.
- iii. Aggregate surface area (Filler content or Crushed Rock Fines).

- on thermal reflection cracking fatigue life have thus been determined. It is proposed that further simulative testing will concentrate upon the remaining mix parameters:-

- i. Bitumen Content
- ii. Air Void Content
- iii. Mix additives and interlayers.

The predictive model, FIG 7.5, indicates that for thermal stresses alone to cause reflection cracking of standard two-course HRA surfacing within 20 Years, roadbase crack spacings would have to be:-

- 23.3m + for a 100mm surfacing
- & 41m + for a 150mm surfacing.

The mix design options considered , FIG 7.5 , TABLE 8.1 , indicate that in extreme cases (mixes containing high filler content , crushed rock fines and heavily oxidised wearing course bitumen , 15 PEN) the fatigue life could be reduced by a factor of 10 which changes the crack spacings where thermal reflection cracking will occur to -

16.4 m + for a 100 mm surfacing
& 29 m + for a 150 mm surfacing .

The observed and "estimated normal" distributions of roadbase crack spacing, FIG 7.1, indicate that the following percentages of roadbase crack spacings are greater than the above values:-

Between 29 and 43% are greater than 16.4m
Between 4 and 14% are greater than 23.3m
Between 0 and 4% are greater than 29m
Between 0 and 0% are greater than 41m.

This indicates that thermal reflection cracking is unlikely to occur with a 150mm surfacing, but will occur within 20 years with a 100mm surfacing at-

between 4% and 14% of roadbase transverse cracks with standard two-course HRA surfacing

and between 29% and 43% of roadbase transverse cracks in extreme cases of brittle surfacing.

8.2 The Combined Effect of Thermal and Traffic Stresses

The survey of reflection cracking indicated 452 transverse cracks in 10.8Km which represents 57% reflection cracking (assuming average roadbase crack spacing = 13.5) after approximately 10 years.

The predictive model can be re-interpreted to give a combined estimate of thermal and traffic stresses that does correspond more closely with observed levels of reflection cracking.

The failure point can be re-defined as when thermal stresses have cracked through the basecourse and began to crack the wearing course, i.e. when the surfacing is cracked to 70% thickness. (The surfacing would then be sufficiently weakened for traffic stresses to rapidly crack the remaining 30%).

This combination of cracking occurs because of the different patterns of development of the crack-tip stress intensity factor with crack growth -

Thermal Stresses, K_1 decreases with crack growth \Rightarrow rapid crack growth in the basecourse and slow crack growth in the wearing course.

Traffic Stresses, K_1 increases with crack growth³² \Rightarrow slow crack growth in the basecourse and rapid crack growth in the wearing course.

These opposing trends of K_1 with crack length for thermal and traffic stresses indicate that the basecourse is most likely to be cracked by thermal stresses and the wearing course is most likely to be cracked by traffic stresses.

The median line of % cracked vs % fatigue life expired for test results, FIG 6.2, indicates that the surfacing is 70% cracked after approximately 7½% fatigue life expired.

This reduces the fatigue lives FIG 7.5, by a factor of 13.3 and indicates that the following roadbase crack spacings will cause reflection cracking within 10 years:-

- 18.6m⁺ for 100mm standard HRA surfacing
- 12.9m⁺ for 100mm extreme brittle surfacing

- 31m⁺ for 150mm standard HRA surfacing
- 23.5m⁺ for 150mm extreme brittle surfacing

The observed and "estimated normal" distributions of roadbase crack spacing, FIG 7.1, indicate that reflection cracking by combined thermal and traffic stresses will occur within 10 years at the following percentages of roadbase transverse cracks:-

- Between 18 and 33% with 100mm Standard HRA surfacing
- Between 55 and 61% with 100mm Extreme brittle surfacing

- Between 0 and 2% with 150mm Standard HRA surfacing
- Between 4 and 14% with 150mm Extreme brittle surfacing.

This modified predictive model for the combined effect of thermal and traffic stresses does predict levels of reflection cracking for 100mm surfacing that correspond reasonably well with observations. However, the model still cannot explain substantial observed levels of reflection cracking with 150-175mm surfacings⁵⁴, nor the 39-45% of observed reflection cracking that occurs at spacings less than 12.9m.

This project is to be continued and further simulative tests will apply a combined simulation of thermal and traffic stresses to asphalt surfacing samples.

Results from these tests will indicate whether a combination of thermal crack opening and traffic induced differential vertical movements are sufficient to explain all reflection cracking, or whether additional mechanisms still have to be considered.

8.3 Surface Crack Initiation

Some indication of the presence of additional mechanisms causing reflection cracking is evident from cores taken at surface transverse cracks on the M4 Motorway⁵⁴.

These cores often reveal a crack in the lean concrete roadbase and the wearing course but no crack in the intervening layer(s). These reflection cracks are considered to initiate at the surface and appear to be caused by a mechanism un-related to the thermal and traffic mechanisms considered here where cracks propagate upwards from the roadbase layer.

These surface cracks on the M4 did tend to occur at short spacings such as 4 → 5m where the predictive model, FIG 7.5, indicates that thermal stresses would only slightly crack the basecourse, and so these observations of uncracked basecourse layers are consistent with the predictive model.

Also, it is apparent that if reflection cracks are present in the wearing course only then they will not require sealing and so will

not constitute as serious a maintenance problem as complete reflection cracks.

There are a range of possible mechanisms that can produce surface initiation of reflection cracks.

- i. Upward thermal warping of slab ends.
- ii. Thermal contraction of the surfacing with minimal thermal movement at underlying roadbase cracks.
- iii. Environmental oxidation of the wearing course at the surface.
- iv. Overall shrinkage of the wearing course, possibly by absorption of bitumen into the aggregate.
- v. A combination of a very stiff wearing course laid over an unusually soft DBM basecourse. This would tend to concentrate thermal and traffic stresses in the very stiff wearing course.

This surface crack initiation could possibly be related to the thermal crack opening mechanism considered here because some surface cracking was observed in the simulative tests performed.

After the initial upwardly propagating reflection crack had reached approx 60% surfacing thickness, then surface cracking tended to occur to either side of the upwardly propagating crack.

This "secondary" surface cracking was also observed in similar simulative testing at Texas University⁵⁵ and was termed the "Hinge" effect.

In simulative testing these "secondary" cracks increase the ability of the surfacing to absorb horizontal strains and this tends to increase the time required for the initial upwardly propagating crack to reach the surface. However once the upwardly propagating crack reaches the surface, the "secondary" cracks tend to heal and disappear.

It was also observed in simulative tests that the reflection cracks tended to heal at the compressive end of each cycle to the extent that at the end of each test considerable force was required to separate the two "broken" halves of each sample.

In actual pavements, debris at the surface would accumulate in the "secondary" surface cracks and this would prevent them from healing.

Also, this surface debris would not accumulate in upwardly propagating basecourse cracks and these would still tend to heal at the compressive end of each cycle. Thus cores taken at reflection cracks may not give a true indication of the extent of cracking in the basecourse, especially because reflection cracks tend to follow the films of bitumen within the mix and the traces of healed cracks would be disguised by the blackness of the bitumen.

9.0 CONCLUSIONS

9.1 The Occurrence of Reflection Cracking

9.1.1 A large proportion of roads constructed in the UK contain a lean concrete roadbase. This proportion has been declining from 75% in 1960/3 to 50% in 1971 and 24% in 1975. The increased thicknesses of roadbase and surfacing for composite pavements in the 1984 Review (LR1132) indicate that this decline is likely to continue.

9.1.2 The existence of many possible mechanisms for cracking of lean concrete roadbases and reflection cracking of surfacings above, has led to uncertainty concerning the performance of composite pavements which is responsible for the increased thickness recommendations in LR 1132.

9.1.3 Composite pavements containing relatively high strength lean concrete have rarely required full-depth reconstruction. High strength lean concrete is thus desirable but may produce long roadbase slabs that are likely to cause thermally induced reflection cracking in the surfacing.

9.1.4 A survey of reflection cracking at 6 sites in Devon with 90-175mm bituminous surfacing indicated 452 transverse cracks in 10.8Km of carriageway. These cracks varied in severity from $\frac{1}{2}$ to 2 lane widths and the average age of the roads at the time of the survey was 10 years.

9.1.5 The survey of reflection cracking indicated spacings between 3 and 30m and an estimated distribution of roadbase crack spacings was found to have a mean value of 13.5m and a 90% scatter-band of 5.8m to 21.8m.

9.1.6 The roadbase transverse crack spacing is related to its tensile strength and thermal coefficient of expansion and the temperature fall in the days after laying. The variability of these factors can easily account for the factor of 4 in the 90% scatter band of estimated roadbase crack spacings.

9.1.7 The mean roadbase crack spacing, 13.5m, indicates that the observed frequency of reflection cracking was 57% after 10 years. The survey was, however, biased towards more heavily cracked sites and so the overall incidence of reflection cracking is likely to be less than this.

9.1.8 Reflection cracks can be sealed by a 50mm wide x 3mm thick film of rubberised asphalt (overbanding) but often the entire wearing course is planed off and replaced or occasionally strips of surfacing 300mm either side of the transverse cracks are broken out and replaced.

9.1.9 The survey of reflection cracking indicated a large range of roadbase crack spacings, but adjacent slabs tend to be of similar length and regular spacings of reflection cracks have been observed to extend for over 100m with both 4+5m and 16+20m crack spacings, indicating that the latter are probably true roadbase crack spacings.

9.2 Assessment of Temperatures and Thermal Movements

9.2.1 The lack of comprehensive temperature data for composite pavements in the UK climate has required the development of a temperature model for composite pavements using temperature data from full depth bituminous and concrete pavements.

9.2.2. Daily temperature ranges in composite pavements closely resemble those in bituminous pavements because the absorption effect of the bituminous surfacing is the same. Daily temperature ranges at roadbase depth are greater in composite pavements because of the relatively higher thermal conductivity of the lean concrete.

9.2.3 Daily temperature ranges in composite pavements determined from this temperature model are greater than implied by the results of a 1955 TRRL survey, but are still considered to be reasonable because the earlier survey related to a site that was both sheltered and shaded to the North and South.

9.2.4 The temperature model indicates that the temperature gradients across a 200mm lean concrete roadbase are unlikely to exceed (3°C mean monthly value, 5°C extreme value) during the night-time upward warping and (5°C mean monthly value, 8°C extreme value) during the day-time downward warping. These values indicate that self-weight restraint to warping of lean concrete roadbases will be almost absolute and warping will be restricted to the end ½ metre of roadbase slabs which is not considered sufficient to require modelling.

9.2.5 This near-absolute restraint of thermal warping indicates that thermal stresses can be adequately modelled by cyclic crack-opening in the roadbase and that daily cyclic crack opening movements are closely related to the daily cycles of depth-averaged mean roadbase temperature.

9.2.6 Thermal reflection cracking is considered to result from a daily cycle fatigue mechanism, based on daily crack opening movements in the roadbase, rather than an extreme low temperature mechanism, based on annual cycles of movement.

The late springtime is the critical period for thermal reflection cracking with 36% of crack growth occurring in April, 87% of crack growth occurring in (April, May and June) and 95% of crack growth occurring in (March, April, May, June and July).

9.2.7 Mean and "Equivalent Mean" values have been evaluated for each month of the year for both daily cyclic crack opening movements in the roadbase and the temperature in the surfacing.

These indicate the magnitude of thermal movements that the surfacing must resist and its "brittleness".

9.3 Simulative Testing and Fracture Mechanics Analysis

9.3.1 A test rig has been developed to perform "controlled strain type" cyclic crack opening fatigue tests on asphalt surfacing samples 100mm wide and up to 2m long, although tests can only be performed at controlled temperatures on samples up to 1.5m long.

9.3.2 The effect of acceleration of testing from a 24 hr cycle to 0.12 hz with a visco-elastic material, can be accounted for by the use of either a higher temperature or a softer grade of bitumen that results in the same test conditions of bitumen stiffness.

9.3.3 This "bitumen stiffness" fatigue criterion whereby bitumen stiffness accounts for the influence of test temperature, test frequency and bitumen grade on fatigue life, is apparent from the work of SHELL researchers and is confirmed by test results at low stiffness conditions between 10^4 and 10^6 N/m² where the predominant failure mechanism is flow in the bitumen.

9.3.4 Over 60 simulative thermal reflection cracking fatigue tests have been performed with the test rig at fixed values of cyclic crack opening and bitumen stiffness. At higher stiffness conditions ($> 10^5$ N/m²) the test rig was unable to apply constant cyclic crack opening in the early stages of tests, but adequate values of dc/dN and K_1 could still be obtained from these tests for fracture mechanics analysis of test results.

9.3.5 Finite element analyses of partially cracked samples have been performed and the results combined with -

- i. Displacement in the samples recorded during testing to determine crack length and thus dc/dN during testing.
- ii. Tensile creep test results to determine mix stiffness and thus K_1 during testing.

9.3.6 The fracture mechanics analysis of test results uses experimental dc/dN and K_1 values to determine material constants A and n. (n) values between 6-7 implied by Schapery's Theory and the results of tensile creep tests were found to be reasonable for these low void content mixes. The corresponding variations of A when these n values were used were expressed as functions of bitumen stiffness.

9.3.7 The finite element analyses also enabled a "master curve" of equivalent mean K_1 (\bar{K}_1) during crack growth to be plotted. A predictive model for thermal reflection cracking has been developed that uses \bar{K}_1 , A & n to determine fatigue life (N_F) for a given thickness of bituminous surfacing (h) for each of the 12 monthly combinations of cyclic crack opening and bitumen stiffness. Miner's Law is then used to determine the equivalent annual N_F from the 12 "monthly" N_F values

9.3.8 Miner's Law is considered to be valid in cases such as this because the cycles of movement are continuous with no rest periods. Miner's Law is in effect an early formulation of fracture mechanics where the quantity ($1/N_F$) the net damage per cycle, is analogous to (dc/dN) the crack growth per cycle, in Paris' Law.

9.3.9 A large number of tests were performed with standard HRA two-course surfacing samples and the variation of fatigue life (N_F) with cyclic crack opening (CO) and bitumen stiffness (S_{BIT}) has been evaluated. This enables equivalent annual combinations of CO and S_{BIT} to be determined for any S_{BIT} value, such that N_F = equivalent annual N_F .

These equivalent annual combinations of CO and S_{BIT} greatly simplify further testing to determine the relative fatigue life for other mixes and the effect of a combined simulation of thermal and traffic stresses.

9.3.10 The experimental fatigue life for the test samples was subject to considerable scatter but this is not considered to be significant in the prediction of reflection cracking because each lane width of surfacing is equivalent to forty 100mm wide test samples in parallel.

9.4 The Influence of Thermal Stresses in Reflection Cracking

9.4.1 Thermal reflection cracking fatigue life has been evaluated as a function of roadbase crack spacing, surfacing thickness and bitumen oxidation for standard HRA surfacing mixes. Tests to

determine relative fatigue life were also performed on surfacings with DBM basecourse and a range of filler contents or crushed rock fine aggregate in the wearing course. Results indicate that extreme cases of brittle surfacing could reduce thermal reflection cracking fatigue life by a factor of 10.

9.4.2 These results indicate that thermal reflection cracking within 10 years will only occur at longer than average roadbase crack spacings, i.e.

i. 23.3 → 16.4m for 100mm thickness of (standard HRA → extremely brittle) surfacing. This corresponds to 9 → 36% of roadbase crack spacings.

ii. 41 → 29m for 150mm thickness of (standard HRA → extremely brittle) surfacing. This corresponds to 0 → 2% of roadbase crack spacings.

9.4.3 These predictions for thermal reflection cracking are consistent with observations of reflection cracks in a 100mm surfacing on an untrafficked section of road at Camborne where the roadbase crack spacing could not be precisely determined. Thermal reflection cracking of surfacings thicker than 150mm is not likely to occur under the UK climate and this has not been observed.

9.4.4 It is probable that factors not evaluated in this project such as, (i) the unrestrained warping of the end $\frac{1}{2}$ metre of roadbase slabs, (ii) the effect of high air void contents which may occur in the road (but were not produced in test samples), (iii) the presence of moisture and fine grit in the road, will reduce thermal reflection cracking fatigue life, but not sufficiently to account for the discrepancy between predicted and observed levels of reflection cracking.

9.4.5 Finite element analyses indicate that the basecourse is more likely to be cracked by thermal stresses and the wearing course is more likely to be cracked by traffic stresses. The predictive model for thermal reflection cracking can be modified by defining the failure

point as when the surfacing is 70% cracked. (It can be assumed that the remainder of the wearing course is rapidly cracked by traffic stresses).

9.4.6 This "modified" model however, implies that the relative significance of thermal and traffic stresses is constant regardless of roadbase crack spacing. Consequently, this "thermal + traffic" model can predict levels of reflection cracking for 100mm surfacing that are consistent with observations, but still cannot explain observed reflection cracking with 150-175mm surfacing and also reflection cracking at short crack spacings down to 4 + 5m, where the relative significance of thermal and traffic stresses is different.

9.4.7 It is apparent that a combination of thermal and traffic stresses are responsible for the bulk of reflection cracking. Further simulative tests are to be performed with a combination of thermal and traffic stresses. This combined simulation is considered to be necessary because traffic stresses alone may have difficulty in initiating reflection cracking.

9.4.8 Some indication of the possible influence of other mechanisms is evident from observations of reflection cracking in the wearing course only that does not appear to be related to the thermal and traffic mechanisms considered here.

Some surface crack initiation was observed in the simulative tests and this was considered to be of secondary importance to cracking initiating in the basecourse, although this may not be so in the actual pavement because of the effect of debris which may accumulate in surface cracks.

9.4.9 The following tentative conclusions can be stated concerning reflection cracking fatigue life (factors that increase fatigue life under thermal stresses may reduce fatigue life under traffic stresses).

- i. The most significant variable is the roadbase transverse crack spacing which is related to its early-life tensile strength. The probable range of 90% of roadbase crack spacings varies between 5.8m and 21.8m which corresponds to a variation in fatigue life of a factor of 3300.
- ii. The second most significant variable is the surfacing thickness. Increasing the surfacing thickness from 90mm to 175mm will increase fatigue life by a factor of 550.
- iii. The least significant variable that has been quantified at present is the bitumen stiffness. The usual range of oxidation of 50 PEN bitumen from 45 to 25 PEN will only reduce fatigue life by a factor of 2.7, with most of this reduction occurring between 35 and 25 PEN.

It is therefore concluded that bitumen softer than 45 PEN may not increase fatigue life with HRA mixes, but that bitumen oxidised beyond 25 PEN may reduce fatigue life considerably.

REFERENCES

1. ROAD RESEARCH LABORATORY. A guide to the structural design of pavements for new roads. Road Note No. 29, 3rd edition, London, 1970. H.M.S.O.
2. LAKE J.R. Road pavement design, Technical Memorandum No H6/78, Department of Transport London, 1978.
3. POWELL, W.D., POTTER, J.F., MAYHEW, H.C. AND NUNN , M.E. The structural design of bituminous roads. T.R.R.L.report LR 1132, Crowthorne, 1984.
4. DEPARTMENT OF TRANSPORT. Specification for road and bridge works/Notes for guidance on the specification for road and bridge works. London, 1976. H.M.S.O.
5. BRITISH STANDARDS INSTITUTION. Specification for rolled asphalt (hot process). BS 594. London, 1973..
6. BRITISH STANDARDS INSTITUTION. Specification for coated macadam for roads and other paved areas. BS 4987, London, 1973.
7. LISTER, N.W. AND PORTER, J. Methodology for the design of bituminous roads. Highways and Transportation, November 1984.
8. KENNEDY, C.K. and LISTER, N.W. Prediction of pavement performance and the design of overlays. T.R.R.L. report LR833. Crowthorne, 1978.
9. ROAD RESEARCH LABORATORY. Bituminous materials in road construction. London, 1962 H.M.S.O. pp 542-573.

10. MONISMITH, C.L. and COETZEE, N.F. Reflection cracking: Analyses, laboratory studies and design considerations. Proceedings, AAPT Vol 49, 1980.
11. CRONEY, D. The design and performance of road pavements. Transport and Road Research Laboratory. London 1977 H.M.S.O.
12. TAYLOR G.D., and WILLIAMS, R.I.T. Restrained thermal contraction of lean concrete roadbases. Highways and Public Works, July 1981.
13. LISTER N.W. Design and performance of cement-bound bases. Journal of the Institution of Highway Engineers, Vol 14, No 2. London, Feb 1972.
14. BONNELL, D.G.R. and HARPER F.C. The thermal expansion of concrete . Building Research Station, National Building Studies, Technical Paper No 7, London H.M.S.O. 1951.
15. CHANG, H.S., LYTTON, R.L. and CARPENTER. Prediction of thermal reflection cracking in West Texas. Texas Transportation Inst'. Research Report 18-3, March 1976.
16. MAJIDZADEH, K. and SUCKARIEH, G. The study of pavement overlay design. Final Report. Ohio State Univ. Columbus 1977.
17. COETZEE, N.F. Some considerations on reflection cracking for asphalt concrete overlay pavements. PhD Dissertation Univ of California, Berkeley, November 1979.
18. GERMANN, F.P. and LYTTON, R.L. Methodology for predicting the reflection cracking life of asphaltic concrete overlays. Research Report 207-5, Texas Transportation Institute, March 1979.

19. JIMINEZ, R.A., MORRIS, G.R. and DaDEPPO, D.A. Tests for a strain attenuating asphaltic material. Proceedings. AAPT Vol 48, 1979.
20. GRIFFITH, A.A. The phenomena of rupture and flow in solids. Transactions, Royal Society, London 1920.
21. WESTERGAARD, H.M. Bearing pressures and cracks, Journal of Applied Mechanics, 61, A49, 1939.
22. IRWIN, G.R. Analysis of stresses and strains near the end of a crack traversing a plate. Transactions, ASME, Journal of Applied Mechanics, Vol 24, 1957.
23. PARIS, P.C. and ERDOGAN, F. A critical analysis of crack propagation laws. Transactions of the ASME, Journal of Basic Engineering, SERIES D, 85, No 3, 1963.
24. PARIS, P.C. and SIH, G.C. "Stress analysis of cracks", Fracture toughness testing and its applications. ASTM. STP 381, Philadelphia 1965.
25. MAJIDZADEH, K and RAMSAMOOJ, D.V. Mechanistic approach to the solution of cracking in pavements. Special Report 140, Transport Research Board, Washington D.C. 1973.
26. MAJIDZADEH, K, BURANOM, C. and KARAKOUZIAN, M. Application of fracture mechanics for improved design of bituminous concrete, Vol I: Plan of research, state of the art and mathematical investigations. Report FHWA-RD-76-91, Federal Highways Administration, Washington D.C. 1976.
27. SCHAPERLY, R.A. A theory of crack growth in viscoelastic media. Mechanics and Materials Research Center, Texas A&M University, College Station, Texas. 1973.

28. PELL, P.S. Fatigue characteristics of bitumen and bituminous mixes. Proceedings; 1st Int. Conference on the structural design of asphalt pavements. Univ of Michigan, Ann Arbor, 1962.
29. BANZIN, P. and SAUNIER, J.B. Deformability, fatigue and healing properties of asphalt mixes.. 2nd Int. Conference on the structural design of asphalt pavements, Univ. of Michigan, Ann Arbor. 1967.
30. KIRK, J.M. Results of fatigue tests on different types of bituminous mixtures. Proceedings, 2nd Int. conference on the structural design of asphalt pavements, Univ. of Michigan Ann Arbor, 1967.
31. MARCHAND, J.P. and GOACOLON, H. Cracking in wearing courses. Proceedings, 5th Int. Conference on the structural design of asphalt pavements, Univ. of Michigan, Ann Arbor, 1982.
32. MOLENAAR, A.A.A. Structural performance and design of flexible road constructions and asphalt concrete overlays. Ph.D. Thesis, Delft University, 1983.
33. LUTHER, M.W., MAJIDZADEH, K. and CHANG, C.W. Mechanistic investigation of reflection cracking of asphalt overlays. Transportation Research Record 572, National Research Council, Washington D.C. 1976.
34. VAN DER POEL, C. Time and Temperature effects on the deformation of asphaltic bitumens and bitumen - mineral mixtures. SPE Journal, Sep 1955.
35. GALLOWAY, J.W. Temperature durations at various depths in bituminous roads. R.R.L. report No. LR 138. Crowthorne, 1968.

36. PRICE, W.I.J. Temperatures in concrete slabs covered with bituminous surfacings and stone layers. R.R.L. unpublished report. 1955.
37. WILSON, A.H. The distribution of temperatures in experimental pavements at Alconbury by-pass. TRRL report LR 719. Crowthorne, 1976.
38. BRITISH STANDARDS INSTITUTION. Bitumen Road Emulsions (Anionic and Cationic) Part I : Requirements , Part II : Recommendations for use, BS 434, 1973.
39. MECHANICAL ENGINEERING PUBLICATIONS LTD. A general introduction to fracture mechanics, London, 1978.
40. SCHAPERLY, R.A. Non-linear fracture analysis of visco-elastic composite materials based on a generalised J-Integral theory. Proceedings Japan-USA Conference on composite materials, Tokyo - 1981.
41. SAYEGH, G. Visco-elastic-properties of bituminous mixtures. Proceedings, 2nd Int. Conference on the structural design of asphalt pavements, Univ. of Michigan, Ann Arbor, 1967.
42. HEUKELOM, W. Observations on the rheology and fracture of bitumens and asphalt mixes. Proceedings AAPT, Vol 35, 1966.
43. MAJIDZADEH, K. and HERRIN, M. Modes of failure and strength of asphalt films subjected to tensile stresses. Highways Research Record 67. Washington D.C. 1965.
44. STILL, P.B. Thermal stresses in bituminous flexible pavements. TRRL report LR 433, Crowthorne, 1972.

45. VAN DIJK, W. Practical fatigue characterisation of bituminous mixes, Proceedings AAPT, Vol 44, 1975.
46. CLAESSEN, A.J.M. et al. Asphalt-Pavement Design - The SHELL Method Proceedings, 4th Int. Conference on the structural design of asphalt pavements. Univ. of Michigan. Ann Arbor, 1977.
47. HILLS, J.F., BRIEN, D and VEN DE LOO, P.J. The correlation of rutting and creep tests on asphalt mixes. Institute of Petroleum, Paper IP 74-001, 1974.
48. OROWAN, E. Energy criteria of fracture, Weld. J. Res. Suppl, 20, 1955.
49. MINER, M.A. Cumulative damage in fatigue, J. Applied Mechanics 67, 1945.
50. FRANCKEN, L. Fatigue performance of a bituminous road mix under realistic test conditions. Transportation Research Record 712, Washington D.C. 1979.
51. JACOBS, F.A. A33 Winchester by-pass : the performance of rolled asphalts designed by the Marshall Test, TRRL report No LR 1082, Crowthorne, 1983.
52. FOULKES, M.D. and KENNEDY, C.K. The limitation of reflection cracking in flexible pavements containing cement bound layers. Proceedings, Int. Conference Bearing Capacity of Roads and Airfields, Plymouth, 1986.
53. HILL, J. Discussion on slippage of rolled asphalt wearing courses, Proceedings of conference entitled - The Performance of Rolled Asphalt Road Surfacing, Institution of Civil Engineers, London, 1979.

54. BURT, M.A. M4 Motorway, a composite pavement : the mechanism of failure. Int. Conference, The Bearing Capacity of Roads and Airfields Plymouth, 1986.

55. PICKETT, D.L. and LYTTON, R.L. Laboratory evaluation of selected fabrics for reinforcement of asphaltic concrete overlays. Texas Transportation Institute, Texas A & M University Texas, August 1983.

APPENDIX

A TEMPERATURE MODEL FOR COMPOSITE PAVEMENTS

This appendix describes a method of using measurements of the annual and daily cycle of pavement temperature from Full-Depth BITUMINOUS and CONCRETE Pavements, to estimate Temperature Variations in COMPOSITE Pavements. These are required for calculation of Thermal Stresses and thus of the likelihood of REFLECTION CRACKING resulting from this mechanism, at various times of the year.

The BITUMINOUS and CONCRETE Pavement Data is used to plot HOURLY TEMP PROFILES. These are compared in order to deduce the relative Thermal Properties of the 2 materials.

The information represented by the profiles can be broken down into 3 Independent Components. The relevant values of each of these components can be estimated for COMPOSITE Pavements and re-combined to give HOURLY TEMP PROFILES from which the relevant Temperature Variations for calculating Thermal Stresses can be found.

CONTENTS

1 INTRODUCTION

- 1.1 The Temperature Model for COMPOSITE Pavements
- 1.2 The Relationship between AIR & PAVEMENT temperature
- 1.3 HOURLY TEMP PROFILES
- 1.4 Components of the HOURLY TEMP PROFILES

2 TABULATION OF THE DAILY CYCLE OF PAVEMENT TEMP

- 2.1 BITUMINOUS PAVEMENT Data
- 2.2. CONCRETE PAVEMENT Data
- 2.3 Observations from the Tabulated Daily Cycle
- 2.4 Comparison of Daily Temp Ranges and Mean Pavement Temps
- 2.5 The Average Year Variation of Daily Temp Range

3 THE VARIATION OVER THE AVERAGE YEAR OF MEAN & "MEDIAN" PAVEMENT TEMPERATURES

- 3.1 The Use of monthly values for "MEDIAN" Pavement Temp
- 3.2 Plotting the Annual Variation of "MEDIAN" Pavement Temp
- 3.3 The Relationship between MEAN & "MEDIAN" Temps
- 3.4 Correction from "MEDIAN" to MEAN Temps
- 3.5 Comparison of MMPTs for BITUMINOUS & CONCRETE Pavements

4 HOURLY TEMPERATURE PROFILES

- 4.1 Adjustment of Tabulated Data
- 4.2 Plotting of Hourly Temp Profiles
- 4.3 Observations from Hourly Temp Profiles
- 4.4 Thermal Conductivity
- 4.5 Deducing COMPOSITE PAVEMENT Hourly Temp Profiles

5 MATCHING OF ISOCHRONE DISTRIBUTIONS (IDs)

- 5.1 Comparison of BITUMINOUS & CONCRETE IDs
- 5.2 Thermal Properties of Pavement Materials
- 5.3 Comparison of Thermal Behaviour of Pavements

- 5.4 Hypothesis for Matching Isochrones
- 5.5 Interpolation of (IDs) for other months

6 COMPOSITE PAVEMENT MMPTs

- 6.1 The LR138 Comparison
- 6.2 (BITUMINOUS-CONCRETE) MMPT DIFFERENCES
- 6.3 Estimated COMPOSITE PAVEMENT MMPTs

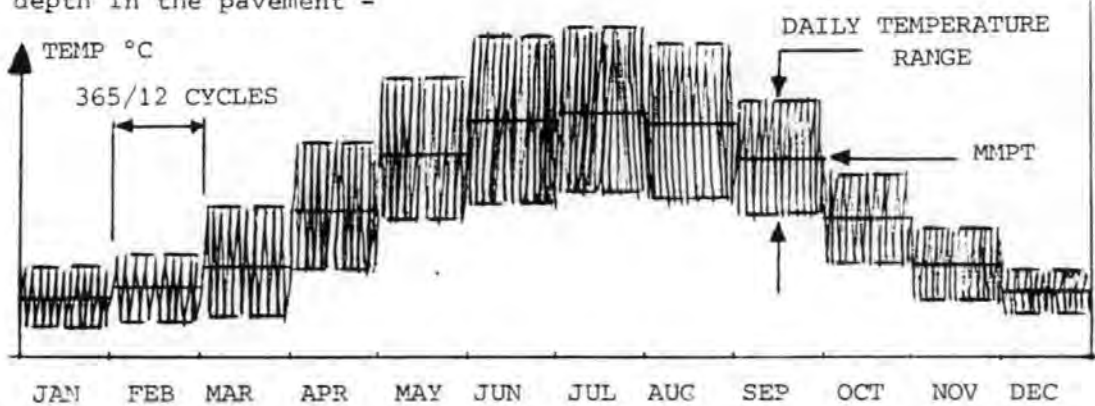
7 COMPOSITE PAVEMENT DAILY TEMP RANGES

- 7.1 Composite Pavement ENVELOPE SHAPE
- 7.2 Composite Pavement ENVELOPE AREA
- 7.3 Solving the Heat Balance Equation
- 7.4 HEAT GAIN of Pavement Materials
- 7.5 HEAT LOSS to the air from the Pavement Surface
- 7.6 SURFACE HEAT ABSORPTION, A
- 7.7 SURFACE HEAT ABSORPTION for a BITUMINOUS SURFACE
- 7.8 ENVELOPE AREA Temp Ranges at Depths
- 7.9 Conclusion

1. INTRODUCTION

1.1 The Temperature Model for COMPOSITE Pavements

In view of the innate unpredictability of the U.K. climate, the following is considered to be a reasonable representation of the annual and daily variations of Pavement Temperature for a given depth in the pavement -



whereby the year is split into 12 "Monthly" Periods, over which -

- i) Mean Daily Pavement Temperature is constant and thus equal to Mean Monthly Pavement Temperature (MMPT)
- ii) The "RANGE" of the Daily Cycle is also constant and equal to the linear average value for that month. This may underestimate the effect of extremes of DAILY TEMP RANGE, in which case it could be expressed as a statistical distribution with a mean and standard deviation which may vary from month to month.

1.2 The Relationship between AIR AND PAVEMENT Temperature

The BITUMINOUS and CONCRETE Pavement Data relates to separate sites at Alconbury and Long Bennington, both of which lie within the Central Zone of the U.K. but ambient air temperatures are slightly different. In order to be able to compare them directly, both sets of Data can be corrected to correspond to Long-Term Mean Air-Temperatures for the Central Zone using a method similar to

that developed by CRONEY (1) which involves establishing a graphical relationship between Mean Monthly Air and Pavement Temperatures over the Annual Cycle.

This relationship can also be used to estimate MMPTs from Met Office Mean Monthly Air Temperatures elsewhere in the U.K. In this manner, the Temperature Model can be applied to any site in the U.K., although for extreme regions, some correction of DAILY TEMP RANGES may be necessary, based on either % cloud cover, wind speed or hours of sunshine.

1.3 HOURLY TEMP PROFILES

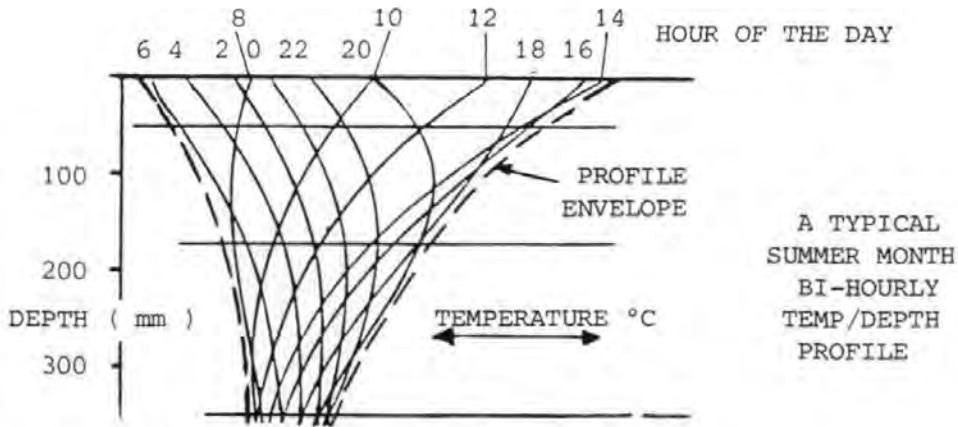
The Temperature Model is based on "Characteristic Monthly" Hourly Temp Profiles produced by combining the Daily Cycle of Pavement Temperature at 3 Depths, i.e. A, B and C. The lines on the profile are ISOCHRONES (lines of equal time, in hours).

The Experimental Data used is that referred to by CRONEY (1) Chapter 10. It relates to the period 1969/70 which is an average year insofar as it is not remembered for either a hot summer or a severe winter.

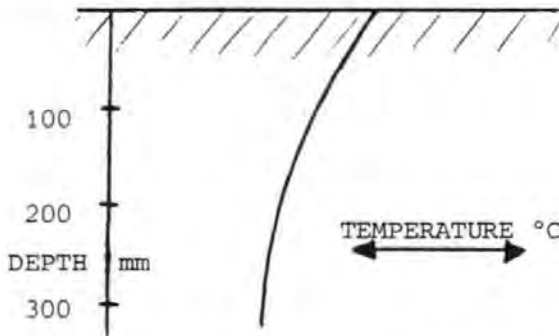
The original Data could only be obtained for BITUMINOUS Pavement Temperatures, and so comparable HOURLY TEMP PROFILES can only be plotted for the months APR/JUL/OCT/JAN. These months are however, key points in the annual cycle and so information for other months can be interpolated with a reasonable expectation of accuracy.

Also, the Data for some of these months is not very representative in terms of the magnitude of DAILY TEMP RANGE and the MMPT at various depths in the pavement. The Annual Variation of these quantities was investigated by graphing and re-tabulation, and more representative "AVERAGE YEAR" values obtained and used to adjust the Data before using it to plot HOURLY TEMP PROFILES.

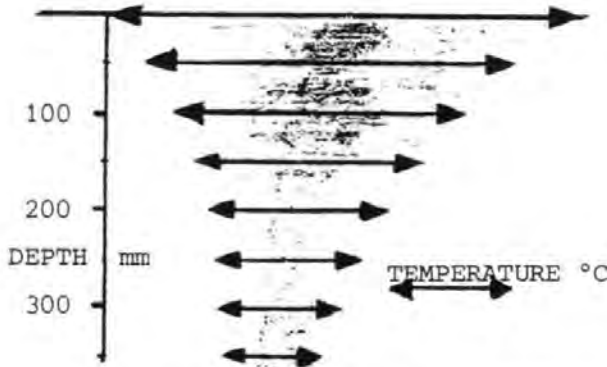
PAVEMENT HOURLY TEMPERATURE / DEPTH PROFILES .



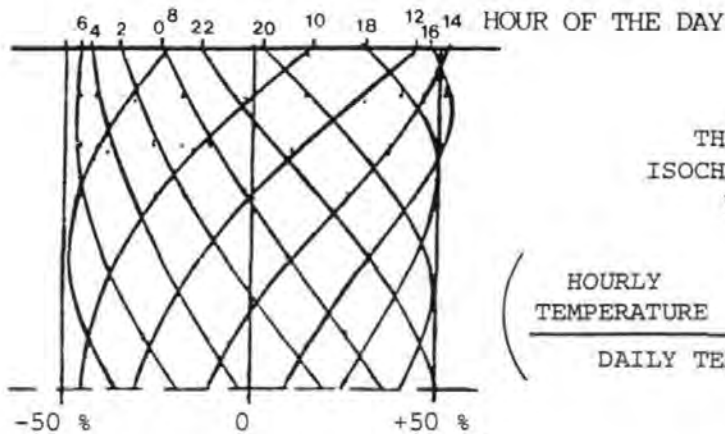
TEMPERATURE / DEPTH PROFILES HAVE THREE INDEPENDANT COMPONENTS



THE VARIATION OF MEAN PAVEMENT TEMPERATURE WITH DEPTH IN THE PAVEMENT



THE ATTENUATION OF DAILY TEMPERATURE RANGE WITH DEPTH IN THE PAVEMENT



THE NORMALISED ISOCHRONE DISTRIBUTION WAVEFORM

$$\left(\frac{\text{HOURLY TEMPERATURE} - \text{MEAN PAVEMENT TEMPERATURE}}{\text{DAILY TEMPERATURE RANGE}} \right) \left(\text{DEPTH IN PAVEMENT} \right)$$

1.4 Components of the HOURLY TEMP PROFILES

MMPT and DAILY TEMP RANGE are both functions of depth in the pavement. Relevant Monthly Values for COMPOSITE Pavements can be determined from

i) Data from LR138 (4) which describes a comparison of temperature durations in FULL-DEPTH BITUMINOUS and COMPOSITE BITUMINOUS/LEAN CONCRETE Pavements.

ii) The Attenuation of DAILY TEMP RANGE with depth in the material, combined with a HEAT BALANCE EQN which relates the "swept area" of the HOURLY TEMP PROFILES to the HEAT GAIN of the pavement material during the daytime.

When MMPT and DAILY TEMP RANGE are eliminated from the HOURLY TEMP PROFILES, the remaining component can be referred to as the, ISOCHRONE DISTRIBUTION (ID), defined by -

$$ID (\text{depth, time}) = \frac{\text{TEMP} (\text{depth, time}) - \text{MMPT} (\text{depth})}{\text{DAILY TEMP RANGE} (\text{depth})}$$

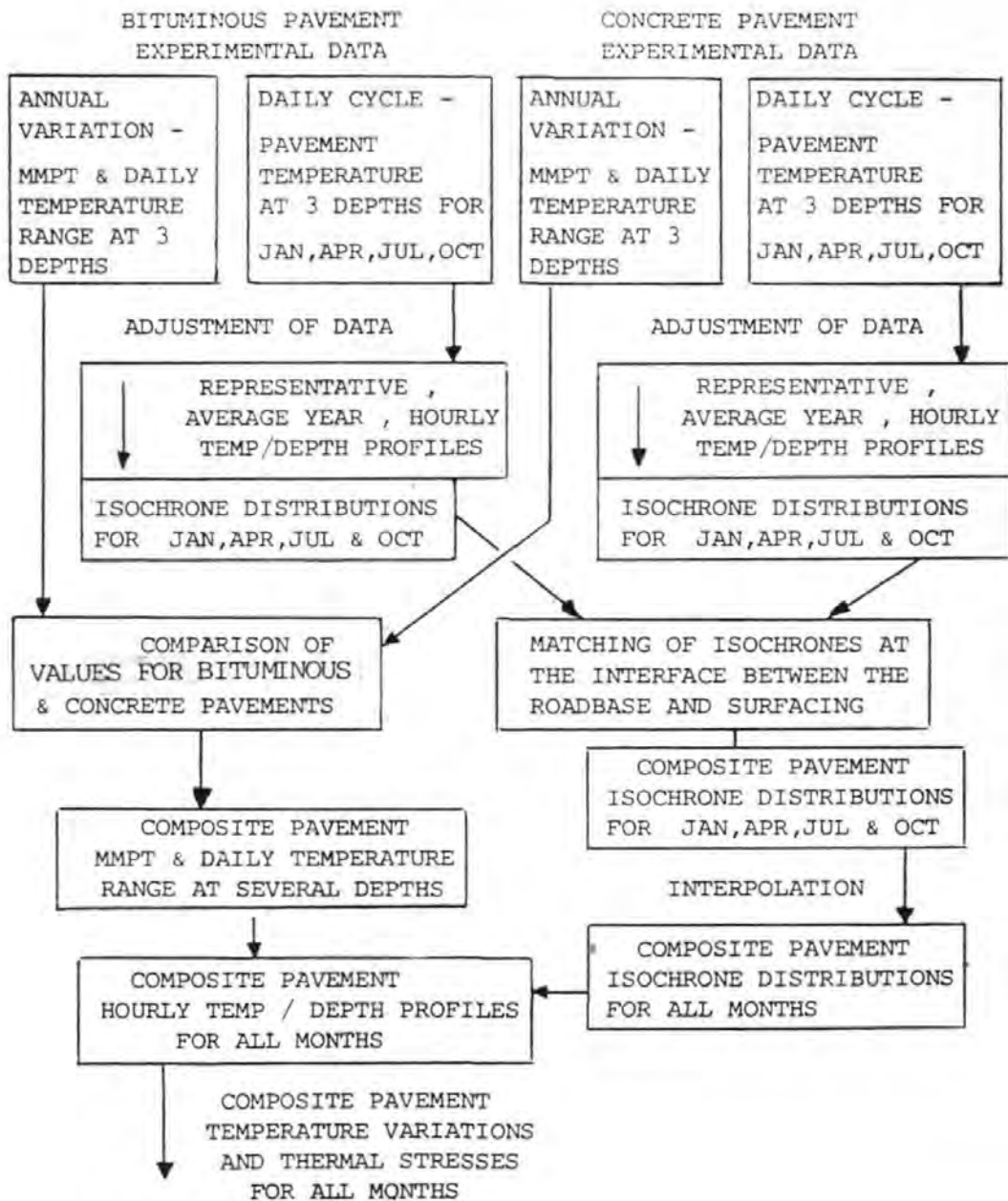
where TEMP (depth, time) are the Individual Hourly Readings of Pavement Temperature.

The ISOCHRONE DISTRIBUTION is a temperature independent measure of the pavement's response to a varying HEAT INPUT at the surface due to the absorption of solar radiation. Its shape will vary from month to month because the duration of the heating period varies over the year, from c 6hrs in WINTER to c 12hrs in SUMMER.

The ISOCHRONE DISTRIBUTION for a COMPOSITE Pavement can be estimated by combining that for the top 100mm of a BITUMINOUS Pavement with that for depths > 100mm in a CONCRETE Pavement. Differences between the position of ISOCHRONES in the 2 sections, at the Interface, can be relaxed with depth by considering the Response to Heating of a COMPOSITE Pavement, and how it differs from that of FULL-DEPTH BITUMINOUS and CONCRETE Pavements.

This method of independently matching MMPT and DAILY TEMP RANGE reduces the effect of errors introduced by this form of matching ISOCHRONES, on the resulting COMPOSITE Pavement HOURLY TEMP PROFILES, by ensuring that they are accurate in terms of size and shape.

The Procedure for Deducing COMPOSITE Pavement HOURLY TEMP PROFILES can be summarised by a flowchart.



2 Tabulation of the Daily Cycle of Pavement Temp

The Daily Cycle of Pavement Temp can be determined from Hourly Readings of Temperature at 3 depths in the Pavement.

2.1 BITUMINOUS PAVEMENT Data

For the BITUMINOUS Pavement, the Original Experimental Data was obtained from TRRL (2)

Mean Temperatures for each Hourly Interval of the Day could be calculated for all months of the year and for depths of 19, 38, 102, 203, and 356 mm in the pavement, but only the Data for JAN/APR/JUL and OCTOBER and for depths of 19, 102 and 356 mm was used, APPENDIX A.

2.2 CONCRETE PAVEMENT DATA

CONCRETE Pavement Data, The Original Experimental Data could not be found and so the Hourly Temp Readings (Fig. 10.12) were photocopied from CRONEY (1).

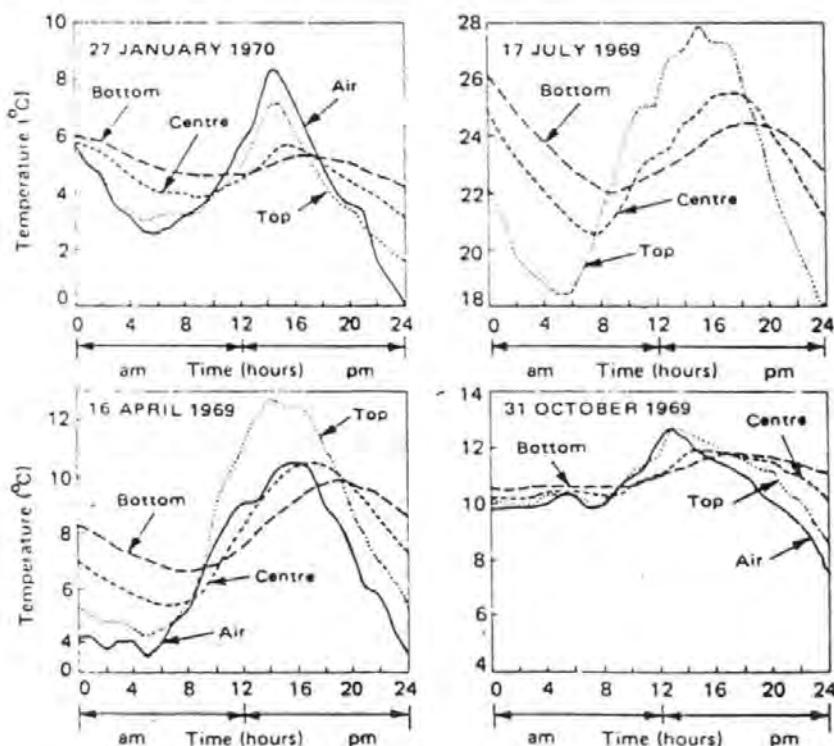


Fig. 10.12. Temperature distribution through 254-mm concrete slab at four times of year.

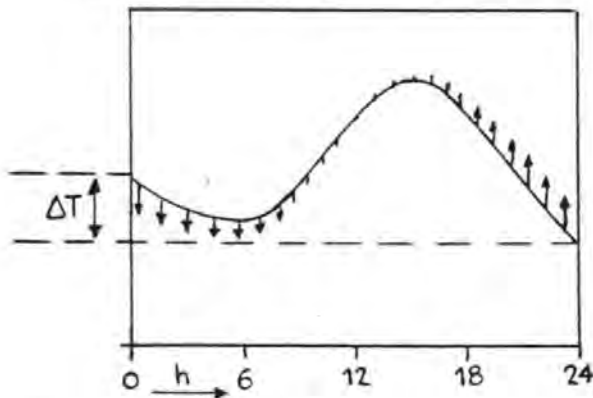
A grid was drawn on the figures and the Temperatures were estimated to the nearest 0.1°C for each hour of the day.

It was noted that, because the curves represent hourly readings from a particular day rather than mean hourly readings over a whole month, i.e. -

The temperatures at hours, $h=0$ and $h=24$ were not always the same, varying by up to 4°C .

This represents a general cooling of the pavement over the day in question, and can be corrected for by "levelling" the curves.

A Correction Factor -



$$T \frac{12 - h}{24}$$

has been subtracted from each Tabulated Hourly Reading of Temperature, APPENDIX A

2.3 Observations from the Tabulated Daily Cycle,

The Maximum and Minimum Temperatures of The Daily Cycle have been highlighted in Heavy Type.

It was noticed that, apart from the main peak of pavement Temperature which occurs at mid-afternoon at the surface and at early evening at lower depths, the Daily Cycle for some months appears to have subsidiary peaks during the early hours of the morning.

i.e. at 03/04.00 hrs for the BITUMINOUS Pavement in JANUARY and at 05/06.00 hrs for the CONCRETE Pavement in OCTOBER.

These peaks are only evident in the upper layers of the pavement and are probably due to some night-time temperature inversion

phenomena, in the air,

For the purposes of estimating the Daily Range of Pavement Temperature, only the daytime peak that results from solar radiation will be used.

The Temperature Ranges at the various depths in BITUMINOUS and CONCRETE Pavements were compared.

2.4 Comparison of Daily Temp Ranges and Mean Pavement Temps

| Daily Temperature Ranges at Depths | | | | TABULATED DATA | | |
|------------------------------------|---------------------|--------|--------|-------------------|--------|--------|
| MONTH | BITUMINOUS Pavement | | | CONCRETE Pavement | | |
| | 19 mm | 102 mm | 356 mm | 0 mm | 127 mm | 254 mm |
| JAN | 1.3 | 1.0 | 0.5 | 5.8 | 2.7 | 1.4 |
| APR | 17.0 | 11.2 | 1.2 | 8.4 | 4.9 | 3.0 |
| JUL | 16.8 | 10.8 | 2.0 | 11.1 | 6.6 | 4.0 |
| OCT | 8.2 | 5.7 | 1.3 | 3.1 | 1.6 | 1.0 |

The Temperature Ranges for some of the months do not seem very representative.

i.e. with BITUMINOUS Pavement; OCT Range \gg JAN Range

but with CONCRETE Pavement; JAN Range $>$ OCT Range

Also, (time averaged) Mean Pavement Temperatures for the Tabulated Data were compared,

| Mean Pavement Temperatures at Depths (° C) MMPT | | | | | | |
|---|---------------------|--------|--------|-------------------|--------|--------|
| MONTH | BITUMINOUS Pavement | | | CONCRETE Pavement | | |
| | 19 mm | 102 mm | 356 mm | 0 mm | 127 mm | 254 mm |
| JAN | 5.5 | 5.4 | 6.1 | 4.1 | 4.6 | 5.0 |
| APR | 12.8 | 12.0 | 10.5 | 8.1 | 7.8 | 8.2 |
| JUL | 25.9 | 25.1 | 23.5 | 22.6 | 23.1 | 23.6 |
| OCT | 14.8 | 14.4 | 14.8 | 10.9 | 10.9 | 11.1 |

The Monthly Mean Pavement Temperatures (MMPTs) are not constant for all depths in the Pavement, but can vary across the full thickness of the Pavement by up to -

1° C with CONCRETE Pavements and
2.4° C with BITUMINOUS Pavements

Average Year Values can be found, for the variation of Daily Temp Range and MMPT with depth in the pavement.

These values can be used as a check on the representativity of the Tabulated Data, which can then be adjusted before being used to plot HOURLY TEMP PROFILES, that are representative of the Average Year.

2.5 The Variation over the Average Year of Daily Temp Range

BITUMINOUS PAVEMENTS, Daily Temp Ranges at depths for all months of the Year, can be found from the MAX and MIN values of the Monthly Mean Temperatures for each Hourly Interval of the day (2).

CONCRETE PAVEMENTS, the MAX and MIN Pavement Temperatures for each day of the Year can be estimated to the nearest 1° C from fig. 10.11 p.327 (1). The combination of c30 readings per month

can be used to give reasonable average values of Daily Temp Range to the nearest 0.1°C , in view of the tedious method of calculating this. The Data for MAY and AUGUST was omitted. TABLE 2

The Data for each Monthly Interval was then graphed and re-tabulated to give a more even progression from month to month which corresponds to the variation over the Average Year. FIG.2.1

This, Average Year, Mean Monthly, variation of Temperature Range with Depth was then plotted to enable the Temperature Range at all depths to be found by interpolation. FIG.2.2.

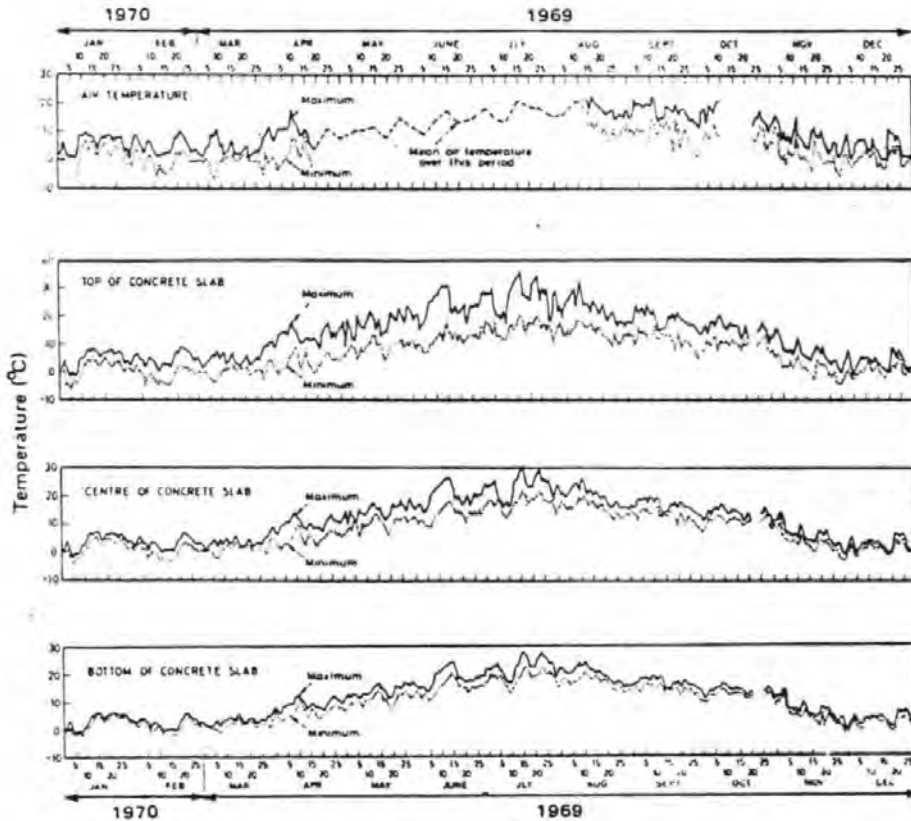


Fig. 10.11. Daily variation of slab and air temperatures measured in a concrete road - central temperature zone.

TABLE 2

AIR , BITUMINOUS, AND CONCRETE PAVEMENT , DAILY TEMPERATURE RANGES
AT VARIOUS DEPTHS (°C) .

MEAN MONTHLY VALUES OBTAINED FROM THE ORIGINAL DATA (1) (2) .

| MONTH | AIR TEMPERATURE DAILY RANGE | BITUMINOUS PAVEMENT DAILY RANGE AT DEPTHS | | | CONCRETE PAVEMENT DAILY RANGE AT DEPTHS | | |
|-------|-----------------------------------|--|--------|--------|--|--------|--------|
| | | 19 mm | 102 mm | 356 mm | 0 mm | 127 mm | 254 mm |
| JAN | 4.5 | 1.3 | 1.0 | 0.5 | 3.5 | 2.0 | 1.2 |
| FEB | 5.9 | 7.7 | 5.3 | 0.9 | 5.8 | 2.9 | 1.6 |
| MAR | 5.3 | 7.9 | 5.3 | 0.65 | 4.8 | 2.9 | 1.7 |
| APR | 8.3 | 17.0 | 11.2 | 1.2 | 9.0 | 5.2 | 3.0 |
| MAY | | 15.4 | 9.7 | 2.0 | | | |
| JUN | | 21.1 | 13.0 | 2.3 | 12.2 | 6.9 | 3.9 |
| JUL | | 16.8 | 10.8 | 2.0 | 10.8 | 5.9 | 3.6 |
| AUG | | 13.5 | 8.4 | 1.5 | | | |
| SEP | 8.5 | 11.5 | 7.2 | 1.2 | 7.3 | 3.8 | 2.5 |
| OCT | 7.5 | 8.2 | 5.7 | 1.3 | 5.4 | 2.6 | 1.9 |
| NOV | 6.3 | 3.7 | 3.1 | 0.7 | 5.4 | 2.7 | 1.8 |
| DEC | 3.9 | 2.1 | 1.4 | 0.3 | 3.4 | 1.8 | 1.3 |

"AVERAGE YEAR" VALUES OBTAINED BY GRAPHING AND RE-TABULATION OF THE
DATA (FIG 2.1) .

| | | | | | | | |
|-----|------|------|------|------|------|-----|-----|
| JAN | 4.0 | 2.1 | 1.3 | 0.4 | 3.5 | 2.0 | 1.2 |
| FEB | 4.6 | 5.2 | 3.2 | 0.6 | 4.3 | 2.4 | 1.4 |
| MAR | 6.4 | 9.9 | 6.5 | 0.95 | 6.6 | 3.5 | 2.0 |
| APR | 8.3 | 14.3 | 9.6 | 1.4 | 9.0 | 5.2 | 3.0 |
| MAY | 9.8 | 18.4 | 11.9 | 1.9 | 11.2 | 6.5 | 3.7 |
| JUN | 10.5 | 21.1 | 13.0 | 2.3 | 12.2 | 6.8 | 3.9 |
| JUL | 10.4 | 17.6 | 11.1 | 2.0 | 10.9 | 6.0 | 3.7 |
| AUG | 9.7 | 14.1 | 9.0 | 1.65 | 9.2 | 4.9 | 3.2 |
| SEP | 8.6 | 10.6 | 6.9 | 1.3 | 7.5 | 3.9 | 2.6 |
| OCT | 7.5 | 7.3 | 4.9 | 0.95 | 5.9 | 2.9 | 2.1 |
| NOV | 6.0 | 4.0 | 3.1 | 0.6 | 4.5 | 2.3 | 1.6 |
| DEC | 4.5 | 1.9 | 1.5 | 0.4 | 3.5 | 1.9 | 1.3 |

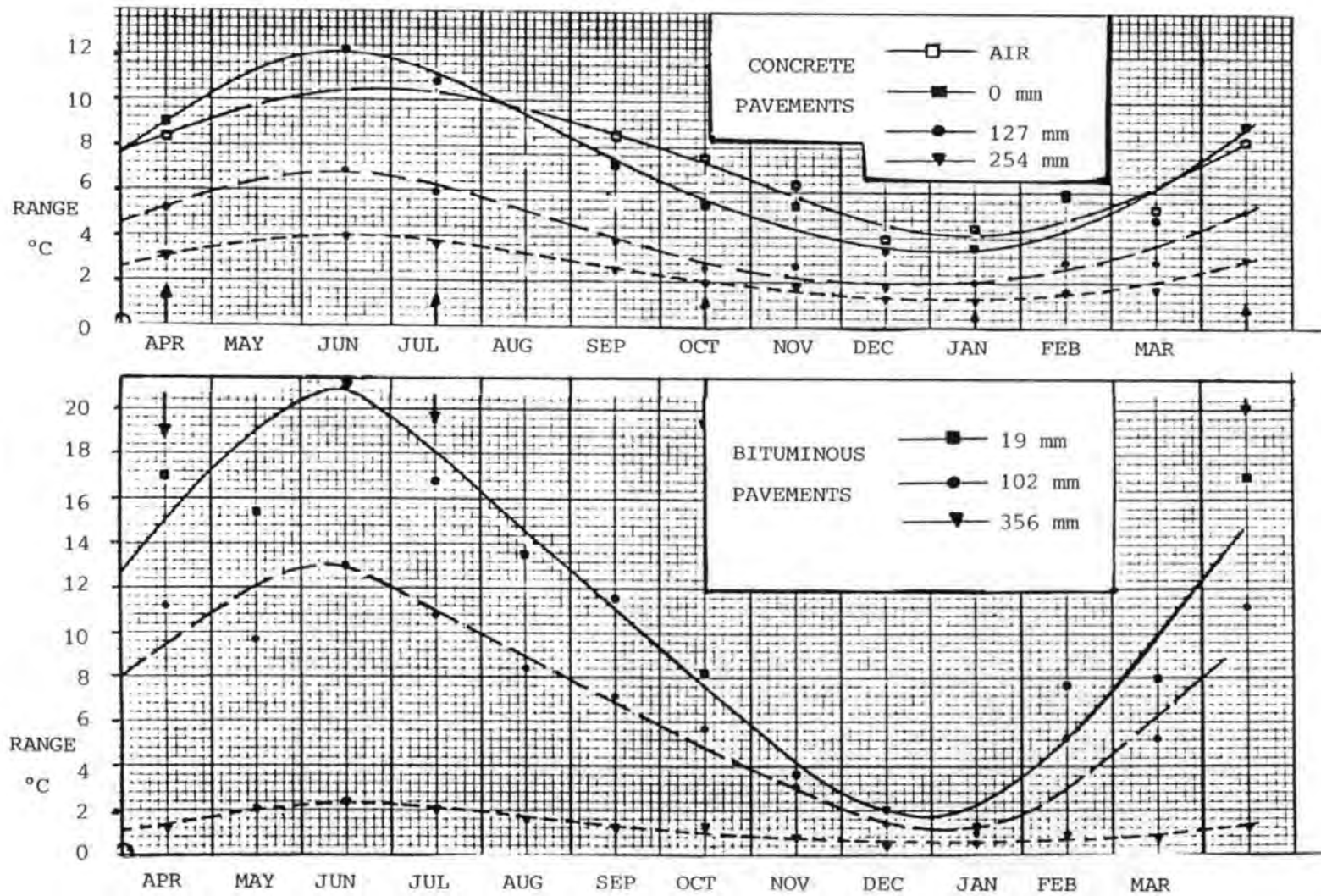
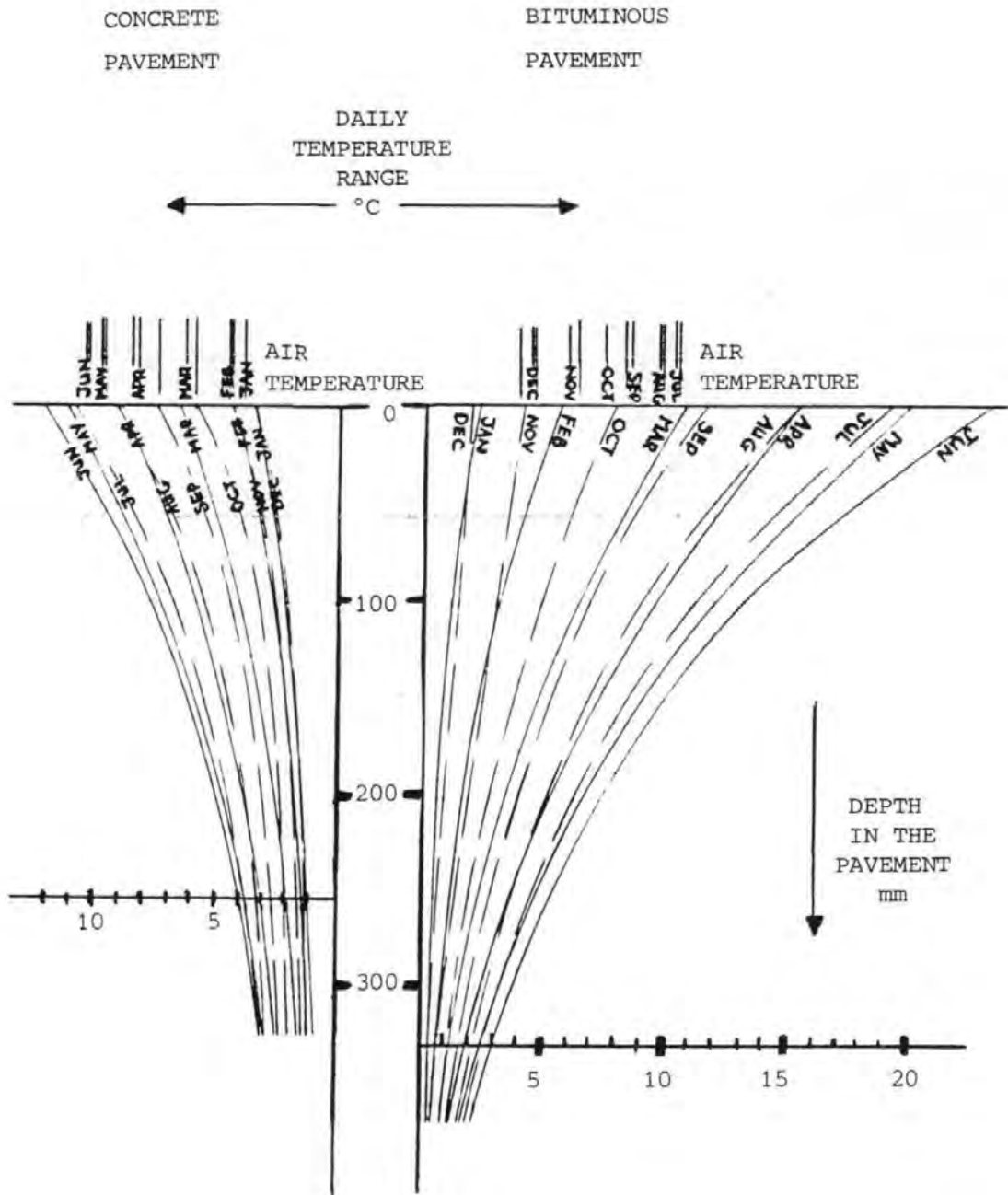


FIG 2 . 1
THE ANNUAL VARIATION OF AVERAGE MONTHLY VALUES FOR -
DAILY TEMPERATURE RANGE AT 3 DEPTHS IN THE PAVEMENT .

FIG 2 . 2

THE VARIATION OF DAILY TEMPERATURE RANGE WITH DEPTH IN THE PAVEMENT (AVERAGE YEAR , MEAN MONTHLY VALUES) .



3 The Variation over the Average Year of MEAN and "MEDIAN" Pavement Temperatures

The determination of the Annual Variation of MMPT for BITUMINOUS and CONCRETE Pavements is not quite as straightforward as for Daily Temp Range.

3.1 The Use of Monthly Values for "MEDIAN" Pavement Temp

MMPTs for all months of the year can only be found for BITUMINOUS Pavements, but "MEDIAN" Pavement Temperatures can be found for all months of the year for both —

BITUMINOUS PAVEMENTS, from the Original Data (2)

and CONCRETE PAVEMENTS, from the MAX and MIN Pavement Temperatures in fig. 10.11 p.327 (1)

thus it was decided to investigate the Annual Variation over the Average Year in terms of "MEDIAN" pavement temperatures.

A relationship can then be developed to convert individual monthly values from "MEDIAN" to MEAN temperatures.

3.2 Plotting of the Annual Variation of "Median" Pavement Temp

The Variation in "Median" Pavement temperature can be plotted over each month of the year by relating it to Met-Office "Mean" air temperatures estimated for the site (2), which are in fact the average of MAX and MIN Temperature and thus "Median" rather than mean air temperatures.

For both BITUMINOUS and CONCRETE Pavements, the "MEDIAN" Pavement Temperatures at 3 depths were Tabulated, TABLE 3.1

The Difference between "Median" Pavement and Air Temperature was then calculated, and plotted over the 12 monthly intervals

TABLE 3 . 1

"MEDIAN", (MAX + MIN) / 2 , AIR & PAVEMENT TEMPERATURES AT VARIOUS DEPTHS AND (PAVEMENT - AIR) TEMPERATURE DIFFERENCES (°C) .

BITUMINOUS PAVEMENT

| MONTH | AIR & PAVEMENT TEMPERATURES AT DEPTHS | | | | (PAVEMENT-AIR) TEMPERATURE DIFF' | | | (PAVEMENT-AIR) TEMPERATURE DIFF' * | | |
|-------|---------------------------------------|-------|-------|-------|------------------------------------|-------|-------|--------------------------------------|-------|-------|
| | AIR | 19mm | 102mm | 356mm | 19mm | 102mm | 356mm | 19mm | 102mm | 356mm |
| JAN | 3.6 | 5.55 | 5.30 | 6.15 | 1.95 | 1.70 | 2.55 | 1.7 | 1.5 | 1.9 |
| FEB | 3.2 | 5.95 | 5.25 | 5.35 | 2.75 | 2.05 | 2.15 | 2.4 | 1.9 | 1.9 |
| MAR | 3.4 | 6.10 | 5.35 | 4.75 | 2.70 | 1.95 | 1.35 | 3.6 | 2.8 | 2.2 |
| APR | 7.6 | 14.10 | 12.40 | 10.50 | 6.50 | 4.80 | 2.90 | 5.6 | 4.3 | 2.9 |
| MAY | 12.0 | 19.30 | 17.95 | 15.95 | 7.30 | 5.95 | 3.95 | 8.1 | 6.5 | 4.4 |
| JUN | 13.8 | 24.25 | 22.80 | 20.55 | 10.45 | 9.00 | 6.75 | 10.1 | 9.0 | 6.7 |
| JUL | 17.4 | 26.70 | 25.60 | 23.60 | 9.30 | 8.20 | 6.20 | 9.3 | 8.2 | 6.2 |
| AUG | 16.4 | 22.85 | 21.40 | 20.55 | 6.40 | 5.00 | 4.15 | 6.8 | 5.5 | 4.6 |
| SEP | 14.3 | 19.65 | 18.30 | 17.70 | 5.35 | 4.00 | 3.40 | 4.6 | 3.2 | 3.5 |
| OCT | 13.1 | 15.90 | 14.85 | 14.85 | 2.80 | 1.75 | 1.75 | 2.8 | 1.8 | 2.8 |
| NOV | 5.7 | 7.50 | 6.85 | 8.75 | 1.80 | 1.15 | 3.05 | 1.8 | 1.3 | 2.4 |
| DEC | 3.1 | 4.55 | 4.40 | 5.65 | 1.45 | 1.30 | 2.55 | 1.5 | 1.2 | 2.1 |

CONCRETE PAVEMENT

| MONTH | AIR & PAVEMENT TEMPERATURES AT DEPTHS | | | | (PAVEMENT-AIR) TEMPERATURE DIFF' | | | (PAVEMENT-AIR) TEMPERATURE DIFF' * | | |
|-------|---------------------------------------|------|-------|-------|------------------------------------|-------|-------|--------------------------------------|-------|-------|
| | AIR | 0mm | 127mm | 254mm | 0mm | 127mm | 254mm | 0mm | 127mm | 254mm |
| JAN | 3.5 | 2.7 | 2.8 | 2.8 | -0.8 | -0.7 | -0.7 | -0.9 | -0.8 | -0.7 |
| FEB | 2.1 | 1.7 | 1.5 | 1.6 | -0.4 | -0.6 | -0.5 | -0.4 | -0.5 | -0.4 |
| MAR | 2.3 | 2.6 | 2.4 | 2.5 | 0.3 | 0.1 | 0.2 | 0.3 | 0.0 | 0.1 |
| APR | 7.0 | 8.4 | 7.6 | 7.9 | 1.4 | 0.6 | 0.9 | 1.3 | 0.8 | 1.0 |
| MAY | | | | | | | | 2.4 | 2.0 | 1.9 |
| JUN | 14.2 | 17.8 | 17.1 | 17.0 | 3.6 | 2.9 | 2.8 | 3.6 | 2.9 | 2.8 |
| JUL | 17.3 | 22.0 | 20.3 | 20.4 | 4.7 | 3.0 | 3.1 | 4.7 | 2.9 | 3.1 |
| AUG | | | | | | | | 4.0 | 2.2 | 2.6 |
| SEP | 13.7 | 15.1 | 14.7 | 15.0 | 1.4 | 1.0 | 1.3 | 1.6 | 1.1 | 1.3 |
| OCT | 12.2 | 12.5 | 12.4 | 12.6 | 0.3 | 0.2 | 0.4 | 0.0 | 0.1 | 0.4 |
| NOV | 5.0 | 4.0 | 4.5 | 4.8 | -1.0 | -0.5 | -0.2 | -1.0 | -0.5 | -0.2 |
| DEC | 2.7 | 1.6 | 1.8 | 2.1 | -1.1 | -0.9 | -0.6 | -1.1 | -0.8 | -0.6 |

* "AVERAGE YEAR" VALUES OBTAINED BY GRAPHING & RE-TABULATION (FIG 3.1)

of the year.

Best-fit curves were then drawn to represent the variation of this quantity over the Average Year, FIG.3.1, and the Data was re-tabulated TABLE 3.1.

These "Average Year" values of the Difference between "Median" Pavement and Air Temperatures can be combined with -

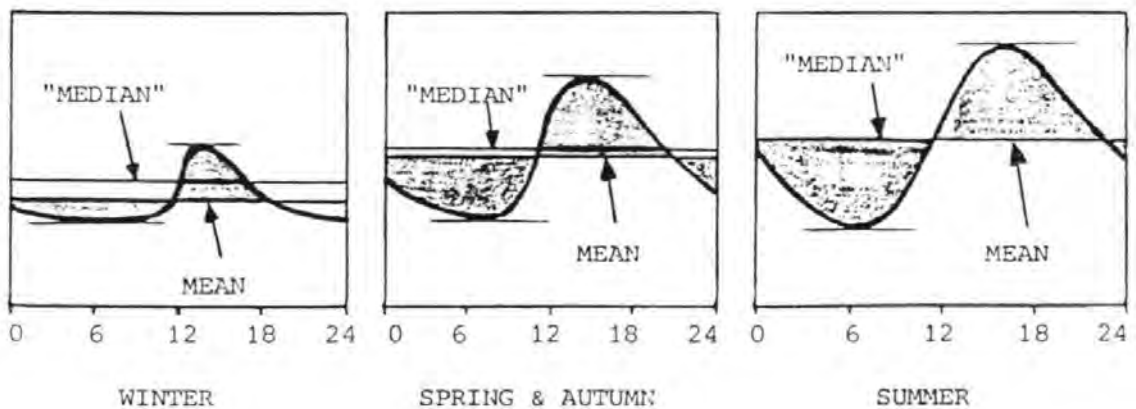
MET OFFICE Long Term "MEDIAN" Air Temperatures for The Central Zone of the U.K. (1)

to give "MEDIAN" Pavement Temperatures for BITUMINOUS and CONCRETE Pavements, that both correspond to the same ambient air temperatures. TABLE 3.2

3.3 The Relationship between MEAN and "MEDIAN" temperatures

The Difference between MEAN and "MEDIAN" temperatures arises from the fact that the duration of the Hump in the Daily Cycle is not always equal to $\frac{1}{2}$ of the wavelength, and varies from month to month.

The Duration of the Hump in the Daily Cycle



GRAPHING AND RETABULATION OF (PAVEMENT - AIR) TEMPERATURE DIFFERENCES FOR DETERMINATION OF AVERAGE YEAR VALUES .

FIG 3 . 1

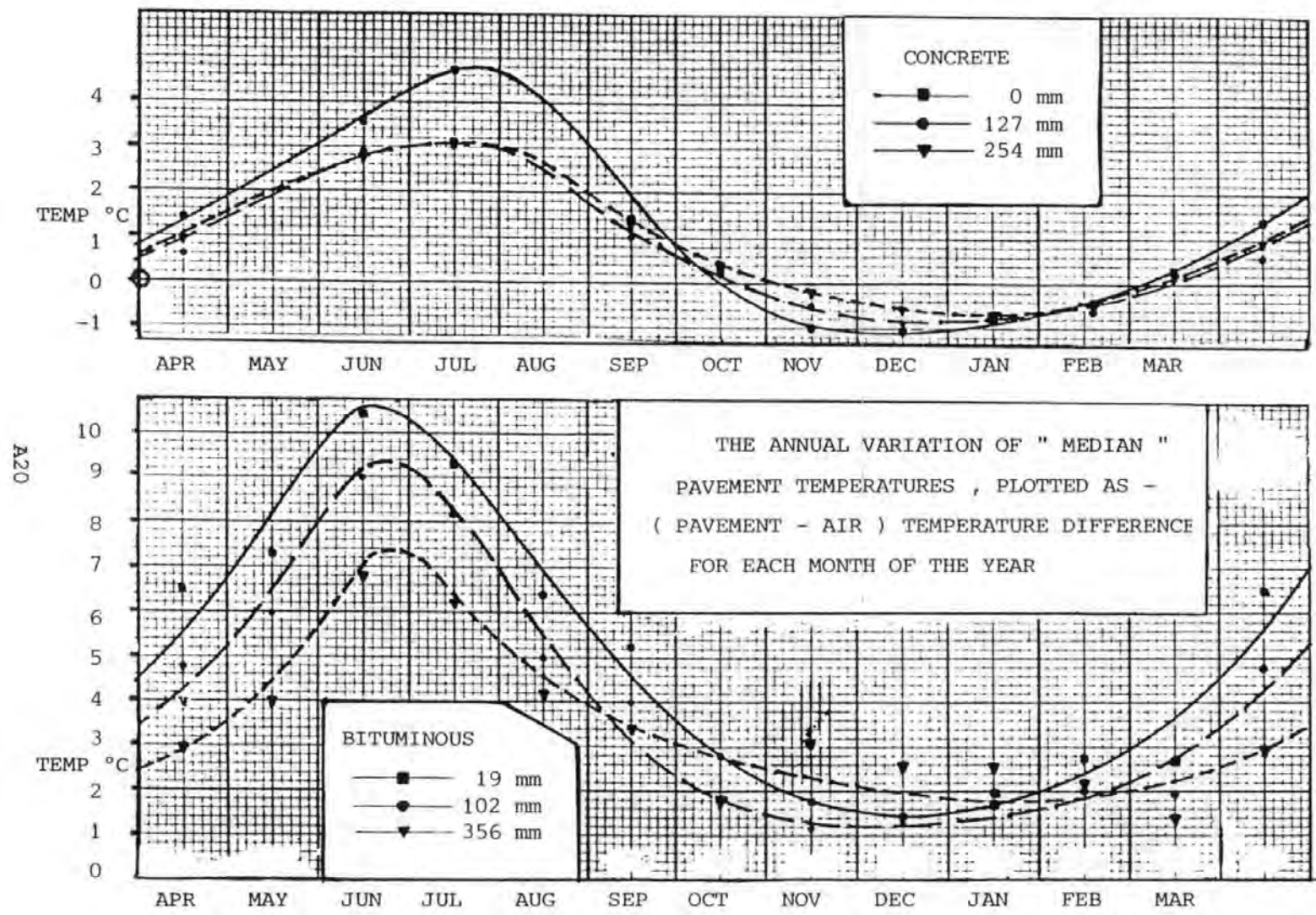


TABLE 3 . 2

"AVERAGE YEAR", "MEDIAN" PAVEMENT TEMPERATURES (°C) .

| MONTH | UK CENTRAL ZONE LONG TERM MEAN AIR TEMPERATURE | BITUMINOUS PAVEMENT TEMPERATURES AT DEPTHS | | | CONCRETE PAVEMENT TEMPERATURES AT DEPTHS | | |
|-------|--|---|-------|-------|---|-------|-------|
| | | 19mm | 102mm | 356mm | 0mm | 127mm | 254mm |
| JAN | 3.3 | 5.0 | 4.8 | 5.2 | 2.4 | 2.5 | 2.6 |
| FEB | 3.7 | 6.1 | 5.6 | 5.6 | 3.3 | 3.2 | 3.3 |
| MAR | 5.7 | 9.3 | 8.5 | 7.9 | 6.0 | 5.7 | 5.8 |
| APR | 8.5 | 14.1 | 12.8 | 11.4 | 9.8 | 9.3 | 9.5 |
| MAY | 11.3 | 19.4 | 17.8 | 15.7 | 13.7 | 13.3 | 13.2 |
| JUN | 14.4 | 24.9 | 23.4 | 21.1 | 18.0 | 17.3 | 17.2 |
| JUL | 16.0 | 25.3 | 24.2 | 22.2 | 20.7 | 18.9 | 19.1 |
| AUG | 15.6 | 22.4 | 21.1 | 20.2 | 19.6 | 17.8 | 18.2 |
| SEP | 14.0 | 18.6 | 17.2 | 17.5 | 15.6 | 15.1 | 15.3 |
| OCT | 10.2 | 13.0 | 12.0 | 13.0 | 10.2 | 10.3 | 10.6 |
| NOV | 6.6 | 8.4 | 7.9 | 9.0 | 5.6 | 6.1 | 6.4 |
| DEC | 4.5 | 6.0 | 5.7 | 6.6 | 3.4 | 3.7 | 3.9 |

The Daily Range of Pavement Temperature also varies considerably from month to month, which makes it difficult to consider the variation of (MEDIAN-MEAN) Temperatures in absolute terms, however a reasonable relationship should exist between -

(MEDIAN-MEAN) TEMPERATURE as % DAILY RANGE, and The Duration of the HUMP (TEMP>MEDIAN); hours.

Sample values for these quantities can be found for both BITUMINOUS and CONCRETE Pavements, from the TABULATED DAILY CYCLE, APPENDIX A , The data from periods with a subsidiary peak in the night-time was not used as it was difficult to decide on representative values for "MEDIAN" TEMPERATURE and the Daily Temp Range.

The Sample Data was Tabulated, TABLE 3.3 and plotted on a graph to illustrate the relationship. FIG 3.2..

The best-fit lines were obtained by Linear Regression, performed separately on the BITUMINOUS and CONCRETE pavement Data Points, with the following results.

| | Intercept | Slope | Correlation Coeff |
|------------|------------|---------|-------------------|
| BITUMINOUS | 11.930 hrs | - 0.336 | 0.885 |
| CONCRETE | 11.959 hrs | - 0.343 | 0.976 |

These two lines are almost coincident and can be combined as a single relationship to give values of (MEDIAN - MEAN) Temp as % Daily Range for both BITUMINOUS and CONCRETE Pavements.

$$(\text{MEDIAN} - \text{MEAN}) = \text{DAILY RANGE} \left(\frac{11.945 - H}{0.340 \times 100} \right) \text{ } ^\circ\text{C} \dots\dots\dots (3.1)$$

where H is the Duration of the Hump, (Temp > MED), in hours.

TABLE 3 . 3

SAMPLE DATA FOR COMPARISON OF -

THE DIFFERENCE BETWEEN "MEDIAN" AND MEAN TEMPERATURES AND THE DURATION OF THE HUMP (TEMP > "MEDIAN") IN THE DAILY CYCLE .

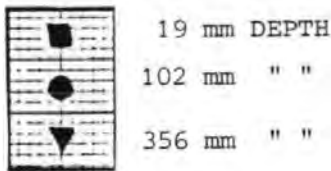
| MONTH | "MEDIAN" TEMP' °C | MEAN TEMP' °C | "MEDIAN" - MEAN TEMP' °C | DAILY TEMP' RANGE °C | "MEDIAN" - MEAN AS % RANGE | TIME AT "MEDIAN" TEMP' IN MORNING | TIME AT "MEDIAN" TEMP' IN EVENING | HUMP (H) HOURS |
|-------------------------------------|-------------------------|---------------------|--------------------------------|-------------------------------|-------------------------------------|--|--|------------------------|
| 19 mm DEPTH IN BITUMINOUS PAVEMENT | | | | | | | | |
| APR | 14.1 | 12.8 | 1.3 | 17.0 | 7.6 | 09,24 | 19,12 | 9.8 |
| JUL | 26.7 | 25.9 | 0.8 | 16.8 | 4.8 | 09,48 | 20,00 | 10.2 |
| OCT | 15.9 | 14.8 | 1.1 | 8.2 | 13.4 | 10,30 | 18,30 | 8.0 |
| 102 mm DEPTH IN BITUMINOUS PAVEMENT | | | | | | | | |
| APR | 12.4 | 12.0 | 0.4 | 11.2 | 3.6 | 10,48 | 21,48 | 11.0 |
| JUL | 25.6 | 25.1 | 0.5 | 10.8 | 4.6 | 11,36 | 21,24 | 9.8 |
| OCT | 14.85 | 14.4 | 0.45 | 5.7 | 7.9 | 11,12 | 20,18 | 9.1 |
| 356 mm DEPTH IN BITUMINOUS PAVEMENT | | | | | | | | |
| JAN | 6.15 | 6.1 | 0.05 | 0.5 | 10.0 | 17,00 | 00,30 | 7.5 |
| APR | 10.5 | 10.5 | 0.0 | 1.2 | - | 15,50 | 04,10 | 12.3 |
| JUL | 23.6 | 23.5 | 0.1 | 2.0 | 5.0 | 17,30 | 04,50 | 11.3 |
| OCT | 14.85 | 14.8 | 0.05 | 1.3 | 4.0 | 17,24 | 03,06 | 9.7 |
| 0 mm DEPTH IN CONCRETE PAVEMENT | | | | | | | | |
| JAN | 4.8 | 4.1 | 0.7 | 5.8 | 12.0 | 11,45 | 19,00 | 7.2 |
| APR | 8.5 | 8.1 | 0.4 | 8.4 | 4.8 | 09,45 | 20,18 | 10.5 |
| JUL | 22.75 | 22.6 | 0.15 | 11.1 | 1.4 | 09,24 | 20,54 | 11.5 |
| 127 mm DEPTH IN CONCRETE PAVEMENT | | | | | | | | |
| JAN | 4.8 | 4.6 | 0.2 | 2.7 | 7.0 | 12,45 | 22,21 | 9.6 |
| APR | 8.0 | 7.8 | 0.2 | 4.9 | 4.0 | 11,42 | 22,24 | 10.7 |
| JUL | 23.1 | 23.1 | 0.0 | 6.6 | 0.0 | 11,40 | 23,50 | 12.2 |
| 254 mm DEPTH IN CONCRETE PAVEMENT | | | | | | | | |
| JAN | 5.0 | 5.0 | 0.0 | 1.4 | 0.0 | 14,00 | 02,00 | 12.0 |
| APR | 8.3 | 8.2 | 0.1 | 3.0 | 3.3 | 13,36 | 00,30 | 10.9 |
| JUL | 23.5 | 23.6 | -0.1 | 4.0 | -2.5 | 13,48 | 02,00 | 12.2 |
| OCT | 11.2 | 11.1 | 0.1 | 1.0 | 10.0 | 13,00 | 22,00 | 9.0 |
| AIR TEMPERATURE | | | | | | | | |
| JAN | 5.0 | 4.3 | 0.7 | 8.0 | 8.8 | 11,21 | 20,33 | 9.2 |
| APR | 7.2 | 6.4 | 0.8 | 7.1 | 11.3 | 09,40 | 20,16 | 10.6 |

FIG 3 . 2

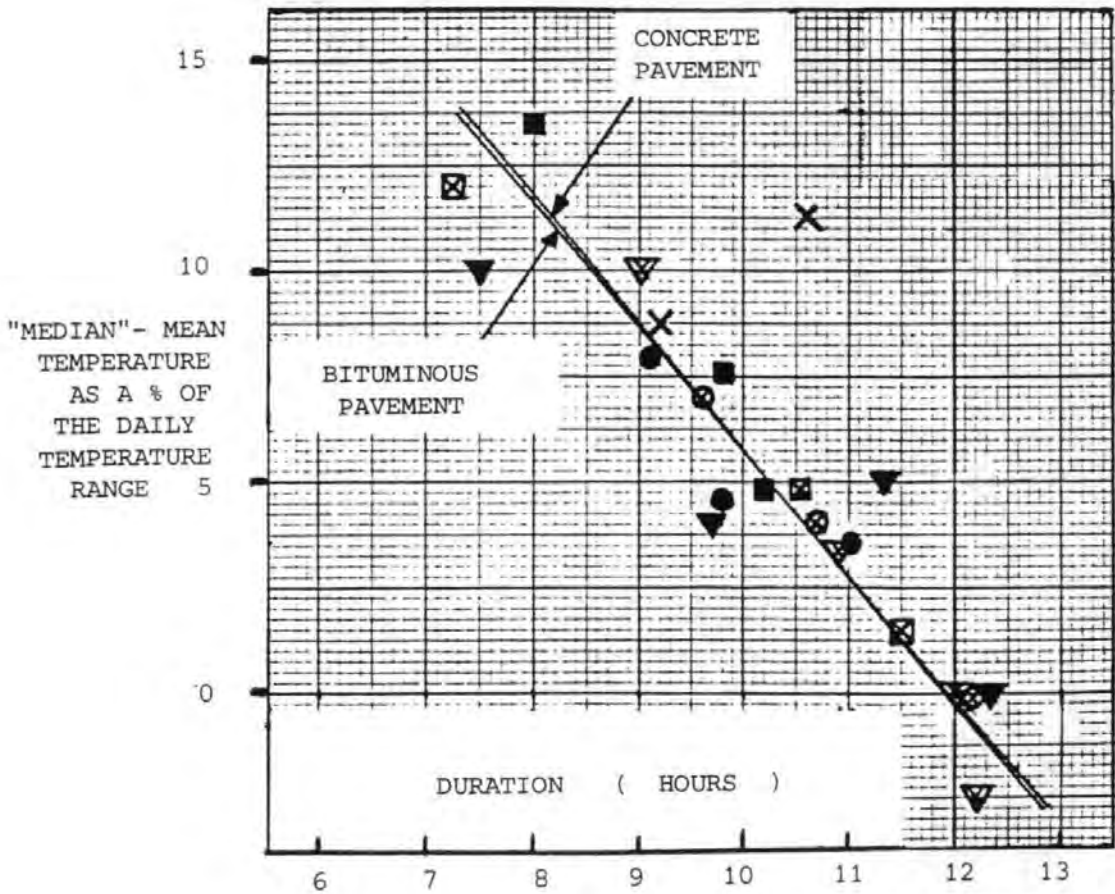
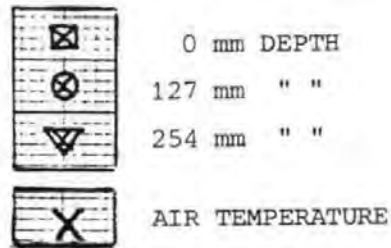
THE VARIATION OF ("MEDIAN " - MEAN) PAVEMENT TEMPERATURE WITH THE SHAPE OF THE DAILY CYCLE .

KEY TO SYMBOLS USED

BITUMINOUS
PAVEMENT



CONCRETE
PAVEMENT



DURATION OF THE HUMP IN THE DAILY CYCLE (WHEN THE TEMPERATURE IS GREATER THAN THE "MEDIAN") .

3.4 Correction from "MEDIAN" to MEAN temperatures

Values for H can be found for all months of the Year for BITUMINOUS Pavements(2) and for the months JAN/APR/JUL/OCT for CONCRETE Pavements(1). Again, the data can be graphed and re-tabulated to make it more representative of the Average Year. FIG 3.3 and TABLE 3.4.

Equation 3.1 above can now be used to give corresponding values of (MEDIAN - MEAN) Temperature for the Average Year, which can be used to correct Average Year MEDIAN Temperatures (TABLE 3.2) to MEAN temperatures, TABLE 3.5.

3.5 Comparison of MMPT for BITUMINOUS and CONCRETE Pavements

The BITUMINOUS and CONCRETE Data was recorded at different depths in the pavement. In order to make a direct comparison the Variation of MMPT with depth must be plotted and re-tabulated for both BITUMINOUS and CONCRETE PAVEMENTS at specified depths i.e. -

0/100/150/250/300 mm FIG 3.4 and TABLE 3.5 .

TABLE 3 . 4

THE DETERMINATION OF "AVERAGE YEAR" VALUES FOR THE DURATION OF THE HUMP (H) IN THE DAILY CYCLE AND ("MEDIAN" - MEAN) TEMPERATURE DIFFERENCES .

| BITUMINOUS PAVEMENT | | | | | | | CORRESPONDING | | |
|---------------------|---|-------|-------|--|-------|-------|-------------------------------------|-------|-------|
| MONTH | DURATION OF H, HOURS AT VARIOUS DEPTHS | | | "AVERAGE YEAR" VALUES FOR (H*) AT DEPTHS- | | | "MEDIAN - MEAN TEMP' DIFFERENCES | | |
| | 19mm | 102mm | 356mm | 19mm | 102mm | 356mm | 19mm | 102mm | 356mm |
| JAN | 10.5 | 18.5 | 7.5 | 7.1 | 8.5 | 10.0 | 0.3 | 0.1 | 0 |
| FEB | 7.0 | 8.7 | 17.0 | 7.6 | 9.0 | 10.3 | 0.7 | 0.3 | 0 |
| MAR | 8.2 | 9.3 | 9.5 | 8.4 | 9.6 | 10.7 | 1.0 | 0.4 | 0 |
| APR | 9.8 | 11.0 | 12.5 | 9.4 | 10.5 | 11.3 | 1.1 | 0.4 | 0 |
| MAY | 9.7 | 10.6 | 8.5 | 10.2 | 11.0 | 11.6 | 0.9 | 0.3 | 0 |
| JUN | 10.8 | 11.5 | 11.0 | 10.5 | 11.2 | 11.7 | 0.9 | 0.3 | 0 |
| JUL | 10.2 | 9.8 | 11.5 | 10.2 | 10.9 | 11.5 | 0.9 | 0.3 | 0 |
| AUG | 9.3 | 10.1 | 15.0 | 9.4 | 10.3 | 11.1 | 1.1 | 0.4 | 0 |
| SEP | 8.6 | 9.9 | 7.5 | 8.5 | 9.6 | 10.7 | 1.1 | 0.5 | 0 |
| OCT | 8.0 | 9.1 | 10.0 | 7.7 | 9.1 | 10.3 | 0.9 | 0.4 | 0 |
| NOV | 6.3 | 8.5 | 13.0 | 7.2 | 8.6 | 10.0 | 0.6 | 0.3 | 0 |
| DEC | 6.6 | 10.5 | 6.0 | 7.0 | 8.4 | 9.8 | 0.3 | 0.2 | 0 |

| CONCRETE PAVEMENT | | | | | | | | CORRESPONDING | | | | |
|-------------------|--|------|-------|-------|--|------|-------|---------------|-------------------------------------|-----|-------|-------|
| MONTH | DURATION OF H , HOURS AT VARIOUS DEPTHS | | | | "AVERAGE YEAR" VALUES FOR (H*) AT DEPTHS- | | | | "MEDIAN - MEAN TEMP' DIFFERENCES | | | |
| | AIR | 0mm | 127mm | 254mm | AIR | 0mm | 127mm | 254mm | AIR | 0mm | 127mm | 254mm |
| JAN | 9.2 | 7.3 | 9.6 | 12.0 | 9.0 | 8.7 | 9.6 | 10.0 | 0.3 | 0.3 | 0.1 | 0.1 |
| FEB | | | | | 9.2 | 9.0 | 9.7 | 10.1 | 0.4 | 0.4 | 0.2 | 0.1 |
| MAR | | | | | 9.8 | 9.6 | 10.2 | 10.6 | 0.4 | 0.5 | 0.2 | 0.1 |
| APR | 10.6 | 10.5 | 10.7 | 10.9 | 10.6 | 10.4 | 10.9 | 11.2 | 0.3 | 0.4 | 0.2 | 0.1 |
| MAY | | | | | 11.2 | 11.0 | 11.5 | 11.7 | 0.2 | 0.3 | 0.1 | 0 |
| JUN | | | | | 11.6 | 11.4 | 11.9 | 12.1 | 0.1 | 0.2 | 0 | 0 |
| JUL | | 11.5 | 12.2 | 12.2 | 11.7 | 11.5 | 12.0 | 12.2 | 0.1 | 0.1 | 0 | 0 |
| AUG | | | | | 11.4 | 11.2 | 11.7 | 12.0 | 0.2 | 0.2 | 0 | 0 |
| SEP | | | | | 10.8 | 10.6 | 11.1 | 11.5 | 0.3 | 0.3 | 0.1 | 0 |
| OCT | 9.8 | 11.0 | 10.5 | 9.0 | 10.2 | 9.9 | 10.5 | 10.9 | 0.4 | 0.4 | 0.1 | 0.1 |
| NOV | | | | | 9.6 | 9.2 | 10.0 | 10.4 | 0.4 | 0.4 | 0.1 | 0.1 |
| DEC | | | | | 9.1 | 8.8 | 9.7 | 10.1 | 0.4 | 0.3 | 0.1 | 0.1 |

* "AVERAGE YEAR" VALUES FOR H OBTAINED BY GRAPHING & RE-TABULATION (FIG 3 . 3)

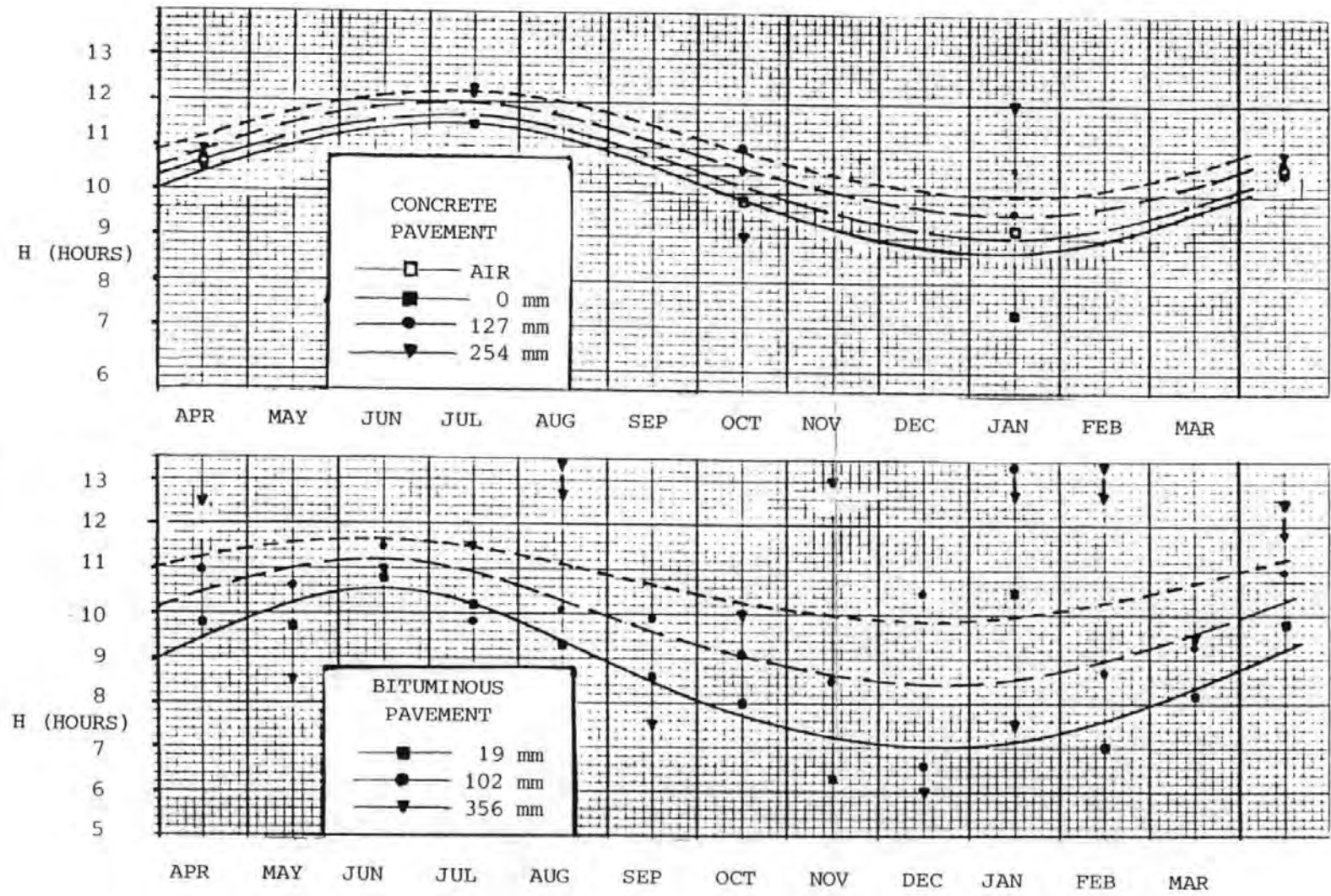


FIG 3 . 3
 THE ANNUAL VARIATION OF H , THE DURATION OF THE HUMP IN THE DAILY CYCLE OF PAVEMENT TEMPERATURE , AT SEVERAL DEPTHS .

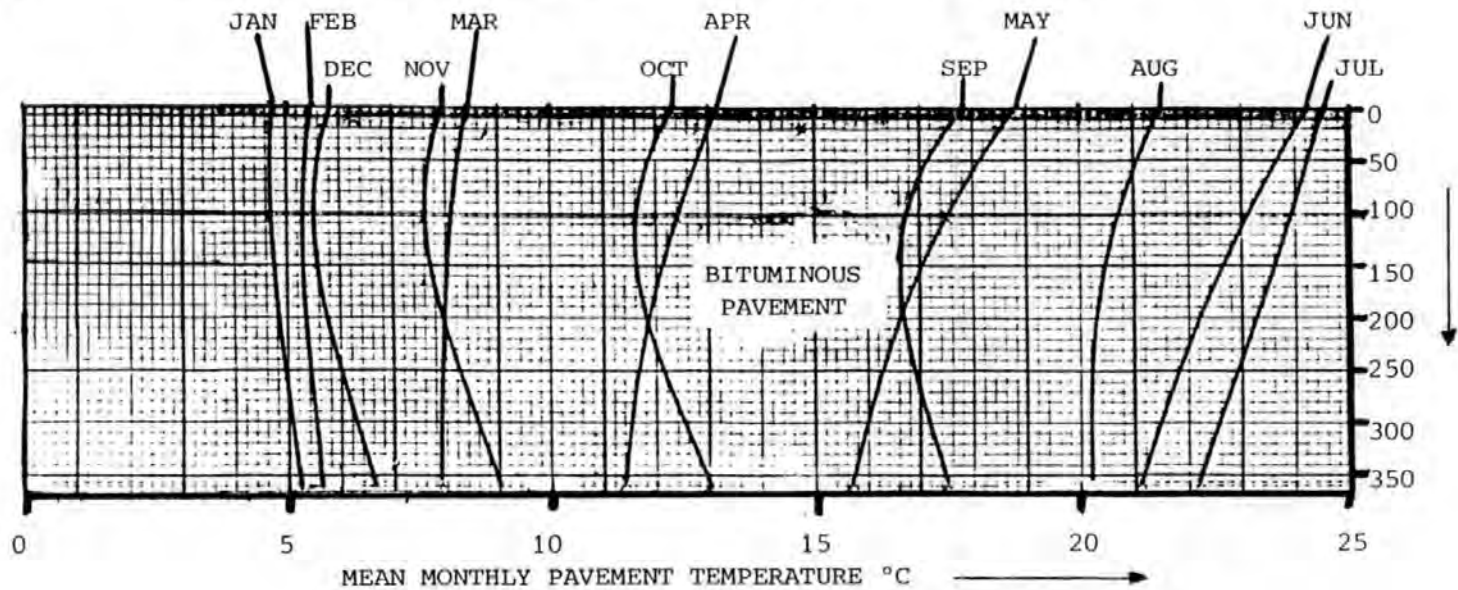
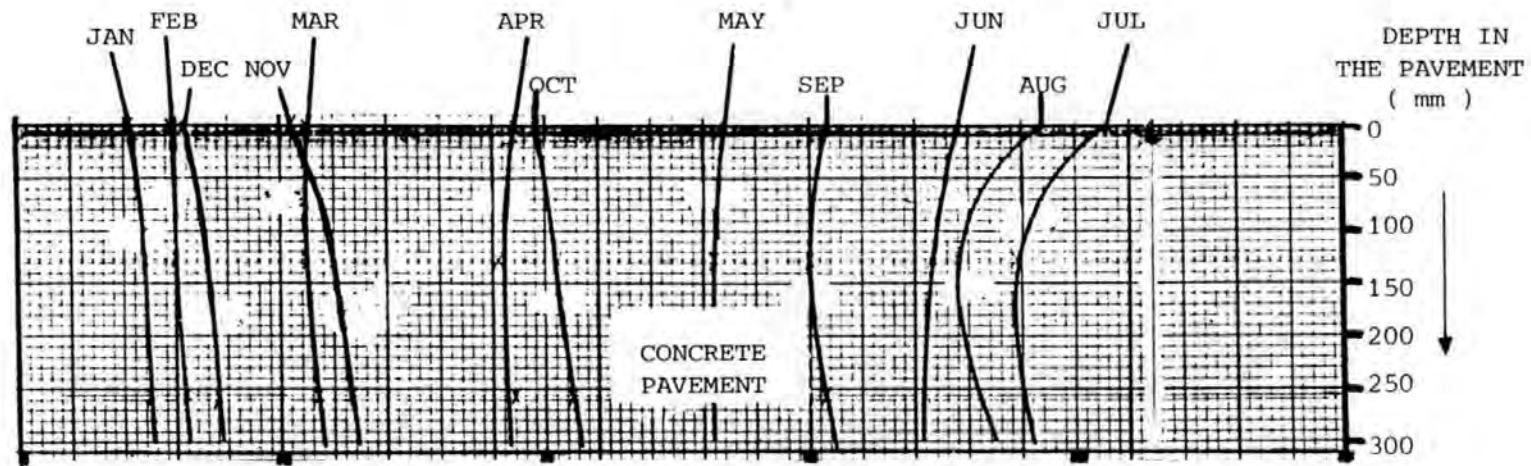
TABLE 3 . 5

"AVERAGE YEAR" MEAN PAVEMENT & AIR TEMPERATURES DETERMINED USING "MEDIAN"- MEAN TEMPERATURE DIFFERENCES (TABLE 3 . 4) .

| DEPTH IN THE PAVEMENT | MONTH OF THE YEAR | | | | | | | | | | | |
|-----------------------------|-------------------|-----|-----|------|------|------|------|------|------|------|-----|-----|
| | JAN | FEB | MAR | APR | MAY | JUN | JUL | AUG | SEP | OCT | NOV | DEC |
| BITUMINOUS PAVEMENT | | | | | | | | | | | | |
| 19mm | 4.7 | 5.4 | 8.3 | 13.0 | 18.5 | 24.0 | 24.4 | 21.3 | 17.5 | 12.1 | 7.8 | 5.7 |
| 102mm | 4.7 | 5.3 | 8.1 | 12.4 | 17.5 | 23.1 | 23.9 | 20.7 | 16.7 | 11.6 | 7.6 | 5.5 |
| 356mm | 5.2 | 5.6 | 7.9 | 11.4 | 15.7 | 21.1 | 22.2 | 20.2 | 17.5 | 13.0 | 9.0 | 6.6 |
| CONCRETE PAVEMENT | | | | | | | | | | | | |
| 0mm | 2.1 | 2.9 | 5.5 | 9.4 | 13.4 | 17.8 | 20.6 | 19.4 | 15.3 | 9.8 | 5.2 | 3.1 |
| 127mm | 2.4 | 3.0 | 5.5 | 9.1 | 13.2 | 17.3 | 18.9 | 17.8 | 15.0 | 10.2 | 6.0 | 3.6 |
| 254mm | 2.5 | 3.2 | 5.7 | 9.4 | 13.2 | 17.2 | 19.1 | 18.2 | 15.3 | 10.5 | 6.3 | 3.8 |
| AIR TEMPERATURE | | | | | | | | | | | | |
| | 3.0 | 3.3 | 5.3 | 8.2 | 11.1 | 14.3 | 15.9 | 15.4 | 13.7 | 9.8 | 6.2 | 4.1 |

MEAN PAVEMENT TEMPERATURES AT REGULAR DEPTHS OBTAINED BY GRAPHING AND RE-TABULATION (FIG 3 . 4) .

| | | | | | | | | | | | | |
|---------------------|-----|-----|-----|------|------|------|------|------|------|------|-----|-----|
| BITUMINOUS PAVEMENT | | | | | | | | | | | | |
| 0mm | 4.8 | 5.3 | 8.3 | 13.2 | 18.9 | 24.4 | 24.6 | 21.6 | 17.9 | 12.2 | 8.0 | 5.8 |
| 100mm | 4.7 | 5.3 | 8.1 | 12.4 | 17.5 | 23.1 | 23.9 | 20.7 | 16.8 | 11.6 | 7.6 | 5.5 |
| 150mm | 4.8 | 5.3 | 8.0 | 12.1 | 17.0 | 22.6 | 23.6 | 20.5 | 16.6 | 11.6 | 7.7 | 5.6 |
| 250mm | 4.9 | 5.4 | 7.9 | 11.7 | 16.3 | 21.8 | 22.9 | 20.2 | 16.9 | 12.1 | 8.3 | 6.0 |
| 300mm | 5.1 | 5.5 | 7.9 | 11.5 | 16.0 | 21.5 | 22.6 | 20.2 | 17.2 | 12.5 | 8.6 | 6.3 |
| CONCRETE PAVEMENT | | | | | | | | | | | | |
| 0mm | 2.2 | 2.9 | 5.5 | 9.4 | 13.4 | 17.8 | 20.7 | 19.5 | 15.4 | 9.9 | 5.3 | 3.1 |
| 100mm | 2.3 | 3.0 | 5.5 | 9.2 | 13.2 | 17.4 | 19.1 | 18.0 | 15.0 | 10.1 | 5.9 | 3.6 |
| 150mm | 2.4 | 3.0 | 5.5 | 9.2 | 13.2 | 17.3 | 18.9 | 17.8 | 15.0 | 10.2 | 6.1 | 3.7 |
| 250mm | 2.5 | 3.2 | 5.7 | 9.3 | 13.2 | 17.2 | 19.0 | 18.2 | 15.3 | 10.5 | 6.3 | 3.8 |
| 300mm | 2.5 | 3.2 | 5.8 | 9.3 | 13.2 | 17.2 | 19.2 | 18.5 | 15.5 | 10.6 | 6.4 | 3.9 |



THE VARIATION OF MEAN MONTHLY PAVEMENT TEMPERATURE WITH DEPTH IN BITUMINOUS AND CONCRETE PAVEMENTS .

FIG 3 . 4

4 HOURLY TEMP PROFILES

4.1 Adjustment of Tabulated Data

The Average Year Values of Daily Temp Range and MMPT can now be used to adjust the Tabulated Daily Cycle of Pavement Temperature at 3 Depths in BITUMINOUS and CONCRETE Pavements, APPENDIX A .

A Table of correction differences for MMPT and correction factors for Daily Temp Range was drawn up, TABLE 4.1, to correct the Tabulated Data as it was plotted to give the HOURLY TEMP PROFILES, APPENDIX B, except for the JANUARY Data for BITUMINOUS Pavements —

For each of the WINTER MONTHS (NOV - MAR), the Daily Cycle of Pavement Temperature at a depth of 19 mm was plotted, (2). FIG 4.1

It can be seen that the Data for JANUARY is not very representative of the WINTER MONTHS in terms of the Shape of the cycle as it includes a subsidiary peak during the nighttime which is even greater than that in the daytime.

In view of this, it was decided to replace the JANUARY DATA (for all 3 Depths) by the mean of the DECEMBER and FEBRUARY DATA, with the amplitude of each reduced to JANUARY levels before averaging, because the peaks and troughs of the 2 curves did not coincide exactly, the amplitude of the resulting DEC/FEB mean data still had to be adjusted slightly in order to correspond to Average Year Values for JANUARY.

TABLE 4 . 1

ADJUSTMENT OF THE DAILY CYCLE OF PAVEMENT TEMPERATURE TO CORRESPOND TO AN "AVERAGE YEAR" .

MEAN MONTHLY PAVEMENT TEMPERATURE : THESE DIFFERENCES MUST BE ADDED TO EACH TEMPERATURE READING OF THE TABULATED DAILY CYCLE , APPENDIX A , SO THAT MMPT'S WILL CORRESPOND TO "AVERAGE YEAR" VALUES .

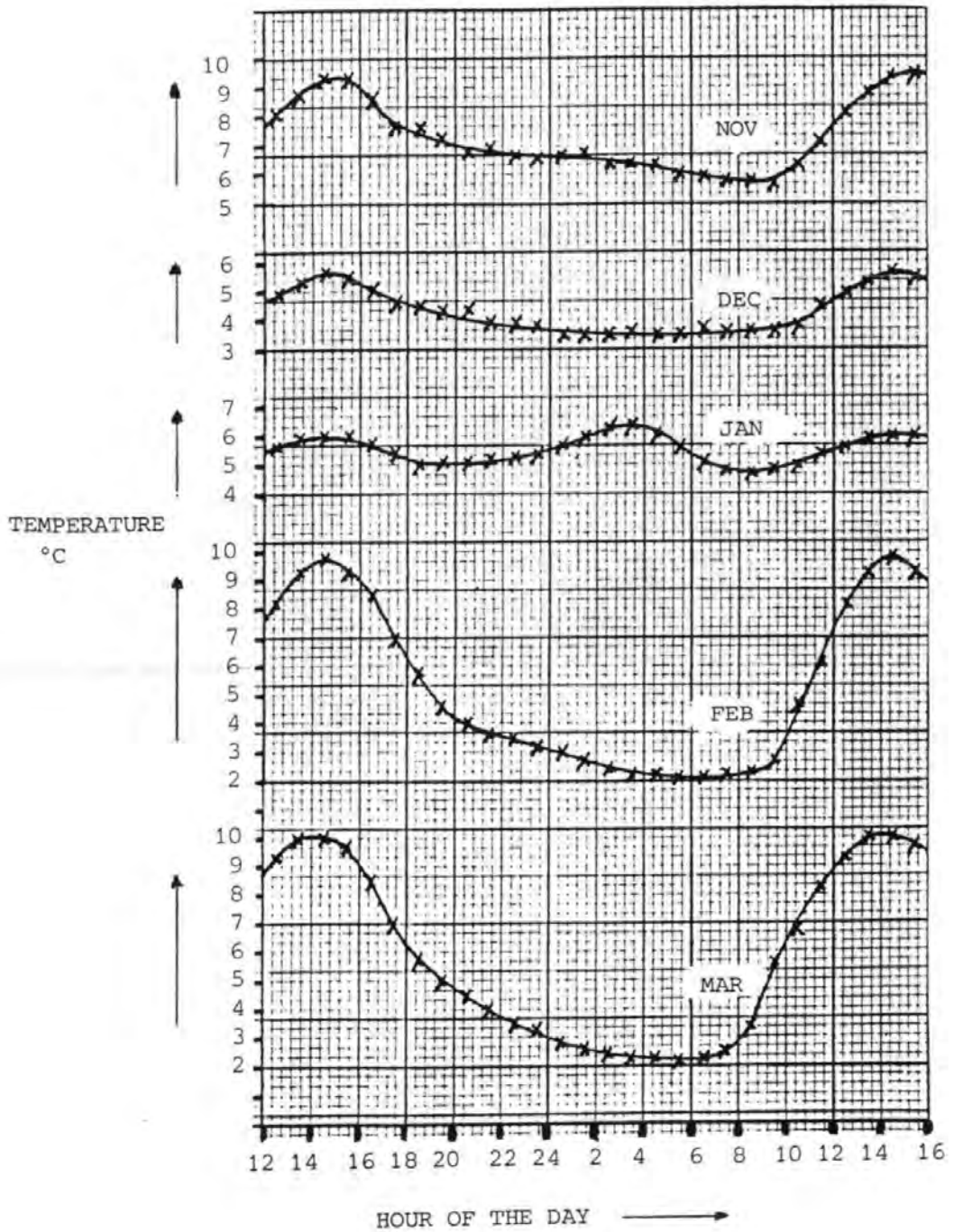
| MONTH | MEAN TEMPERATURE FOR TABULATED DAILY CYCLE AT DEPTHS (mm) | | | "AVERAGE YEAR" MEAN PAVEMENT TEMPERATURE (TABLE 3 . 5) | | | DIFFERENCE °C | | |
|-------|---|-------|-------|--|-------|-------|---------------|-------|-------|
| | BITUMINOUS PAVEMENT | | | | | | | | |
| | 19mm | 102mm | 356mm | 19mm | 102mm | 356mm | 19mm | 102mm | 356mm |
| JAN | 5.5 | 5.4 | 6.1 | 4.7 | 4.7 | 5.2 | -0.8 | -0.7 | -0.9 |
| APR | 12.8 | 12.0 | 10.5 | 13.0 | 12.4 | 11.4 | 0.2 | 0.4 | 0.9 |
| JUL | 25.9 | 25.1 | 23.5 | 24.4 | 23.9 | 22.2 | -1.5 | -1.2 | -1.3 |
| OCT | 14.8 | 14.4 | 14.8 | 12.1 | 11.6 | 13.0 | -2.7 | -2.8 | -1.8 |
| | CONCRETE PAVEMENT | | | | | | | | |
| | 0mm | 127mm | 254mm | 0mm | 127mm | 254mm | 0mm | 127mm | 254mm |
| JAN | 4.1 | 4.6 | 5.0 | 2.1 | 2.4 | 2.5 | -2.0 | -2.2 | -2.5 |
| APR | 8.1 | 7.8 | 8.2 | 9.4 | 9.1 | 9.4 | 1.3 | 1.3 | 1.2 |
| JUL | 22.6 | 23.1 | 23.6 | 20.6 | 18.9 | 19.1 | -2.0 | -4.2 | -4.5 |
| OCT | 10.9 | 10.9 | 11.1 | 9.8 | 10.2 | 10.5 | -1.1 | -0.7 | -0.6 |

DAILY TEMPERATURE RANGE : THE DEVIATION OF EACH TEMPERATURE READING OF THE TABULATED DAILY CYCLE , APPENDIX A , MUST BE INCREASED BY THIS FACTOR , SO THAT DAILY TEMP' RANGES WILL CORRESPOND TO THE "AVERAGE YEAR" VALUES .

| MONTH | DAILY TEMP' RANGE FOR TABULATED DAILY CYCLE AT DEPTHS (mm) | | | "AVERAGE YEAR" VALUE FOR DAILY TEMPERATURE RANGE (TABLE 2) | | | CORRECTION FACTOR | | |
|-------|--|-------|-------|--|-------|-------|-------------------|-------|-------|
| | BITUMINOUS PAVEMENT | | | | | | | | |
| | 19mm | 102mm | 356mm | 19mm | 102mm | 356mm | 19mm | 102mm | 356mm |
| JAN | 1.3 | 1.0 | 0.5 | 2.1 | 1.3 | 0.4 | 1.62 | 1.30 | 0.80 |
| APR | 17.0 | 11.2 | 1.2 | 14.3 | 9.6 | 1.4 | 0.84 | 0.86 | 1.17 |
| JUL | 16.8 | 10.8 | 2.0 | 17.6 | 11.1 | 2.0 | 1.05 | 1.03 | 1.00 |
| OCT | 8.2 | 5.7 | 1.3 | 7.3 | 4.9 | 0.9 | 0.89 | 0.86 | 0.73 |
| | CONCRETE PAVEMENT | | | | | | | | |
| | 0mm | 127mm | 254mm | 0mm | 127mm | 254mm | 0mm | 127mm | 254mm |
| JAN | 5.8 | 2.7 | 1.4 | 3.5 | 2.0 | 1.2 | 0.60 | 0.74 | 0.86 |
| APR | 8.4 | 4.9 | 3.0 | 9.0 | 5.2 | 3.0 | 1.07 | 1.06 | 1.00 |
| JUL | 11.1 | 6.6 | 4.0 | 10.9 | 6.0 | 3.7 | 0.98 | 0.91 | 0.93 |
| OCT | 3.1 | 1.6 | 1.0 | 5.9 | 2.9 | 2.1 | 1.69 | 1.61 | 2.10 |

FIG 4 . 1

THE DAILY CYCLE OF PAVEMENT TEMPERATURE DURING THE WINTER MONTHS
AT DEPTH , 19 mm , IN A BITUMINOUS PAVEMENT .



4.2 Plotting of HOURLY TEMP PROFILES

The Hourly Temp Profiles were plotted as a series of best-fit curves for the adjusted Tabulated Data with the aid of the following assumptions.

- i) there is a smooth progression of the shape of the hourly curve (Isochrone) from each hour to the next.
- ii) The Area on the profile represents Heat Stored in the pavement, there should be a smooth progression of the change in stored Heat in the pavement from hour to hour, i.e. of the area between subsequent Isochrones.

The Resulting Profiles, APPENDIX B, are somewhat idealised in that they assume this smooth build-up of Heat in the pavement during the day, whilst in reality, Intermittant Cloud Cover and a Cooling Breeze would result in a stepped build up at the surface, becoming smoother at greater depths.

Thus the changes in the Thermal Stresses in the Pavement may be significantly more rapid at times, than implied by the Profiles, and this may affect the degree of stress relief by creep in Bituminous Materials.

4.3 Observations from Hourly Temp Profiles

When the BITUMINOUS and CONCRETE Hourly Temp Profiles are plotted adjacent to each other it can be seen that for all months, at depths of c350mm, the Temperature Range is greater with CONCRETE Pavements.

At the surface however, the Temperature Range is greater with BITUMINOUS Pavements for the months APR/JUL and OCT.

This indicates that the attenuation of Temperature Range with depth is significantly greater with BITUMINOUS Pavements. The comparison can be extended to all months by considering the variation of Temp Range with Depth, FIG 2.2, from which the attenuation of Temperature Range with Depth can be found for all months. TABLE 4.2

It can be seen that Temperature Ranges are Greater with CONCRETE for the following months at Depths -

| | |
|------------|---|
| 0 - 200 mm | JAN, DEC |
| 250 mm | JAN, FEB, NOV, DEC |
| 300 mm | JAN, FEB, MAR, JUL, AUG, SEP, OCT, NOV, DEC |

This Temperature Range is due to a combination of Surface Absorption of Solar Energy and Heat Transfer between the air and the pavement surface. The Surface Absorption is almost certainly greater at all times with BITUMINOUS PAVEMENTS, thus Heat Transfer effects must be significant in the Winter months in order to explain the greater ranges in CONCRETE at all depths during DEC, JAN.

The greater temp range in CONCRETE at lower depths during most of the year is a result of the greater attenuation of Temp Range with depth in BITUMINOUS Pavements which implies that thermal conductivity is lower for BITUMINOUS than for CONCRETE materials.

4.4 Thermal Conductivity

This conclusion that Thermal Conductivity is lower for BITUMINOUS

TABLE 4 . 2

"AVERAGE YEAR" DAILY TEMPERATURE RANGES AT REGULAR DEPTHS , OBTAINED BY GRAPHING AND RETABULATION (FIG 2 . 2),AND THE ATTENUATION OF DAILY TEMPERATURE RANGE WITH DEPTH .

DAILY TEMPERATURE RANGE (°C)

| DEPTH IN THE PAVEMENT | MONTH OF THE YEAR | | | | | | | | | | | |
|-----------------------------|-------------------|-----|-----|-----|-----|-----|-----|-----|-----|-----|-----|-----|
| | JAN | FEB | MAR | APR | MAY | JUN | JUL | AUG | SEP | OCT | NOV | DEC |

BITUMINOUS PAVEMENT

| | | | | | | | | | | | | |
|-------|-----|-----|------|------|------|------|------|------|------|-----|-----|-----|
| 0mm | 2.4 | 5.8 | 10.8 | 15.5 | 20.3 | 23.3 | 19.5 | 15.5 | 11.6 | 8.0 | 4.3 | 2.0 |
| 50mm | 1.8 | 4.4 | 8.5 | 12.4 | 15.7 | 17.7 | 14.9 | 12.0 | 9.1 | 6.3 | 3.6 | 1.7 |
| 100mm | 1.3 | 3.2 | 6.6 | 9.7 | 12.0 | 13.1 | 11.2 | 9.1 | 7.0 | 5.0 | 3.1 | 1.5 |
| 150mm | 1.0 | 2.4 | 4.9 | 7.3 | 8.8 | 9.6 | 8.3 | 6.8 | 5.3 | 3.8 | 2.5 | 1.2 |
| 200mm | 0.7 | 1.7 | 3.5 | 5.3 | 6.5 | 7.1 | 6.1 | 5.0 | 3.8 | 2.8 | 2.0 | 1.0 |
| 250mm | 0.6 | 1.2 | 2.4 | 3.7 | 4.6 | 5.1 | 4.5 | 3.6 | 2.8 | 2.0 | 1.5 | 0.7 |
| 300mm | 0.4 | 0.9 | 1.6 | 2.5 | 3.1 | 3.6 | 3.1 | 2.5 | 2.0 | 1.4 | 1.0 | 0.5 |

CONCRETE PAVEMENT

| | | | | | | | | | | | | |
|-------|------|------|------|-----|------|------|------|------|------|------|------|------|
| 0mm | 3.5* | 4.3 | 6.6 | 9.0 | 11.2 | 12.2 | 10.9 | 9.2 | 7.5 | 5.9 | 4.5* | 3.5* |
| 50mm | 2.8* | 3.5 | 5.1 | 7.2 | 9.1 | 9.7 | 8.6 | 7.2 | 5.8 | 4.3 | 3.4 | 2.8* |
| 100mm | 2.2* | 2.7 | 3.9 | 5.8 | 7.3 | 7.7 | 6.8 | 5.6 | 4.4 | 3.3 | 2.6 | 2.1* |
| 150mm | 1.8* | 2.1 | 3.1 | 4.7 | 5.8 | 6.1 | 5.4 | 4.5 | 3.5 | 2.7 | 2.1 | 1.7* |
| 200mm | 1.4* | 1.7 | 2.5 | 3.8 | 4.6 | 4.9 | 4.4 | 3.7 | 3.0 | 2.3 | 1.8 | 1.4* |
| 250mm | 1.2* | 1.4* | 2.0 | 3.1 | 3.7 | 3.9 | 3.7 | 3.2 | 2.6 | 2.1* | 1.6* | 1.3* |
| 300mm | 1.0* | 1.2* | 1.8* | 2.5 | 3.0 | 3.3 | 3.2* | 2.9* | 2.4* | 1.9* | 1.5* | 1.2* |

THE ATTENUATION OF DAILY TEMPERATURE RANGE WITH DEPTH IN THE PAVEMENT (% RANGE AT THE SURFACE)

BITUMINOUS PAVEMENT

| | | | | | | | | | | | | |
|-------|----|----|----|----|----|----|----|----|----|----|----|----|
| 50mm | 75 | 76 | 79 | 80 | 77 | 76 | 77 | 77 | 78 | 79 | 84 | 85 |
| 100mm | 54 | 55 | 61 | 63 | 59 | 64 | 57 | 59 | 60 | 63 | 72 | 75 |
| 150mm | 42 | 41 | 45 | 47 | 43 | 47 | 43 | 44 | 46 | 47 | 58 | 60 |
| 200mm | 29 | 29 | 32 | 34 | 32 | 30 | 31 | 32 | 33 | 35 | 47 | 50 |
| 250mm | 25 | 21 | 22 | 24 | 23 | 22 | 23 | 23 | 24 | 25 | 35 | 35 |
| 300mm | 17 | 16 | 15 | 16 | 15 | 18 | 16 | 16 | 17 | 18 | 23 | 25 |

CONCRETE PAVEMENT

| | | | | | | | | | | | | |
|-------|----|----|----|----|----|----|----|----|----|----|----|----|
| 50mm | 80 | 81 | 77 | 80 | 81 | 80 | 79 | 78 | 77 | 73 | 76 | 80 |
| 100mm | 63 | 63 | 59 | 64 | 65 | 63 | 62 | 61 | 59 | 56 | 58 | 60 |
| 150mm | 51 | 49 | 47 | 52 | 52 | 50 | 50 | 49 | 47 | 46 | 47 | 49 |
| 200mm | 40 | 40 | 38 | 42 | 41 | 40 | 40 | 40 | 40 | 39 | 40 | 40 |
| 250mm | 34 | 33 | 30 | 34 | 33 | 32 | 34 | 35 | 35 | 36 | 36 | 37 |
| 300mm | 29 | 28 | 27 | 28 | 27 | 27 | 29 | 32 | 32 | 32 | 33 | 34 |

* DAILY TEMPERATURE RANGE GREATER IN CONCRETE PAVEMENT THAN IN BITUMINOUS PAVEMENT .

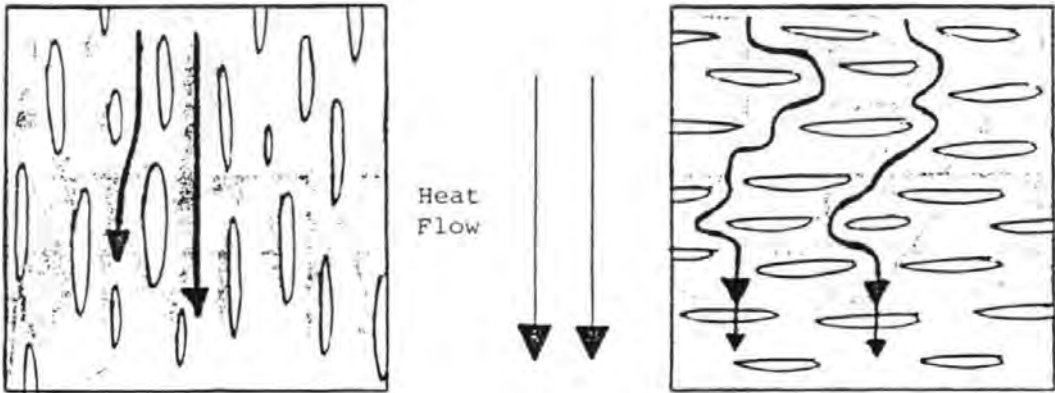
Materials is in contrast to values quoted by some reference works (3)

i.e. 0.84 Btu/(hr)(ft²)(°F)(ft) for BITUMINOUS concrete
& 0.54 Btu/(hr)(ft²)(°F)(ft) for PORTLAND CEMENT concrete

However, there are several factors which could influence the thermal conductivity of PAVEMENT MATERIALS i.e.

1) The comparatively, much lower thermal conductivity of Air (0.014) will mean that the presence of even a small volume fraction of air voids, if inconveniently orientated with respect to HEAT FLOW, could significantly influence the bulk value for the material, i.e. -

by being effectively in Series, rather than in Parallel with the Pavement Material.



AIR VOIDS
IN PARALLEL

AIR VOIDS
IN SERIES

This is likely to happen with Vertical Heat Flow in Materials Compacted Horizontally by Rolling.

2) The Bitumen/Asphalt will undergo significant changes in state over the normal climatic range of temperature and this must also affect its Thermal Conductivity.

These factors will make it difficult to determine reliable experimental values for the Thermal Conductivity of Pavement Materials, which incidentally, adds justification to the use of an empirical Temperature Model based on Actual measurements, rather than a mathematically derived one using Surface Absorption Coefficients and Thermal Conductivity.

There are also other observations from the HOURLY TEMP PROFILES; such as the more pronounced "bunching" of the Isochrones for BITUMINOUS Pavements during the nighttime, despite the greater Temperature Gradients across the Pavement which indicate greater Insulation Properties, and thus lower thermal conductivity for BITUMINOUS Materials.

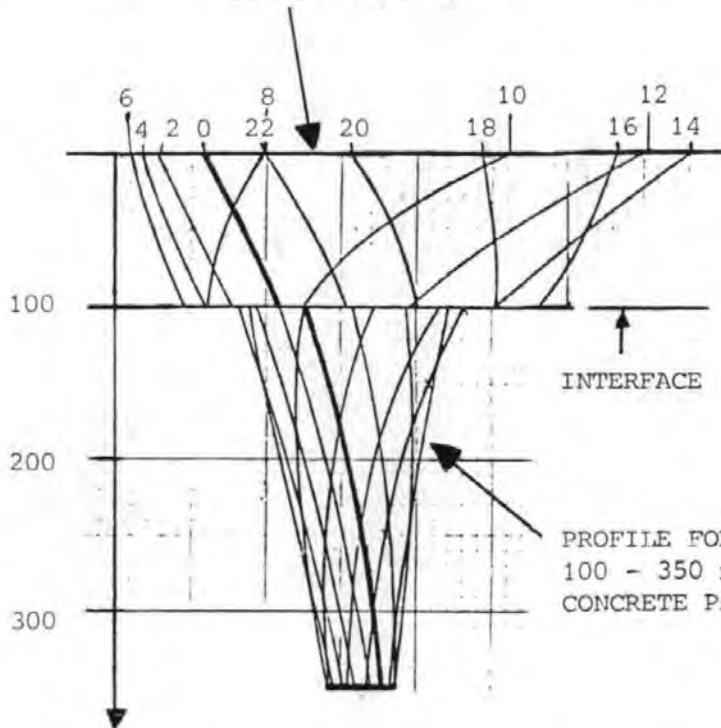
4.5 Deducing COMPOSITE Pavement Hourly Temp Profiles

The main assumption to be used in deducing Hourly Temp Profiles for composite pavements is that Temperature Gradients are similar at all hours of the day -

- | | | |
|---|---|--|
| (i) In the Surfacing Layer of a COMPOSITE pavement | & | In the Surfacing Layer of a BITUMINOUS Pavement |
| (ii) In the Roadbase Layer of a COMPOSITE pavement | & | In the Roadbase Layer of a CONCRETE Pavement |

Thus, the HOURLY TEMP PROFILE for a COMPOSITE Pavement, comprising 100 mm BITUMINOUS Surfacing and c 200 mm LEAN CONCRETE Roadbase, can be crudely approximated by combining that for 0 - 100 mm BITUMINOUS Pavement with that for 100 mm + CONCRETE Pavement.

PROFILE FOR DEPTHS 0-100 mm IN A
BITMINOUS PAVEMENT



It can be seen that there is a broad general agreement between the trends of the Isochrones either side of the interface.

PROFILE FOR DEPTHS
100 - 350 mm IN A
CONCRETE PAVEMENT

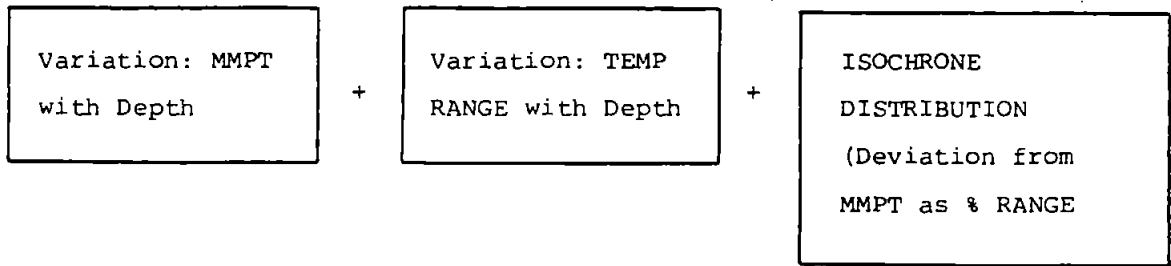
DEPTH IN THE
PAVEMENT (mm)

THE "CRUDE" COMPOSITE PAVEMENT
BI-HOURLY TEMPERATURE / DEPTH
PROFILE FOR APRIL

In order to maintain continuity at a depth of 100 mm, both sections of this crude profile will have to be adjusted.

- i) The upper and lower sections will have to be expanded/contracted laterally so that the Temperature Range at 100 mm will be equal in both.
- ii) Even then, the position of Individual Isochrones within the profiles may have to be adjusted in order to match the two halves at the Interface.

This adjustment can best be done by splitting the Information contained in the profiles into 3 Components.



The relevant values of each component for COMPOSITE Pavements can then be deduced independently, by COMPARING/MATCHING the BITUMINOUS x CONCRETE pavement data.

The 3 Components can then be re-combined to give HOURLY TEMP PROFILES for COMPOSITE Pavements.

5 Matching of ISOCHRONE DISTRIBUTIONS

The ISOCHRONE DISTRIBUTION is also a function of depth in the pavement, x , and the hour of the day, h .

For the purposes of calculating the ISOCHRONE DISTRIBUTIONS, the relevant sections of the APR/JUL/OCT/JAN HOURLY TEMP PROFILES were retabulated, in terms of the Deviation of each Hourly Temp Reading from the MMPT at a Depth of 100 mm. i.e.

At Depths, 0/50/100 mm for BITUMINOUS Pavements

& At Depths, 100/150/300 mm for CONCRETE Pavements

The MMPTs for the retabulated data at these depths were then calculated, also in terms of the Deviation from the MMPT at 100 mm.

5.1 Comparison of BITUMINOUS and CONCRETE ID's

The ID's were calculated using each hourly Temp Reading $T(x, h)$ and the equation.

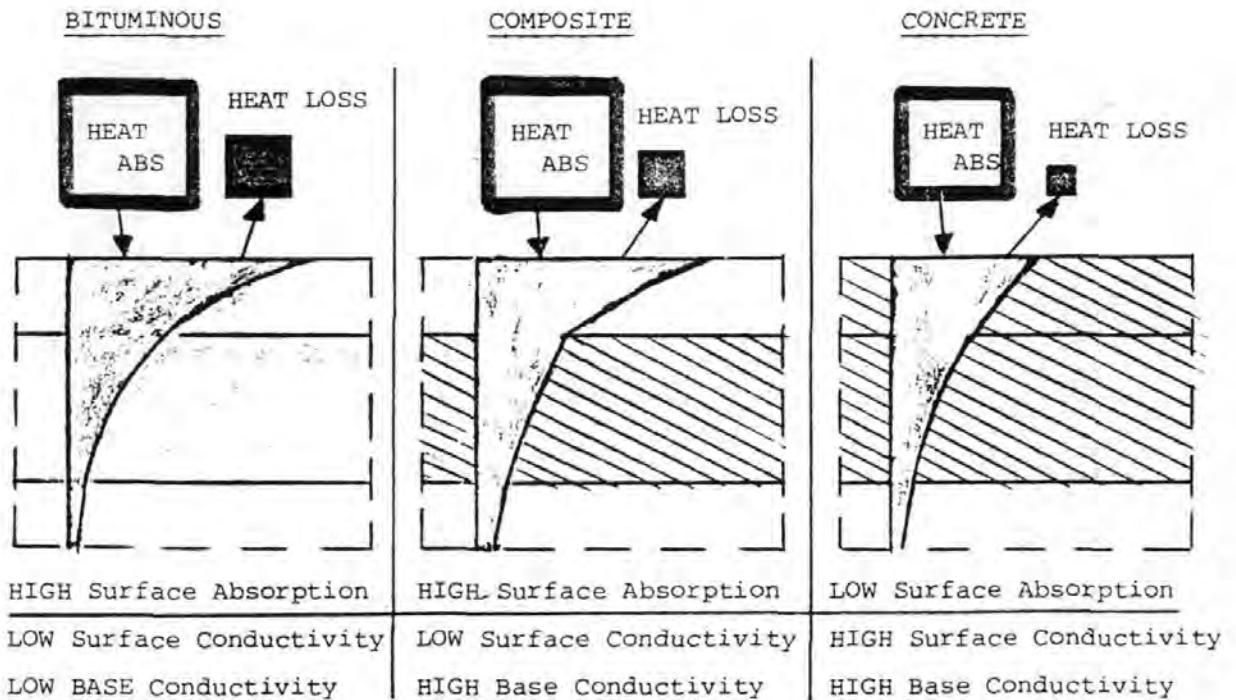
$$ID(x, h) = \left(\frac{T(x, h) - MMPTx}{\text{Daily Temp Range } x} \right) \times 100\% \quad \text{----- (5.1)}$$

These two sections of the BITUMINOUS and CONCRETE Pavement ID's together comprise the crude (unmatched) COMPOSITE Pavement ID. They are Tabulated together for each month JAN/APR/JUL/OCT, APPENDIX C , so as to illustrate the magnitude of the difference at the interface (DI) that must be resolved by matching.

5.2 Thermal Properties of Pavement Materials

The knowledge of relative thermal properties of Pavement Materials can now be used to formulate a Hypothesis for matching the upper and lower sections of the Isochrone Distribution.

Consider the 3 types of Pavement Warming up during the morning from the idealised situation of Zero Temperature Gradient across the pavement at Dawn.



5.3 Comparisons of Thermal Behaviour of Pavements

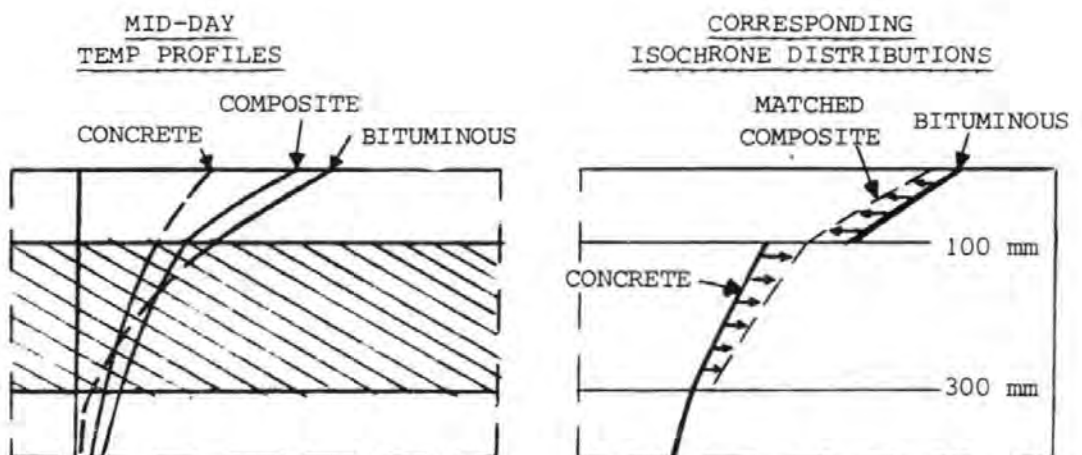
i) COMPOSITE and BITUMINOUS : The Surface Absorption is the same, but HEAT CONDUCTION through to the lower layers is more rapid with COMPOSITE Pavements, resulting in lower surface temperatures and thus less HEAT LOSS to the air. This in turn, implies a greater HEAT GAIN for the Pavement which implies greater temperature gradients across the surfacing to generate this greater HEAT FLOW.

ii) COMPOSITE and CONCRETE : The COMPOSITE pavement has greater Surface Heat Absorption, some of the excess will be lost as greater HEAT LOSS to the air but the bulk will remain in the pavement implying; greater Temperature Gradients and Pavement Temperatures at all depths.

i.e. for both layers of a COMPOSITE Pavement, both Temperature Gradients and Layer Extremity Temperatures will differ slightly from the values for full-depth construction with the component materials.

5.4 Hypothesis for Matching ISOCHRONES

The "mid-day" Temperature Profiles from this warming of the Pavement can be compared directly.



The following hypothesis was deduced, where the following proportions of the Difference at the Interface (DI) are used as correction factors to give ID comp from ID bit and ID conc, at the various depths in the pavement.

| Depth in Pavement | ID comp = |
|-------------------|---------------------|
| 0 mm | ID bit - 0.25 DI |
| 50 mm | ID bit - 0.375 DI |
| 100 mm | ID bit - 0.5 DI |
| | |
| " | or ID conc + 0.5 DI |
| 150 mm | ID conc + 0.44 DI |
| 300 mm | ID conc + 0.25 DI |

whereby the difference is resolved as -

25% BITUMINOUS Layer TEMP GRADIENT Adjustment
 + 25% " " SURFACE TEMP "
 + 25% CONCRETE " TEMP GRADIENT "
 + 25% " " BASE TEMP "

It can be seen from 5.3 that the difference will be a mixture of these four quantities. The exact proportions are difficult to define and so a 25/25/25/25 split was decided on as the best approximation.

These differences in terms of °C are small anyway and so errors introduced by this assumption will be even smaller.

5.5 INTERPOLATION OF IDs for the other months

This, and the subsequent conversion of IDs into COMPOSITE PAVEMENT Hourly Temp Profiles is best done by a computer program.

6 COMPOSITE Pavement MMPT's

COMPOSITE Pavement MMPT's for all months of the year and for depths of 0/50/100/150 x 300 mm, need to be ascertained as part of the procedure for converting the ISOCHRONE DISTRIBUTIONS (ID) back into HOURLY TEMP PROFILES.

It is the variation of MMPT with Depth that is responsible for the "TWIST" in the tail of the Hourly Temp Profiles, which significantly influences Temp Gradients in the Roadbase Layer.

6.1 The LRL38 COMPARISON

From 1961-6, an experiment was conducted at TRRL to investigate the Duration of Temperature Levels throughout the year in both

FULL-DEPTH (14") BITUMINOUS Pavements, and
COMPOSITE (4":10") BITUMINOUS/LEAN CONCRETE Pavements

at a variety of Depths in the Pavement. The report of this experiment(LRL38)was published in 1968. (4)

Unfortunately, from the way in which the Data is grouped for publishing, it is only possible to ascertain the mean pavement temperature at depths for -

- i) The SUMMER PERIOD (JUN, JUL & AUG)
- ii) The REST OF THE YEAR.

TABLE 6.1

The DIFFERENCE between BITUMINOUS and COMPOSITE Mean Pavement Temperatures can be ascertained for these 2 Periods by plotting the Data as a function of Depth in the Pavement. Fig. 6.1

TABLE 6 . 1

LR 138 DATA : COMPOSITE PAVEMENT MEAN TEMPERATURES AT DEPTHS .

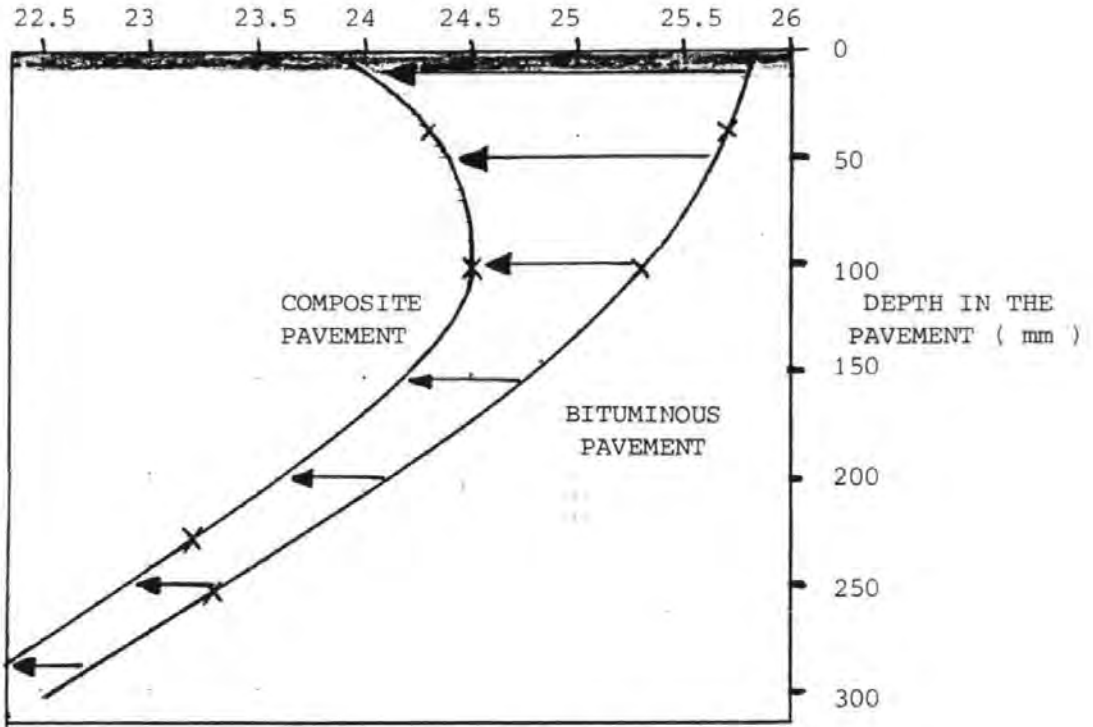
| NUMBER OF DAYS PER YEAR WHEN PAVEMENT TEMPERATURE WAS WITHIN THE FOLLOWING INTERVALS (MEAN OF 5 YEARS 1961-5) . | | | | | | |
|---|----------------------------------|-------|-------|--------------------|-------|-------|
| TEMPERATURE INTERVAL °C | FULL - DEPTH BITUMINOUS PAVEMENT | | | COMPOSITE PAVEMENT | | |
| | 38mm | 102mm | 254mm | 38mm | 102mm | 229mm |
| -5 0 | 10 | 5½ | 2 | 12 | 5½ | 3 |
| 0 5 | 48 | 49½ | 42 | 59½ | 53 | 52½ |
| 5 10 | 76 | 75½ | 84½ | 75½ | 82½ | 88½ |
| 10 15 | 58 | 59 | 62½ | 55½ | 58½ | 58½ |
| 15 20 | 59½ | 57½ | 61 | 63 | 57 | 56½ |
| 20 25 | 51 | 59½ | 74 | 49 | 59 | 69½ |
| 25 30 | 29½ | 33½ | 33 | 27 | 32 | 30 |
| 30 35 | 17 | 16½ | 5 | 15½ | 14 | 6½ |
| 35 40 | 8½ | 6 | ½ | 5½ | 3 | ½ |
| 40 45 | 6 | 1 | | 2½ | ½ | |
| 45 50 | 2 | ½ | | ½ | | |
| MEAN ANNUAL PAVEMENT TEMPERATURE °C | 15.35 | 15.15 | 14.65 | 14.15 | 14.40 | 14.00 |

| NUMBER OF DAYS IN JUNE , JULY & AUGUST WHEN PAVEMENT TEMPERATURE WAS WITHIN THE FOLLOWING INTERVALS (MEAN OF 5 YEARS 1961-5) . | | | | | | |
|--|----------------------------------|-------|-------|--------------------|-------|-------|
| TEMPERATURE INTERVAL °C | FULL - DEPTH BITUMINOUS PAVEMENT | | | COMPOSITE PAVEMENT | | |
| | 38mm | 102mm | 254mm | 38mm | 102mm | 229mm |
| 10 15 | 1½ | ½ | ½ | 1½ | ½ | ½ |
| 15 20 | 19½ | 15½ | 10 | 24 | 16½ | 13½ |
| 20 25 | 29 | 34 | 49½ | 30 | 37 | 46 |
| 25 30 | 18 | 22½ | 25½ | 18 | 23 | 24 |
| 30 35 | 11 | 12 | 4½ | 10½ | 10½ | 5½ |
| 35 40 | 5½ | 5 | | 4 | 2½ | ½ |
| 40 45 | 4 | 1 | | 2 | ½ | |
| 45 50 | 1½ | ½ | | | | |
| MEAN SUMMER PAVEMENT TEMPERATURE °C | 25.7 | 25.3 | 23.8 | 24.3 | 24.5 | 23.7 |
| MEAN PAVEMENT TEMPERATURE FOR THE REST OF THE YEAR °C | 11.9 | 11.75 | 11.6 | 10.75 | 11.0 | 10.8 |

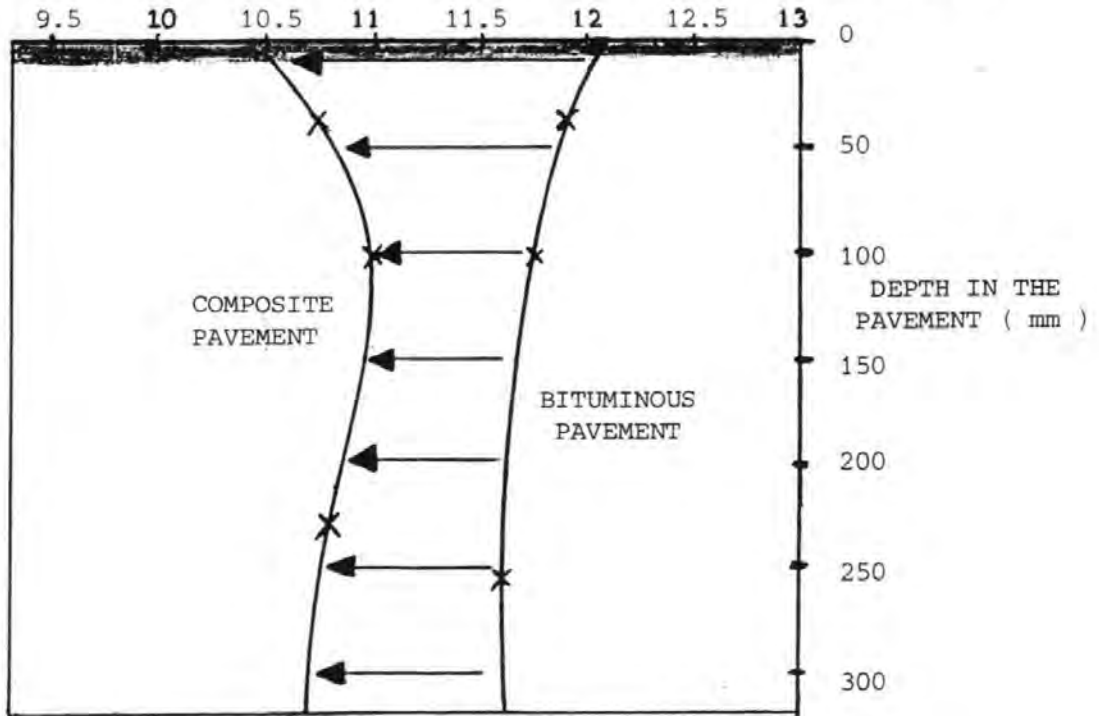
FIG 6 . 1

THE DIFFERENCES BETWEEN MEAN PAVEMENT TEMPERATURES AT VARIOUS DEPTHS IN BITUMINOUS AND COMPOSITE PAVEMENTS .

MEAN PAVEMENT TEMPERATURE FOR THE SUMMER MONTHS , °C
(JUNE , JULY & AUGUST)



MEAN PAVEMENT TEMPERATURE FOR THE REST OF THE YEAR , °C
(SEP , OCT , NOV , DEC , JAN , FEB , MAR , APR & MAY)



If values for this DIFFERENCE could be found for individual months of the year, then COMPOSITE PAVEMENT MMPT's could be estimated by correction from BITUMINOUS PAVEMENT MMPT's.

The Deviation of COMPOSITE MMPT's from the values for BITUMINOUS Pavements, will follow a similar trend over the year to the Deviation of CONCRETE MMPT's from the BITUMINOUS values, as both are due to the presence of CONCRETE in the Pavement.

Thus (BITUMINOUS - CONCRETE) MMPT DIFFERENCES, reduced such that their mean value over the relevant period is equal to the (BITUMINOUS - COMPOSITE) DIFFERENCE from the LRL38 Comparison, can be used as estimated (BITUMINOUS - COMPOSITE) MMPT DIFFERENCES.

6.2 (BITUMINOUS-CONCRETE) MMPT DIFFERENCES

These can be calculated for depths of 0/100/150, 250 and 300 mm in the pavement, for all months of the year, from the Average Year Mean Pavement Temperatures in TABLE 3.2.

For each depth in the pavement, the mean value for the SUMMER and REST OF THE YEAR periods was calculated and compared to the relevant (BITUMINOUS-COMPOSITE) DIFFERENCE from FIG. 6.1, to give a reduction factor for estimating monthly (BITUMINOUS-COMPOSITE) DIFFERENCES for that period. TABLE 6.2.

6.3 Estimated COMPOSITE Pavement MMPT's

The estimated (BITUMINOUS-COMPOSITE) MMPT DIFFERENCES can be combined with the Average Year MMPT's for BITUMINOUS PAVEMENTS in TABLE 3.2 to give Average Year COMPOSITE PAVEMENT MMPT's. TABLE 6.3

A graph was plotted to illustrate the Annual Variation of COMPOSITE PAVEMENT MMPT with depth, and also to enable the COMPOSITE PAVEMENT MMPT at a depth of 50 mm to be obtained by interpolation. FIG. 6.2

For most months, the peak of MMPT with depth occurs at c 100 mm, this is consistent with the expected build-up of stored heat underneath the LOW-CONDUCTIVITY BITUMINOUS LAYER.

TABLE 6 . 2

USE OF THE ANNUAL TREND OF (BITUMINOUS - CONCRETE) MMPT DIFFERENCES TO ESTIMATE THE ANNUAL TREND OF (BITUMINOUS - COMPOSITE) MMPT DIFFERENCES AND THUS COMPOSITE PAVEMENT MMPT'S .

| THE SUMMER PERIOD | | DEPTH IN THE PAVEMENT | | | | |
|---------------------------------|-----|-----------------------|-------|-------|-------|-------|
| | | 0mm | 100mm | 150mm | 250mm | 300mm |
| (BITUMINOUS - CONCRETE) | JUN | 6.6 | 5.7 | 5.4 | 4.4 | 4.0 |
| MMPT DIFFERENCES °C | JUL | 4.0 | 4.7 | 4.6 | 3.7 | 3.2 |
| | AUG | 2.1 | 2.6 | 2.6 | 2.0 | 1.7 |
| MEAN VALUE FOR SUMMER PERIOD | | 4.25 | 4.35 | 4.20 | 3.35 | 2.95 |
| (BITUMINOUS - COMPOSITE) | | 2.0 | 0.8 | 0.55 | 0.35 | 0.30 |
| MMPT DIFFERENCE °C | | | | | | |
| REDUCTION FACTOR | | 0.470 | 0.184 | 0.131 | 0.104 | 0.102 |
| ESTIMATED | JUN | 3.1 | 1.0 | 0.7 | 0.5 | 0.4 |
| (BITUMINOUS - COMPOSITE) | JUL | 1.9 | 0.9 | 0.6 | 0.4 | 0.3 |
| MMPT DIFFERENCES °C | AUG | 1.0 | 0.5 | 0.3 | 0.2 | 0.2 |
| THE REST OF THE YEAR | | DEPTH IN THE PAVEMENT | | | | |
| | | 0mm | 100mm | 150mm | 250mm | 300mm |
| (BITUMINOUS - CONCRETE) | SEP | 2.5 | 1.7 | 1.6 | 1.5 | 1.5 |
| MMPT DIFFERENCES °C | OCT | 2.3 | 1.5 | 1.3 | 1.5 | 1.8 |
| | NOV | 2.7 | 1.8 | 1.5 | 1.9 | 2.1 |
| | DEC | 2.7 | 2.0 | 1.8 | 2.1 | 2.3 |
| | JAN | 2.6 | 2.4 | 2.3 | 2.4 | 2.6 |
| | FEB | 2.4 | 2.3 | 2.3 | 2.2 | 2.3 |
| | MAR | 2.8 | 2.5 | 2.4 | 2.2 | 2.1 |
| | APR | 3.8 | 3.2 | 2.9 | 2.2 | 2.0 |
| | MAY | 5.5 | 4.3 | 3.8 | 3.1 | 2.8 |
| MEAN VALUE FOR REST OF THE YEAR | | 3.05 | 2.40 | 2.20 | 2.10 | 2.15 |
| (BITUMINOUS - COMPOSITE) | | 1.65 | 0.75 | 0.70 | 0.75 | 0.80 |
| MMPT DIFFERENCE °C | | | | | | |
| REDUCTION FACTOR | | 0.540 | 0.313 | 0.318 | 0.357 | 0.372 |
| ESTIMATED | SEP | 1.3 | 0.5 | 0.5 | 0.5 | 0.6 |
| (BITUMINOUS - COMPOSITE) | OCT | 1.2 | 0.5 | 0.4 | 0.5 | 0.7 |
| MMPT DIFFERENCES °C | NOV | 1.5 | 0.6 | 0.5 | 0.7 | 0.8 |
| | DEC | 1.5 | 0.6 | 0.6 | 0.7 | 0.9 |
| | JAN | 1.4 | 0.8 | 0.7 | 0.9 | 1.0 |
| | FEB | 1.3 | 0.7 | 0.7 | 0.8 | 0.9 |
| | MAR | 1.5 | 0.8 | 0.8 | 0.8 | 0.8 |
| | APR | 2.1 | 1.0 | 0.9 | 0.8 | 0.7 |
| | MAY | 3.0 | 1.3 | 1.2 | 1.1 | 1.0 |

FIG 6 . 2

ESTIMATED COMPOSITE PAVEMENT MEAN MONTHLY PAVEMENT TEMPERATURES AT VARIOUS DEPTHS .

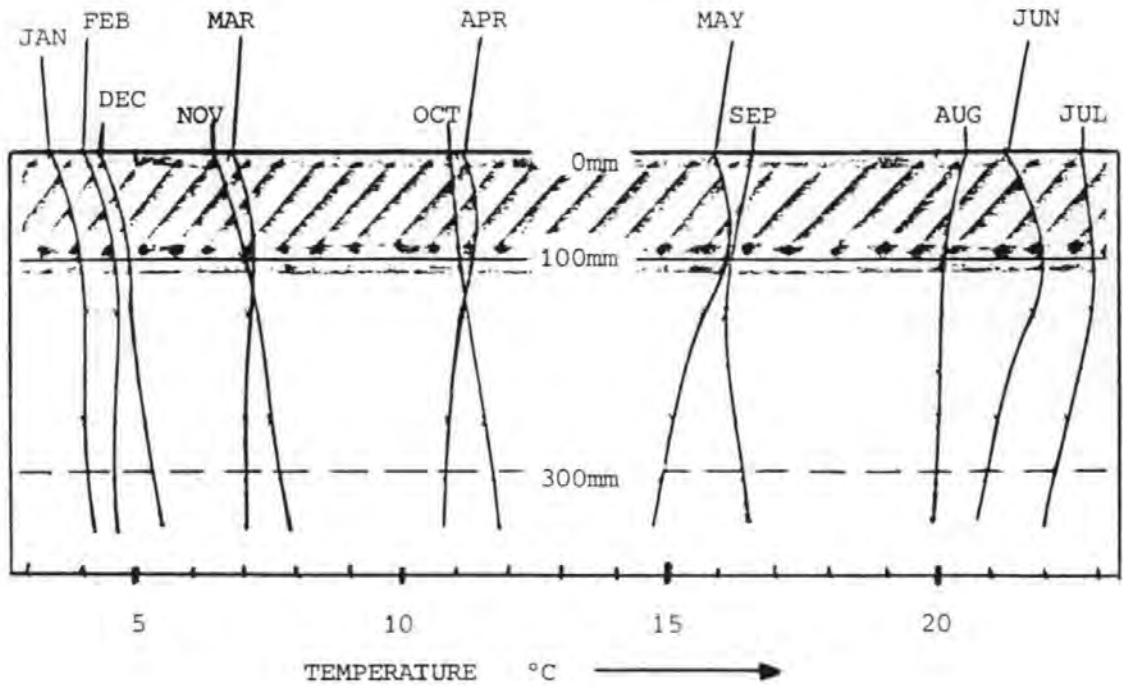


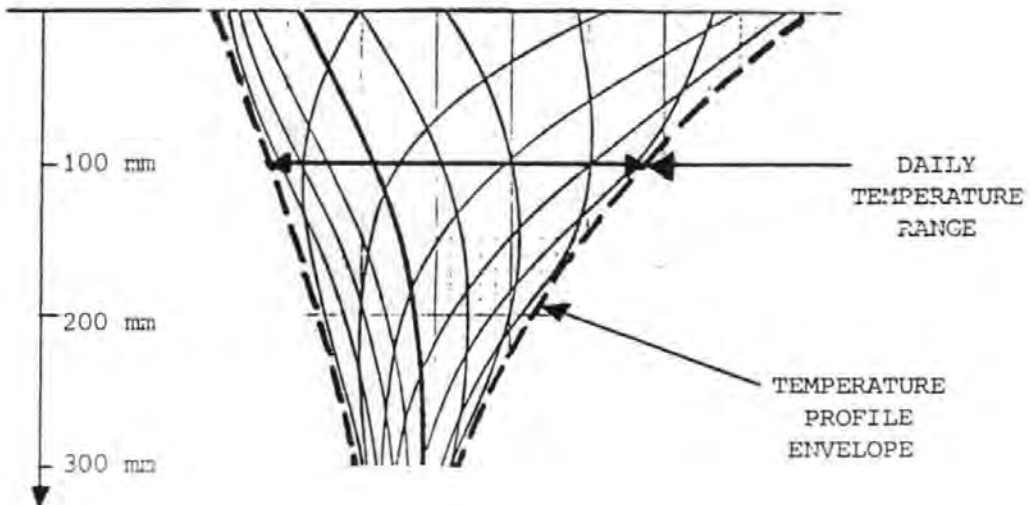
TABLE 6 . 3

"AVERAGE YEAR" COMPOSITE PAVEMENT MMPT'S AT REGULAR DEPTHS .

| DEPTH IN THE PAVEMENT | MONTH OF THE YEAR | | | | | | | | | | | |
|-----------------------------|-------------------|-----|-----|------|------|------|------|------|------|------|-----|-----|
| | JAN | FEB | MAR | APR | MAY | JUN | JUL | AUG | SEP | OCT | NOV | DEC |
| 0mm | 3.4 | 4.0 | 6.8 | 11.1 | 15.9 | 21.3 | 22.7 | 20.6 | 16.6 | 10.9 | 6.5 | 4.3 |
| 50mm | 3.8 | 4.4 | 7.1 | 11.4 | 16.2 | 21.8 | 22.9 | 20.3 | 16.4 | 11.0 | 6.8 | 4.7 |
| 100mm | 3.9 | 4.6 | 7.2 | 11.3 | 16.1 | 22.0 | 22.9 | 20.1 | 16.2 | 11.1 | 7.0 | 4.9 |
| 150mm | 4.1 | 4.6 | 7.1 | 11.1 | 15.7 | 21.8 | 22.9 | 20.1 | 16.1 | 11.2 | 7.3 | 4.9 |
| 250mm | 4.0 | 4.6 | 7.1 | 10.8 | 15.1 | 21.1 | 22.4 | 20.0 | 16.3 | 11.5 | 7.5 | 5.2 |
| 300mm | 4.1 | 4.6 | 7.1 | 10.8 | 14.9 | 20.9 | 22.2 | 20.0 | 16.4 | 11.7 | 7.7 | 5.3 |

7 COMPOSITE PAVEMENT Daily Temp Ranges

The Variation of Daily Temp Range with depth must be found for all months of the Year, for use in converting the COMPOSITE PAVEMENT ISOCHRONE DISTRIBUTIONS back into HOURLY TEMP PROFILES.



The Variation of Daily Temp Range with depth is the "envelope" of the HOURLY TEMP PROFILE shown by the dotted line on the figure above.

The Variation of COMPOSITE PAVEMENT Daily Temp Ranges with depth can thus be found by considering COMPOSITE PAVEMENT TEMP PROFILE ENVELOPES, which are defined by -

i) ENVELOPE SHAPE, The attenuation of Temp Range with depth.

ii) ENVELOPE AREA, This represents the change in STORED HEAT of a unit column of the Pavement Material.

7.1 COMPOSITE PAVEMENT ENVELOPE SHAPE

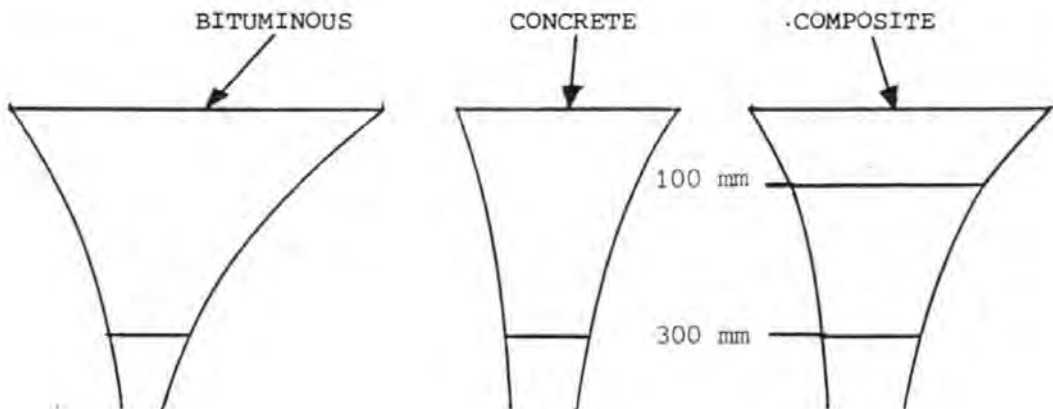
The Attenuation of Temperature Range with depth is determined by the Thermal Conductivity and Heat Storage capacity of the material and is thus a material property.

The Heat Storage capacities of BITUMINOUS and CONCRETE Materials are similar and so any significant difference in the Attenuation will be due to differing Thermal Conductivities.

Thus, Composite Pavement Envelope Shape can be estimated from The Attenuation of Temperature Range

- i) for Bituminous Pavements for depths 0 - 100 mm
- ii) for Concrete Pavements for depths 100 - 300+ mm

Envelope Shapes



The Attenuation has already been calculated for both BITUMINOUS and CONCRETE Pavements in terms of % Range at the Surface, TABLE 4.2. The Attenuation for CONCRETE Pavements from a depth of 100 mm can be re-calculated from this and used to calculate COMPOSITE PAVEMENT ENVELOPE SHAPE in terms of % Range at the Surface. TABLE 7.1

7.2 COMPOSITE PAVEMENT ENVELOPE AREA

The ENVELOPE AREA is analogous to the HEAT GAIN of the Pavement Material during the Warming Part of the Daily Cycle, which can be found by considering the Heat Balance eqn for unit column of the Pavement Material -

TABLE 7 . 1

COMPOSITE PAVEMENT TEMPERATURE PROFILE ENVELOPE "SHAPE" IN TERMS OF THE ATTENUATION OF DAILY TEMPERATURE RANGE WITH DEPTH IN THE PAVEMENT .

| DEPTH IN THE PAVEMENT | DAILY TEMPERAURE RANGE AT DEPTHS AS A % THE SURFACE VALUE | | | | | | | | | | | |
|-----------------------------|---|-----|-----|-----|-----|-----|-----|-----|-----|-----|-----|-----|
| | MONTH OF THE YEAR | | | | | | | | | | | |
| | JAN | FEB | MAR | APR | MAY | JUN | JUL | AUG | SEP | OCT | NOV | DEC |
| 0mm | 100 | 100 | 100 | 100 | 100 | 100 | 100 | 100 | 100 | 100 | 100 | 100 |
| 50mm | 75 | 76 | 79 | 80 | 77 | 76 | 77 | 77 | 78 | 79 | 84 | 85 |
| 100mm | 54 | 55 | 61 | 63 | 59 | 64 | 57 | 59 | 60 | 63 | 72 | 75 |
| 150mm | 44 | 43 | 48 | 51 | 46 | 51 | 45 | 47 | 48 | 51 | 58 | 61 |
| 200mm | 35 | 35 | 39 | 42 | 37 | 41 | 37 | 39 | 41 | 44 | 50 | 50 |
| 250mm | 30 | 29 | 31 | 33 | 30 | 33 | 31 | 34 | 35 | 39 | 45 | 46 |
| 300mm | 24 | 24 | 28 | 27 | 24 | 27 | 27 | 31 | 33 | 36 | 42 | 43 |

TABLE 7 . 2

HEAT GAIN OF THE PAVEMENT MATERIAL DURING THE DAYTIME , DETERMINED FROM THE SWEEP AREA OF THE TEMPERATURE / DEPTH PROFILES

| MONTH | HEAT GAIN AREA ON THE PROFILE m . °C | VOLUMETRIC HEAT OF THE PAVEMENT (3) $\frac{\text{Btu}}{\text{m}^3 \text{ } ^\circ\text{C}}$ | HEAT GAIN PER m ² PAVEMENT SURFACE Btu / m ² | |
|------------------------|--|---|--|------|
| | | | | |
| BITUMINOUS PAVEMENT | JAN | 0.295 | 1427 | 421 |
| | APR | 2.100 | 1427 | 2997 |
| | JUL | 2.405 | 1427 | 3432 |
| | OCT | 1.158 | 1427 | 1653 |
| CONCRETE PAVEMENT | JAN | 0.593 | 1529 | 907 |
| | APR | 1.558 | 1529 | 2382 |
| | JUL | 1.805 | 1529 | 2760 |
| | OCT | 1.045 | 1529 | 1598 |

TABLE 7 . 3

USE OF THE TOTAL ENVELOPE AREA TO A DEPTH OF 300 mm TO ESTIMATE THE HEAT GAIN AREA FOR ALL MONTHS OF THE YEAR .

| MONTH | BITUMINOUS PAVEMENT AREA (m . °C) | | | | CONCRETE PAVEMENT AREA (m . °C) | | | | COMPOSITE PAVEMENT |
|-------|--|-----------|-------|-------|--------------------------------------|-----------|-------|-------|-----------------------|
| | ENVELOPE | HEAT GAIN | | RATIO | ENVELOPE | HEAT GAIN | | RATIO | RATIO |
| | | ACT' | EST' | | | ACT' | EST' | | |
| JAN | .340 | .295 | | 1.15 | .583 | .593 | | 0.98 | 1.07* |
| FEB | .813 | | .713 | | .708 | | .722 | | 1.06* |
| MAR | 1.605 | | 1.408 | | 1.040 | | 1.065 | | 1.06* |
| APR | 2.370 | 2.100 | | 1.13 | 1.518 | 1.558 | | 0.97 | 1.05* |
| MAY | 2.965 | | 2.601 | | 1.880 | | 1.914 | | 1.06* |
| JUN | 3.302 | | 2.847 | | 2.003 | | 2.025 | | 1.07* |
| JUL | 2.814 | 2.405 | | 1.17 | 1.800 | 1.805 | | 1.00 | 1.08* |
| AUG | 2.275 | | 2.013 | | 1.513 | | 1.574 | | 1.05* |
| SEP | 1.740 | | 1.582 | | 1.213 | | 1.310 | | 1.01* |
| OCT | 1.230 | 1.158 | | 1.06 | .930 | 1.045 | | 0.89 | 0.98* |
| NOV | .767 | | .704 | | .725 | | .787 | | 1.00* |
| DEC | .368 | | .329 | | .583 | | .613 | | 1.04* |

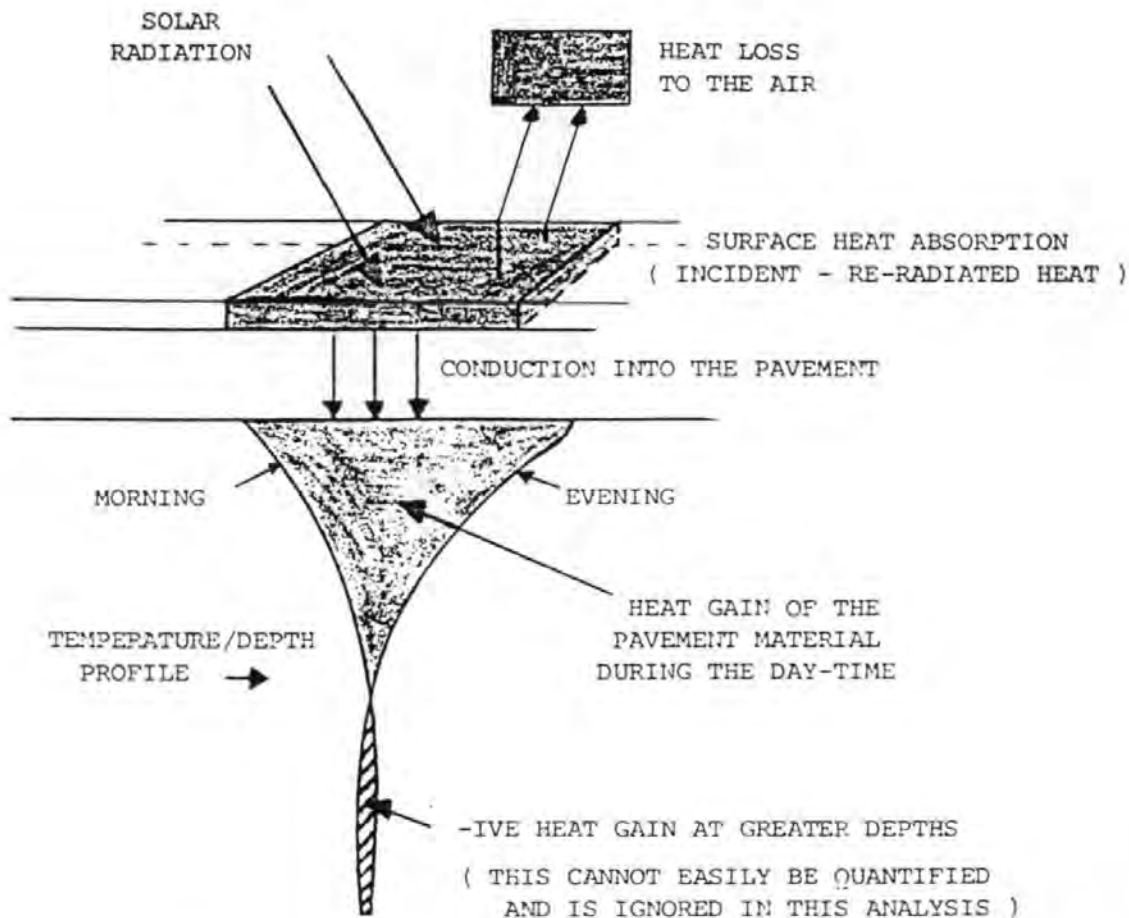
* COMPOSITE PAVEMENT ESTIMATED VALUES ARE THE AVERAGE OF THOSE FOR BITUMINOUS AND CONCRETE PAVEMENTS .

SURFACE HEAT
ABSORPTION FROM
SOLAR RADIATION

= HEAT GAIN
OF THE PAVEMENT
MATERIAL

+ HEAT LOSS TO
THE AIR BY
CONDUCTION &
CONVECTION

THE HEAT BALANCE EQUATION PER m² PAVEMENT SURFACE



for a COMPOSITE (BITUMINOUS/LEAN CONCRETE) Pavement. The SURFACE HEAT ABSORPTION will be the same as for a BITUMINOUS Pavement, but The HEAT LOSS to the air will be different, (5.3) , HEAT GAIN for COMPOSITE pavements can be found if the HEAT LOSS term in the equation can be determined, i.e., by solving the equation.

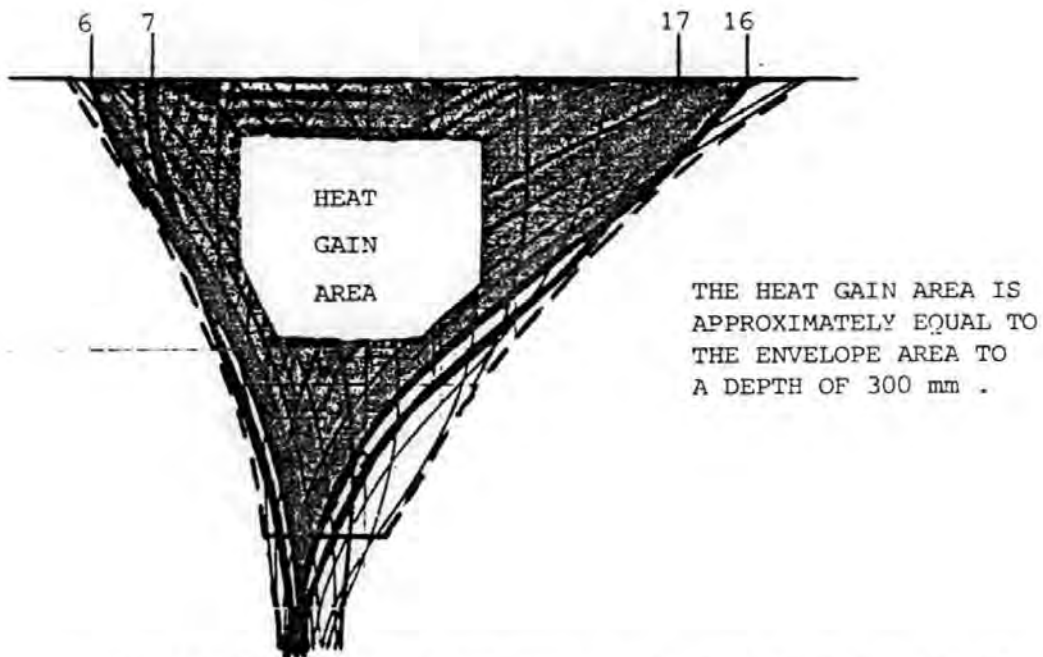
7.3 Solving the Heat Balance Eqn

The only Term that can be found directly is the HEAT GAIN for BITUMINOUS and CONCRETE Pavements, from the Hourly Temp Profiles for JAN/APR/JUL/OCT, and from the ENVELOPE AREAS to a depth of 300 mm for all months.

The SURFACE HEAT ABSORPTION for BITUMINOUS and CONCRETE Pavements can be expressed as a ratio, and The HEAT LOSS can be related to the DIFFERENCE between PAVEMENT SURFACE and AIR TEMPERATURES.

The equation can be solved simultaneously for BITUMINOUS and CONCRETE pavements to determine these quantities.

7.4 HEAT GAIN of the Pavement Material



On a Typical HOURLY TEMP PROFILE, there will be Two Pairs of ISOCHRONES (Morning and Evening) between which the HEAT GAIN of the upper and lower sections of the Pavement is equal and opposite. These times (usually 06 - 07, and 16 - 17 hrs) represent turning points in the daily cycle of heating and cooling of the bulk of the pavement.

The enclosed area on the profile represents the HEAT GAIN of the PAVEMENT, in terms of the heat stored in a unit column of pavement material.

The HEAT GAIN was estimated in this manner using 50 mm Layers and the Trapezium Rule on the Hourly Temp Profiles for both BITUMINOUS

and CONCRETE Pavements for the months JAN/APR/JUL/OCT. TABLE 7.2

It can be seen from the Typical Hourly Temp Profile that the HEAT GAIN AREA is not exactly equal to the ENVELOPE AREA, but it can be approximated by, the ENVELOPE AREA to a depth of 300 mm.

The ENVELOPE AREA to 300 mm can be found from the Attenuation of Temp Range, TABLE 4.2, again using 50 mm Layers and the Trapezium Rule.

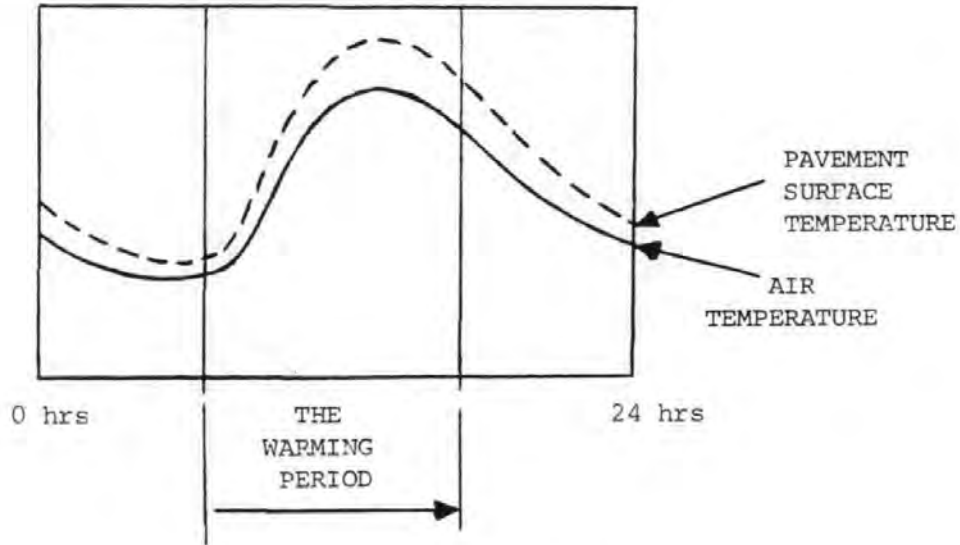
For those months (JAN/APR/JUL/OCT) where both are known, correction factors can be found to correct ENVELOPE AREA 300 mm to the HEAT GAIN AREA. TABLE 7.3

The correction factors do not vary much from month to month. Values for the other months can be interpolated and used to correct the ENVELOPE AREA: 300 mm. Thus HEAT GAIN of the Pavement can be found for all months.

7.5 HEAT LOSS to the Air from the Pavement Surface

This will be by a combination of CONDUCTION and CONVECTION, both of which are dependant on the Temperature Difference between the air and the Surface. (The evaporation of moisture may also be significant, but this is an intermittant factor and therefore difficult to quantify).

From Fig. 10.12 CRONEY it can be seen that Pavement Surface Temperature and Air Temperature follow almost exactly the same Hourly Variation.



The Mean Difference for the Warming Period is very similar to that for the rest of the Daily Cycle and thus to that for the complete Daily Cycle.

Mean Monthly Values of Mean Daily Air and Pavement Surface Temperature have already been evaluated, from which the Difference can be found, for each of the 3 Pavement Types. The HEAT LOSS from the Pavement Surface to the Air can be assumed to be proportional to this Difference. TABLE 7.4

$$\text{i.e. HEAT LOSS} = \lambda (\text{DIFF } ^\circ\text{C})$$

7.6 Surface Heat Absorption, A

The Surface Heat Absorption for Bituminous and Concrete Surfaces will vary considerably over the year, but for any particular month, the ratio of the two is likely to be constant.

$$\begin{aligned} \text{let } \beta &= \text{the ratio } A \text{ conc} : A \text{ bit} \\ \rightarrow A \text{ conc} &= \beta \cdot A \text{ bit} \end{aligned}$$

TABLE 7 . 4

PAVEMENT SURFACE - AIR TEMPERATURE DIFFERENCES FOR DETERMINATION OF PAVEMENT HEAT LOSS TO THE AIR DURING THE WARMING PERIOD .

| MEAN | MONTH OF THE YEAR | | | | | | | | | | | |
|---------------------|-------------------|------|-----|-----|------|------|------|------|------|-----|------|------|
| | JAN | FEB | MAR | APR | MAY | JUN | JUL | AUG | SEP | OCT | NOV | DEC |
| AIR TEMP' | 3.0 | 3.3 | 5.3 | 8.2 | 11.1 | 14.3 | 15.9 | 15.4 | 13.7 | 9.8 | 6.2 | 4.1 |
| BITUMINOUS PAVEMENT | 1.8 | 2.0 | 3.0 | 5.0 | 7.8 | 10.1 | 8.7 | 6.2 | 4.2 | 2.4 | 1.8 | 1.7 |
| CONCRETE PAVEMENT | -0.8 | -0.4 | 0.2 | 1.2 | 2.3 | 3.5 | 4.8 | 4.1 | 1.7 | 0.1 | -0.9 | -1.0 |
| COMPOSITE PAVEMENT | 0.4 | 0.7 | 1.5 | 2.9 | 4.8 | 7.0 | 6.8 | 5.2 | 2.9 | 1.1 | 0.3 | 0.2 |

TABLE 7 . 5

THE HEAT BALANCE EQUATION FOR BITUMINOUS AND CONCRETE PAVEMENTS FOR EACH MONTH OF THE YEAR (Btu / m² PAVEMENT SURFACE) .

| MONTH | BITUMINOUS PAVEMENT | CONCRETE PAVEMENT |
|-------|---------------------|----------------------|
| JAN | 421 = A1 - 1.8 λ | 907 = β.A1 + 0.8 λ |
| FEB | 1017 = A2 - 2.0 λ | 1104 = β.A2 + 0.4 λ |
| MAR | 2009 = A3 - 3.0 λ | 1628 = β.A3 - 0.2 λ |
| APR | 2997 = A4 - 5.0 λ | 2382 = β.A4 - 1.2 λ |
| MAY | 3712 = A5 - 7.8 λ | 2927 = β.A5 - 2.3 λ |
| JUN | 4063 = A6 - 10.1 λ | 3096 = β.A6 - 3.5 λ |
| JUL | 3432 = A7 - 8.7 λ | 2760 = β.A7 - 4.8 λ |
| AUG | 2873 = A8 - 6.2 λ | 2407 = β.A8 - 4.1 λ |
| SEP | 2258 = A9 - 4.2 λ | 2003 = β.A9 - 1.7 λ |
| OCT | 1653 = A10 - 2.4 λ | 1598 = β.A10 - 0.1 λ |
| NOV | 1005 = A11 - 1.8 λ | 1203 = β.A11 + 0.9 λ |
| DEC | 469 = A12 - 1.7 λ | 937 = β.A12 + 1.0 λ |

A1 → A12 = BITUMINOUS SURFACE HEAT ABSORPTION FOR EACH MONTH

TABLE 7 . 6

CORRESPONDING PAIRS OF VALUES FOR λ AND β FOR EACH MONTH , FOR GRAPHICAL SOLUTION OF THE HEAT BALANCE EQUATION .

| MONTH | VALUES OF λ (Btu / m ² / °C) FOR GIVEN β | | | | |
|-------|---|---------|---------|---------|---------|
| | β = 0.9 | β = 0.8 | β = 0.7 | β = 0.6 | β = 0.5 |
| JAN | 218 | 255 | 297 | 348 | 410 |
| FEB | 86 | 145 | 217 | 308 | 425 |
| MAR | -72 | 9 | 117 | 264 | 480 |
| APR | -96 | -6 | 123 | 324 | 680 |
| MAY | -88 | -11 | 104 | 294 | 670 |
| JUN | -100 | -33 | 70 | 257 | 687 |
| JUL | -105 | 6 | 257 | 1346 | -2982 |
| AUG | -121 | 126 | 1649 | -1797 | -970 |
| SEP | -14 | 118 | 341 | 790 | 2185 |
| OCT | 54 | 152 | 279 | 452 | 701 |
| NOV | 118 | 170 | 231 | 303 | 389 |
| DEC | 203 | 238 | 278 | 325 | 380 |

The Values of Heat Gain, Heat Loss and Surface Heat Absorption can now be used to formulate 24 examples of the Heat Balance Eqn, TABLE 7.5 for both BITUMINOUS and CONCRETE Pavements for all 12 months of the year.

For each month, The BITUMINOUS and CONCRETE Pavement equations can be combined as equations in β and λ . These 12 equations can be "SOLVED" simultaneously by plotting them as curves on a graph of λ vs β .

It was known that the probable value of β was in the range 0.5 + 0.9 and so values of λ were calculated corresponding to $\beta = 0.5/0.6/0.7/0.8/0.9$, TABLE 7.6, and used for plotting the equations, FIG. 7.1.

Each equation on FIG. 7.1 is only an approximation for the actual relationship for that month, therefore each intersection of lines represents an estimate for Average Annual Values of λ and β .

All visible intersections were marked on FIG. 7.1 and the best "General Solution" was estimated as

$$\beta = 0.675, \quad \lambda = 250$$

These values are the best Year-Round estimates for β , the relative surface Heat Absorption of CONCRETE and BITUMINOUS Surfaces, and for λ , the ratio of Heat Loss to the Air during the daytime to the mean Pavement Surface - Air Temperature Difference, in Btu/ $^{\circ}$ C.

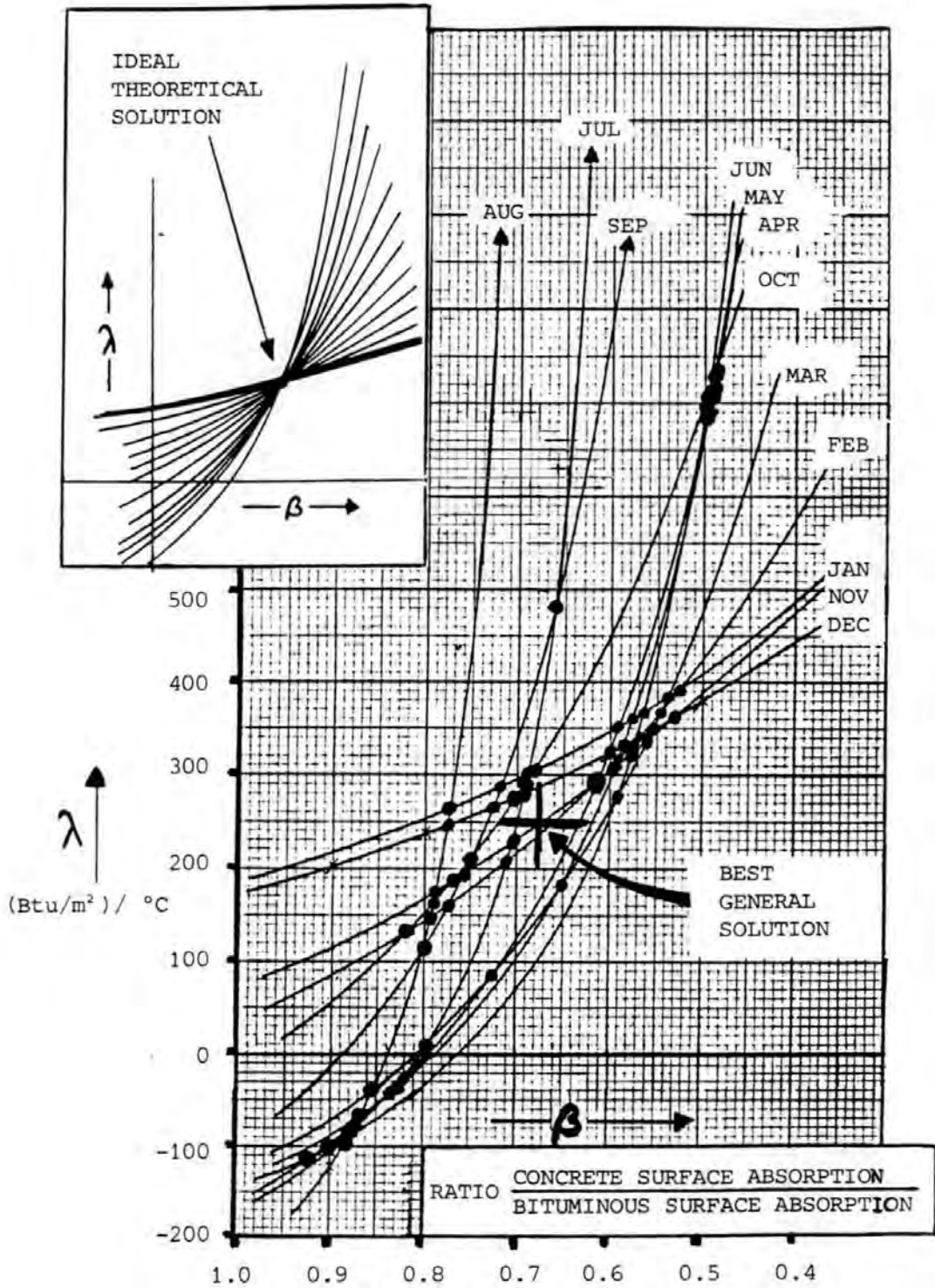
7.7 The Surface Heat Absorption for a BITUMINOUS SURFACING

The First Stage in using the HEAT BALANCE EQN to calculate COMPOSITE PAVEMENT HEAT GAIN is to calculate the Heat Absorption for BITUMINOUS SURFACING.

This can be done in two ways, for all months -

FIG 7 . 1

GRAPHICAL SOLUTION OF THE HEAT BALANCE EQUATION IN TERMS OF λ & β .



- i) using BITUMINOUS PAVEMENT HEAT GAIN (TABLE 7.3) and λ
- ii) using CONCRETE PAVEMENT HEAT GAIN (TABLE 7.3) and λ and β . TABLE 7.7

The Average Values for BITUMINOUS Surface HEAT ABSORPTION can now be combined with values for

COMPOSITE Pavement HEAT LOSS to air, to give
 COMPOSITE Pavement HEAT GAIN and thus,
 COMPOSITE Pavement ENVELOPE AREA, to 300 mm

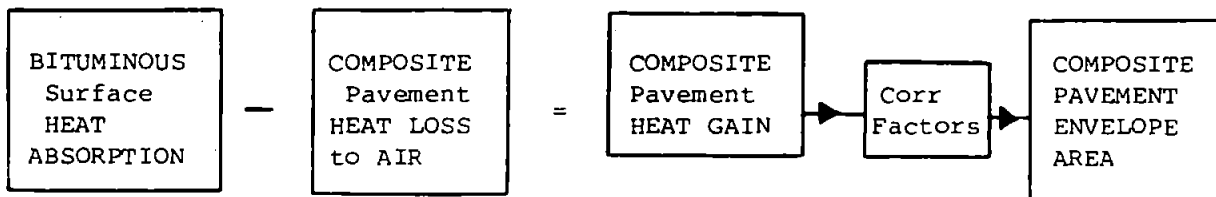


TABLE 7.8

* The HEAT GAIN for a composite pavement is almost exactly divided between the BITUMINOUS Material and the LEAN CONCRETE. Thus a Value for Volumetric Heat, equal to the average for BITUMINOUS and CONCRETE has been used.

$$(1427 + 1529) / 2 = 1478$$

7.8 ENVELOPE AREA → TEMP RANGES at Depths

ENVELOPE SHAPE, in terms of Attenuation of Temperature Range with depth, can be used to relate -

ENVELOPE AREA to 300 mm, to the Temperature Range at the Surface,
 from which the Temperature Range at all depths can be found.
considering Envelope Shape, with a 1°C Range at the Surface

The Attenuation with depth to 300 mm can be summed using the Trapezium Rule to give, for each month of the Year -

ENVELOPE AREA per 1°C range at the Surface.

TABLE 7.9

TABLE 7 . 7

DETERMINATION OF BITUMINOUS SURFACE HEAT ABSORPTION A_n FROM THE HEAT BALANCE EQUATIONS FOR BOTH BITUMINOUS AND COMPOSITE PAVEMENTS .

| MONTH | BITUMINOUS PAVEMENT (Btu / m ²) | | | | CONCRETE PAVEMENT (Btu / m ²) | | | | A_n ($\beta=0.675$) |
|-------|---|-----------------------------|------------------|-------|---|-----------------------------|------------------|-------------------|----------------------------|
| | HEAT GAIN | SURFACE - AIR TEMP' DIFF °C | HEAT LOSS TO AIR | A_n | HEAT GAIN | SURFACE - AIR TEMP' DIFF °C | HEAT LOSS TO AIR | $\beta \cdot A_n$ | |
| JAN | 421 | 1.8 | 450 | 870 | 907 | -0.8 | -200 | 710 | 1050 |
| FEB | 1017 | 2.0 | 500 | 1520 | 1104 | -0.4 | -100 | 1000 | 1480 |
| MAR | 2009 | 3.0 | 750 | 2760 | 1628 | 0.2 | 50 | 1680 | 2490 |
| APR | 2997 | 5.0 | 1250 | 4250 | 2382 | 1.2 | 300 | 2680 | 3970 |
| MAY | 3712 | 7.8 | 1950 | 5660 | 2927 | 2.3 | 575 | 3500 | 5190 |
| JUN | 4063 | 10.1 | 2525 | 6590 | 3096 | 3.5 | 875 | 3970 | 5880 |
| JUL | 3432 | 8.7 | 2175 | 5610 | 2760 | 4.8 | 1200 | 3960 | 5870 |
| AUG | 2873 | 6.2 | 1550 | 4420 | 2407 | 4.1 | 1025 | 3430 | 5080 |
| SEP | 2258 | 4.2 | 1050 | 3310 | 2003 | 1.7 | 425 | 2430 | 3600 |
| OCT | 1653 | 2.4 | 600 | 2250 | 1598 | 0.1 | 25 | 1620 | 2400 |
| NOV | 1005 | 1.8 | 450 | 1455 | 1203 | -0.9 | -225 | 980 | 1450 |
| DEC | 469 | 1.7 | 425 | 894 | 937 | -1.0 | -250 | 690 | 1020 |

TABLE 7 . 8

DETERMINATION OF COMPOSITE PAVEMENT HEAT GAIN AREA AND COMPOSITE PAVEMENT TEMPERATURE PROFILE "ENVELOPE AREA" TO A DEPTH OF 300mm .

| MONTH | SURFACE HEAT ABS' TABLE 7.7 MEAN VALUE | SURFACE -AIR TEMP' DIFF °C | HEAT LOSS TO THE AIR | HEAT GAIN | VOLUMETRIC HEAT OF PAVEMENT Btu /m ³ °C | HEAT GAIN AREA | RATIO TABLE 7.3 | COMPOSITE PAVEMENT ENVELOPE AREA _{300mm} |
|-------|--|----------------------------|----------------------|-----------|--|----------------|-----------------|---|
| JAN | 960 | 0.4 | 100 | 860 | 1478 | .582 | 1.07 | .623 |
| FEB | 1500 | 0.7 | 175 | 1325 | 1478 | .896 | 1.06 | .950 |
| MAR | 2620 | 1.5 | 375 | 2245 | 1478 | 1.520 | 1.06 | 1.610 |
| APR | 4110 | 2.9 | 725 | 3385 | 1478 | 2.290 | 1.05 | 2.405 |
| MAY | 5420 | 4.8 | 1200 | 4220 | 1478 | 2.855 | 1.06 | 3.025 |
| JUN | 6240 | 7.0 | 1750 | 4490 | 1478 | 3.040 | 1.07 | 3.250 |
| JUL | 5470 | 6.8 | 1700 | 4040 | 1478 | 2.733 | 1.08 | 2.950 |
| AUG | 4750 | 5.2 | 1300 | 3450 | 1478 | 2.334 | 1.05 | 2.450 |
| SEP | 3450 | 2.9 | 725 | 2725 | 1478 | 1.844 | 1.01 | 1.860 |
| OCT | 2330 | 1.1 | 275 | 2055 | 1478 | 1.390 | 0.98 | 1.355 |
| NOV | 1450 | 0.3 | 75 | 1375 | 1478 | .930 | 1.00 | .930 |
| DEC | 960 | 0.2 | 50 | 910 | 1478 | .616 | 1.04 | .640 |

The values of COMPOSITE PAVEMENT ENVELOPE AREA for each month can now be divided by this factor to give the corresponding range at the Surface, the attenuation of range with depth, TABLE 7.1, for each month can then be used to give - Daily Temp Ranges at Depths for all months of the Year. TABLE 7.9

7.9 CONCLUSION

The Mean Monthly Pavement Temperatures , Isochrone Distributions and Daily Temperature Ranges have now been evaluated for various depths in a 100 mm surfacing Composite Pavement and can be used to determine Composite Pavement Hourly Temperature / Depth Profiles . The same method can also be used to determine Hourly Temperature / Depth Profiles for 150 and 200 mm surfacing Composite Pavements .

Hourly Temperature / Depth profiles for a 100 mm surfacing Composite Pavement. are tabulated in APPENDIX D .

TABLE 7 . 9

COMPOSITE PAVEMENT DAILY TEMPERATURE RANGES AT DEPTHS 0 - 300 mm .

| MONTH | ENVELOPE AREA TO DEPTH 300mm | ENVELOPE AREA PER 1°C RANGE AT THE SURFACE | COMPOSITE PAVEMENT DAILY TEMPERATURE RANGES AT VARIOUS DEPTHS (°C) | | | | | |
|-------|------------------------------|--|--|------|-------|-------|-------|-------|
| | m ³ °C | m ³ | 0mm | 50mm | 100mm | 150mm | 250mm | 300mm |
| JAN | .623 | .1500 | 4.15 | 3.10 | 2.25 | 1.85 | 1.25 | 1.00 |
| FEB | .950 | .1500 | 6.35 | 4.80 | 3.50 | 2.70 | 1.85 | 1.50 |
| MAR | 1.610 | .1610 | 10.0 | 7.60 | 5.50 | 4.30 | 2.90 | 2.40 |
| APR | 2.405 | .1663 | 14.5 | 11.6 | 9.10 | 7.40 | 4.75 | 3.90 |
| MAY | 3.025 | .1555 | 19.5 | 15.0 | 11.5 | 8.95 | 5.85 | 4.65 |
| JUN | 3.250 | .1643 | 19.8 | 15.0 | 12.7 | 10.1 | 6.55 | 5.35 |
| JUL | 2.950 | .1553 | 19.0 | 14.6 | 10.8 | 8.55 | 5.90 | 5.10 |
| AUG | 2.450 | .1608 | 15.2 | 11.7 | 9.00 | 7.15 | 5.20 | 4.70 |
| SEP | 1.860 | .1642 | 11.3 | 8.85 | 6.80 | 5.45 | 3.95 | 3.75 |
| OCT | 1.355 | .1732 | 7.80 | 6.15 | 4.90 | 4.00 | 3.05 | 2.80 |
| NOV | .930 | .1900 | 4.90 | 4.10 | 3.50 | 2.85 | 2.20 | 2.05 |
| DEC | .640 | .1945 | 3.30 | 2.80 | 2.45 | 2.00 | 1.55 | 1.40 |

The difference between Bituminous Pavement and Concrete Pavement Hourly Temperature/Depth Profiles , APPENDIX B , is only a few °C and so the accuracy of interpolated data for Composite Pavements will be of the order of 1°C .

REFERENCES

1. CRONEY, D ; The Design and Performance of Road Pavements.
TRRL, HMSO, 1977.
2. FORSGATE, J.A. ; Tables of Temperature Frequency Distributions
in Flexible Road Pavements. Unpublished Report, TRRL, 1971.
3. KREBS, R.D. & WALKER, R.D. ; Highway Materials. McGraw-Hill, 1971.
4. GALLOWAY, J.W. ; Temperature Durations at various depths in
Bituminous Roads. RRL Report LR138. 1968.

APPENDIX A

BITUMINOUS PAVEMENT EXPERIMENTAL TEMPERATURE DATA , MEAN MONTHLY TEMPERATURES FOR EACH HOURLY INTERVAL OF THE DAY AT 3 DEPTHS IN THE PAVEMENT (mm) .

| HOUR | TEMPERATURE (°C) | | | | | | | | | | | |
|-------|--------------------|------|-----|-------|------|------|------|------|------|---------|------|------|
| | JANUARY | | | APRIL | | | JULY | | | OCTOBER | | |
| | 19 | 102 | 356 | 19 | 102 | 356 | 19 | 102 | 356 | 19 | 102 | 356 |
| 0- 1 | 5.7* | 5.5* | 6.2 | 7.0 | 9.3 | 10.9 | 21.2 | 22.6 | 24.6 | 12.6 | 13.6 | 15.5 |
| 1- 2 | 6.0* | 5.6* | 6.1 | 6.3 | 8.9 | 10.9 | 20.1 | 22.3 | 24.2 | 12.6 | 13.3 | 15.2 |
| 2- 3 | 6.3* | 5.6* | 6.0 | 6.2 | 8.7 | 10.8 | 19.2 | 21.8 | 24.1 | 12.2 | 13.1 | 15.1 |
| 3- 4 | 6.4* | 5.7* | 6.0 | 6.1 | 8.1 | 10.7 | 18.8 | 21.7 | 23.8 | 11.9 | 12.9 | 14.7 |
| 4- 5 | 6.1* | 5.5* | 6.0 | 5.9 | 7.5 | 10.4 | 18.3 | 20.4 | 23.7 | 11.9 | 12.5 | 14.6 |
| 5- 6 | 5.6* | 5.4* | 5.9 | 5.6 | 7.2 | 10.4 | 18.3 | 20.5 | 23.4 | 11.8 | 12.3 | 14.7 |
| 6- 7 | 5.1* | 5.3* | 6.0 | 5.8 | 6.8 | 10.3 | 18.5 | 20.2 | 23.2 | 11.8 | 12.0 | 14.6 |
| 7- 8 | 4.8* | 5.2* | 5.9 | 7.5 | 7.2 | 10.1 | 20.6 | 20.8 | 23.1 | 11.9 | 12.1 | 14.4 |
| 8- 9 | 4.7 | 5.0* | 6.0 | 10.6 | 8.6 | 10.0 | 22.9 | 21.5 | 22.9 | 12.4 | 12.2 | 14.3 |
| 9-10 | 4.9 | 4.8 | 5.9 | 14.4 | 10.0 | 9.9 | 25.6 | 22.6 | 22.7 | 13.8 | 12.9 | 14.3 |
| 10-11 | 5.0 | 5.2 | 5.9 | 16.8 | 11.7 | 9.9 | 29.1 | 24.0 | 22.6 | 15.9 | 14.1 | 14.3 |
| 11-12 | 5.4 | 5.3 | 6.0 | 19.4 | 13.7 | 9.9 | 31.9 | 25.3 | 22.8 | 17.7 | 15.2 | 14.2 |
| 12-13 | 5.6 | 5.5 | 5.9 | 20.3 | 15.0 | 9.9 | 33.5 | 27.6 | 22.9 | 19.4 | 16.1 | 14.3 |
| 13-14 | 5.9 | 5.5 | 5.9 | 21.4 | 16.3 | 10.1 | 34.8 | 29.1 | 22.7 | 20.0 | 17.1 | 14.4 |
| 14-15 | 6.0 | 5.7 | 6.0 | 22.6 | 17.0 | 10.3 | 35.1 | 30.0 | 22.8 | 20.0 | 17.7 | 14.4 |
| 15-16 | 6.0 | 5.8 | 6.0 | 22.4 | 17.8 | 10.5 | 35.1 | 30.5 | 23.1 | 19.8 | 17.6 | 14.4 |
| 16-17 | 5.8 | 5.7 | 6.1 | 18.5 | 18.0 | 10.6 | 33.9 | 31.0 | 23.2 | 18.2 | 17.2 | 14.5 |
| 17-18 | 5.4 | 5.6 | 6.2 | 17.8 | 17.3 | 10.8 | 32.3 | 30.8 | 23.6 | 16.7 | 16.3 | 14.9 |
| 18-19 | 5.0 | 5.6 | 6.2 | 15.5 | 16.2 | 10.9 | 30.3 | 29.8 | 24.1 | 15.9 | 15.9 | 15.3 |
| 19-20 | 5.1* | 5.4 | 6.3 | 13.6 | 14.6 | 11.0 | 27.9 | 28.4 | 24.2 | 14.9 | 15.4 | 15.4 |
| 20-21 | 5.1* | 5.4 | 6.3 | 12.0 | 14.0 | 10.9 | 25.4 | 27.2 | 24.2 | 14.0 | 14.7 | 15.4 |
| 21-22 | 5.2* | 5.3 | 6.3 | 10.4 | 12.8 | 11.1 | 23.7 | 25.5 | 24.4 | 13.4 | 14.1 | 15.3 |
| 22-23 | 5.3* | 5.4* | 6.2 | 9.6 | 11.5 | 11.1 | 22.7 | 24.5 | 24.1 | 13.1 | 14.0 | 15.3 |
| 23-24 | 5.4* | 5.5* | 6.4 | 9.0 | 10.7 | 10.8 | 21.5 | 23.9 | 24.2 | 12.8 | 13.8 | 15.2 |

* SUBSIDIARY PEAK IN CYCLE , PROBABLY RELATED TO THE MOVEMENT OF "WARM FRONTS" IN THE ATMOSPHERE .

APPENDIX A CONTINUED

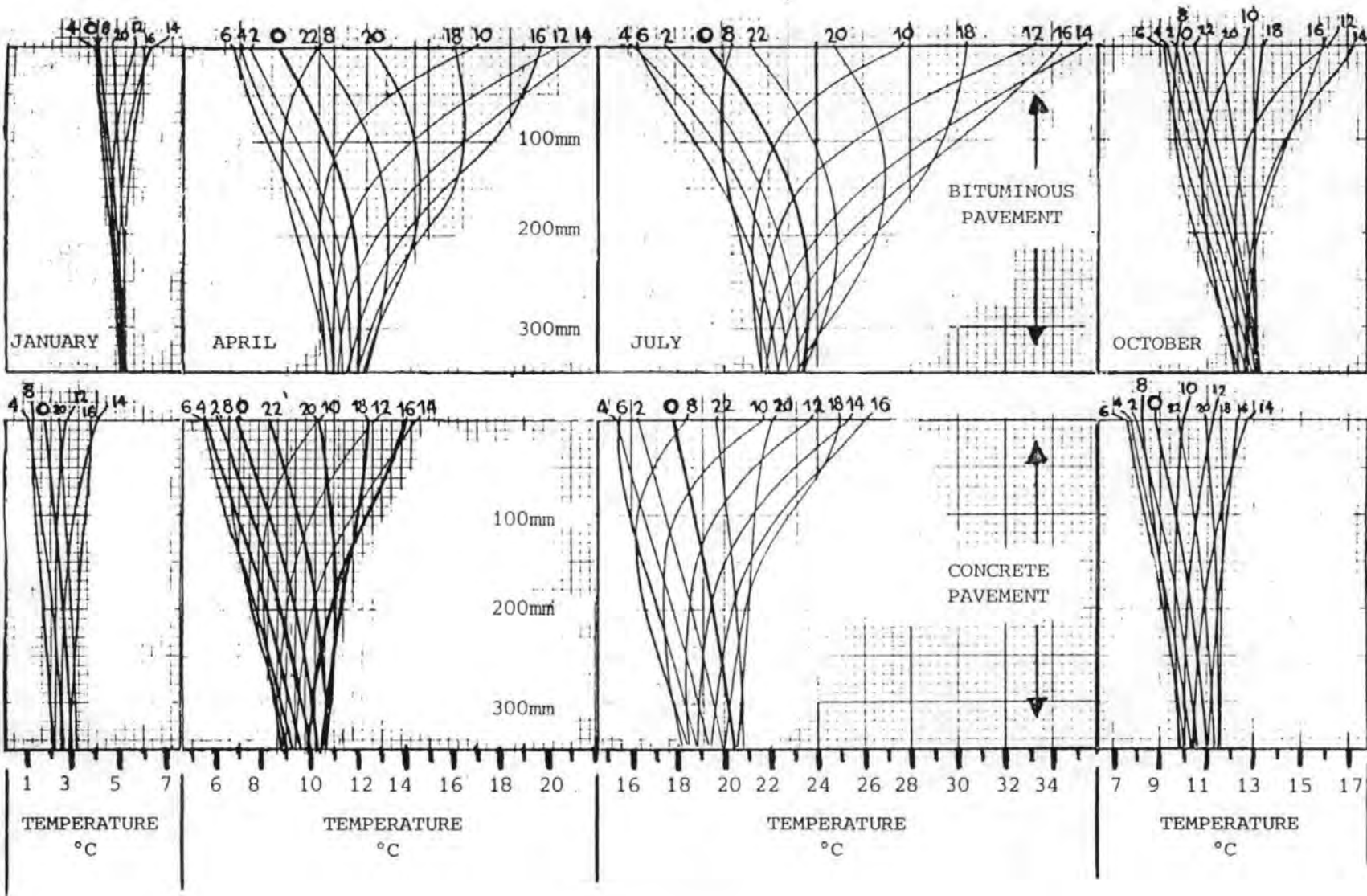
CONCRETE PAVEMENT EXPERIMENTAL TEMPERATURE DATA , HOURLY TEMPERATURES AT 3 DEPTHS IN THE PAVEMENT (mm) FOR SELECTED DAYS FROM FOUR MONTHS OF THE YEAR .

| HOUR | TEMPERATURE (°C) | | | | | | | | | | | |
|------|--------------------|-----|-----|-------|------|-----|------|------|------|---------|-------|------|
| | JANUARY | | | APRIL | | | JULY | | | OCTOBER | | |
| | 0 | 127 | 254 | 0 | 127 | 254 | 0 | 127 | 254 | 0 | 127 | 254 |
| 0 | 3.5 | 4.5 | 5.1 | 5.3 | 7.2 | 8.4 | 20.0 | 23.0 | 24.4 | 9.4 | 10.2 | 10.9 |
| 1 | 3.3 | 4.5 | 5.1 | 5.0 | 6.9 | 8.2 | 19.3 | 22.3 | 24.0 | 9.4 | 10.1 | 10.8 |
| 2 | 3.0 | 4.4 | 5.0 | 4.8 | 6.5 | 7.9 | 18.1 | 21.7 | 23.5 | 9.3 | 10.1 | 10.8 |
| 3 | 2.2 | 4.2 | 4.8 | 4.7 | 6.2 | 7.5 | 17.7 | 21.3 | 23.0 | 9.4* | 10.2* | 10.8 |
| 4 | 2.0 | 3.8 | 4.7 | 4.5 | 5.9 | 7.4 | 17.4 | 20.8 | 22.8 | 9.8* | 10.4* | 10.8 |
| 5 | 1.9 | 3.6 | 4.6 | 4.3 | 5.7 | 7.2 | 17.2 | 20.5 | 22.4 | 9.8* | 10.5* | 10.8 |
| 6 | 2.1 | 3.4 | 4.4 | 4.5 | 5.5 | 7.0 | 17.5 | 20.1 | 22.1 | 9.9* | 10.5* | 10.8 |
| 7 | 2.4 | 3.5 | 4.3 | 4.9 | 5.5 | 6.8 | 18.7 | 19.8 | 21.8 | 9.8* | 10.4* | 10.8 |
| 8 | 2.6 | 3.6 | 4.3 | 5.5 | 5.6 | 6.8 | 20.5 | 20.0 | 21.5 | 9.7 | 10.3 | 10.8 |
| 9 | 2.8 | 3.5 | 4.4 | 7.0 | 5.9 | 6.8 | 22.1 | 20.6 | 21.6 | 10.4 | 10.4 | 10.7 |
| 10 | 3.7 | 3.8 | 4.5 | 9.0 | 6.7 | 6.9 | 23.9 | 21.7 | 21.9 | 11.0 | 10.6 | 10.7 |
| 11 | 4.2 | 4.2 | 4.6 | 10.2 | 7.5 | 7.2 | 24.8 | 22.7 | 22.4 | 11.3 | 10.8 | 10.8 |
| 12 | 5.0 | 4.5 | 4.7 | 11.1 | 8.2 | 7.5 | 25.0 | 23.3 | 22.7 | 11.7 | 11.0 | 10.9 |
| 13 | 6.1 | 4.9 | 4.9 | 12.1 | 8.9 | 8.0 | 26.8 | 23.9 | 23.1 | 12.8 | 11.3 | 11.2 |
| 14 | 7.2 | 5.4 | 5.0 | 12.7 | 9.6 | 8.5 | 27.3 | 24.7 | 23.6 | 12.7 | 11.8 | 11.3 |
| 15 | 7.7 | 6.0 | 5.3 | 12.5 | 10.1 | 8.8 | 28.3 | 25.3 | 24.1 | 12.5 | 11.9 | 11.5 |
| 16 | 6.8 | 6.1 | 5.6 | 12.5 | 10.3 | 9.1 | 28.1 | 25.9 | 24.6 | 12.4 | 11.9 | 11.6 |
| 17 | 6.0 | 5.9 | 5.7 | 12.0 | 10.4 | 9.5 | 28.1 | 26.3 | 25.0 | 12.1 | 11.8 | 11.7 |
| 18 | 5.3 | 5.6 | 5.7 | 11.0 | 10.3 | 9.7 | 27.1 | 26.4 | 25.2 | 12.0 | 11.7 | 11.7 |
| 19 | 4.8 | 5.4 | 5.6 | 10.1 | 10.0 | 9.8 | 25.9 | 26.2 | 25.4 | 11.8 | 11.6 | 11.6 |
| 20 | 4.6 | 5.1 | 5.6 | 8.8 | 9.5 | 9.7 | 24.2 | 25.6 | 25.4 | 11.6 | 11.5 | 11.6 |
| 21 | 4.1 | 5.0 | 5.5 | 7.8 | 9.0 | 9.5 | 22.7 | 25.1 | 25.5 | 11.2 | 11.3 | 11.5 |
| 22 | 3.9 | 4.9 | 5.4 | 7.0 | 8.3 | 9.2 | 21.8 | 24.4 | 25.2 | 10.9 | 11.1 | 11.2 |
| 23 | 3.6 | 4.6 | 5.2 | 6.3 | 7.6 | 8.8 | 20.9 | 23.6 | 24.9 | 10.1 | 10.9 | 11.1 |
| 24 | 3.5 | 4.5 | 5.1 | 5.3 | 7.2 | 8.4 | 20.0 | 23.0 | 24.4 | 9.4 | 10.2 | 10.9 |

* SUBSIDIARY PEAK IN CYCLE , PROBABLY RELATED TO THE MOVEMENT OF A "WARM FRONT" IN THE ATMOSPHERE .

APPENDIX B
 BI-HOURLY TEMPERATURE / DEPTH PROFILES FOR BITUMINOUS AND CONCRETE
 PAVEMENTS, 0 - 300 mm.

ABI



APPENDIX C

ISOCHRONE DISTRIBUTIONS FOR 0-100 mm DEPTH IN A BITUMINOUS PAVEMENT AND 100-300 mm DEPTH IN A CONCRETE PAVEMENT, FOR ESTIMATION OF THE ISOCHRONE DISTRIBUTION AT DEPTHS 0-300 mm IN A COMPOSITE PAVEMENT .

| HOUR | JANUARY (% DAILY RANGE) | | | | | | | | | | | |
|------|---------------------------|-----|-----|-------------------|-----|-----|-----------------------------|---|-----|-----|-----|-----|
| | BITUMINOUS PAVEMENT | | | CONCRETE PAVEMENT | | | DIFFERENCE AT THE INTERFACE | "MATCHED" DISTRIBUTION FOR COMPOSITE PAVEMENT | | | | |
| | 0 | 50 | 100 | 100 | 150 | 300 | | 0 | 50 | 100 | 150 | 300 |
| 0 | -26 | -20 | -15 | -4 | 0 | 17 | -11 | -23 | -16 | -10 | -5 | 14 |
| 1 | -28 | -23 | -19 | -9 | -5 | 9 | -10 | -26 | -19 | -14 | -9 | 6 |
| 2 | -28 | -26 | -22 | -16 | -11 | 4 | -6 | -27 | -24 | -19 | -14 | 2 |
| 3 | -30 | -29 | -26 | -22 | -19 | -4 | -4 | -29 | -27 | -24 | -21 | -5 |
| 4 | -33 | -31 | -30 | -31 | -27 | -13 | 1 | -33 | -31 | -30 | -27 | -13 |
| 5 | -33 | -31 | -33 | -38 | -38 | -22 | 5 | -34 | -33 | -35 | -36 | -23 |
| 6 | -33 | -34 | -37 | -42 | -43 | -35 | 5 | -34 | -36 | -39 | -41 | -36 |
| 7 | -30 | -34 | -37 | -40 | -46 | -48 | 3 | -31 | -35 | -39 | -45 | -47 |
| 8 | -28 | -31 | -41 | -40 | -43 | -52 | -1 | -28 | -31 | -40 | -43 | -52 |
| 9 | -24 | -29 | -37 | -33 | -41 | -48 | -4 | -23 | -27 | -35 | -42 | -49 |
| 10 | -15 | -20 | -26 | -24 | -30 | -39 | -2 | -15 | -19 | -25 | -31 | -39 |
| 11 | 9 | 0 | -7 | -11 | -19 | -30 | 4 | 8 | -1 | -9 | -17 | -29 |
| 12 | 39 | 20 | 7 | 2 | -5 | -26 | 5 | 38 | 18 | 4 | -3 | -25 |
| 13 | 61 | 43 | 26 | 18 | 8 | -18 | 8 | 59 | 40 | 22 | 11 | -16 |
| 14 | 67 | 57 | 44 | 36 | 24 | -9 | 8 | 65 | 54 | 40 | 27 | -7 |
| 15 | 65 | 66 | 56 | 58 | 43 | 9 | -2 | 65 | 67 | 57 | 42 | 9 |
| 16 | 52 | 60 | 59 | 58 | 54 | 35 | 1 | 52 | 60 | 59 | 54 | 35 |
| 17 | 33 | 46 | 48 | 44 | 46 | 48 | 4 | 32 | 44 | 46 | 48 | 49 |
| 18 | 17 | 29 | 37 | 33 | 41 | 48 | 4 | 16 | 27 | 35 | 43 | 49 |
| 19 | 7 | 17 | 26 | 27 | 32 | 48 | -1 | 7 | 17 | 26 | 32 | 48 |
| 20 | -2 | 9 | 15 | 18 | 24 | 43 | -3 | -1 | 10 | 16 | 23 | 42 |
| 21 | -9 | 0 | 7 | 11 | 19 | 39 | -4 | -8 | 1 | 9 | 18 | 38 |
| 22 | -15 | -9 | 0 | 7 | 14 | 35 | -7 | -13 | -6 | 3 | 11 | 33 |
| 23 | -22 | -14 | -7 | 2 | 8 | 26 | -9 | -20 | -11 | -3 | 4 | 24 |
| 24 | -26 | -20 | -15 | -4 | 0 | 17 | -11 | -23 | -16 | -10 | -5 | 14 |

APPENDIX C CONTINUED

ISOCHRONE DISTRIBUTIONS FOR 0-100 mm DEPTH IN A BITUMINOUS PAVEMENT AND 100-300 mm DEPTH IN A CONCRETE PAVEMENT , FOR ESTIMATION OF THE ISOCHRONE DISTRIBUTION AT DEPTHS 0-300 mm IN A COMPOSITE PAVEMENT .

| HOUR | APRIL (% DAILY RANGE) | | | | | | | | | | | |
|------|-------------------------|-----|-----|-------------------|-----|-----|-----------------------------|---|-----|-----|-----|-----|
| | BITUMINOUS PAVEMENT | | | CONCRETE PAVEMENT | | | DIFFERENCE AT THE INTERFACE | "MATCHED" DISTRIBUTION FOR COMPOSITE PAVEMENT | | | | |
| | 0 | 50 | 100 | 100 | 150 | 300 | | 0 | 50 | 100 | 150 | 300 |
| 0 | -30 | -25 | -19 | -18 | -10 | 21 | -1 | -30 | -25 | -18 | -10 | 21 |
| 1 | -36 | -32 | -27 | -23 | -16 | 13 | -4 | -35 | -30 | -25 | -18 | 12 |
| 2 | -37 | -36 | -32 | -28 | -22 | 2 | -4 | -36 | -34 | -30 | -24 | 1 |
| 3 | -39 | -38 | -36 | -34 | -30 | -11 | -2 | -38 | -37 | -35 | -31 | -12 |
| 4 | -40 | -40 | -40 | -39 | -36 | -19 | -1 | -40 | -40 | -39 | -36 | -19 |
| 5 | -41 | -42 | -43 | -43 | -41 | -26 | 0 | -41 | -42 | -43 | -41 | -26 |
| 6 | -42 | -44 | -45 | -47 | -46 | -32 | 2 | -42 | -44 | -46 | -45 | -31 |
| 7 | -35 | -40 | -45 | -46 | -48 | -43 | 1 | -35 | -40 | -45 | -48 | -43 |
| 8 | -19 | -28 | -37 | -42 | -46 | -45 | 5 | -20 | -30 | -39 | -44 | -44 |
| 9 | 8 | -12 | -25 | -34 | -40 | -47 | 9 | 6 | -15 | -29 | -36 | -45 |
| 10 | 24 | 6 | -11 | -17 | -27 | -47 | 6 | 22 | 4 | -14 | -24 | -45 |
| 11 | 35 | 23 | 6 | -1 | -11 | -45 | 5 | 34 | 21 | 2 | -9 | -44 |
| 12 | 46 | 35 | 21 | 14 | 3 | -36 | 7 | 44 | 32 | 17 | 6 | -34 |
| 13 | 52 | 45 | 32 | 28 | 18 | -23 | 4 | 51 | 43 | 30 | 20 | -22 |
| 14 | 56 | 51 | 43 | 42 | 32 | -2 | 1 | 56 | 51 | 42 | 32 | -2 |
| 15 | 58 | 56 | 49 | 51 | 41 | 9 | -2 | 58 | 57 | 50 | 40 | 8 |
| 16 | 42 | 51 | 55 | 53 | 48 | 21 | 2 | 41 | 50 | 54 | 49 | 21 |
| 17 | 28 | 40 | 52 | 52 | 52 | 36 | 0 | 28 | 40 | 52 | 52 | 36 |
| 18 | 19 | 31 | 43 | 47 | 52 | 47 | -4 | 20 | 32 | 45 | 50 | 46 |
| 19 | 7 | 19 | 31 | 39 | 48 | 53 | -8 | 9 | 22 | 35 | 44 | 51 |
| 20 | -4 | 9 | 21 | 27 | 38 | 53 | -6 | -2 | 11 | 24 | 35 | 51 |
| 21 | -12 | -1 | 11 | 17 | 29 | 51 | -6 | -10 | 1 | 14 | 26 | 49 |
| 22 | -19 | -9 | 1 | 4 | 15 | 45 | -3 | -18 | -8 | 2 | 14 | 44 |
| 23 | -24 | -17 | -9 | -8 | 1 | 34 | -1 | -24 | -17 | -8 | 1 | 34 |
| 24 | -30 | -25 | -19 | -18 | -10 | 21 | -1 | -30 | -25 | -18 | -10 | 21 |

APPENDIX C CONTINUED

ISOCHROME DISTRIBUTIONS FOR 0-100 mm DEPTH IN A BITUMINOUS PAVEMENT AND 100-300 mm DEPTH IN A CONCRETE PAVEMENT , FOR ESTIMATION OF THE ISOCHROME DISTRIBUTION AT DEPTHS 0-300 mm IN A COMPOSITE PAVEMENT .

| HOUR | JULY (% DAILY RANGE) | | | | | | | | | | | |
|------|------------------------|-----|-----|-------------------|-----|-----|-----------------------------|---|-----|-----|-----|-----|
| | BITUMINOUS PAVEMENT | | | CONCRETE PAVEMENT | | | DIFFERENCE AT THE INTERFACE | "MATCHED" DISTRIBUTION FOR COMPOSITE PAVEMENT | | | | |
| | 0 | 50 | 100 | 100 | 150 | 300 | | 0 | 50 | 100 | 150 | 300 |
| 0 | -28 | -23 | -17 | -7 | 2 | 28 | -10 | -25 | -19 | -12 | -2 | 25 |
| 1 | -33 | -29 | -24 | -16 | -8 | 17 | -8 | -31 | -26 | -20 | -11 | 15 |
| 2 | -37 | -33 | -29 | -25 | -16 | 9 | -4 | -36 | -31 | -27 | -18 | 8 |
| 3 | -40 | -38 | -34 | -32 | -24 | -2 | -2 | -40 | -37 | -33 | -25 | -2 |
| 4 | -44 | -42 | -38 | -38 | -32 | -12 | 0 | -44 | -42 | -38 | -32 | -12 |
| 5 | -45 | -46 | -43 | -43 | -39 | -22 | 0 | -45 | -46 | -43 | -39 | -22 |
| 6 | -44 | -46 | -46 | -47 | -45 | -29 | 1 | -44 | -46 | -46 | -45 | -29 |
| 7 | -37 | -40 | -43 | -48 | -52 | -38 | 5 | -38 | -42 | -45 | -50 | -37 |
| 8 | -22 | -29 | -36 | -43 | -50 | -45 | 7 | -24 | -32 | -39 | -47 | -43 |
| 9 | -3 | -18 | -28 | -34 | -42 | -48 | 6 | -4 | -20 | -31 | -39 | -46 |
| 10 | 15 | -2 | -15 | -18 | -27 | -45 | 3 | 14 | -3 | -16 | -26 | -44 |
| 11 | 34 | 16 | -4 | -4 | -13 | -35 | 0 | 34 | 16 | -4 | -13 | -35 |
| 12 | 44 | 32 | 14 | 7 | -3 | -28 | 7 | 42 | 29 | 10 | 0 | -26 |
| 13 | 52 | 44 | 31 | 17 | 8 | 20 | 14 | 48 | 39 | 24 | 14 | -16 |
| 14 | 54 | 50 | 42 | 30 | 20 | -9 | 12 | 51 | 45 | 36 | 25 | -6 |
| 15 | 55 | 54 | 49 | 37 | 29 | -2 | -12 | 52 | 49 | 43 | 34 | -5 |
| 16 | 49 | 54 | 54 | 46 | 39 | 12 | 8 | 47 | 51 | 50 | 42 | 14 |
| 17 | 40 | 48 | 54 | 50 | 45 | 23 | 4 | 39 | 46 | 52 | 47 | 24 |
| 18 | 29 | 38 | 48 | 52 | 48 | 31 | -4 | 30 | 39 | 50 | 47 | 30 |
| 19 | 16 | 25 | 37 | 45 | 47 | 38 | -8 | 18 | 28 | 41 | 43 | 36 |
| 20 | 0 | 11 | 24 | 32 | 40 | 46 | -8 | 2 | 14 | 28 | 36 | 44 |
| 21 | -12 | -1 | 11 | 23 | 33 | 52 | -12 | -9 | 3 | 17 | 28 | 49 |
| 22 | -18 | -11 | -1 | 14 | 24 | 48 | -15 | -14 | -5 | 6 | 17 | 44 |
| 23 | -24 | -18 | -9 | 4 | 14 | 38 | -13 | -21 | -13 | -2 | 8 | 35 |
| 24 | -28 | -23 | -17 | -7 | 2 | 28 | -10 | -25 | -19 | -12 | -2 | 25 |

APPENDIX C CONTINUED

ISOCHRONE DISTRIBUTIONS FOR 0-100 mm DEPTH IN A BITUMINOUS PAVEMENT AND 100-300 mm DEPTH IN A CONCRETE PAVEMENT , FOR ESTIMATION OF THE ISOCHRONE DISTRIBUTION AT DEPTHS 0-300 mm IN A COMPOSITE PAVEMENT .

| HOUR | OCTOBER (% DAILY RANGE) | | | | | | | | | | | |
|------|---------------------------|-----|-----|-------------------|-----|-----|-----------------------------|---|-----|-----|-----|-----|
| | BITUMINOUS PAVEMENT | | | CONCRETE PAVEMENT | | | DIFFERENCE AT THE INTERFACE | "MATCHED" DISTRIBUTION FOR COMPOSITE PAVEMENT | | | | |
| | 0 | 50 | 100 | 100 | 150 | 300 | | 0 | 50 | 100 | 150 | 300 |
| 0 | -27 | -21 | -15 | -14 | -10 | 17 | -1 | -27 | -21 | -14 | -10 | 17 |
| 1 | -29 | -23 | -18 | -24 | -20 | 3 | 6 | -30 | -25 | -21 | -17 | 4 |
| 2 | -31 | -26 | -22 | -32 | -29 | -8 | 10 | -33 | -30 | -27 | -25 | -5 |
| 3 | -32 | -29 | -27 | -38 | -37 | -19 | 11 | -35 | -33 | -32 | -32 | -16 |
| 4 | -35 | -31 | -30 | -42 | -42 | -28 | 12 | -38 | -35 | -36 | -37 | -25 |
| 5 | -36 | -33 | -34 | -46 | -46 | -33 | 12 | -39 | -37 | -40 | -41 | -28 |
| 6 | -36 | -35 | -38 | -48 | -49 | -39 | 10 | -38 | -39 | -43 | -45 | -36 |
| 7 | -35 | -36 | -42 | -46 | -49 | -42 | 4 | -36 | -38 | -44 | -47 | -41 |
| 8 | -30 | -33 | -41 | -37 | -39 | -44 | -4 | -29 | -32 | -39 | -41 | -45 |
| 9 | -16 | -25 | -33 | -23 | -27 | -42 | -10 | -13 | -21 | -28 | -31 | -44 |
| 10 | 7 | -8 | -16 | -10 | -19 | -42 | -6 | 8 | -6 | -13 | -22 | -43 |
| 11 | 32 | 14 | 4 | -1 | -10 | -39 | 5 | 31 | 12 | 1 | -8 | -38 |
| 12 | 52 | 33 | 22 | 11 | 2 | -31 | 11 | 49 | 29 | 16 | 7 | -28 |
| 13 | 63 | 52 | 39 | 25 | 15 | -17 | 14 | 59 | 47 | 32 | 21 | -13 |
| 14 | 64 | 60 | 53 | 42 | 32 | 0 | 11 | 61 | 56 | 47 | 37 | 3 |
| 15 | 59 | 64 | 58 | 52 | 44 | 22 | 6 | 57 | 62 | 55 | 47 | 23 |
| 16 | 49 | 53 | 53 | 52 | 51 | 36 | 1 | 49 | 53 | 52 | 51 | 36 |
| 17 | 30 | 36 | 41 | 48 | 49 | 47 | -7 | 32 | 39 | 44 | 46 | 45 |
| 18 | 16 | 22 | 31 | 42 | 46 | 53 | -11 | 19 | 26 | 36 | 41 | 50 |
| 19 | 4 | 12 | 20 | 37 | 41 | 56 | -17 | 8 | 18 | 28 | 33 | 52 |
| 20 | -7 | 2 | 10 | 30 | 36 | 56 | -20 | -2 | 9 | 20 | 27 | 51 |
| 21 | -15 | -8 | -1 | 20 | 27 | 50 | -21 | -10 | 0 | 9 | 18 | 45 |
| 22 | -21 | -14 | -7 | 8 | 15 | 42 | -15 | -17 | -8 | 0 | 8 | 38 |
| 23 | -24 | -17 | -11 | -3 | 3 | 31 | -8 | -26 | -14 | -7 | -1 | 29 |
| 24 | -27 | -21 | -15 | -14 | -10 | 17 | -1 | -27 | -21 | -14 | -10 | 17 |

APPENDIX D

COMPOSITE PAVEMENT HOURLY TEMPERATURE / DEPTH PROFILES , DEDUCED FROM BITUMINOUS , CONCRETE AND COMPOSITE PAVEMENT TEMPERATURES .

| HOUR | TEMPERATURE (°C) | | | | | | | | | |
|------|--------------------|------|-------|-------|-------|-------|------|-------|-------|-------|
| | JANUARY | | | | | APRIL | | | | |
| | 0mm | 50mm | 100mm | 150mm | 300mm | 0mm | 50mm | 100mm | 150mm | 300mm |
| 0 | 2.45 | 3.30 | 3.65 | 4.00 | 4.25 | 6.75 | 8.55 | 9.65 | 10.4 | 11.7 |
| 1 | 2.30 | 3.25 | 3.60 | 3.95 | 4.15 | 6.00 | 7.95 | 9.00 | 9.75 | 11.3 |
| 2 | 2.25 | 3.10 | 3.45 | 3.85 | 4.10 | 5.90 | 7.50 | 8.55 | 9.30 | 10.8 |
| 3 | 2.20 | 3.00 | 3.35 | 3.70 | 4.05 | 5.60 | 7.15 | 8.10 | 8.80 | 10.3 |
| 4 | 2.00 | 2.85 | 3.20 | 3.60 | 3.95 | 5.30 | 6.80 | 7.75 | 8.45 | 10.0 |
| 5 | 1.95 | 2.80 | 3.10 | 3.45 | 3.85 | 5.15 | 6.60 | 7.40 | 8.05 | 9.75 |
| 6 | 1.95 | 2.70 | 3.00 | 3.35 | 3.75 | 5.00 | 6.35 | 7.10 | 7.75 | 9.55 |
| 7 | 2.10 | 2.75 | 3.00 | 3.25 | 3.65 | 6.00 | 6.80 | 7.20 | 7.55 | 9.05 |
| 8 | 2.25 | 2.85 | 3.00 | 3.30 | 3.60 | 8.20 | 7.95 | 7.75 | 7.85 | 9.00 |
| 9 | 2.45 | 3.00 | 3.10 | 3.30 | 3.60 | 12.0 | 9.70 | 8.65 | 8.45 | 8.95 |
| 10 | 2.75 | 3.25 | 3.35 | 3.50 | 3.70 | 14.3 | 11.9 | 10.0 | 9.30 | 8.95 |
| 11 | 3.75 | 3.75 | 3.70 | 3.80 | 3.80 | 16.0 | 13.8 | 11.5 | 10.4 | 9.00 |
| 12 | 5.00 | 4.35 | 4.00 | 4.05 | 3.85 | 17.5 | 15.1 | 12.8 | 11.5 | 9.40 |
| 13 | 5.85 | 5.00 | 4.40 | 4.30 | 3.95 | 18.5 | 16.3 | 14.0 | 12.6 | 9.90 |
| 14 | 6.15 | 5.45 | 4.80 | 4.60 | 4.05 | 19.2 | 17.3 | 15.1 | 13.5 | 10.7 |
| 15 | 6.15 | 5.80 | 5.20 | 4.90 | 4.20 | 19.5 | 17.9 | 15.8 | 14.1 | 11.1 |
| 16 | 5.60 | 5.60 | 5.25 | 5.10 | 4.45 | 17.0 | 17.1 | 16.2 | 14.7 | 11.7 |
| 17 | 4.75 | 5.10 | 4.95 | 5.00 | 4.60 | 15.2 | 16.0 | 16.0 | 14.9 | 12.3 |
| 18 | 4.05 | 4.60 | 4.70 | 4.90 | 4.60 | 14.0 | 15.1 | 15.4 | 14.8 | 12.7 |
| 19 | 3.70 | 4.30 | 4.50 | 4.70 | 4.60 | 12.4 | 13.9 | 14.5 | 14.4 | 12.9 |
| 20 | 3.35 | 4.10 | 4.25 | 4.55 | 4.50 | 10.8 | 12.7 | 13.5 | 13.7 | 12.9 |
| 21 | 3.05 | 3.85 | 4.10 | 4.45 | 4.50 | 9.65 | 11.5 | 12.6 | 13.0 | 12.8 |
| 22 | 2.85 | 3.60 | 3.95 | 4.30 | 4.45 | 8.50 | 10.5 | 11.5 | 12.1 | 12.6 |
| 23 | 2.55 | 3.45 | 3.85 | 4.15 | 4.35 | 7.60 | 9.45 | 10.6 | 11.2 | 12.2 |
| 24 | 2.45 | 3.30 | 3.65 | 4.00 | 4.25 | 6.75 | 8.55 | 9.65 | 10.4 | 11.7 |

APPENDIX D CONTINUED

COMPOSITE PAVEMENT HOURLY TEMPERATURE / DEPTH PROFILES , DEDUCED FROM BITUMINOUS , CONCRETE AND COMPOSITE PAVEMENT TEMPERATURES .

| HOUR | TEMPERATURE (°C) | | | | | | | | | |
|------|--------------------|------|-------|-------|-------|---------|------|-------|-------|-------|
| | JULY | | | | | OCTOBER | | | | |
| | 0mm | 50mm | 100mm | 150mm | 300mm | 0mm | 50mm | 100mm | 150mm | 300mm |
| 0 | 17.8 | 20.0 | 21.6 | 22.7 | 23.5 | 8.80 | 9.70 | 10.4 | 10.8 | 12.2 |
| 1 | 16.6 | 19.0 | 20.7 | 21.9 | 23.0 | 8.55 | 9.50 | 10.1 | 10.5 | 11.8 |
| 2 | 15.6 | 18.2 | 20.0 | 21.3 | 22.6 | 8.35 | 9.15 | 9.75 | 10.2 | 11.6 |
| 3 | 14.9 | 17.3 | 19.3 | 20.7 | 22.1 | 8.15 | 9.00 | 9.50 | 9.90 | 11.2 |
| 4 | 14.1 | 16.6 | 18.7 | 20.1 | 21.6 | 7.95 | 8.85 | 9.30 | 9.70 | 11.0 |
| 5 | 13.9 | 16.0 | 18.2 | 19.5 | 21.0 | 7.85 | 8.75 | 9.10 | 9.55 | 10.9 |
| 6 | 14.1 | 16.0 | 17.8 | 18.9 | 20.6 | 7.95 | 8.65 | 8.95 | 9.35 | 10.7 |
| 7 | 15.3 | 16.6 | 17.9 | 18.5 | 20.2 | 8.10 | 8.70 | 8.90 | 9.30 | 10.5 |
| 8 | 18.0 | 18.1 | 18.6 | 18.8 | 19.9 | 8.65 | 9.05 | 9.15 | 9.55 | 10.4 |
| 9 | 21.9 | 19.9 | 19.5 | 19.5 | 19.7 | 9.90 | 9.70 | 9.70 | 9.95 | 10.4 |
| 10 | 25.4 | 22.4 | 21.1 | 20.7 | 19.8 | 11.5 | 10.6 | 10.5 | 10.3 | 10.5 |
| 11 | 29.4 | 25.3 | 22.5 | 21.8 | 20.3 | 13.3 | 11.7 | 11.1 | 10.9 | 10.6 |
| 12 | 30.9 | 27.3 | 24.0 | 22.9 | 20.8 | 14.7 | 12.8 | 11.9 | 11.5 | 10.9 |
| 13 | 32.1 | 28.8 | 25.5 | 24.1 | 21.3 | 15.5 | 13.9 | 12.7 | 12.1 | 11.3 |
| 14 | 32.7 | 29.7 | 26.9 | 25.1 | 21.9 | 15.7 | 14.4 | 13.4 | 12.7 | 11.8 |
| 15 | 32.9 | 30.3 | 27.6 | 25.9 | 22.5 | 15.3 | 14.8 | 13.8 | 13.1 | 12.4 |
| 16 | 31.9 | 30.6 | 28.4 | 26.6 | 23.0 | 14.7 | 14.2 | 13.7 | 13.3 | 12.7 |
| 17 | 30.3 | 29.8 | 28.6 | 27.0 | 23.5 | 13.4 | 13.4 | 13.3 | 13.1 | 13.0 |
| 18 | 28.6 | 28.8 | 28.4 | 27.0 | 23.8 | 12.4 | 12.6 | 12.9 | 12.9 | 13.1 |
| 19 | 26.2 | 27.1 | 27.4 | 26.7 | 24.1 | 11.5 | 12.1 | 12.5 | 12.5 | 13.2 |
| 20 | 23.1 | 25.0 | 26.0 | 26.0 | 24.6 | 10.7 | 11.5 | 12.1 | 12.3 | 13.2 |
| 21 | 20.9 | 23.4 | 24.8 | 25.4 | 24.8 | 10.1 | 11.0 | 11.5 | 11.9 | 13.0 |
| 22 | 20.0 | 22.1 | 23.6 | 24.4 | 24.6 | 9.55 | 10.5 | 11.1 | 11.5 | 12.8 |
| 23 | 18.6 | 20.9 | 22.7 | 23.6 | 24.1 | 8.90 | 10.1 | 10.8 | 11.2 | 12.5 |
| 24 | 17.8 | 20.0 | 21.6 | 22.7 | 23.5 | 8.80 | 9.70 | 10.4 | 10.8 | 12.2 |